Cell-Derived Extracellular Matrix Scaffolds Developed using Macromolecular Crowding

A dissertation submitted to the faculty of Worcester Polytechnic Institute in partial fulfillment of the requirements for the degree of Doctor of Philosophy in Biomedical Engineering

June 11th, 2019

By

Dalia M. Shendi

Approved By:

Marsha W. Rolle, PhD
Associate Professor, Advisor
Biomedical Engineering
Worcester Polytechnic Institute

Tanja Dominko, PhD
Associate Professor
Biology & Biotechnology
Worcester Polytechnic Institute

Kristen L. Billiar, PhD
Department Head and Professor
Biomedical Engineering
Worcester Polytechnic Institute

Michael P. Zimber, PhD
Director of Applied Research
Histogen, Inc

Jeannine M. Coburn, PhD
Assistant Professor
Biomedical Engineering
Worcester Polytechnic Institute

Table of Contents

Acknowledgements

Thank you to my dedicated advisor, Marsha Rolle, who was always there supporting me in research, and in life. You are one of the best advisors WPI has to offer; and because of a dramatic change in fate, I am very fortunate to have walked into your lab and became one of your PhD students. I will definitely miss my time working in the Rolle lab.

Thank you to Terri Camesano and Kristin Billiar for providing their support during my transition period into a new lab, and a special thank you to my committee members for providing scientific feedback on my project.

I would like to acknowledge all of our special collaborators that have provided significant contribution in completing my research story. Thank you to Julia Marzi and Katja Schenke-Layland (Raman microspectroscopy) as well as for hosting me during my IGERT international research experience at the Fraunhofer Institute; Ariel Kauss and Todd McDevitt (decellularization strategies and surface coatings); Will Linthicum and Qi Wen (AFM); David Dolivo (qRT-PCR training); Silke Keller (confocal LSM training), and Daniel Lawler (Image J data analysis macros) for their support on the project.

I would like to acknowledge our funding sources for supporting our work: NSF IGERT (DGE 1144804) and STTR Grant (NSF IIP 1521294), as well as the Trachea grant (1R01EB023907-01).

I would also like to thank our several wonderful undergraduate researchers and volunteers, Paige Waligora, Jillian Schilp, Vincent Tanguilig, Michelle Philpot, Quillyn Smith, Kevin D'Augustine, and many more! A special thank you to Amanda Rickards, our REU student, for her help in completing the HA-dosage studies. And, a special thank you to our MQP team, Allison Mills and Hanna Gru Shiman, for their help in the Histogen project. It was a delight working with each of you, and I am honored to have mentored you during my time at WPI. I would also like to thank Jyotsna Patel, Victoria Huntress, Daryl Johnson, and Eric Sabacinski for their core support in the program.

To the amazing lifetime friends that I have made at WPI, you were my family away from home, and I am forever grateful to have you in my life. I truly thank you for all the emotional support, encouragement, advice, and laughs that we have shared in this roller coaster of a PhD journey: Lindsay Lozeau, Todd Alexander, Daniel Lawler, Hannah Strobel, Anne-Marie Bryant. A special thank you to my lab mates, especially Jonian Grosha, for always having a smile on, and being a delight to work with.

To my family, I cannot thank you enough for your love, patience, support, and guidance throughout these years, especially during the difficult past couple of months. I would not have accomplished everything I have if you were not there believing in me, and cheering me on.

Abstract

Cell-derived (CDM) matrix scaffolds provide a 3-dimensional (3D) matrix material that recapitulates a native, human extracellular matrix (ECM) microenvironment. CDMs are a heterogeneous source of ECM proteins with a composition dependent on the cell source and its phenotype. CDMs have several applications, such as for development of cell culture substrates to study stromal cell propagation and differentiation, as well as cell or drug delivery vehicles, or for regenerative biomaterial applications. Although CDMs are versatile and exhibit advantageous structure and activity, their use has been hindered due to the prolonged culture time required for ECM deposition and maturation *in vitro*. Macromolecular crowding (MMC) has been shown to increase ECM deposition and organization by limiting the diffusion of ECM precursor proteins and allowing the accumulation of matrix at the cell layer. A commonly used crowder that has been shown to increase ECM deposition *in vitro* is Ficoll, and was used in this study as a positive control to assess matrix deposition. Hyaluronic acid (HA), a natural crowding macromolecule expressed at high levels during fetal development, has been shown to play a role in ECM production, organization, and assembly *in vivo*. HA has not been investigated as a crowding molecule for matrix deposition or development of CDMs *in vitro*.

This dissertation focused on 2 aims supporting the development of a functional, human dermal fibroblast-derived ECM material for the delivery deliver an antimicrobial peptide, cCBD-LL37, and for potentially promoting a pro-angiogenic environment. The goal of this thesis was to evaluate the effects of high molecular weight (HMW) HA as a macromolecular crowding agent on *in vitro* deposition of ECM proteins important for tissue regeneration and angiogenesis. A pilot proteomics study supported the use of HA as a crowder, as it preliminarily showed increases in ECM proteins and increased retention of ECM precursor proteins at the cell layer; thus supporting the use of HA as a crowder molecule. In the presence of HA, human dermal fibroblasts demonstrated an increase in ECM deposition comparable to the effects of Ficoll 70/400 at day 3 using Raman microspectroscopy. It was hypothesized that HA promotes matrix deposition through changes on ECM gene expression. However, qRT-PCR results indicate that HA and Ficoll 70/400 did not have a direct effect on collagen gene expression, but differences in matrix crosslinking and proteinase genes were observed. Decellularized CDMs were then used to assess CDM stiffness and endothelial sprouting, which indicated differences in structural organization of collagen, and preliminarily suggests that there are differences in endothelial cell migration depending on the crowder agent used in culture. Finally, the collagen retained in the decellularized CDM matrix prepared under MMC supported the binding of cCBD-LL37 with retention of antimicrobial activity when tested against E.*coli*. Overall, the differences in matrix deposition profiles in HA versus Ficoll crowded cultures may be attributed to crowder molecule-mediated differences in matrix crosslinking, turnover, and organization as indicated by differences in collagen deposition, matrix metalloproteinase expression, and matrix stiffness.

MMC is a valuable tool for increasing matrix deposition, and can be combined with other techniques, such as low oxygen and bioreactor cultures, to promote development of a biomanufactured CDM-ECM biomaterial. Successful development of scalable CDM materials that stimulate angiogenesis and support antimicrobial peptide delivery would fill an important unmet need in the treatment of non-healing, chronic, infected wounds.

Table of Abbreviations

AFM	Atomic force microscopy
AMP	Antimicrobial peptide
ANOVA	Analysis of Variance
BSA	Bovine serum albumin
CDM	Cell-derived matrix / Cell-derived matrices/ Cell-derived materials
CS	Chondroitin sulfate
DAPI	4′,6-diamidino-2-phenylindole
DMEM	Dulbecco modified eagle medium
ECM	Extracellular matrix
ECs	Endothelial cells
FGF	Fibroblast growth factor
FBS	Fetal bovine serum
GAG	Glycosaminoglycans
HA	Hyaluronic acid
hECM	human ECM (cell-derived; provided by Histogen, Inc.)
HS	Heparan sulfate
LCMS	Liquid chromatography/ mass spectrometry
LOX	Lysyl oxidase
MIC	Minimum inhibitory concentration
MMC	Macromolecular crowding
MMP	matrix metalloproteinase
MS	Mass spectrometry
MSC	Mesenchymal stem/stromal cells
PCOLCE	procollagen C-endopeptidase enhancer
PDGF	Platelet-derived growth factor
PG	Proteoglycan
PLOD	Procollagen-lysine,2-oxoglutarate 5-dioxygenase 1
TIMP	Tissue inhibitor of metalloproteinase
TGF	Transforming-growth factor
TGM	Transglutaminase

Table of Figures

Table of Tables

Previous Publications

Shendi, D., Marzi, J., Linthicum, W., Rickards, A.J., Dolivo, D.M., Keller, S., Kauss, M.A.,Wen, Q., McDevitt, T.C., Dominko, T., Schenke-Layland, K., Rolle, M.W. (2019). Hyaluronic acid as a macromolecular crowding agent for production of cell-derived matrices. *In revision: Acta Biomateriala*

Ding, I., Shendi, D. M., Rolle, M. W., & Peterson, A. M. (2017). Growth-factor-releasing polyelectrolyte multilayer films to control the cell culture environment. *Langmuir*, *34*(3), 1178-1189.

Shendi, D., Albrecht, D., Jain, A. (2017). Anti-F as conjugated hyaluronic acid microsphere gels for neural stem cell delivery. *Journal of Biomedical Materials Research Part A,* 105(2), 608-618.

Shendi, D., Dede, A., Yin, Y., Wang, C., Valmikinathan, C., Jain, A. (2016). Tunable, bioactive protein conjugated hyaluronic acid hydrogel for neural engineering applications. *Journal of Materials Chemistry B,* 4(16), 2803-2818.

Accelerate WPI

In the Fall of 2016, my advisor, Marsha Rolle, and I participated in Accelerate WPI, which was an 8-week program offered by the WPI Office of Technology Commercialization in collaboration with the Foisie School of Business, and modeled after the NSF iCorps programs. Accelerate WPI provided coaching and training on customer discovery, to evaluate commercialization strategy of our proposed product, a regenerative, antimicrobial dressing for chronic wound healing.

A significant portion of this program focused on customer discovery and being able to match your value proposition to the identified customer segments. In this program, we completed over 30 interviews with people of various backgrounds, from clinicians to VPs of biotechnology companies, to regulatory individuals.

From the interviews, we learned a lot of key information. Speaking to wound care nurses and physicians we learned that the reason why there are so many wound products on the market is that one has not yet been developed that addresses all aspects of wound healing, specifically the problem of impaired blood flow. Wounds have a delayed healing response because dressings currently available in the market do not address vascularization in clinical studies, and thus research efforts need to focus on this aspect of wound repair. This take home message inspired formulation of the endothelial sprouting experiments described in Appendix B, which are focused on assessing capillary network formation as a quantifiable outcome for angiogenesis.

Accelerate WPI was an excellent opportunity to develop the mindset for applying research to develop a product with clinical translation potential. It provided guidance on how to engage with prospective stakeholders and knowledge of how products are used in a clinical setting, as well as the limitations that need to be addressed.

Abstract

Cell-derived matrix (CDM) scaffolds provide a 3-dimensional (3D) matrix material that recapitulates a native, human extracellular matrix (ECM) microenvironment. CDMs are a heterogeneous source of ECM proteins with a composition dependent on the cell source and phenotype. CDMs have several applications, such as for development of cell culture substrates to study stromal cell propagation and differentiation, as well as cell or drug delivery vehicles for regenerative biomaterial applications. Although CDMs are versatile and exhibit advantageous structure and activity, their use has been hindered due to the prolonged culture time required for ECM deposition and maturation *in vitro*. Macromolecular crowding (MMC) has been shown to increase ECM deposition and organization by limiting the diffusion of ECM precursor proteins and allowing the accumulation of matrix at the cell layer. A commonly used crowder that has been shown to increase ECM deposition *in vitro* is Ficoll, and was used in this study as a positive control. Hyaluronic acid (HA), a natural crowding macromolecule expressed at high levels during fetal development, has been shown to play a role in ECM production, organization, and assembly *in vivo*. HA has not been investigated as a crowding molecule for matrix deposition or development of CDMs *in vitro*.

This dissertation focused on two aims supporting the development of a functional, human dermal fibroblast-derived ECM material to deliver an antimicrobial peptide, cCBD-LL37, and for potentially promoting a pro-angiogenic environment. The goal of this thesis was to evaluate the effects of high molecular weight (HMW) HA as a macromolecular crowding agent on *in vitro* deposition of ECM proteins important for tissue regeneration and angiogenesis. A pilot proteomics study supported the use of HA as a crowder, as it preliminarily showed increases in ECM proteins and increased retention of ECM precursor proteins at the cell layer; thus supporting the use of HA as a crowder molecule. In the presence of HA, human dermal fibroblasts demonstrated an increase in ECM deposition comparable to the effects of Ficoll 70/400 after 3 days in culture, although increases were not statistically significant. Furthermore, Sircol and hydroxyproline assays indicated that Ficoll 70/400-treated cultures had significantly lower collagen production compared to HA and untreated, which was also qualitatively supported by the SDS-PAGE. HA and Ficoll 70/400 did not have a direct effect on collagen gene expression, but differences in matrix crosslinking and proteinase genes were observed. Decellularized CDMs were then used to assess CDM stiffness and endothelial sprouting, which indicated differences in structural organization of collagen, and preliminarily suggests that there are differences in endothelial cell migration depending on the crowder agent used in culture. Finally, the collagen retained in the decellularized CDM matrix prepared under MMC supported the binding of cCBD-LL37 with retention of antimicrobial activity when tested against E.*coli*. Overall, the differences in matrix deposition profiles in HA versus Ficoll crowded cultures may be attributed to crowder molecule-mediated differences in matrix crosslinking, turnover, and organization as indicated by differences in collagen deposition, matrix metalloproteinase expression, and matrix stiffness.

MMC may be a valuable tool for increasing matrix deposition, and can be combined with other techniques, such as low oxygen and bioreactor cultures, to promote development of a biomanufactured CDM-ECM biomaterial. Successful development of scalable CDM materials that stimulate angiogenesis and support antimicrobial peptide delivery would fill an important unmet need in the treatment of non-healing, chronic, infected wounds.

Chapter 1 : Overview

1.1. Introduction

In the United States alone, there is a total of 130 million cases of skin wounds caused by injury or disease [1-4]. Skin wounds can occur due to surgical incisions, lacerations, trauma, burns, and various types of ulcers such as pressure, venous, and diabetic foot ulcers. Chronic wounds affect approximately 6.5 million patients [5] in the United States with an estimated annual healthcare cost of $24 billion [5]. Furthermore, chronic wounds are characterized by high recurrence rates; 23-40% for pressure ulcers [6], 30-78% for venous ulcers [7], and 40-65% for diabetic foot ulcers [8].

The failure to undergo a reparative wound healing process has been attributed to defective composition and remodeling of the extracellular matrix (ECM) at the wound site [9]. As a result of the altered ECM structure, as well as the delayed epithelialization, impaired angiogenesis, and prolonged inflammatory state, chronic wounds have a higher chance of becoming infected [10]. Wound infections nearly double the cost of treating chronic wounds [11-13]. In order to reduce the likelihood of infection, principal goals in wound management focus on promoting epithelization and restoring the protective barrier at the wound bed [9].

Current treatment strategies for chronic wounds involve the use of autologous skin grafts [14], engineered natural polymer ECM scaffolds [15], or natural biologic ECM based scaffolds [16, 17]. These products are rich in ECM proteins, and provide signaling molecules to promote cell migration. While these approaches have been successful in promoting wound closure and epithelialization of the wound bed, the wound is subject to dehiscence and recurrence as proper tissue regeneration generally does not occur [15]. Impaired blood flow to the wound site is another factor that is also implicated in the delayed healing response [18, 19], however many

treatment strategies do not address angiogenesis. The delay in wound closure increases the likelihood of infection [10], which requires additional treatment strategies.

ECM-based products have also been used for the delivery of antimicrobial agents, such as silver, to treat chronic infected wounds. While these products have been shown to effectively treat infection, there have been reports of silver induced cytotoxicity [20, 21] as well as adverse effects on other important aspects of wound healing, such as angiogenesis [22, 23]. Antimicrobial peptides (AMPs), specifically LL37, have been shown to induce fibroblast proliferation [24], neutralize inflammatory mediators [25], and inhibit endothelial cell apoptosis [26], thus suggesting a role in reduction of inflammation and promotion of healing and angiogenesis. *In vivo* studies involving LL37 have also shown improved wound healing in diabetic mouse models by increasing re-epithelialization rate and granulation tissue formation [27]. While AMPs have several advantages, challenges associated with their cytotoxicity at higher doses, poor *in vivo* stability, and high costs of production have hindered their commercial application in wound healing [28]. To address this challenge, LL37 can be modified with a collagenase (cCBD) or fibronectin –derived collagen binding domain (fCBD). CBD modified LL37 has been successfully shown to bind to commercially available collagen scaffolds [29] and provide an anti-infective therapy through reduction of bioburden [29, 30] .

Decellularized, xenogeneic ECM based products have been shown to promote wound closure, and deliver antimicrobials, such as silver, to treat an infection [31-33]. Despite their success, these products also have their limitations. Xenogeneic derived ECM products present limitations in donor tissue availability as well as variability in composition/structure between different donors. Thus, there is a need to develop a product that not only promotes healing

through matrix regeneration and vascularization, but also inhibit or treat infection without adverse cytotoxicity.

Cell derived matrices (CDMs) are currently being investigated as alternative biomaterials for tissue repair, and other applications, such as surface substrates for stromal cell propagation [34] and differentiation [35-39]. CDMs have several advantages in that they can be human derived, are non-immunogenic, can be customized depending on cell source and culture conditions, and contain ECM structures and growth factors important for tissue repair and angiogenesis. However, commercialization of CDMs is hindered due to the prolonged culture time, often on the order of several weeks to months, required for ECM deposition [40]. Recent publications have shown that modification of cell culture conditions, such as using chemically-defined media [41] and low oxygen [42-44], can help promote increased matrix production and deposition *in vitro*. Macromolecular crowding (MMC), which involves the addition of macromolecules to the cell culture media, is a biophysical phenomenon that promotes sequestration of ECM precursor proteins and the accumulation of matrix at the cell layer [45-49]. The addition of macromolecules to the media creates what is known as an excluded volume effect. The excluded volume effect, or the volume occupied by different macromolecules in the media, is represented by: 1) the space occupied by the added macromolecules themselves, and 2) the space created due to steric and electrostatic repulsions between the macromolecules [50]. Viscosity has also been shown to play a contributing role to the effects of crowding [51, 52].

Several synthetic, inert polymers with different molecular weights, charges, and radii have been used as macromolecular crowders, including Ficoll [46, 49, 53-55], carrageenan [42], dextran sulfate (DxS) [47, 48], and polyvinylpyrrolidone (PVP) [56]. Hyaluronic acid (HA) also shares many properties with crowders reported in literature, and has been shown to play a role in

collagen assembly and organization in acellular systems [57]. However, it has not been reported as a crowder in cell-based systems for driving ECM deposition and assembly, or for the development of CDM scaffolds. Hyaluronic acid (HA), an *in vivo* crowder that is ubiquitously present during fetal development [58], and has been shown to be involved in matrix production [59-62] and promotion of angiogenesis [59, 63]. Therefore, we hypothesized that adding HA to cell culture medium as a macromolecular crowder can ultimately increase matrix production compared to a untreated control, while also providing a CDM that can be tailored for collagen content and crosslinks, mechanical properties, and matrix distribution. Furthermore, we hypothesized that a modified AMP with a collagen binding domain (CBD), cCBD-LL37, can adsorb to human-derived CDMs and maintain their antimicrobial activity against bacteria.

1.2. Specific Aims

The overall goal of the work presented in this document is to develop and characterize a tunable, cell-derived matrix biomaterial that can promote wound closure and angiogenesis. This approach may ultimately create a human, cell-derived material that promotes tissue regeneration and angiogenesis, while also acting as a vehicle for delivery of exogenous therapeutic agents to the wound site, such as antimicrobial peptides. To achieve this goal, we proposed the following aims:

1.2.1. Aim 1: Investigate the effects of hyaluronic acid (HA) as a macromolecular crowding agent on ECM gene expression, protein deposition, structure, and organization in human fibroblast cultures

In this aim, we investigated the effects of high molecular weight hyaluronic acid (HA) in culture as a MMC agent for development of cell-derived matrix (CDM) scaffolds **(Figure 1-1)**.

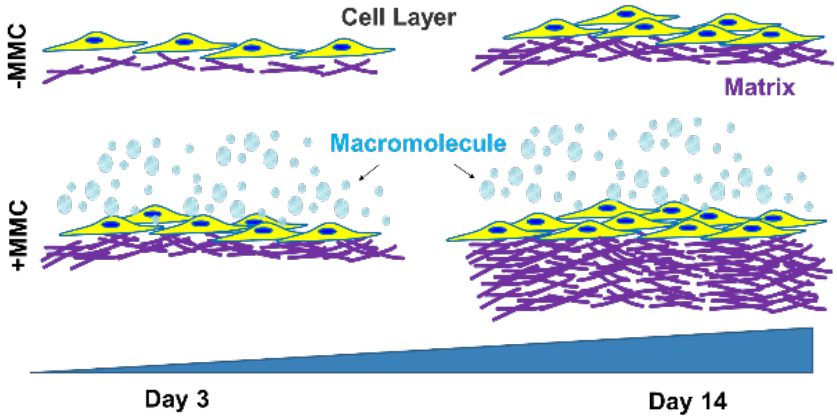

Figure 1-1: Aim 1 Overview: Effects of HA crowding. Schematic illustrating matrix deposition under macromolecular crowding

We characterized ECM deposition and composition using two different HA concentrations, 0.05% and 0.5%. Ficoll 70/400 has been well established in literature as a macromolecular crowder for increased matrix production, and was used as a positive control [46, 53-55]. Non-treated fibroblast cultures served as a negative control (0% HA). It was shown that ECM production with HA treatment is increased compared to a non-treated controls. Furthermore, HA had comparable effects on matrix deposition and composition compared to Ficoll 70/400, thus supporting the use of HA as a crowder molecule. Ficoll 70/400 treatment also increased cell number over time, indicating that the increased matrix may be due to increased cell number or the maintenance of cells in a proliferative state. There were no differences in cell number with HA treatment, indicating that increased matrix may be due to increased cell matrix production. Assessment of gene expression showed no changes in collagen gene expression between all crowded cultures, however, significant differences were observed in expression of crosslinking enzymes and matrix metalloproteinases.

In order to use the CDM as a potential biomaterial source, and characterize ECM structure and organization, it is important to remove the cellular components. The decellularization protocol selected must remove dsDNA content without altering matrix structure and composition [64]. A hyperosmotic decellularization strategy combined with endonuclease treatment was used to avoid use of harmful detergents and surfactants that would alter matrix properties [65]. After decellularization, approximately 95% of DNA was removed from the CDMs, supporting the efficacy of the process. ECM retention post-decellularization was maintained. The decellularized CDM developed under HA and Ficoll 70/400 crowding and non-treated controls was used to assess stiffness using atomic force microscopy (AFM). CDM stiffness was dependent on the macromolecule and concentration used, as a decrease in stiffness was seen under the 0.5% and Ficoll 70/400 crowders. Preliminary results were also obtained to assess endothelial cell migration as a function of sprouting. Capillary sprouting was assessed using a Cytodex bead assay [66] with human umbilical vein endothelial cells cultured on the CDMs.

1.2.2. Aim 2: Investigate the use of a CDM material for the delivery of antimicrobial peptide, cCBD-LL37.

In this aim, we assessed the feasibility of using human cell-derived ECM as a delivery vehicle for antimicrobial agents.

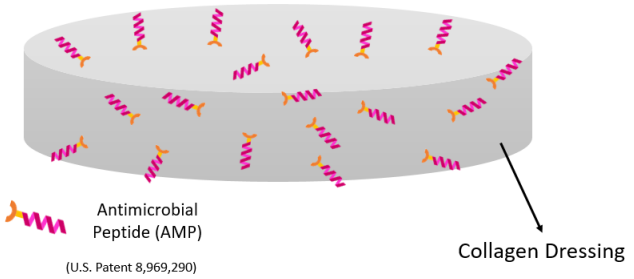

Figure 1-2: Aim 2 Overview: Antimicrobial peptide loaded scaffolds. Cell-derived ECM material loaded with cCBD-LL37 for developed of antimicrobial scaffolds for infected chronic wounds.

In this first part of the aim, we evaluated the efficacy of loading an antimicrobial peptide, cCBD-LL37, into CDMs developed under

MMC culture conditions. The peptide (300 μM) was incubated with CDMs to allow binding to collagen molecules. While microbial killing was not at the level of sterility controls in any conditions, Ficoll 70/400 MMC CDMs appeared to have the highest colony counts. CDMs developed under MMC were only studied as a preliminary approach for peptide binding and antimicrobial activity onto cell-derived materials. However, in order to use this as a biomaterial, a thicker scaffold with higher collagen content is needed. Biomanufactured CDMs from a microcarrier bioreactor culture provided by Histogen, Inc. were used to develop scaffolds for peptide loading. Peptide-loaded ECM slurry (0 μM, 75 μM, 150 μM, 300 μM) retained peptide post lyophilization. The peptide loaded scaffolds were then inoculated with bacteria to assess antimicrobial activity by measuring the turbidity of the media using a plate reader. A decrease in turbidity indicates reduction in bacterial colonies, and thus antimicrobial activity. The antimicrobial activity of the ECM was assessed using turbidity assays. Control and peptide-loaded ECM disks were inoculated with bacteria (*E. coli)*, and microbial activity was assessed using colony count assays. Scaffolds loaded with peptide at a concentration of 75uM and 300uM prevented *E. coli* growth on agar plates.

1.3. Summary

In this thesis, we will discuss commercially available ECM based products for wound treatment as well as their limitations, and discuss cell-derived ECM production as a potential alternative approach to create scaffold matrices. We will specifically focus on changing the cell culture environment by using macromolecular crowding to increase matrix production and deposition. The next chapters will discuss the experimental design and methodology of each aim, and present the results and data analysis related to characterization and development of the ECM

material. The use of macromolecular crowding can be used as a tool to study matrix production and deposition for the development of tailored functional cell-derived matrices.

1.4. References

[1] P. Drisoll, Wound Prevalence and Wound Management, 2012-2020, Mediligence, 2013.
[2] S. King, Burn Statistics, 2017. (Accessed January 2017).
[3] M.D. Peck, Epidemiology of burns throughout the World. Part II: intentional burns in adults, Burns 38(5) (2012) 630-637.
[4] R.K. Sethi, E.D. Kozin, P.J. Fagenholz, D.J. Lee, M.G. Shrime, S.T. Gray, Epidemiological survey of head and neck injuries and trauma in the United States, Otolaryngology--Head and Neck Surgery 151(5) (2014) 776-784.
[5] C.K. Sen, G.M. Gordillo, S. Roy, R. Kirsner, L. Lambert, T.K. Hunt, F. Gottrup, G.C. Gurtner, M.T. Longaker, Human skin wounds: a major and snowballing threat to public health and the economy, Wound Repair and Regeneration 17(6) (2009) 763-771.
[6] M. Kuwahara, H. Tada, K. Mashiba, S. Yurugi, H. Iioka, K. Niitsuma, Y. Yasuda, Mortality and recurrence rate after pressure ulcer operation for elderly long-term bedridden patients, Annals of plastic surgery 54(6) (2005) 629-632.
[7] L.P.F. Abbade, S. Lastória, Venous ulcer: epidemiology, physiopathology, diagnosis and treatment, International journal of dermatology 44(6) (2005) 449-456.
[8] D.G. Armstrong, A.J. Boulton, S.A. Bus, Diabetic foot ulcers and their recurrence, New England Journal of Medicine 376(24) (2017) 2367-2375.
[9] D.J. Leaper, G. Schultz, K. Carville, J. Fletcher, T. Swanson, R. Drake, Extending the TIME concept: what have we learned in the past 10 years?, International wound journal 9(s2) (2012) 1-19.
[10] R.L. Lammers, D.L. Hudson, M.E. Seaman, Prediction of traumatic wound infection with a neural network-derived decision model, The American journal of emergency medicine 21(1) (2003) 1-7.
[11] J.F. Guest, G.W. Fuller, P. Vowden, Costs and outcomes in evaluating management of unhealed surgical wounds in the community in clinical practice in the UK: a cohort study, BMJ open 8(12) (2018) e022591.
[12] P. Bowler, B. Duerden, D.G. Armstrong, Wound microbiology and associated approaches to wound management, Clinical microbiology reviews 14(2) (2001) 244-269.
[13] P.G. Bowler, B.J. Davies, The microbiology of infected and noninfected leg ulcers, International journal of dermatology 38(8) (1999) 573-578.
[14] J. Tam, Y. Wang, W.A. Farinelli, J. Jiménez-Lozano, W. Franco, F.H. Sakamoto, E.J. Cheung, M. Purschke, A.G. Doukas, R.R. Anderson, Fractional skin harvesting: autologous skin grafting without donor-site morbidity, Plastic and Reconstructive Surgery Global Open 1(6) (2013).
[15] L.E. Dickinson, S. Gerecht, Engineered biopolymeric scaffolds for chronic wound healing, Frontiers in physiology 7 (2016).
[16] B. Cullen, R. Smith, E. Mcculloch, D. Silcock, L. Morrison, Mechanism of action of PROMOGRAN, a protease modulating matrix, for the treatment of diabetic foot ulcers, Wound Repair and Regeneration 10(1) (2002) 16-25.
[17] D. Ulrich, R. Smeets, F. Unglaub, M. Wöltje, N. Pallua, Effect of oxidized regenerated cellulose/collagen matrix on proteases in wound exudate of patients with diabetic foot ulcers, Journal of Wound Ostomy & Continence Nursing 38(5) (2011) 522-528.
[18] S.a. Guo, L.A. DiPietro, Factors affecting wound healing, Journal of dental research 89(3) (2010) 219-229.
[19] H. Sinno, S. Prakash, Complements and the wound healing cascade: an updated review, Plastic surgery international 2013 (2013).
[20] S.B. Zou, W.Y. Yoon, S.K. Han, S.H. Jeong, Z.J. Cui, W.K. Kim, Cytotoxicity of silver dressings on diabetic fibroblasts, International wound journal 10(3) (2013) 306-312.

[21] A. Burd, C.H. Kwok, S.C. Hung, H.S. Chan, H. Gu, W.K. Lam, L. Huang, A comparative study of the cytotoxicity of silver-based dressings in monolayer cell, tissue explant, and animal models, Wound repair and regeneration 15(1) (2007) 94-104.
[22] S. Li, N. Ye, Y. Qi, G. Liang, Z. Xiao, Po03. Pathways affected by Fe2o3 nanoparticles with microrna expression profiling, Acta Biochim Biophys Sin 42(20100600) (2010) i19-i66.
[23] S. Sheikpranbabu, K. Kalishwaralal, D. Venkataraman, S.H. Eom, J. Park, S. Gurunathan, Silver nanoparticles inhibit VEGF-and IL-1β-induced vascular permeability via Src dependent pathway in porcine retinal endothelial cells, Journal of nanobiotechnology 7(1) (2009) 8.
[24] L. Tomasinsig, C. Pizzirani, B. Skerlavaj, P. Pellegatti, S. Gulinelli, A. Tossi, F. Di Virgilio, M. Zanetti, The human cathelicidin LL-37 modulates the activities of the P2X7 receptor in a structure-dependent manner, Journal of Biological Chemistry 283(45) (2008) 30471-30481.
[25] I. Nagaoka, S. Hirota, F. Niyonsaba, M. Hirata, Y. Adachi, H. Tamura, S. Tanaka, D. Heumann, Augmentation of the lipopolysaccharide-neutralizing activities of human cathelicidin CAP18/LL-37-derived antimicrobial peptides by replacement with hydrophobic and cationic amino acid residues, Clin. Diagn. Lab. Immunol. 9(5) (2002) 972-982.
[26] K. Suzuki, T. Murakami, K. Kuwahara-Arai, H. Tamura, K. Hiramatsu, I. Nagaoka, Human anti-microbial cathelicidin peptide LL-37 suppresses the LPS-induced apoptosis of endothelial cells, International immunology 23(3) (2011) 185-193.
[27] M. Carretero, M.J. Escamez, M. Garcia, B. Duarte, A. Holguín, L. Retamosa, J.L. Jorcano, M. Del Río, F. Larcher, In vitro and in vivo wound healing-promoting activities of human cathelicidin LL-37, Journal of Investigative Dermatology 128(1) (2008) 223-236.
[28] R. Eckert, Road to clinical efficacy: challenges and novel strategies for antimicrobial peptide development, Future microbiology 6(6) (2011) 635-651.
[29] L.D. Lozeau, J. Grosha, D. Kole, F. Prifti, T. Dominko, T.A. Camesano, M.W. Rolle, Collagen tethering of synthetic human antimicrobial peptides cathelicidin LL37 and its effects on antimicrobial activity and cytotoxicity, Acta biomaterialia 52 (2017) 9-20.
[30] R.E. Hancock, H.-G. Sahl, Antimicrobial and host-defense peptides as new anti-infective therapeutic strategies, Nature biotechnology 24(12) (2006) 1551.
[31] E.P. Brennan, J. Reing, D. Chew, J.M. Myers-Irvin, E. Young, S.F. Badylak, Antibacterial activity within degradation products of biological scaffolds composed of extracellular matrix, Tissue engineering 12(10) (2006) 2949-2955.
[32] N.J. Turner, S.F. Badylak, The use of biologic scaffolds in the treatment of chronic nonhealing wounds, Advances in wound care 4(8) (2015) 490-500.
[33] A.D. Metcalfe, M.W. Ferguson, Tissue engineering of replacement skin: the crossroads of biomaterials, wound healing, embryonic development, stem cells and regeneration, Journal of the Royal Society Interface 4(14) (2006) 413-437.
[34] Y. Peng, M.T. Bocker, J. Holm, W.S. Toh, C.S. Hughes, F. Kidwai, G.A. Lajoie, T. Cao, F. Lyko, M. Raghunath, Human fibroblast matrices bio-assembled under macromolecular crowding support stable propagation of human embryonic stem cells, Journal of tissue engineering and regenerative medicine 6(10) (2012) e74-e86.
[35] H. Ragelle, A. Naba, B.L. Larson, F. Zhou, M. Prijić, C.A. Whittaker, A. Del Rosario, R. Langer, R.O. Hynes, D.G. Anderson, Comprehensive proteomic characterization of stem cell-derived extracellular matrices, Biomaterials 128 (2017) 147-159.
[36] S. Sart, T. Ma, Y. Li, Extracellular matrices decellularized from embryonic stem cells maintained their structure and signaling specificity, Tissue Engineering Part A 20(1-2) (2013) 54-66.
[37] M.L. Decaris, B.Y. Binder, M.A. Soicher, A. Bhat, J.K. Leach, Cell-derived matrix coatings for polymeric scaffolds, Tissue engineering Part A 18(19-20) (2012) 2148-2157.
[38] G. Tour, M. Wendel, I. Tcacencu, Cell-derived matrix enhances osteogenic properties of hydroxyapatite, Tissue Engineering Part A 17(1-2) (2010) 127-137.

[39] Y. Mao, T. Block, A. Singh-Varma, A. Sheldrake, R. Leeth, S. Griffey, J. Kohn, Extracellular matrix derived from chondrocytes promotes rapid expansion of human primary chondrocytes in vitro with reduced dedifferentiation, Acta biomaterialia 85 (2019) 75-83.
[40] M. Peck, D. Gebhart, N. Dusserre, T.N. McAllister, N. L'Heureux, The evolution of vascular tissue engineering and current state of the art, Cells Tissues Organs 195(1-2) (2012) 144-158.
[41] J.-E.W. Ahlfors, K.L. Billiar, Biomechanical and biochemical characteristics of a human fibroblast-produced and remodeled matrix, Biomaterials 28(13) (2007) 2183-2191.
[42] D. Cigognini, D. Gaspar, P. Kumar, A. Satyam, S. Alagesan, C. Sanz-Nogués, M. Griffin, T. O'Brien, A. Pandit, D.I. Zeugolis, Macromolecular crowding meets oxygen tension in human mesenchymal stem cell culture-A step closer to physiologically relevant in vitro organogenesis, Scientific Reports 6 (2016) 30746.
[43] R.S. Kellar, M. Hubka, L.A. Rheins, G. Fisher, G.K. Naughton, Hypoxic conditioned culture medium from fibroblasts grown under embryonic-like conditions supports healing following post-laser resurfacing, Journal of cosmetic dermatology 8(3) (2009) 190-196.
[44] Y. Zhou, M. Zimber, H. Yuan, G.K. Naughton, R. Fernan, W.-J. Li, Effects of human fibroblast-derived extracellular matrix on mesenchymal stem cells, Stem Cell Reviews and Reports 12(5) (2016) 560-572.
[45] R. Clark, P. Henson, The molecular and cellular biology of wound repair. Plenum Press, New York (1996).
[46] P. Kumar, A. Satyam, X. Fan, E. Collin, Y. Rochev, B.J. Rodriguez, A. Gorelov, S. Dillon, L. Joshi, M. Raghunath, Macromolecularly crowded in vitro microenvironments accelerate the production of extracellular matrix-rich supramolecular assemblies, Scientific reports 5 (2015) 8729.
[47] R.R. Lareu, K.H. Subramhanya, Y. Peng, P. Benny, C. Chen, Z. Wang, R. Rajagopalan, M. Raghunath, Collagen matrix deposition is dramatically enhanced in vitro when crowded with charged macromolecules: the biological relevance of the excluded volume effect, FEBS letters 581(14) (2007) 2709-2714.
[48] A. Satyam, P. Kumar, X. Fan, A. Gorelov, Y. Rochev, L. Joshi, H. Peinado, D. Lyden, B. Thomas, B. Rodriguez, M. Raghunath, A. Pandit, D. Zeugolis, Macromolecular crowding meets tissue engineering by self-assembly: A paradigm shift in regenerative medicine, Advanced Materials 26(19) (2014) 3024-3034.
[49] A.S. Zeiger, F.C. Loe, R. Li, M. Raghunath, K.J. Van Vliet, Macromolecular crowding directs extracellular matrix organization and mesenchymal stem cell behavior, PloS one 7(5) (2012) e37904.
[50] R.J. Ellis, Macromolecular crowding: obvious but underappreciated, Trends in biochemical sciences 26(10) (2001) 597-604.
[51] A. Christiansen, Q. Wang, M.S. Cheung, P. Wittung-Stafshede, Effects of macromolecular crowding agents on protein folding in vitro and in silico, Biophysical reviews 5(2) (2013) 137-145.
[52] I. Kuznetsova, B. Zaslavsky, L. Breydo, K. Turoverov, V. Uversky, Beyond the excluded volume effects: mechanistic complexity of the crowded milieu, Molecules 20(1) (2015) 1377-1409.
[53] P. Benny, C. Badowski, E.B. Lane, M. Raghunath, Making more matrix: enhancing the deposition of dermal–epidermal junction components in vitro and accelerating organotypic skin culture development, using macromolecular crowding, Tissue Engineering Part A 21(1-2) (2014) 183-192.
[54] M. Patrikoski, M.H.C. Lee, L. Mäkinen, X.M. Ang, B. Mannerström, M. Raghunath, S. Miettinen, Effects of Macromolecular Crowding on Human Adipose Stem Cell Culture in Fetal Bovine Serum, Human Serum, and Defined Xeno-Free/Serum-Free Conditions, Stem cells international 2017 (2017) 6909163.
[55] M.C. Prewitz, A. Stißel, J. Friedrichs, N. Träber, S. Vogler, M. Bornhäuser, C. Werner, Extracellular matrix deposition of bone marrow stroma enhanced by macromolecular crowding, Biomaterials 73 (2015) 60-69.
[56] R. Rashid, N.S.J. Lim, S.M.L. Chee, S.N. Png, T. Wohland, M. Raghunath, Novel use for polyvinylpyrrolidone as a macromolecular crowder for enhanced extracellular matrix deposition and cell proliferation, Tissue Engineering Part C: Methods 20(12) (2014) 994-1002.

[57] N. Saeidi, K.P. Karmelek, J.A. Paten, R. Zareian, E. DiMasi, J.W. Ruberti, Molecular crowding of collagen: a pathway to produce highly-organized collagenous structures, Biomaterials 33(30) (2012) 7366-7374.
[58] M.T. Longaker, E.S. Chiu, N.S. Adzick, M. Stern, M.R. Harrison, R. Stern, Studies in fetal wound healing. V. A prolonged presence of hyaluronic acid characterizes fetal wound fluid, Annals of surgery 213(4) (1991) 292.
[59] S.P. Evanko, J.C. Angello, T.N. Wight, Formation of hyaluronan-and versican-rich pericellular matrix is required for proliferation and migration of vascular smooth muscle cells, Arteriosclerosis, thrombosis, and vascular biology 19(4) (1999) 1004-1013.
[60] B. Nusgens, Hyaluronic acid and extracellular matrix: a primitive molecule?, Annales de dermatologie et de vénéréologie 137 Suppl 1 (2010) S3-8.
[61] C.B. Knudson, Hyaluronan and CD44: strategic players for cell–matrix interactions during chondrogenesis and matrix assembly, Birth Defects Research Part C: Embryo Today: Reviews 69(2) (2003) 174-196.
[62] C.B. Knudson, W. Knudson, Hyaluronan-binding proteins in development, tissue homeostasis, and disease, The FASEB Journal 7(13) (1993) 1233-1241.
[63] E.L. Pardue, S. Ibrahim, A. Ramamurthi, Role of hyaluronan in angiogenesis and its utility to angiogenic tissue engineering, Organogenesis 4(4) (2008) 203-214.
[64] P.M. Crapo, T.W. Gilbert, S.F. Badylak, An overview of tissue and whole organ decellularization processes, Biomaterials 32(12) (2011) 3233-3243.
[65] A.R. Gillies, L.R. Smith, R.L. Lieber, S. Varghese, Method for decellularizing skeletal muscle without detergents or proteolytic enzymes, Tissue engineering part C: Methods 17(4) (2010) 383-389.
[66] M.N. Nakatsu, C.C. Hughes, An optimized three-dimensional in vitro model for the analysis of angiogenesis, Methods in enzymology 443 (2008) 65-82.

Chapter 2 : Background

In this chapter, we discuss chronic wound development, associated treatment strategies, current limitations with treatment approaches, and alternatives for development of new treatment options. The chapter specifically focuses on the importance of the extracellular matrix components to the wound healing cascade, and how ECM components are supplements in ECM-like substrates that are commercially available for wound care. Macromolecular crowding is introduced as a strategy for the development of cell-derived matrices.

2.1. Skin and its Extracellular Matrix (ECM)

The skin is the largest organ in the body, and its primary function is to act as a protective barrier. Other functions for skin include, temperature and fluid balance regulation, reception of stimuli, and a reservoir for nutrient and water storage. Different cell populations reside in the skin, but it is primarily composed of keratinocytes and fibroblasts, and they are distributed within the epidermis and dermis, respectively. Fibroblasts are the most common connective tissues cells present in the body, and reside in the dermal layer of skin, where they are involved in the production of two main classes of extracellular matrix molecules: 1) glycosaminoglycans (GAGs), and 2) fibrous proteins, such as collagen, elastin, laminin, and fibronectin [1].

GAGs, which are present primarily in the forms of proteoglycans, or polysaccharides covalently linked to proteins, form the hydrated gel-like substance that embeds the fibrous proteins. Fibrous proteins, such as collagen and elastin, play a major role in establishing the structural integrity and architecture of the tissue. Other fibrous proteins, such as fibronectin and

laminin, have adhesive functions; they allow epithelial cells to adhere to the underlying matrix, and form the epidermis, or the protective barrier.

The extracellular matrix components interact with neighboring cells and serve two major functions: 1) provide structural support for cellular populations, thus providing mechanical properties for tissues [2, 3], 2) are a reservoir for bioactive molecules, thus acting as signaling molecule to support cellular activities [4, 5]. Each ECM component plays different roles to support the overall function of the native tissue, and thus tissues would have varying ECM compositions. The extracellular matrix composition of skin primarily consists of collagen, glycoproteins, and GAGs.

2.1.1. Collagens

Collagens are the most abundant proteins present in the body, and consists of 28 different types of collagen molecules. They are grouped together based on the presence of a triple helical structure; and their diversity is due to existence of different α-chains, supramolecular structures and molecular isoforms of the same collagen type, and alternative splicing and promoters [6]. At the primary structural level, the α-chains in the triple helical structure consists of glycine (Gly)-X-Y amino acid triplets, where –X and –Y amino acid residues are different ratios of proline and hydroxyproline amino acid residues [6]. This repeating amino acid sequence forms the collagenous domain, or triple helix motif [6], which is stabilized by the presence of these amino acid residues, hydrogen bonds, and electrostatic interaction between amino acids, lysine and aspartate [7]. The collagenous, helical domain is flanked by short non-helical N- and C-telopeptides at the N- and C- terminals, respectively [6].

The collagen family is divided into serval different classes based on their structural assembly, but the major classifications is based on fiber assembly. Fibrillar collagens consists of collagens types I, II, III, V, and VI; and are the major component of collagen fibers in the body [6]. Fibrillar collagens are structural proteins that provide strength and characterize matrix stiffness, while also providing cellular binding domains and matrix templates for non-collagenous ECM components, such as fibronectin and laminin. Collagen type I is the most abundant fibrillar collagen present in the body, and along with collagen type III is present in skin. Collagen type I is the primary collagen present in scar tissue after repair, and replaces the collagen type III tissue present in the granulation tissue formed during the healing process. Furthermore, within the collagen fiber networks, are supramolecular ECM macromolecules, such as the elastin protein and hyaluronic acid. Non-fibrillar collagens include collagen types IV, VIII, X [6]. Collagen type IV is a basal lamina and basement membrane collagen associated with tissues of epithelial elements, and plays a major role in promotion of angiogenesis [6]. The composition and distribution of non-collagenous ECM proteins and associated ECM macromolecules vary according to specific tissue function.

2.1.2. Collagen Biosynthesis

Fibroblasts secrete tropocollagen, which is a precursor to assembly of collagen aggregates [8]. Collagen synthesis occurs intracellularly, and formation of the triple helical structure is completed extracellularly. After export of collagen mRNA from the nucleus, translation of the sequence occurs in the cytoplasm of the cell. The signal sequence that is present on the N-terminal of the pre-procollagen (pre-pro peptide) is recognized by a signal recognition particle present on the endoplasmic reticulum (ER) [9, 10]. After the pre-pro

sequence enters the ER, it undergoes several post-translational modifications, which involves removal of the signal sequence present on the N-terminal, hydroxylation of the lysine and proline residues present on the propeptide, glycosylation of the lysine and hydroxylysine residues, and sulfation of tyrosine residues [11]. Heat shock protein 47 (HSP 47) also binds to procollagen and acts as a molecular chaperone for procollagen modification [12]. Prolyl-4-hydroxylase and lysyl hydroxylase (LOX) hydroxylate the proline and lysine residues, respectively; and as a result produces hydroxyproline and hydroxylysine residues on what is now referred to as the procollagen molecule (pro-peptide) [13]. The hydroxylation process is dependent on the presence of ascorbic acid, which is an important cofactor in the collagen biosynthesis process as it contributes hydroxyl groups to amino acid residues [14]. As human cells are unable to synthesize ascorbate, there is dependence on exogenous sources for supplementation. Hydroxylation is an important process for the formation of crosslinked alpha peptides, and the lack of hydroxylation causes a loose triple helical structure, as seen in tissue of vitamin C deficient patients. In cell culture, ascorbic acid is added at varying concentrations between 50 μM – 150 μM, where it is involved in the collagen stabilization process [14-16].

After formation of the hydroxylysine residues, glycosylation occurs, which involves addition of glucose or galactose monomers to the hydroxyl groups. The procollagen triple helix molecule is assembled from three hydroxylated and glycosylated alpha peptides, and sent to the golgi for post-translational modification [11]. Recent work suggests that prior to extracellular secretion, the intracellular Secreted Protein Acidic and Rich in Cysteine (SPARC) binds to the triple helical domain of procollagen thus allowing collagen deposition [17]. Formation of the tropocollagen molecule, also known as the collagen fibril, occurs in the presence of collagen peptidases, specifically N- and C-propeptides, to remove the loose end terminals of the

procollagen molecule [6]. The final step involved in the post-translational modification is mediated by lysyl oxidase to allow covalent bonding and crosslinking with other tropocollagen molecules to form the collagen fibril [11].

2.1.3. Laminins

Noncollagenous glycoproteins are also major constituents of the ECM microenvironment. Laminins are the most abundant ECM glycoproteins present in the basement membrane extracellular matrix [18, 19], and were first purified and characterized in the study of the Engelbreth-Hol-Swarm (EHS) mouse tumor model [20]. The laminins are heterotrimers assembled with 3 different subunits: α-chain, β-chain, γ-chain, with various subunit assemblies resulting in a family of 16 different laminin molecules [19, 21]. Laminin heterotrimers are assembled intracellularly where disulfide linked β-chain and γ-chain dimers assemble. The β- γ dimer remains in the cytoplasm until trimerization of the α-subunit, which is required for extracellular secretions [22].

As part of the basement membrane, laminins are involved in several processes such as angiogenesis [23], skin re-epithelialization, and wound healing [18] through their interaction with several functional domains, such as binding sites for cells [24] other glycoproteins, glycosaminoglycans, glycolipids, growth factors [18], and proteases , thus making them central to ECM structure and stability. Laminin deposition and incorporation into the ECM through these functional domains are still under investigation, but several regulating mechanisms have been proposed. Laminin deposition is cell type dependent though regulation of different cell receptors, such as integrins and syndecans, and it has been suggested that laminin deposition patterns vary depending on the laminin-matrix function and/or the stage of laminin deposition

[25]. For example, if laminin fibril formation occurs, as seen in epithelial cells [26] and fibroblasts, it is an indication that is involved in mechanosignal transmission. Alternatively, it has been proposed that laminin deposition is regulated through self- or co-polymerization of the short arms present in the different laminin isoforms. Laminin interacting proteins, such as nidogen, heparan sulfate proteoglycans, and collagen type VII have also been shown to interact with certain laminin domains to effect basement membrane formation and differences in laminin deposition patterns [27].

2.1.4. Fibronectin

Fibronectin is another important ECM glycoprotein present in plasma and tissue. It is a are dimer molecule consisting of two subunits joined by a disulfide bond [1]. Each subunit is organized into its own series of functional domains separated by polypeptide chains [1]. Fibronectin isoforms are produced due to alternative splicing of one large RNA molecule [1]. With the exception of one isoform, all cellular fibronectin forms are incorporated into the ECM due to dimerization of adjacent fibronectin molecules through disulfide bonds to form fibrils. Fibronectin has multiple binding sites allowing interaction with other extracellular substances such as collagen, fibrin, and heparin sulfate proteoglycans allowing it to link different ECM molecules. It also contains a cell binding domain consisting of three amino acids, Arginine-Glycine- Aspartane (RGD), that allows integrin receptors present in cell membranes to bind thus stimulating cellular pathways involved in cell adhesion, migration, and differentiation [28]. The main type of binding domain, the type III fibronectin repeat, is the most common domain present in vertebrates, and binds to integrins [1].

Organization of a fibrillar fibronectin network is primarily cell-mediated through interactions with integrin binding to the RGD cell binding domain [29]. The assembly of fibrils

is a crucial step for the incorporation of other ECM components, such as collagen and elastin [30], tenascin C [31], and latent TGF-β binding proteins [32] through binding domains. Fibronectin's involvement in important wound healing events, such as angiogenesis, is evident through *in vitro* blocking [33] and *in vivo* gene inactivation experiments [34]. Genetically modified mice unable to produce fibronectin during the embryogenesis stage had decreased endothelial cell ability to form blood vessels, thus highlighting the importance of cell interactions with a fibronectin rich matrix [34]. Furthermore, endothelial cells treated with FN blocking antibodies were unable to maintain spherical morphology and had altered migratory profiles, thus inhibiting tubulogenesis potential despite presence of a 3D fibrin matrix in culture [33]. This emphasizes the importance of fibronectin matrix incorporation for angiogenesis and vascularization.

2.1.5. Proteoglycans and Glycosaminoglycans

Glycosaminoglycans (GAGs) are hydrophilic, negatively charged, polysaccharide chains consisting of repeating disaccharide units. Due to the high density of negative charge present in GAGs, they have a high amount of water absorption. As a result, GAGs enable tissues to withstand compression forces. The main non-sulfated GAG present in the ECM is hyaluronic acid (HA). HA is heavily present during embryonic development, where it is creates a cell-free space for cells to migrate and allow for organ development [1]. It is also produced in large quantities during the wound healing process, where it mediates many healing responses. HA stimulates macrophage mediated cytokine production, and is involved in angiogenesis [28, 35]. Sulfated GAGs present in the ECM include chondroitin sulfate, heparan sulfate, keratan sulfate, and dermatan sulfate. Sulfated GAGs are primarily bounds to protein cores for formation of proteoglycans.

Proteoglycans, or glycosylated protein cores, are major ECM components with several different functions, and are characterized by their size and GAG chains. They are synthesized by cellular ribosomes and translocated to the rough endoplasmic reticulum for further processing. Glycosylation of the protein core occurs in the Golgi apparatus prior secretion to the ECM via secretory vesicles. Common proteoglycans include decorin, biglycan, perlecan, and fibromodulin. Decorin and billycan are glycosylated with chondroitin sulfate and dermatan sulfate, and play a role in extracellular matrix assembly [36]. Perlecan, a heparan sulfate and chondroitin sulfate glycosylated proteoglycan, is primarily involved in binding and crosslinking ECM components and cell surface markers [37]. The most notable function of proteoglycans is their ability to sequester growth factors onto the surface of the ECM. Heparan sulfate proteoglycans bind several different growth factors, such as FGFs [38], VEGFs, and PDGFs [18, 39], thus retaining them in tissue matrix and enabling their binding to cell receptors for different cellular functions. Furthermore, the degradation of proteoglycans can release small GAG fragments as well as bound growth factors that can ultimately modulate wound healing and angiogenesis [40]. For example, chondroitin and dermatan sulfate stimulate nitric oxide production; and heparan sulfate promotes interleukin production, thus creating a pro-angiogenic environment [40].

2.1.6. Tissue Proteases and Inhibitors

Matrix metalloproteases (MMPs) and tissue inhibitors of metalloproteases (TIMPs) play a crucial role in extracellular matrix turnover. MMPs are zinc-dependent endopeptidases that degrade matrix proteins such as collagen, laminin, and fibronectin. Some MMPs have specificity towards collagens. MMP1 and MMP8 primarily degrade fibrillar collagen types I and III [41].

MMP2 is also capable of cleaving collagen type I. Denatured collagen molecules (gelatin) and collagen type IV are cleaved by MMP2 and MMP9 [41].While MMPs are involved in collagen degradation, they also aid in the release of bioactive molecules that are bound to full length collagens [42]. The degradation of ECM by MMPs releases sequestered TGFβ, which may subsequently lead to increased ECM deposition [43]. To prevent uncontrolled matrix accumulation and occurrence of pathological disturbances, matrix degradation must be regulated to prevent pathological disturbances. One mechanism is through the secretion of TIMPs. TIMPs are protease specific and act to inhibit the activity of active MMPs with different efficacy. Inhibition of MMPs by TIMPs restricts TGFβ activation thereby decreasing ECM deposition. TIMP1 and -3 are strong inhibitors of latent or proMMP9, with TIMP2, -3, and -4 strongly inhibiting pro-MMP2 [44]. TIMPs can be localized with cell surface receptors. For example, TIMP1 has been shown to mediate angiogenesis though interaction with integrin receptors [45]. Alternatively, TIMP3 has been reported to antagonize VEGF signaling through direct interaction with VEGFR on endothelial cells [46]. MMP and TIMP balance is crucial for matrix proteolysis and stability, therefore, a balance must exist in order to support healthy matrix turnover.

2.2. The normal wound healing response

In the event that the skin barrier is breached, a series of dynamic, yet overlapping events occur instantaneously in order to maintain the closed tissue environment and protect from any invading pathogens. Immediately after injury, fibroblast apoptosis, hypoxia, and ECM disruption initiate the wound healing cascade, which involves four distinct yet overlapping phases of healing that require different soluble chemical mediators and ECM molecules. The initial response to injury is establishment of hemostasis that involves activation of the clotting cascade

and formation of the provisional wound matrix (PWM). The PWM is composed of ECM proteins such as fibrin, fibronectin, and collagen, and acts as a scaffold to support cellular migration and tissue remodeling [2]. In response to tissue injury and chemokine secretion, platelets arrive at the site of injury, where they secrete clot-forming mediators, such as platelet-derived growth factor (PDGF) [47], epidermal growth factor (EGF), and fibronectin [2].

Platelet degranulation and associated chemokine release activates the complement cascade [48] and causes vasodilation and recruitment of inflammatory cells, such as neutrophils and macrophages to the injured site [49]. The increase in vascular permeability causes increased deposition of fibronectin into the PWM to further support inflammatory cell recruitment and matrix formation. The recruited neutrophils remove devitalized tissue, destroy bacteria, and secrete inflammatory mediators, such as TNF-α and IL-1, which recruit and activate fibroblasts for collagen deposition [28]. Circulating monocytes are chemotactically attracted to the wound site and differentiate into macrophages, where they regulate proteolytic destruction of tissue through secretion of MMPs and TIMPs. Macrophages also a play a role in the transition into the proliferative phase where they secrete soluble mediators such as TGF-β, PDGF, FGF-2, TNF-α, IL-1, IL-6, and VEGF [50]. These soluble mediators stimulate the migration of epithelial cells, endothelial cells, and fibroblasts to the PWM, thus promoting formation of the basement membrane, angiogenesis, and new collagen synthesis for formation of granulation tissue [28, 50].

To promote an adequate supply of oxygen and nutrients within the wound space, angiogenesis is initiated through endothelial as well as fibroblast cell migration in response to hypoxic conditions present in the PWM [51, 52]. Endothelial cells interact with the fibronectin present in the PWM via their integrin cell surface receptors to form capillary sprouts [50]. Furthermore, FGF-2 stimulates the release of proteolytic enzymes, such as plasminogen and

collagenase, to digest basement membrane to support capillary sprouting and vascular network formation. Resident dermal fibroblasts [53] and fibroblasts differentiated from mesenchymal stem cells bind to the fibronectin present in the PWM in response to macrophage secreted cytokines [54-57] to support granulation tissue formation as well as angiogenesis.

To form granulation tissue, fibroblasts migrate along fibronectin fibrils and deposit collagen type III [58] while secreting proteases such as MMP-1, to remove any remaining collagen molecules damaged during injury [28]. This process of collagen destruction is balanced through the secretion of TIMPs in order to prevent the degradation of the functional matrix [28]. This balanced organization and destruction of collagen is important in the production of a functional matrix, as degraded collagen will not properly bind to newly formed collagen, thus resulting in a weak, disorganized ECM. Furthermore, peptides of collagen, fibronectin, and elastin that have been degraded by proteolytic enzymes through this process stimulate angiogenesis by promoting migration and proliferation of endothelial cells. In addition to collagen type III deposition [59], fibroblasts replace the PWM with ECM consisting of fibronectin, HA, and sulfated proteoglycans [60]. Dermal repair begins to follow a fibrotic rather than regenerative pathway as HA is replaced with chondroitin and dermatan sulfate, and type I collagen is synthesized [50, 61].

The final phase of wound healing involves remodeling of the ECM and maturation of the granulation tissue. The ECM composition changes from primarily type III collagen to type I enhancing the tensile strength of the tissue [61]. The unorganized fibers formed during granulation become organized through the action of MMPs and crosslinked due to the secretion of lysyl oxidase by fibroblasts [28]. Disruption of this cascade and biochemical cues within the ECM can result in the development of chronic, non-healing wounds.

2.3. Role of the ECM and associated small molecules in the wound healing response

ECM proteins and glycoproteins, such as collagens have been widely studied as a substrate for mechanical signaling cues for the study of cellular migration and adhesion. Due to the role of ECM components, such as collagen, laminin, and fibronectin in *in vivo* wound healing responses, there is an increased research interest in ECM derived biomaterials for wound healing applications.

The collagen in a CDM scaffold provides a substrate to control the elevation in MMP activity by acting as a substrate for MMP activity to prevent degradation of the natural, collagen type III matrix formed at the wound bed. The degraded collagen fragments also provide a chemotactic response, which induce the migration of different cell types to the wound bed in order to promote cytokine production (macrophages and neutrophils), matrix deposition (fibroblasts), and promotion of angiogenesis (endothelial cells) [28, 62].

Laminin and fibronectin have been shown to have high affinity interaction with growth factors through the heparin binding domains that promote migration of fibroblasts and endothelial cells, as seen in an improved wound closure in mice [18, 63]. Under homeostasis, laminin-332 is present as cleaved molecule that is then upregulated in the presence of wounds. The presence of laminin peptide sequences, such as IKVAV, have been shown to promote angiogenesis, promoting the use of laminin derived synthetic peptides as bioactive molecules in development of pro-angiogenic scaffolds [23].

2.4. Obstacles to healing: A chronic wound and the altered ECM environment

Rather than resolving the wound through formation of granulation tissue, chronic wounds remain in a continued state of inflammation. This is primarily due to increased levels of MMP as

well the neutrophil cytokine profile, which prevents wound closure [64]. Histological analysis of ECM components in a chronic wound indicate diffuse presence of fibronectin as well as the presence of fibrin cuffs compared to acute wounds. This inhibits cellular adherence and formation of the dermal-epidermal junction, and angiogenesis, respectively [65, 66]. This is further supported by molecular analysis of wound exudate, which shows fibronectin degradation in the wound bed [67]. Chronic wounds are also characterized by decreased laminin, chondroitin sulfate, and tenascin production which impair cellular proliferation and migration to promote re-epithelialization [65]. The excessive inflammation caused by the continued presence of neutrophils as well as their associated protease and cytokine profiles further inhibits the migration of fibroblasts and, as a result, delays the secretion of growth factors needed for new ECM deposition and induction of angiogenesis [28]. In addition to delayed ECM deposition, the elevated levels of proteases further degrade the collagen present and inactivate growth factors, such as PDGF, TGF-B, and VEGF [68]. As a result, ECM-associated growth factors needed for deposition of new ECM and induction of angiogenesis are delayed. Furthermore, the reduced vascularization at the wound bed contributes to the chronicity of a dermal wound as nutrients and gas exchange are not present at the wound. As a result of the delayed vascularization and wound closure, a chronic wound is also characterized by higher susceptibility to infection. Therefore, treatment strategies that aim to promote dermal repair and promote vascularization are crucial to preventing an infection from occurring at the wound bed.

2.5. Therapies to promote dermal repair

The study of wounded ECM microenvironments have led to the development of treatment strategies that may ultimately lead to restored ECM proteins through inactivation of

proteases and supplementation of the wound bed with ECM-like substrate. These goals of treatment were summarized under the 'TIME' acronym by a group of wound care providers in 2002 [69]. The first approach to treatment is tissue management, accomplished by debridement, in order to restore the wound bed and functional ECM proteins. This is followed by control of infection and inflammation with the use of antimicrobial products to decrease inflammatory cytokines and protease inhibitors while also increasing reparative growth factors. This is done in conjunction with the use of dressings or skin grafts/biologic therapies to aid in moisture balance and epithelialization, thus restoring the protease profile. Unfortunately, chronic wounds often fail to respond to this treatment approach due to the alteration in the underlying ECM structure, which affects epithelization and angiogenesis [66, 70-72].

2.5.1. Autografts

A frequently used regenerative treatment strategy for chronic wound repair is the use of autografts. Autologous skin grafts are used to support functional tissue regeneration because their intact epidermal/dermal layer provide the wound site with a healthy, natural ECM [73]. The extracellular matrix present within the freshly grafted skin helps promote epithelialization and closure by providing the wound bed with proteins, such as collagen, that have been degraded due to an imbalance in growth factors and matrix metalloproteases. However, this approach involves removing healthy skin tissue from another site, thus creating another wound, which may also have potential for healing complications.

2.5.2. Engineered, synthetic biomaterials (acellular)

Wound dressings help create a moist environment to promote faster epithelialization through increased cell migration and growth factor secretion [74]. Occlusive polymer films, foams, hydrocolloids, and hydrogels have been used as to create a moisture balance and prevent bacterial penetration into the wound. Polyurethane-film dressings provide an impermeable barrier to bacteria and liquid, while also supporting oxygen diffusion [75]. Polyurethane-foam based dressings were then developed to address the lack of exudate absorbency in film based dressings [75]. Alternatively, hydrocolloid dressings, that typically consist of agar, alginate, or gelatin, have occlusive, absorbent, as well as oxygen permeability properties compared to the other two classes. Synthetic hydrogel bases materials, with hydrophilic properties similar to hydrocolloids, such as poly(lactide-co-glycolide) (PLGA), polyurethane, and polyethylene glycol (PEG), have also been shown to promote healing.

The limitation to using occlusive dressings is that they are non-absorbent, and can promote accumulation of wound exudate and bacterial contamination [76]. Furthermore, the inert and synthetic nature of these dressings do not interact with the wound bed to promote a regenerative environment and do not represent the native microenvironment. Thus, alternative dressings have been developed to promote faster wound closure and epithelialization due to the presence ECM basement membrane proteins [77, 78].

2.5.3. Engineered, biopolymer scaffolds

Alternative approaches include commercially available products that are naturally derived proteins and polysaccharides that provide a homogenous source of native and denatured collagen [79] and hyaluronic acid [80]. Acellular, naturally-derived polymeric scaffolds, such as

Integra and Promogran, consist of enzymatically degraded or mammalian sourced ECM proteins adhered to a synthetic material, such as polyglycolic acid, polylactic acid, or silicone [77, 81]. The simplest form of these engineered scaffolds act to absorb wound exudate, while also sequestering proteases that can reduce the degradation of naturally produced collagen at the wound bed [77]. Collagen-based products, such as Promogran, have been shown to reduce MMP activity in the wound bed at the expense of degradation of its collagen protein, thus greatly reducing the wound size [79, 82]. Hyaluronic acid-based products, such as Hyalomatrix, have also been shown to promote cellular migration and healing [81, 83, 84]. These scaffolds typically require repeat administration, and thus are not a material that functions to direct tissue repair [77].

From a manufacturing and commercialization perspective, these ECM components are assembled and polymerized onto a synthetic mesh that would allow application to the patient. The advantages of engineered scaffolds is that they can also have tailored characteristics, such as pore size and degradation rate, to promote tissue regeneration [81]. Furthermore, these natural, engineered biopolymer scaffolds are biocompatible, have a long shelf life, and have been shown to provide a degradable substrate for protease balance and act as a mediator for wound repair [85]. However, they are still considered a simplified, homogenous composition that is not representative of the complex, heterogeneous composition of natural ECM, and ultimately lack a basement membrane and fail to fully recapitulate the native ECM environment [86]. It has also been suggested that homogenous protein scaffolds are not optimal for promoting regeneration, and thus a heterogeneous, native structure is recommended [62].

2.5.4. ECM-derived scaffolds

The important role of ECM components in the wound healing response has highlighted the need of ECM-derived biomaterials to address the barriers of healing and limitations provided by the natural, acellular biomaterials described above. In addition to providing a protective and hydrating dressing, biologic ECM also have a functional role in the wound bed. The possible mechanisms of action by which they promote healing is through degradation, and release of various bioactive molecules, such as cytokines and ECM-peptide fragments, which ultimately modulate the immune response, recruit progenitor/stromal cells to the site of tissue remodeling stimulate angiogenesis, granulation tissue formation, and reepithelialization [77]. These products are often sourced from decellularized, animal-derived tissue. Porcine-derived small intestinal submucosa (SIS) (i.e. Oasis) and urinary bladder matrix (UBM) (i.e. Matristem), bovine-derived dermis (i.e. Primatrix), and human cadaver-derived dermal matrices (i.e. Alloderm/Strattice) have been characterized as ECM sources for wound healing dressings. ECM-derived scaffolds release peptide fragments, which promote migration of stromal cells to support tissue remodeling [87]. The ECM scaffolds are primarily composed of collagen type I and modest amounts of collagen types III, IV, V, and VI. GAGs, such as chondroitin sulfate, heparin sulfate, and hyaluronic acid [88] and, growth factors, such as FGF[89] and VEGF [90], have also been identified.

2.5.5. Clinical endpoints and limitations

These treatment strategies utilize synthetic or ECM-based products that provide ECM components to supplement the wound environment with bioactive factors for tissue regeneration. Assessment of the efficacy of these products is frequently based on wound closure as the primary

clinical endpoint. However, this does not necessarily correlate with formation of the desired regenerated tissue that is more resistant to wound recurrence and tissue dehiscence [81]. While these approaches have been shown to promote wound closure and epithelialization of the wound bed, other causes of delayed healing are not addressed. One major cause of chronicity is overexpression of MMP presence and activity in the wound bed, thus strategies to inhibit these proteases may create an environment that is more conducive to healing [91]. Furthermore, impaired blood flow to the wound site is implicated in the delayed healing response [64, 92]; however, many treatment strategies do not address angiogenesis, and thus vascularization measurements are not reported in clinical endpoints. Thus, there is a need to develop a product that not only promotes healing through inflammation control, but also through promotion of angiogenesis.

2.6. Angiogenesis

Angiogenesis is defined as the growth of blood vessels from an existing vessels [93], and is one of the earliest events in embryogenesis that continues throughout the human life span under strictly defined conditions. It is vital to the newly formed tissues during development, as well as during remodeling and repair (wound healing). In a delayed wound healing response, insufficient capillary network formation can lead to hypoxia-induced tissue death [94]. Therefore, strategies to promote angiogenesis within a wound bed are crucial. The process of angiogenesis is mediated by several factors that provide stimulatory or inhibitory signals in response to accumulation of hypoxia induced factor-1-α (HIF-1α). Under hypoxic conditions, HIF-1α accumulates and activates endothelial cells, thus triggering intracellular pathways for upregulation of proteases and growth factors. Proteases are crucial to angiogenesis, as they break

down the basement membrane to support endothelial cell migration via integrin mediated interaction with the extracellular matrix [95]. However, an elevation in proteases must be balanced via proteinase inhibitors in order to maintain a matrix composition to support other cellular functions in the wound bed. Endothelial cells are also known to respond to different growth factors, to support formation of a capillary lumen and network formation. There have been several factors reported in literature that positively regulate angiogenesis, such as fibroblast growth factors (FGF1, FGF2), TGFα and TGFβ, hepatocyte growth factor (HGF), tumor necrosis factor (TNFα), and angiopoietins, however, these factors are not specific to endothelial cells [96]. However, the most important growth factor regulating the process of angiogenesis is vascular endothelium growth factor (VEGF) [97].

In addition to growth factors and proteinases, the ECM composition also plays a central role in promoting angiogenesis. Growth factors bind to the ECM via different proteoglycan chains, thus acting as a reservoir of growth factors for regulated release mediated by different enzymes [98]. As a result, several research efforts have been incorporating growth factors within ECM delivery vehicles. The composition of the delivery vehicle is also crucial. For example, transition of the fibrin provisional matrix to the second order fibronectin/hyaluronic acid provisional matrix, and subsequently to the collagen rich scar, highlights the roles of different ECM components during each phase of wound healing. After formation of collagenous scar in the wound healing process, there is a decrease in vessel density within the wound site; however, protease activity results in the presence of denatured collagen, which, like native collagen, contain RGD binding sites [99] that are also inductive to angiogenesis. Fibronectin and laminin have also been shown to a play a role in promoting angiogenesis. For example, altered fibronectin expression in mice, decreased the ability of endothelial cell to form capillary

networks [34]. Laminin has been shown to interact with other growth factors to promote endothelial cell differentiation, and associated tubule formation [100]. ECM macromolecules can also provide directional cues for vessel outgrowth as well as a gradient for soluble pro-angiogenic factors [101]. The presence of these stimulators enables the formation of capillary sprouts, and development of a microvascular network [102].

2.7. Developing pro-angiogenic biomaterials

Biomaterial scaffolds are currently under investigation to enhance angiogenic stimulus, to promote endothelial cell proliferation, sprouting, and capillary network formation [103, 104]. Synthetic polymers, such as polycaprolactone (PCL) and polylactides (PLA), have been studied [105, 106], but they do not interact with the microenvironment to regulate angiogenesis. These limitations, as well as evidence supporting the important role of ECM and associated molecules in regulating angiogenesis, led a shift towards naturally derived biomaterials with ECM components, such as collagen [107, 108], hyaluronic acid [109], and fibrin gels [53, 61]. Hyaluronic acid scaffolds have been shown to promote capillary network formation in endothelial cells when cultured with fibroblasts, as fibroblasts provided the pro-angiogenic stimulus, and the HA scaffold provided directional cues for endothelial cell migration [109]. These ECM biomaterials can also support controlled release of pro-angiogenic factors that are bound to the material or delivered, such as FGF [108], HGF [110], VEGF [111], and angiopoietin [111]. Finally, ECM based hydrogels have also been developed to promote endothelial cell recruitment and promote a pro-angiogenic microenvironment in tissues, such as the heart [112]. Natural ECM biomaterials provide several advantages in promoting angiogenesis, and can ultimately be used as delivery vehicles for controlled release of

proangiogenic factors or as degradable scaffolds that recruit endothelial cell migration to support capillary network formation.

2.8. Cell-derived matrices (CDMs)

CDMs are mainly composed of collagen types I and III, as well as other types of collagen molecules. Collagen plays a bi-functional role in wound healing as it governs adhesion, differentiation, and migration of keratinocytes and fibroblasts, while also promoting ECM deposition and angiogenesis. In addition, it regulates the wound bed environment by binding excess proteases, inflammatory cytokines, and free radicals [113]. Thus, an imbalance in collagen deposition versus collagen degradation in the wound bed leads to prolonged inflammation. Using an exogenous collagen-based scaffold to control protease activity at the wound bed is desirable, and a reason why many wound healing products are primarily collagen based. An additional advantage of using collagen-derived materials is the ability to incorporate the controlled release of growth factors and proteins via the use collagen-binding domain sequences [114, 115].

The earliest work related to cell-derived products was cultured epithelial autografts (CEA), which used human derived keratinocytes to obtain a metabolically active epidermal cell sheet for clinical treatment of burns. While there was a 69% engraftment rate, there were many complications, including wound contractures, and shearing [116]. Metabolically active cell-sheets, known as living skin equivalents (LSEs), are examples of bioengineered cell-derived biologics that consist of extracellular matrix components deposited by primary human cells, such as keratinocytes, fibroblasts, or stem cells [117]. Primary cells, which may also be derived from patients, are typically seeded within a scaffold and cultured *ex vivo* to support the accumulation

of cell-derived extracellular matrix components. During the culture period, the supporting scaffold ultimately degrades, thus leaving a functional, metabolically-active cell-derived biomaterial. Thus, cell sourcing and selection of scaffolding materials is pivotal to development of a functional biomaterial to support repair of target tissue. LSEs have applications as clinical skin replacements and grafts as well as drug toxicity screening models [117]. Examples of LSEs that have been FDA-approved and used as skin replacement grafts include, Fidia Avanced Biopolymer's LaserSkin®, Advanced Tissue Sciences Transcyte/Dermagraft®, and FortiCell Bioscience's Orcel®. These commercialized products consist of either keratinocytes or fibroblasts cultured *ex vivo* on a mesh or collagen matrix for 4-6 weeks to allow accumulation of ECM molecules. These products provide a biochemically balanced wound environment to support tissue repair and delivery of cytokines and growth factors important to tissue remodeling, and have been shown clinically to promote reepithelialization of the wound [118]. Cell-derived products have also been developed as toxicity screen models. Examples of these commercialized products included SkinEthic® and Episkin®, which are human keratinocyte or fibroblasts *ex vivo* cultures developed on a synthetic or biologic meshes. These applications are provided as alternatives for animal testing for cosmetic drug testing [119], and can provide specific skin models for healthy and diseased tissues to support product development.

Another example of a cell-based product is the development of devitalized, cell-derived matrix for development of blood vessel grafts [120]. Despite the advantages of CDMs compared to synthetically produced scaffolds, the culture time needed for development is a challenge in its clinical applications. However, recent work has shown that the variations in culture conditions, such as oxygen levels or addition of external stimuli can effect matrix production and deposition *in vitro.* While culturing cells under hypoxic culture conditions can promote increased matrix

production, the use external culture stimuli such as macromolecular crowding can promote increased matrix deposition. Macromolecular crowding has shown to be a very promising approach to increasing ECM production, and accelerating the production of CDM [121-124].

2.9. Macromolecular crowding

Macromolecular crowding (MMC), has been shown to increase ECM deposition and assembly in cultured cells *in vitro* [121-124]. Briefly, MMC entails the addition of polymeric materials to the cell culture media to create an excluded volume effect and physically limit diffusion of cellular proteins from the cell layer. Addition of neutral polymers to a human skin fibroblast culture was initially studied by Bateman *et al.* in 1987 [125]. While this approach was not referred to as crowding at the time, nor was it utilized as a method in tissue engineering applications for development of cell-assembled sheets, it highlighted the importance of altering the reaction kinetics of precursor ECM proteins at the cell layer to increase CDM deposition.

2.9.1. Macromolecular crowding in vivo

ECM matrix deposition is strongly dependent on the cellular microenvironment. Under physiological conditions, cells are surrounded by a dense environment crowded with proteins of different size and charge, thus affecting the extent of ECM secretion. Standard culture conditions are very dilute and do not represent the crowded native environment. As a result, ECM precursor materials are discarded as waste during media removal. Animal-derived serum in standard culture conditions provides a source of crowder proteins, with serum concentration in the range of 1-10g/L [126]. This concentration is dilute compared to *in vivo* conditions which, depending on the biological fluid, can vary from 30 – 350 g/L [126]. As a result of the dilute culture

conditions, the reaction kinetics for conversion of pro-collagen to mature collagen, as well as its molecular assembly at the cellular layer *in vitro*, is altered. One approach to increase extracellular matrix secretion and deposition is through the culture of cells under macromolecular crowding (MMC) conditions. Macromolecular crowding has shown to be a promising approach to increase ECM secretion, and accelerate the production of CDM [121-124].

2.9.2. Macromolecular crowding principles: excluded volume effect and fractional volume occupancy

The addition of macromolecules to the media creates an excluded volume effect. The excluded volume effect, or the volume occupied by different macromolecules in the media, is represented by: 1) the space occupied by the added macromolecules themselves (shown schematically in **Figure 2-1** , and 2) the space created due to steric and electrostatic repulsions between the macromolecules **(Figure 2-1, insert)**. This alters the reaction kinetics for conversion of pro-collagen to mature collagen as well as its molecular assembly at the cellular layer. The effects of macromolecular crowding on ECM synthesis and deposition can be varied depending on the fractional volume occupancy (FVO) of the macromolecules in solution. The FVO is the total fraction of the media volume that is occupied by macromolecules used leading to an elevation in the free energy of reactant molecules. This enhances many biological functions specifically enzyme substrate interactions, ultimately leading to more product. FVO is dependent on many parameters such as the molecular weight and hydrodynamic radii of the macromolecules in solution. Therefore, the culture media can be tailored depending on the type of crowder used to enhance biological processes *in vitro.*

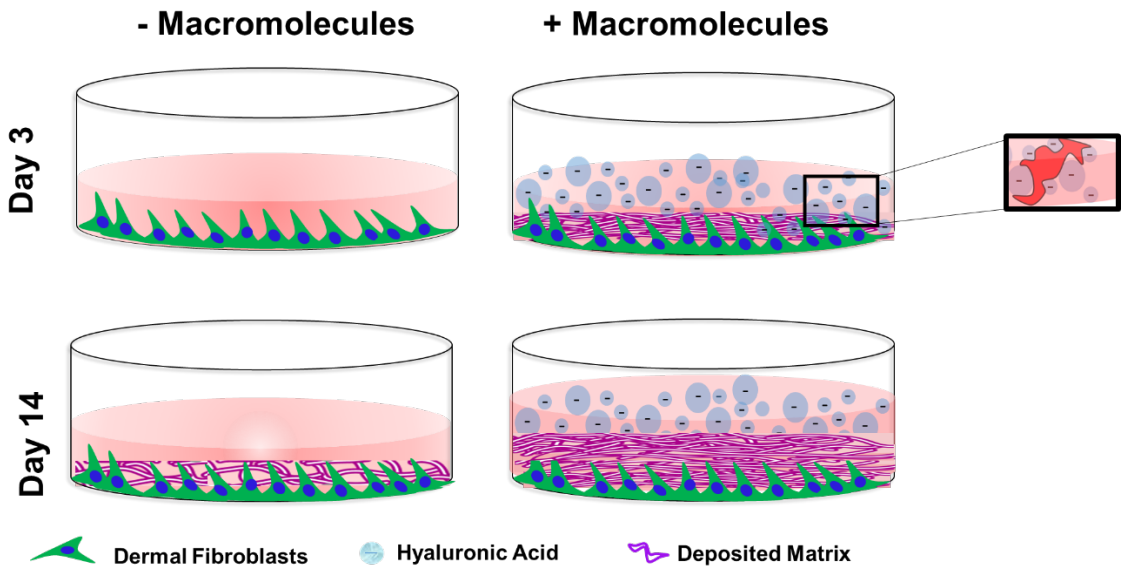

Figure 2-1: Schematic illustrating the macromolecular crowding principle, and its effect on ECM deposition *in vitro*. Macromolecules, such as hyaluronic acid, occupy a volume in the culture environment, thus reducing diffusion of ECM precursor molecules into the media. This results in increased deposition of ECM at the cell layer compared to non-crowded controls. Insert: Illustration of the excluded volume effect, or the total amount of space not available for ECM precursor protein diffusion due to the volume occupied by the macromolecules (spheres) and the void spaces created due to electrostatic and steric repulsion (shaded red).

2.9.3. Macromolecular crowding principles: polydispersity

The majority of studies have focused on the use of monodisperse particles for crowding studies [127], however, it was recognized that the polydisperse nature of spherical particles has a stronger potential to promoting matrix deposition [128]. This is also more accurate representation of the cellular protein microenvironment that is characterized with polydisperse macromolecules of various shapes and sizes. Several research publications have emphasized the contribution of crowder size and molecular weight on the fractional volume occupancy, and thus the excluded volume effect, created by the macromolecule. However, this does not provide the full explanation on the nature of macromolecular crowding effects, as polydispersity is also a contributing factor. Previous studies have explored the effect of particle size on protein stability under crowding, and have shown that the larger sized crowding molecules have an adverse effect

on stability of proteins with small radii [129]. The differently sized particles that are typically used in these studies are often different macromolecules (i.e. Ficoll 70 vs Dextran 40), and thus it is unclear if the effects in protein stability are due to macromolecule composition or the size alone [130]. Despite the effects of different particle sizes on protein stability, a polydisperse crowding solution is optimal as it increases the excluded volume effect [131] without significantly increasing the solution viscosity [132, 133], thus improving the efficacy of MMC overall. Furthermore, a polydisperse crowding environment provides a better representation of conditions *in vivo*.

2.9.4. Macromolecular crowding principles: net charge

The effects of macromolecule charge have also been explored for MMC-mediated effect on ECM deposition. A monodisperse solution of crowders with neutral charge, such as Ficoll, was unable to increase collagen deposition [127]. In addition to the neutral charge, the small hydrodynamic radii of these molecules did not generate a large enough excluded volume in order to have a crowding effect. However, the combination of neutral macromolecules at a reduced concentration increased collagen deposition [128, 134]. Collagen deposition was further improved in cultures with a negatively charged macromolecules as opposed to neutral ones [127, 128]. The presence of a negative charge on the macromolecule backbone creates electrostatic repulsion, and thus contributes to the excluded volume effect.

2.9.5. Macromolecular Crowding Principles: Viscosity

While the excluded volume effect is a major contributing factor to cellular responses to crowding, there are other factors such as viscosity [135, 136], diffusion [137], and direct physical

interactions between crowders and secreted proteins that may also be involved in matrix deposition [138]. It has been previously reported that changes in viscosity due to crowding alter diffusion rates for enzyme and factors involved in different cellular processes [139-141]. Small proteins, such as enzymes, are more sensitive to differences in viscosity than larger proteins, and thus have a reduced diffusion coefficient in the system [137, 140]. It is important to note, that an increase in concentration and viscosity does not necessarily mean that a hydrogel is developed. Thus, a solution with increased viscosity is still considered macromolecular crowding, and not macromolecular confinement, which would occur in the presence of a hydrogel.

2.9.6. Characteristics of an Ideal Crowding Agent

In general, an ideal crowding agent is soluble in media, has a globular molecular shape, an overall negative charge, is biochemically inert, and acts by steric repulsion. Several synthetic, inert polymers with different molecular weights, charges, and radii have been used as macromolecular crowders, including Ficoll [122, 123, 134, 142, 143], carrageenan [121], dextran sulfate (DxS) [124, 127], and polyvinylpyrrolidone (PVP) [128]. Several cell types including fibroblasts [124, 127, 134], embryonic stem cells (ESC) [144], and mesenchymal stem cells (MSCs)[121] have been cultured in the presence of these crowders, and have demonstrated to increase ECM deposition. These crowders affect reaction kinetics primarily through their hydrodynamic radii, which alters reaction kinetics through steric repulsion, or through their charge-induced electrostatic repulsion effects.

2.9.7. Effects of macromolecular crowding on collagen synthesis

Currently, cultures used for CDMs may take up to 180 days in order to allow time for ECM deposition and matrix production [145]. In order to reduce the culture time, increased ECM deposition due to the accelerated conversion of procollagen to collagen would be of significant interest to the development of CDM. Addition of neutral polymers to a human skin fibroblast culture was initially studied thirty years ago by Bateman *et al.* [125]. The addition of these polymers caused accumulation of collagen at the cell layer due to proteolytic cleavage of collagen N- and C-terminal peptides [125]. While reducing the culture period required for matrix deposition is essential, the properties of the developed CDM are also of importance, and can be tailored depending on the cell source and FVO of the macromolecular crowder.

The CDMs developed using synthetic crowding have been primarily applied as a tissue culture surface coating to promote or maintain differentiation of different stem cell types [122], and therefore was tailored to the stem cell microenvironment. To develop a product for wound healing, promotion of angiogenesis and reduction of inflammation are crucial, and the choice of cell source and crowder molecules should support the application.

2.10. Hyaluronic acid: a crowder molecule?

Natural crowders, such as hyaluronic acid (HA), have been investigated in the study of collagen alignment and fibrillogenesis in acellular systems [146]. Other HA studies have reportedly cultured fibroblasts with exogenous HA, and reported effects on cell proliferation and collagen deposition [147, 148]. However, these studies were completed at concentrations not representative of macromolecular crowding, and thus its effects as a natural crowder on ECM deposition have not yet been studied. HA shares many properties with crowders typically reported in the literature. It is water soluble and forms a self-avoiding random coil-like structure

in solution to form a globular shape [149, 150], has an overall net negative charge [151], and interacts with the system via steric as well as electrostatic repulsion. In addition to those properties, HA is bioactive, natural ECM molecule [2, 28, 151], that has been shown to have anti-inflammatory properties [152], and promotes angiogenesis [105].

HA is naturally present *in vivo* and abundantly found in the extracellular matrix microenvironment of different cells types, especially in fibroblast ECM in skin. It is especially abundant in the fetal microenvironment, where it plays a significant role in scar-free wound healing. The increased levels of HA alter the contractility of myofibroblasts as well as the contraction of the surrounding collagen matrix [153]. Furthermore, it causes a decrease in the levels of TGF-β, which leads to a reduction in scarring [154]. As a natural ECM polymer, it regulates healing and inflammation through its interaction with RHAMM and CD44 receptors, thus having a direct effect on gene expression. HA also has anti-inflammatory properties depending on its molecular weight [155]. High molecular weight (HMW) HA in particular has been shown to inhibit secretion of inflammatory cytokines, such as IL-1, IL-4, IL-6, and TNF-α [152]. The presence of enzymes in an inflamed wound site causes degradation of the HA into lower MW HA fragments [151, 152, 156]. While low molecular weight HA fragments tend to generate pro-inflammatory molecules, they also stimulate HA synthase genes that produce HMW HA [156]. In addition, low molecular weight fragments have been shown to bind to CD44 [157] and RHAMM [158] receptors on the surfaces of endothelial cells to promote migration, proliferation, and angiogenic capillary sprouting [157, 158]. Lastly, HA is involved in the development of collagen rich ECM [159-161] as well as its alignment. In scar tissue, collagen is arranged in parallel bundles compared to the basket weave-like collagen arrangement present in the normal skin [2]. Due to its hydrophilic and negatively charged nature [48, 49], HA can

promote collagen alignment, which is important for fibroblast and endothelial cell migration during wound healing [50, 146].

To address the challenge associated with the development of a cell-derived matrix as a material for wound healing, we propose the use of HA as a natural crowder agent that can promote a regenerative tissue environment and angiogenesis. As a naturally occurring macromolecule that has effects on collagen alignment, extracellular matrix deposition, and cytokine and interleukin expression, the CDM deposited in the presence of an HA crowder can ultimately be used as a wound healing scaffold. Other groups have focused on understanding the biochemical effects of crowding on matrix deposition [162, 163]. In this work, our goal is to use these principles to develop a tissue regenerative material with angiogenic properties that can also support delivery of antimicrobial peptides.

2.11. Overall project goal and hypothesis

The overall goal of the proposed research is to develop and characterize a cell-based biomaterial with pro-angiogenic and antimicrobial properties. **We hypothesize that culture conditions, specifically HA-mediated crowding, will increase deposition of pro-angiogenic factors and provide a cell-derived matrix (CDM) biomaterial for the delivery of antimicrobial peptides.**

2.12. References

[1] B. Alberts, D. Bray, K. Hopkin, A.D. Johnson, J. Lewis, M. Raff, K. Roberts, P. Walter, Essential cell biology, Garland Science2013.
[2] M. Xue, C.J. Jackson, Extracellular matrix reorganization during wound healing and its impact on abnormal scarring, Advances in wound care 4(3) (2015) 119-136.
[3] A. Sieminski, R.P. Hebbel, K. Gooch, The relative magnitudes of endothelial force generation and matrix stiffness modulate capillary morphogenesis in vitro, Experimental cell research 297(2) (2004) 574-584.
[4] A. Naba, K.R. Clauser, S. Hoersch, H. Liu, S.A. Carr, R.O. Hynes, The matrisome: in silico definition and in vivo characterization by proteomics of normal and tumor extracellular matrices, Molecular & Cellular Proteomics 11(4) (2012) M111. 014647.
[5] A. Naba, O.M. Pearce, A. Del Rosario, D. Ma, H. Ding, V. Rajeeve, P.R. Cutillas, F.R. Balkwill, R.O. Hynes, Characterization of the extracellular matrix of normal and diseased tissues using proteomics, Journal of proteome research 16(8) (2017) 3083-3091.
[6] S. Ricard-Blum, The collagen family, Cold Spring Harbor perspectives in biology 3(1) (2011) a004978.
[7] J.A. Fallas, V. Gauba, J.D. Hartgerink, Solution structure of an ABC collagen heterotrimer reveals a single-register helix stabilized by electrostatic interactions, Journal of Biological Chemistry 284(39) (2009) 26851-26859.
[8] B. Goldberg, C.J. Sherr, Secretion and extracellular processing of procollagen by cultured human fibroblasts, Proceedings of the National Academy of Sciences 70(2) (1973) 361-365.
[9] C.V. Nicchitta, R.S. Lerner, S.B. Stephens, R.D. Dodd, B. Pyhtila, Pathways for compartmentalizing protein synthesis in eukaryotic cells: the template-partitioning model, Biochemistry and cell biology 83(6) (2005) 687-695.
[10] J.L. Maiers, E. Kostallari, M. Mushref, T.M. deAssuncao, H. Li, N. Jalan-Sakrikar, R.C. Huebert, S. Cao, H. Malhi, V.H. Shah, The unfolded protein response mediates fibrogenesis and collagen I secretion through regulating TANGO1 in mice, Hepatology 65(3) (2017) 983-998.
[11] J. Myllyharju, K.I. Kivirikko, Collagens, modifying enzymes and their mutations in humans, flies and worms, TRENDS in Genetics 20(1) (2004) 33-43.
[12] J.J. Sauk, N. Nikitakis, H. Siavash, Hsp47 a novel collagen binding serpin chaperone, autoantigen and therapeutic target, Front Biosci 10(2) (2005) 107-118.
[13] M. Yamauchi, M. Sricholpech, Lysine post-translational modifications of collagen, Essays in biochemistry 52 (2012) 113-133.
[14] S. Murad, D. Grove, K. Lindberg, G. Reynolds, A. Sivarajah, S. Pinnell, Regulation of collagen synthesis by ascorbic acid, Proceedings of the National Academy of Sciences 78(5) (1981) 2879-2882.
[15] J.-E.W. Ahlfors, K.L. Billiar, Biomechanical and biochemical characteristics of a human fibroblast-produced and remodeled matrix, Biomaterials 28(13) (2007) 2183-2191.
[16] V. Magno, J. Friedrichs, H.M. Weber, M.C. Prewitz, M.V. Tsurkan, C. Werner, Macromolecular crowding for tailoring tissue-derived fibrillated matrices, Acta biomaterialia 55 (2017) 109-119.
[17] N. Martinek, J. Shahab, J. Sodek, M. Ringuette, Is SPARC an evolutionarily conserved collagen chaperone?, Journal of dental research 86(4) (2007) 296-305.
[18] J. Ishihara, A. Ishihara, K. Fukunaga, K. Sasaki, M.J. White, P.S. Briquez, J.A. Hubbell, Laminin heparin-binding peptides bind to several growth factors and enhance diabetic wound healing, Nature communications 9(1) (2018) 2163.
[19] M. Aumailley, N. Smyth, The role of laminins in basement membrane function, The Journal of Anatomy 193(1) (1998) 1-21.
[20] H.K. Kleinman, G.R. Martin, Matrigel: basement membrane matrix with biological activity, Seminars in cancer biology, Elsevier, 2005, pp. 378-386.

[21] R.E. Burgeson, M. Chiquet, R. Deutzmann, P. Ekblom, J. Engel, H. Kleinman, G.R. Martin, G. Meneguzzi, M. Paulsson, J. Sanes, A new nomenclature for the laminins, Matrix Biology 14(3) (1994) 209-211.
[22] P.D. Yurchenco, Y. Quan, H. Colognato, T. Mathus, D. Harrison, Y. Yamada, J. Julian, The α chain of laminin-1 is independently secreted and drives secretion of its β-and γ-chain partners, Proceedings of the National Academy of Sciences 94(19) (1997) 10189-10194.
[23] P. Simon-Assmann, G. Orend, E. Mammadova-Bach, C. Spenlé, O. Lefebvre, Role of laminins in physiological and pathological angiogenesis, International journal of developmental biology 55(4-5) (2011) 455-465.
[24] K.-i. TASHIRO, A. MONJI, I. YOSHIDA, Y. HAYASHI, K. MATSUDA, N. TASHIRO, Y. MITSUYAMA, An IKLLI-containing peptide derived from the laminin α1 chain mediating heparin-binding, cell adhesion, neurite outgrowth and proliferation, represents a binding site for integrin α3β1 and heparan sulphate proteoglycan, Biochemical Journal 340(1) (1999) 119-126.
[25] K.J. Hamill, K. Kligys, S.B. Hopkinson, J.C. Jones, Laminin deposition in the extracellular matrix: a complex picture emerges, J Cell Sci 122(24) (2009) 4409-4417.
[26] J.C. Jones, K. Lane, S.B. Hopkinson, E. Lecuona, R.C. Geiger, D.A. Dean, E. Correa-Meyer, M. Gonzales, K. Campbell, J.I. Sznajder, Laminin-6 assembles into multimolecular fibrillar complexes with perlecan and participates in mechanical-signal transduction via a dystroglycan-dependent, integrin-independent mechanism, Journal of cell science 118(12) (2005) 2557-2566.
[27] D. Breitkreutz, N. Mirancea, C. Schmidt, R. Beck, U. Werner, H.-J. Stark, M. Gerl, N.E. Fusenig, Inhibition of basement membrane formation by a nidogen-binding laminin γ1-chain fragment in human skin-organotypic cocultures, Journal of Cell Science 117(12) (2004) 2611-2622.
[28] G.S. Schultz, G. Ladwig, A. Wysocki, Extracellular matrix: review of its roles in acute and chronic wounds, World wide wounds 2005 (2005) 1-18.
[29] R.O. Hynes, Interactions of fibronectins, Fibronectins, Springer1990, pp. 84-112.
[30] K.E. Kadler, A. Hill, E.G. Canty-Laird, Collagen fibrillogenesis: fibronectin, integrins, and minor collagens as organizers and nucleators, Current opinion in cell biology 20(5) (2008) 495-501.
[31] C.Y. Chung, H.P. Erickson, Glycosaminoglycans modulate fibronectin matrix assembly and are essential for matrix incorporation of tenascin-C, Journal of cell science 110(12) (1997) 1413-1419.
[32] S.L. Dallas, P. Sivakumar, C.J. Jones, Q. Chen, D.M. Peters, D.F. Mosher, M.J. Humphries, C.M. Kielty, Fibronectin regulates latent transforming growth factor-β (TGFβ) by controlling matrix assembly of latent TGFβ-binding protein-1, Journal of Biological Chemistry 280(19) (2005) 18871-18880.
[33] X. Zhou, R.G. Rowe, N. Hiraoka, J.P. George, D. Wirtz, D.F. Mosher, I. Virtanen, M.A. Chernousov, S.J. Weiss, Fibronectin fibrillogenesis regulates three-dimensional neovessel formation, Genes & development 22(9) (2008) 1231-1243.
[34] P.A. Murphy, S. Begum, R.O. Hynes, Tumor angiogenesis in the absence of fibronectin or its cognate integrin receptors, PLoS One 10(3) (2015) e0120872.
[35] D. Park, Y. Kim, H. Kim, K. Kim, Y.-S. Lee, J. Choe, J.-H. Hahn, H. Lee, J. Jeon, C. Choi, Hyaluronic acid promotes angiogenesis by inducing RHAMM-TGFβ receptor interaction via CD44-PKCδ, Molecules and cells 33(6) (2012) 563-574.
[36] R.V. Iozzo, The family of the small leucine-rich proteoglycans: key regulators of matrix assembly and cellular growth, Critical reviews in biochemistry and molecular biology 32(2) (1997) 141-174.
[37] M.C. Farach-Carson, D.D. Carson, Perlecan—a multifunctional extracellular proteoglycan scaffold, Oxford University Press, 2007.
[38] L. Pellegrini, D.F. Burke, F. von Delft, B. Mulloy, T.L. Blundell, Crystal structure of fibroblast growth factor receptor ectodomain bound to ligand and heparin, Nature 407(6807) (2000) 1029.
[39] E. Ruoslahti, Y. Yamaguchi, Proteoglycans as modulators of growth factor activities, Cell 64(5) (1991) 867-869.
[40] P.V. Peplow, Glycosaminoglycan: a candidate to stimulate the repair of chronic wounds, Thrombosis and Haemostasis 94(07) (2005) 4-16.

[41] T. Klein, R. Bischoff, Physiology and pathophysiology of matrix metalloproteases, Amino acids 41(2) (2011) 271-290.
[42] S. Ricard-Blum, L. Ballut, Matricryptins derived from collagens and proteoglycans, Frontiers in bioscience (Landmark edition) 16 (2011) 674-697.
[43] M. Selman, V. Ruiz, S. Cabrera, L. Segura, R. Ramírez, R. Barrios, A. Pardo, TIMP-1,-2,-3, and-4 in idiopathic pulmonary fibrosis. A prevailing nondegradative lung microenvironment?, American Journal of Physiology-Lung Cellular and Molecular Physiology 279(3) (2000) L562-L574.
[44] A.H. Baker, D.R. Edwards, G. Murphy, Metalloproteinase inhibitors: biological actions and therapeutic opportunities, Journal of cell science 115(19) (2002) 3719-3727.
[45] M. Toricelli, F.H. Melo, G.B. Peres, D.C. Silva, M.G. Jasiulionis, Timp1 interacts with beta-1 integrin and CD63 along melanoma genesis and confers anoikis resistance by activating PI3-K signaling pathway independently of Akt phosphorylation, Molecular cancer 12(1) (2013) 1095.
[46] J.H. Qi, Q. Ebrahem, N. Moore, G. Murphy, L. Claesson-Welsh, M. Bond, A. Baker, B. Anand-Apte, A novel function for tissue inhibitor of metalloproteinases-3 (TIMP3): inhibition of angiogenesis by blockage of VEGF binding to VEGF receptor-2, Nature medicine 9(4) (2003) 407.
[47] C.-H. Heldin, B. Westermark, Mechanism of action and in vivo role of platelet-derived growth factor, Physiological reviews 79(4) (1999) 1283-1316.
[48] J. Björk, T. Hugli, G. Smedegård, Microvascular effects of anaphylatoxins C3a and C5a, The Journal of Immunology 134(2) (1985) 1115-1119.
[49] R. Clark, P. Henson, The molecular and cellular biology of wound repair. Plenum Press, New York (1996).
[50] D.L. Stocum, Regenerative biology and medicine, Academic Press2012.
[51] T.K.H.a.Z. Hussain, Wound Microenvironmemt, in: I.K. Cohen, R.F. Die-gelmann, W.J. Lindblad, N.E. Hugo (Eds.), Wound Healing: Biochemical and Clinical Aspects, Philadelphia, 1992.
[52] A.E. Koch, P.J. Polverini, S.L. Kunkel, L.A. Harlow, L.A. DiPietro, V.M. Elner, S.G. Elner, R.M. Strieter, Interleukin-8 as a macrophage-derived mediator of angiogenesis, SCIENCE-NEW YORK THEN WASHINGTON- 258 (1992) 1798-1798.
[53] D. Greiling, R. Clark, Fibronectin provides a conduit for fibroblast transmigration from collagenous stroma into fibrin clot provisional matrix, Journal of cell science 110(7) (1997) 861-870.
[54] C. Fathke, L. Wilson, J. Hutter, V. Kapoor, A. Smith, A. Hocking, F. Isik, Contribution of bone marrow–derived cells to skin: collagen deposition and wound repair, Stem cells 22(5) (2004) 812-822.
[55] G. Song, D.T. Nguyen, G. Pietramaggiori, S. Scherer, B. Chen, Q. Zhan, R. Ogawa, I. Yannas, A.J. Wagers, D.P. Orgill, Use of the parabiotic model in studies of cutaneous wound healing to define the participation of circulating cells, Wound repair and regeneration 18(4) (2010) 426-432.
[56] J. Verstappen, C. Katsaros, A.M. Kuijpers-Jagtman, R. Torensma, J.W. Von den Hoff, The recruitment of bone marrow-derived cells to skin wounds is independent of wound size, Wound repair and regeneration 19(2) (2011) 260-267.
[57] R. Yamaguchi, Y. Takami, Y. Yamaguchi, S. Shimazaki, Bone marrow-derived myofibroblasts recruited to the upper dermis appear beneath regenerating epidermis after deep dermal burn injury, Wound repair and regeneration 15(1) (2007) 87-93.
[58] M.G. Tonnesen, X. Feng, R.A. Clark, Angiogenesis in wound healing, Journal of Investigative Dermatology Symposium Proceedings, Elsevier, 2000, pp. 40-46.
[59] D. Whitby, M. Ferguson, The extracellular matrix of lip wounds in fetal, neonatal and adult mice, Development 112(2) (1991) 651-668.
[60] M.W.a.M.R. Bernfield, Proteoglycan glycoconjugates, in: I.K. Cohen, R.F. Die-gelmann, W.J. Lindblad, N.E. Hugo (Eds.), Wound Healing: Biochemical and Clinical Aspects, Philadelphia, 1992, p. 926.
[61] D.J. Geer, S.T. Andreadis, A novel role of fibrin in epidermal healing: plasminogen-mediated migration and selective detachment of differentiated keratinocytes, Journal of investigative dermatology 121(5) (2003) 1210-1216.

[62] S.F. Badylak, The extracellular matrix as a biologic scaffold material, Biomaterials 28(25) (2007) 3587-3593.
[63] M.M. Martino, F. Tortelli, M. Mochizuki, S. Traub, D. Ben-David, G.A. Kuhn, R. Müller, E. Livne, S.A. Eming, J.A. Hubbell, Engineering the growth factor microenvironment with fibronectin domains to promote wound and bone tissue healing, Science translational medicine 3(100) (2011) 100ra89-100ra89.
[64] H. Sinno, S. Prakash, Complements and the wound healing cascade: an updated review, Plastic surgery international 2013 (2013).
[65] T.N. Demidova-Rice, M.R. Hamblin, I.M. Herman, Acute and impaired wound healing: pathophysiology and current methods for drug delivery, part 1: normal and chronic wounds: biology, causes, and approaches to care, Advances in skin & wound care 25(7) (2012) 304.
[66] S. Herrick, P. Sloan, M. McGurk, L. Freak, C. McCollum, M. Ferguson, Sequential changes in histologic pattern and extracellular matrix deposition during the healing of chronic venous ulcers, The American journal of pathology 141(5) (1992) 1085.
[67] F. Grinnell, M. Zhu, Fibronectin degradation in chronic wounds depends on the relative levels of elastase, α1-proteinase inhibitor, and α2-macroglobulin, Journal of investigative dermatology 106(2) (1996) 335-341.
[68] G. Lauer, S. Sollberg, M. Cole, T. Krieg, S.A. Eming, I. Flamme, J. Stürzebecher, K. Mann, Expression and proteolysis of vascular endothelial growth factor is increased in chronic wounds, Journal of Investigative Dermatology 115(1) (2000) 12-18.
[69] D.J. Leaper, G. Schultz, K. Carville, J. Fletcher, T. Swanson, R. Drake, Extending the TIME concept: what have we learned in the past 10 years?, International wound journal 9(s2) (2012) 1-19.
[70] R.D. Galiano, O.M. Tepper, C.R. Pelo, K.A. Bhatt, M. Callaghan, N. Bastidas, S. Bunting, H.G. Steinmetz, G.C. Gurtner, Topical vascular endothelial growth factor accelerates diabetic wound healing through increased angiogenesis and by mobilizing and recruiting bone marrow-derived cells, The American journal of pathology 164(6) (2004) 1935-1947.
[71] M.A. Loots, E.N. Lamme, J. Zeegelaar, J.R. Mekkes, J.D. Bos, E. Middelkoop, Differences in cellular infiltrate and extracellular matrix of chronic diabetic and venous ulcers versus acute wounds, Journal of Investigative Dermatology 111(5) (1998) 850-857.
[72] K. Lundqvist, A. Schmidtchen, Immunohistochemical studies on proteoglycan expression in normal skin and chronic ulcers, British Journal of Dermatology 144(2) (2001) 254-259.
[73] J. Tam, Y. Wang, W.A. Farinelli, J. Jiménez-Lozano, W. Franco, F.H. Sakamoto, E.J. Cheung, M. Purschke, A.G. Doukas, R.R. Anderson, Fractional skin harvesting: autologous skin grafting without donor-site morbidity, Plastic and Reconstructive Surgery Global Open 1(6) (2013).
[74] C.K. Field, M.D. Kerstein, Overview of wound healing in a moist environment, The American journal of surgery 167(1) (1994) S2-S6.
[75] M. Mir, M.N. Ali, A. Barakullah, A. Gulzar, M. Arshad, S. Fatima, M. Asad, Synthetic polymeric biomaterials for wound healing: a review, Progress in biomaterials 7(1) (2018) 1-21.
[76] D.T. Ubbink, H. Vermeulen, A. Goossens, R.B. Kelner, S.M. Schreuder, M.J. Lubbers, Occlusive vs gauze dressings for local wound care in surgical patients: a randomized clinical trial, Archives of Surgery 143(10) (2008) 950-955.
[77] N.J. Turner, S.F. Badylak, The use of biologic scaffolds in the treatment of chronic nonhealing wounds, Advances in wound care 4(8) (2015) 490-500.
[78] A.S. Halim, T.L. Khoo, S.J.M. Yussof, Biologic and synthetic skin substitutes: An overview, Indian journal of plastic surgery: official publication of the Association of Plastic Surgeons of India 43(Suppl) (2010) S23.
[79] B. Cullen, R. Smith, E. Mcculloch, D. Silcock, L. Morrison, Mechanism of action of PROMOGRAN, a protease modulating matrix, for the treatment of diabetic foot ulcers, Wound Repair and Regeneration 10(1) (2002) 16-25.
[80] S.R. Myers, V.N. Partha, C. Soranzo, R.D. Price, H.A. Navsaria, Hyalomatrix: a temporary epidermal barrier, hyaluronan delivery, and neodermis induction system for keratinocyte stem cell therapy, Tissue engineering 13(11) (2007) 2733-2741.

[81] L.E. Dickinson, S. Gerecht, Engineered biopolymeric scaffolds for chronic wound healing, Frontiers in physiology 7 (2016).
[82] D. Ulrich, R. Smeets, F. Unglaub, M. Wöltje, N. Pallua, Effect of oxidized regenerated cellulose/collagen matrix on proteases in wound exudate of patients with diabetic foot ulcers, Journal of Wound Ostomy & Continence Nursing 38(5) (2011) 522-528.
[83] G. Galassi, P. Brun, M. Radice, R. Cortivo, G.F. Zanon, P. Genovese, G. Abatangelo, In vitro reconstructed dermis implanted in human wounds: degradation studies of the HA-based supporting scaffold, Biomaterials 21(21) (2000) 2183-2191.
[84] N.J. Turner, C.M. Kielty, M.G. Walker, A.E. Canfield, A novel hyaluronan-based biomaterial (Hyaff-11®) as a scaffold for endothelial cells in tissue engineered vascular grafts, Biomaterials 25(28) (2004) 5955-5964.
[85] L. Gould, P. Abadir, H. Brem, M. Carter, T. Conner-Kerr, J. Davidson, L. DiPietro, V. Falanga, C. Fife, S. Gardner, Chronic wound repair and healing in older adults: current status and future research, Wound Repair and Regeneration 23(1) (2015) 1-13.
[86] D.M. Yoon, J.P. Fisher, Natural and synthetic polymeric scaffolds, Biomedical Materials, Springer2009, pp. 415-442.
[87] E.P. Brennan, X.H. Tang, A.M. Stewart-Akers, L.J. Gudas, S.F. Badylak, Chemoattractant activity of degradation products of fetal and adult skin extracellular matrix for keratinocyte progenitor cells, Journal of tissue engineering and regenerative medicine 2(8) (2008) 491-498.
[88] J.P. Hodde, S.F. Badylak, A.O. Brightman, S.L. Voytik-Harbin, Glycosaminoglycan content of small intestinal submucosa: a bioscaffold for tissue replacement, Tissue engineering 2(3) (1996) 209-217.
[89] J. Hodde, D. Ernst, M. Hiles, An investigation of the long-term bioactivity of endogenous growth factor in OASIS Wound Matrix, Journal of wound care 14(1) (2005) 23-25.
[90] J. Hodde, R. Record, H. Liang, S. Badylak, Vascular endothelial growth factor in porcine-derived extracellular matrix, Endothelium 8(1) (2001) 11-24.
[91] D. Brett, A review of collagen and collagen-based wound dressings, Wounds 20(12) (2008) 347-356.
[92] S.a. Guo, L.A. DiPietro, Factors affecting wound healing, Journal of dental research 89(3) (2010) 219-229.
[93] T.H. Adair, J.-P. Montani, Overview of angiogenesis, Angiogenesis (2010) 1-8.
[94] D.M. Castilla, Z.-J. Liu, O.C. Velazquez, Oxygen: implications for wound healing, Advances in wound care 1(6) (2012) 225-230.
[95] A. Neve, F.P. Cantatore, N. Maruotti, A. Corrado, D. Ribatti, Extracellular matrix modulates angiogenesis in physiological and pathological conditions, BioMed research international 2014 (2014).
[96] A. Karamysheva, Mechanisms of angiogenesis, Biochemistry (Moscow) 73(7) (2008) 751.
[97] M.J. Cross, L. Claesson-Welsh, FGF and VEGF function in angiogenesis: signalling pathways, biological responses and therapeutic inhibition, Trends in pharmacological sciences 22(4) (2001) 201-207.
[98] D.M. Ornitz, FGFs, heparan sulfate and FGFRs: complex interactions essential for development, Bioessays 22(2) (2000) 108-112.
[99] G.E. Davis, Affinity of integrins for damaged extracellular matrix: αvβ3 binds to denatured collagen type I through RGD sites, Biochemical and biophysical research communications 182(3) (1992) 1025-1031.
[100] J. Dixelius, L. Jakobsson, E. Genersch, S. Bohman, P. Ekblom, L. Claesson-Welsh, Laminin-1 promotes angiogenesis in synergy with fibroblast growth factor by distinct regulation of the gene and protein expression profile in endothelial cells, Journal of Biological Chemistry 279(22) (2004) 23766-23772.
[101] T. Lühmann, H. Hall, Cell guidance by 3D-gradients in hydrogel matrices: importance for biomedical applications, Materials 2(3) (2009) 1058-1083.
[102] S.J. Phillips, Physiology of wound healing and surgical wound care, ASAIO journal 46(6) (2000) S2-S5.

[103] D.A. Narmoneva, O. Oni, A.L. Sieminski, S. Zhang, J.P. Gertler, R.D. Kamm, R.T. Lee, Self-assembling short oligopeptides and the promotion of angiogenesis, Biomaterials 26(23) (2005) 4837-4846.
[104] K.A. Landman, A.Q. Cai, Cell proliferation and oxygen diffusion in a vascularising scaffold, Bulletin of mathematical biology 69(7) (2007) 2405-2428.
[105] E.L. Pardue, S. Ibrahim, A. Ramamurthi, Role of hyaluronan in angiogenesis and its utility to angiogenic tissue engineering, Organogenesis 4(4) (2008) 203-214.
[106] H.-J. Sung, C. Meredith, C. Johnson, Z.S. Galis, The effect of scaffold degradation rate on three-dimensional cell growth and angiogenesis, Biomaterials 25(26) (2004) 5735-5742.
[107] A. Callegari, S. Bollini, L. Iop, A. Chiavegato, G. Torregrossa, M. Pozzobon, G. Gerosa, P. De Coppi, N. Elvassore, S. Sartore, Neovascularization induced by porous collagen scaffold implanted on intact and cryoinjured rat hearts, Biomaterials 28(36) (2007) 5449-5461.
[108] A.V. Vashi, K.M. Abberton, G.P. Thomas, W.A. Morrison, A.J. O'connor, J.J. Cooper-White, E.W. Thompson, Adipose tissue engineering based on the controlled release of fibroblast growth factor-2 in a collagen matrix, Tissue Engineering 12(11) (2006) 3035-3043.
[109] C. Tonello, B. Zavan, R. Cortivo, P. Brun, S. Panfilo, G. Abatangelo, In vitro reconstruction of human dermal equivalent enriched with endothelial cells, Biomaterials 24(7) (2003) 1205-1211.
[110] R. Morishita, M. Aoki, N. Hashiya, K. Yamasaki, H. Kurinami, S. Shimizu, H. Makino, Y. Takesya, J. Azuma, T. Ogihara, Therapeutic angiogenesis using hepatocyte growth factor (HGF), Current gene therapy 4(2) (2004) 199-206.
[111] A.J. Rufaihah, N.A. Johari, S.R. Vaibavi, M. Plotkin, T. Kofidis, D. Seliktar, Dual delivery of VEGF and ANG-1 in ischemic hearts using an injectable hydrogel, Acta biomaterialia 48 (2017) 58-67.
[112] J.W. Wassenaar, R. Gaetani, J.J. Garcia, R.L. Braden, C.G. Luo, D. Huang, A.N. DeMaria, J.H. Omens, K.L. Christman, Evidence for mechanisms underlying the functional benefits of a myocardial matrix hydrogel for post-MI treatment, Journal of the American College of Cardiology 67(9) (2016) 1074-1086.
[113] C. Wiegand, U. Schönfelder, M. Abel, P. Ruth, M. Kaatz, U.-C. Hipler, Protease and pro-inflammatory cytokine concentrations are elevated in chronic compared to acute wounds and can be modulated by collagen type I in vitro, Archives of dermatological research 302(6) (2010) 419-428.
[114] C. Addi, F. Murschel, G. De Crescenzo, Design and use of chimeric proteins containing a collagen-binding domain for wound healing and bone regeneration, Tissue Engineering Part B: Reviews 23(2) (2017) 163-182.
[115] L.D. Lozeau, J. Grosha, D. Kole, F. Prifti, T. Dominko, T.A. Camesano, M.W. Rolle, Collagen tethering of synthetic human antimicrobial peptides cathelicidin LL37 and its effects on antimicrobial activity and cytotoxicity, Acta biomaterialia 52 (2017) 9-20.
[116] J.N. Mcheik, C. Barrault, G. Levard, F. Morel, F.-X. Bernard, J.-C. Lecron, Epidermal healing in burns: autologous keratinocyte transplantation as a standard procedure: update and perspective, Plastic and Reconstructive Surgery Global Open 2(9) (2014).
[117] Z. Zhang, B.B. Michniak-Kohn, Tissue engineered human skin equivalents, Pharmaceutics 4(1) (2012) 26-41.
[118] K. Vyas, H. Vasconez, Wound healing: biologics, skin substitutes, biomembranes and scaffolds, Healthcare, Multidisciplinary Digital Publishing Institute, 2014, pp. 356-400.
[119] S.o.T.a.A. OECD Environmental Health and Safety Publications, Guidance Document for the Conduct of Skin Absorption Studies, in: r.f.E.C.-O.a. Development (Ed.) Paris, France, 2004.
[120] M. Peck, D. Gebhart, N. Dusserre, T.N. McAllister, N. L'Heureux, The evolution of vascular tissue engineering and current state of the art, Cells Tissues Organs 195(1-2) (2012) 144-158.
[121] D. Cigognini, D. Gaspar, P. Kumar, A. Satyam, S. Alagesan, C. Sanz-Nogués, M. Griffin, T. O'Brien, A. Pandit, D.I. Zeugolis, Macromolecular crowding meets oxygen tension in human mesenchymal stem cell culture-A step closer to physiologically relevant in vitro organogenesis, Scientific Reports 6 (2016) 30746.

[122] M.C. Prewitz, A. Stißel, J. Friedrichs, N. Träber, S. Vogler, M. Bornhäuser, C. Werner, Extracellular matrix deposition of bone marrow stroma enhanced by macromolecular crowding, Biomaterials 73 (2015) 60-69.
[123] A.S. Zeiger, F.C. Loe, R. Li, M. Raghunath, K.J. Van Vliet, Macromolecular crowding directs extracellular matrix organization and mesenchymal stem cell behavior, PloS one 7(5) (2012) e37904.
[124] A. Satyam, P. Kumar, X. Fan, A. Gorelov, Y. Rochev, L. Joshi, H. Peinado, D. Lyden, B. Thomas, B. Rodriguez, M. Raghunath, A. Pandit, D. Zeugolis, Macromolecular crowding meets tissue engineering by self-assembly: A paradigm shift in regenerative medicine, Advanced Materials 26(19) (2014) 3024-3034.
[125] J.F. Bateman, J.J. Pillow, T. Mascara, S. Medvedec, J.A. Ramshaw, W. Cole, Cell-layer-associated proteolytic cleavage of the telopeptides of type I collagen in fibroblast culture, Biochemical Journal 245(3) (1987) 677-682.
[126] R.J. Ellis, Macromolecular crowding: obvious but underappreciated, Trends in biochemical sciences 26(10) (2001) 597-604.
[127] R.R. Lareu, K.H. Subramhanya, Y. Peng, P. Benny, C. Chen, Z. Wang, R. Rajagopalan, M. Raghunath, Collagen matrix deposition is dramatically enhanced in vitro when crowded with charged macromolecules: the biological relevance of the excluded volume effect, FEBS letters 581(14) (2007) 2709-2714.
[128] R. Rashid, N.S.J. Lim, S.M.L. Chee, S.N. Png, T. Wohland, M. Raghunath, Novel use for polyvinylpyrrolidone as a macromolecular crowder for enhanced extracellular matrix deposition and cell proliferation, Tissue Engineering Part C: Methods 20(12) (2014) 994-1002.
[129] A. Christiansen, Q. Wang, A. Samiotakis, M.S. Cheung, P. Wittung-Stafshede, Factors defining effects of macromolecular crowding on protein stability: an in vitro/in silico case study using cytochrome c, Biochemistry 49(31) (2010) 6519-6530.
[130] L.A. Benton, A.E. Smith, G.B. Young, G.J. Pielak, Unexpected effects of macromolecular crowding on protein stability, Biochemistry 51(49) (2012) 9773-9775.
[131] C. Chen, F. Loe, A. Blocki, Y. Peng, M. Raghunath, Applying macromolecular crowding to enhance extracellular matrix deposition and its remodeling in vitro for tissue engineering and cell-based therapies, Advanced drug delivery reviews 63(4) (2011) 277-290.
[132] H. Booij, H. Schoffeleers, M. Haex, Effect of polydispersity on the shear rate dependence of the intrinsic viscosity of flexible linear polymers, Macromolecules 24(11) (1991) 3334-3339.
[133] X. Ye, T. Sridhar, Effects of the polydispersity on rheological properties of entangled polystyrene solutions, Macromolecules 38(8) (2005) 3442-3449.
[134] P. Kumar, A. Satyam, X. Fan, E. Collin, Y. Rochev, B.J. Rodriguez, A. Gorelov, S. Dillon, L. Joshi, M. Raghunath, Macromolecularly crowded in vitro microenvironments accelerate the production of extracellular matrix-rich supramolecular assemblies, Scientific reports 5 (2015) 8729.
[135] T. Laurent, A. Ogston, The interaction between polysaccharides and other macromolecules. 4. The osmotic pressure of mixtures of serum albumin and hyaluronic acid, Biochemical Journal 89(2) (1963) 249.
[136] T.C. Laurent, An early look at macromolecular crowding, Biophysical chemistry 57(1) (1995) 7-14.
[137] M.M. Hansen, L.H. Meijer, E. Spruijt, R.J. Maas, M.V. Rosquelles, J. Groen, H.A. Heus, W.T. Huck, Macromolecular crowding creates heterogeneous environments of gene expression in picolitre droplets, Nature nanotechnology 11(2) (2016) 191.
[138] I. Kuznetsova, B. Zaslavsky, L. Breydo, K. Turoverov, V. Uversky, Beyond the excluded volume effects: mechanistic complexity of the crowded milieu, Molecules 20(1) (2015) 1377-1409.
[139] M. Golkaram, S. Hellander, B. Drawert, L.R. Petzold, Macromolecular crowding regulates the gene expression profile by limiting diffusion, PLoS computational biology 12(11) (2016) e1005122.
[140] M. Tabaka, T. Kalwarczyk, J. Szymanski, S. Hou, R. Holyst, The effect of macromolecular crowding on mobility of biomolecules, association kinetics, and gene expression in living cells, Frontiers in Physics 2 (2014) 54.

[141] M.J. Morelli, R.J. Allen, P.R. Ten Wolde, Effects of macromolecular crowding on genetic networks, Biophysical journal 101(12) (2011) 2882-2891.
[142] P. Benny, C. Badowski, E.B. Lane, M. Raghunath, Making more matrix: enhancing the deposition of dermal–epidermal junction components in vitro and accelerating organotypic skin culture development, using macromolecular crowding, Tissue Engineering Part A 21(1-2) (2014) 183-192.
[143] M. Patrikoski, M.H.C. Lee, L. Mäkinen, X.M. Ang, B. Mannerström, M. Raghunath, S. Miettinen, Effects of Macromolecular Crowding on Human Adipose Stem Cell Culture in Fetal Bovine Serum, Human Serum, and Defined Xeno-Free/Serum-Free Conditions, Stem cells international 2017 (2017) 6909163.
[144] Y. Peng, M.T. Bocker, J. Holm, W.S. Toh, C.S. Hughes, F. Kidwai, G.A. Lajoie, T. Cao, F. Lyko, M. Raghunath, Human fibroblast matrices bio-assembled under macromolecular crowding support stable propagation of human embryonic stem cells, Journal of tissue engineering and regenerative medicine 6(10) (2012) e74-e86.
[145] J. Baldwin, M. Antille, U. Bonda, E.M. De-Juan-Pardo, K. Khosrotehrani, S. Ivanovski, E.B. Petcu, D.W. Hutmacher, In vitro pre-vascularisation of tissue-engineered constructs A co-culture perspective, Vascular cell 6(1) (2014) 13.
[146] N. Saeidi, K.P. Karmelek, J.A. Paten, R. Zareian, E. DiMasi, J.W. Ruberti, Molecular crowding of collagen: a pathway to produce highly-organized collagenous structures, Biomaterials 33(30) (2012) 7366-7374.
[147] B.A. Mast, R.F. Diegelmann, T.M. Krummel, I.K. Cohen, Hyaluronic acid modulates proliferation, collagen and protein synthesis of cultured fetal fibroblasts, Matrix 13(6) (1993) 441-446.
[148] M.R. Monteiro, I.L. dos Santos Tersario, S.V. Lucena, Culture of human dermal fibroblast in the presence of hyaluronic acid and polyethylene glycol: effects on cell proliferation, collagen production, and related enzymes linked to the remodeling of the extracellular matrix, Surg Cosmet Dermatol 5(3) (2013) 222-5.
[149] J.P. Berezney, O.A. Saleh, Electrostatic effects on the conformation and elasticity of hyaluronic acid, a moderately flexible polyelectrolyte, Macromolecules 50(3) (2017) 1085-1089.
[150] A. La Gatta, M. De Rosa, I. Marzaioli, T. Busico, C. Schiraldi, A complete hyaluronan hydrodynamic characterization using a size exclusion chromatography–triple detector array system during in vitro enzymatic degradation, Analytical biochemistry 404(1) (2010) 21-29.
[151] C.B. Knudson, W. Knudson, Hyaluronan-binding proteins in development, tissue homeostasis, and disease, The FASEB Journal 7(13) (1993) 1233-1241.
[152] C.A. Cooper, K.K. Brown, C.D. Meletis, N. Zabriskie, Inflammation and hyaluronic acid, Alternative & complementary therapies 14(2) (2008) 78-84.
[153] L.L. Huang-Lee, J.H. Wu, M.E. Nimni, Effects of hyaluronan on collagen fibrillar matrix contraction by fibroblasts, Journal of Biomedical Materials Research Part A 28(1) (1994) 123-132.
[154] M. Hu, E.E. Sabelman, Y. Cao, J. Chang, V.R. Hentz, Three-dimensional hyaluronic acid grafts promote healing and reduce scar formation in skin incision wounds, Journal of Biomedical Materials Research Part B: Applied Biomaterials 67(1) (2003) 586-592.
[155] P. Ghosh, The role of hyaluronic acid (hyaluronan) in health and disease: interactions with cells, cartilage and components of synovial fluid, Clinical and experimental rheumatology 12(1) (1994) 75-82.
[156] D. Jiang, J. Liang, P.W. Noble, Hyaluronan as an immune regulator in human diseases, Physiological reviews 91(1) (2011) 221-264.
[157] G. Cao, R.C. Savani, M. Fehrenbach, C. Lyons, L. Zhang, G. Coukos, H.M. DeLisser, Involvement of endothelial CD44 during in vivo angiogenesis, The American journal of pathology 169(1) (2006) 325-336.
[158] F. Gao, C. Yang, W. Mo, Y. Liu, Y. He, Hyaluronan oligosaccharides are potential stimulators to angiogenesis via RHAMM mediated signal pathway in wound healing, Clinical & Investigative Medicine 31(3) (2008) 106-116.

[159] M. Smith, P. Ghosh, The synthesis of hyaluronic acid by human synovial fibroblasts is influenced by the nature of the hyaluronate in the extracellular environment, Rheumatology international 7(3) (1987) 113-122.
[160] B.P. Toole, R.L. Trelstad, Hyaluronate production and removal during corneal development in the chick, Developmental biology 26(1) (1971) 28-35.
[161] M. SOLURSH, M. FISHER, C.T. SINGLEY, The synthesis of hyaluronic acid by ectoderm during early organogenesis in the chick embryo, Differentiation 14(1-3) (1979) 77-85.
[162] Y. Phillip, E. Sherman, G. Haran, G. Schreiber, Common crowding agents have only a small effect on protein-protein interactions, Biophysical journal 97(3) (2009) 875-885.
[163] H.-X. Zhou, G. Rivas, A.P. Minton, Macromolecular crowding and confinement: biochemical, biophysical, and potential physiological consequences, Annu. Rev. Biophys. 37 (2008) 375-397.

Chapter 3 : Proteomic Analysis of Cell-Derived Matrices

3.1. Introduction

The extracellular matrix (ECM) microenvironment is a complex signaling network of fibrillar and non-fibrillar structural proteins, 2) glycoproteins and proteoglycans, 3) glycosaminoglycans, and 4) growth factors, which provide cells with chemical and mechanical signals to support cellular adhesion and growth, direct cell migration, and regulate differentiation [1, 2]. The overall assembly and organization of the ECM is controlled through a series of complex, yet fascinating, multi-molecular signaling processes. Collagen, for example, undergoes several post-translational modification, such as hydroxylation, terminal peptide cleavage, and crosslinking prior to its incorporation in the ECM [3-6]. After processing and incorporation into the ECM, collagen fibrils may undergo enzyme-mediated changes to support binding of other ECM proteins such as fibronectin through protein binding domains, thus providing binding sites for cellular adhesion [7, 8]. The presence of a polymerized fibronectin matrix also supports the incorporation of other ECM components, such a fibrillin [9], heparin [10], and fibrin [8]. Thus, it is evident that the ECM is an overcrowded environment, with various proteins of distinct chemical structure and interactions.

Due to its role as the largest biochemical and mechanical cellular signaling complex, the ECM has served as a design guideline for the development of engineered three-dimensional (3D) tissue scaffolds for remodeling and regeneration of damaged tissues. The bidirectional communication between cells and their microenvironment also provides insightful information into pathological and physiological conditions, as ECM dysregulation is indicative of disease progression [1]. And, through studying the ECM, several extracellular candidates have been identified as markers and therapeutics [11]. As a result of these complex interactions,

understanding these cell-cell, cell-matrix, and matrix-matrix interactions go beyond methods of independently assessing uni-molecular structures.

Proteomics provides a valuable research tool for the large-scale study of proteins. Mass spectrometry (MS) based-techniques have emerged as promising tools for sensitive, quantitative, and global analysis of proteins [12]. MS techniques are high-throughput approaches allowing the detection of femtomole amounts of peptides, and sequencing of thousands of peptides simultaneously [13]. This approach is often combined with reverse-phase high performance liquid chromatography (HPLC) to allow for separation of the ionized sample molecules, and thus allowing measurement of ion signal intensity.

Liquid chromatography/mass spectrometry (LC/MS/MS) techniques have been commonly used to separate and quantify protein composition. Extracellular and transmembrane proteins, however, present analytical challenges due to their biochemical structure, and insolubility in solution [1, 14]. Due to the large, dynamic range of analytes present in the multi-molecular ECM structure, strategies must be employed to increase the signal to noise ratio and enable the detection of the wide molecular range present in an ECM sample. Naba *et al.* developed a method for the depletion of cytosolic, nuclear, membrane, and cytoskeletal proteins, and the subsequent enrichment of ECM proteins [1]. This method has been successfully used to characterize ECM from several different tissues and tumor types [1], and cell-derived ECM [15]. Other techniques, such as *in-situ* digestion have also been used to separate and desalt a protein sample prior to LC/MS.

We utilized proteomics as a preliminary approach to characterize the ECM composition of CDMs developed under macromolecular crowding (MMC) conditions. Corresponding media samples from each cell layer sample were also analyzed to assess protein secretion into the

media. This approach provided a global analysis of how dermal fibroblasts are affected by addition of different macromolecules, and how macromolecular crowding sequesters precursor proteins. Proteomics provided preliminary results to motivate further studies, and also provided insight into cell-dependent responses to MMC in order to support development of CDM biomaterials using HMW HA as a macromolecular crowder.

3.2. Methods

3.2.1. Cell culture

Human dermal fibroblasts (HDF, ATCC, CRL 2097) were cultured as previously described in complete DMEM (Corning, 15-017 CV) supplemented with 10% v/v fetal bovine serum (Gibco, 16000-044) , 1% v/v penicillin/streptomycin (Corning, 30-002-Cl), 1% v/v non-essential amino acids (Corning, 25-025Cl), 1% L-glutamine (Corning, 25- 005Cl) and 1% v/v sodium pyruvate (Corning, 25-001-Cl). Cells were trypsinized and centrifuged. Supernatant was removed, and pellet was resuspended in complete DMEM, and maintained in T75 flasks.

3.2.2. Culture of cell-derived matrices (in vitro)

HDFs (p3-p8) were plated at a density of 25,000 cells/cm^2 at n = 4 wells/ condition and cultured in complete DMEM for 24 hours prior to culture with crowding media. Crowding media was supplemented with 0.05% w/v or 0.5% w/v high molecular weight hyaluronic acid (HA) (HA15M-5, 1.5MDa, LifeCore Biomedical, USA). Ficoll media was prepared by mixing 37.5 mg/mL Ficoll 70 (Sigma, F2878) and 40 mg/mL Ficoll 400 (Sigma, F4375) in standard DMEM. Crowded conditions were compared to a non-crowded treated negative control condition. All conditions were supplemented with 100 μM ascorbic acid (Wako, 013-19641). Cells were

cultured at standard culture conditions (37°C, 5% CO_2), and media was replaced every 2-3 days. CDMs were cultured for 14 days prior to protein harvest as this time point was expected to have the highest protein concentration for analysis.

3.2.3. Protein sample collection

Media was collected and pooled from n = 4 wells/condition, flash frozen in liquid nitrogen, and stored at -80°C until lyophilization. The samples were lyophilized at -55°C, -0.25°C/min ramp temperature, with a hold at -25°C. Media samples were reconstituted in RIPA buffer (ThermoFisher Scientific, 89900) supplemented with protease inhibitor (ThermoFisher Scientific, A32965) and phosphatase inhibitor tablet (ThermoFisher Scientific, A32957) at a final sample protein concentration of 65 mg/mL. Cell layers were rinsed three times with 1XDPBS prior to being collected. Cell layers were lysed in 50 µL RIPA buffer prepared as specified above on ice for 15minutes. Lysates from each condition were from n =4 wells to increase protein concentration. Samples were disrupted using a Missonix CL-2000 ultrasonic cell disruptor five times at power level 1. A Bradford assay was used to determine protein concentration. A bovine serum albumin (BSA) standard was prepared to calculate protein concentration of unknown experimental samples. Samples were loaded with 5X Lamelli Buffer (60mM Tris-HCl pH 6.8, 25% v/v glycerol, 2% v/v SDS, 0.1% v/v bromophenol

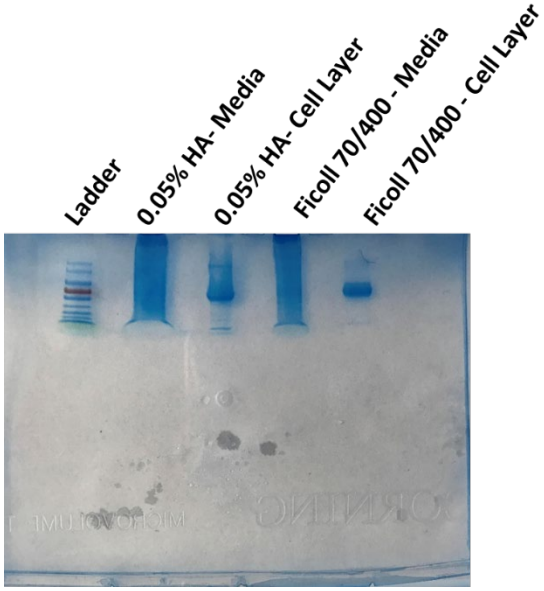

Figure 3-1: Cell layer and media samples for the 0.05% HA and Ficoll 70/400 conditions were loaded in a 4-20% acrylamide gradient gel and stained using FastBlue. The 0% and 0.5% HA conditions were loaded on a separate gradient gel (not shown). Short gel was run to allow for protein denaturation and separation for LC/MS sample preparation.

blue) and 5% v/v β-mercaptoethanol. All samples were boiled at 95°C and stored at -20°C until use.

3.2.4. SDS-PAGE and coomassie blue staining

Samples were loaded in a Biorad mini protean TGX 4-20% acrylamide gradient gel at a loading mass of 30 µg/condition. The non-treated control and the 0.5% HA cell layer and media samples were run on gel 1 with alternating lanes. The 0.05% and the Ficoll 70/400 cell layer and media samples were run on a separate gel **(Figure 3-1)**. Gels were run at 100V for 25 minutes, or until dye front reached 2 cm below each well to allow for protein separation and desalting. After short gel was run, it was rinsed in MilliQ water, and incubated in Fast Blue (ThermoFisher Scientific, LC6060) staining solution for 1 hour. Gel was destained using MilliQ water rinse prior to excising from the acrylamide gel. Protein was stored in MilliQ water, and immediately transferred to UMass Core Proteomics Facility located in Worcester, MA.

3.2.5. LC/MS proteomics and data analysis

LC/MS sample preparation was completed at the UMass Proteomics core facility according to their established protocols. Excised gel plugs were reduced, alkylated, and digested *in situ* followed by peptide extraction for LC/MS. Label free spectral count was completed on Thermo Scientific Q-Exactive w/Water NanoAcquity UPLC system. Tandem mass spectra were extracted. Charge state deconvolution and deisotoping were not performed as specified in the UMass protocol. All MS/MS samples were analyzed using Mascot, which was set up to search the SwissProt_Human database. Mascot was searched with a fragment mass tolerance of 0.05 Da and a parent ion tolerance of 10 ppm. Scaffold software was used to validate MS/MS based

peptide and protein identification. Peptides were accepted if they could be established at greater than 70% probability by the Peptide Prophet algorithm [16]. Protein probabilities were assigned by the protein prophet algorithm [17]; and proteins sharing significant peptides evidence were grouped into clusters. Proteins were annotated with GO terms from gene_associate.goa_uniprot.

Data are quantified and presented as a function of intensity based absolute quantification (iBAQ). This measure corresponds to the sum of all peptides intensities divided by the number of observable peptides of a protein [18]. Statistical analysis was not completed on this data set due to small sample size (N =1).

3.3. Results

3.3.1. Characterization of human cell-derived extracellular matrix

LC/MS techniques identified a total of 1, 840 proteins, of which 83 were identified as core matrisome proteins, and 76 identified as matrisome-associated proteins (**Figure 3-2**) across all experimental conditions. Core matrisome proteins include collagen, ECM glycoproteins, and proteoglycans [2, 19], and included a total of 17, 58, and 8 proteins, respectively. Matrisome-associated proteins includes ECM regulators, ECM-affiliated and secreted factors [2, 19], and accounted for 48, 15, and 13 total proteins, respectively.

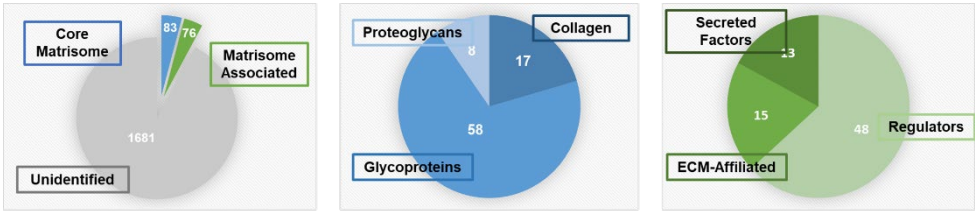

Category	# Proteins
Core Matrisome	83
Matrisome-Associated	76
Unidentified	1681
Total	**1840**

Core Matrisome	# Proteins
Collagen	17
ECM Glycoproteins	58
Proteoglycans	8
Total	**83**

Matrisome Associated	# Proteins
ECM Regulators	48
ECM Affiliated Proteins	15
Secreted Factors	13
Total	**76**

Figure 3-2: Characterization of the protein expression profile of CDMs developed under MMC conditions (0%, 0.05%, 0.5%, and Ficoll 70/400) for 14 days based on classifications from the Matrisome Project (Hynes Lab, MIT).

3.3.2. Quantification of ECM proteins in cell layer and media samples

Collagen types I, III, IV, V, VI, XII, XIV, XV, XVI, and XVIII were identified in the untreated as well as HA and Ficoll 70/400 treated cell layers of CDMs prepared at 14 days. Collagens type I, III, and IV are of specific interest due to their role in wound healing and angiogenesis. For collagen types I and III, the 0.05% HA cell layer sample had the highest iBAQ values compared to the control and other crowding conditions **(Figure 3-3 A-C)**. The 0.5% HA and Ficoll 70/400 had the lowest collagen type I iBAQ values, and were comparable in intensities **(Figure 3-3 A, C)**. Ficoll 70/400 had higher collagen type III compared to the 0.5% HA condition **(Figure 3-3 B)**. In addition to the cell layers, media samples indicated the presence of collagen types I and III in the in the non-crowded media condition **(Figure 3-3 A-C)**. Collagen secretion into the media decreased in the high and low HA conditions. Collagen was not present in the Ficoll 70/400 media condition. Collagen type IV had a different trend with 0.05% and Ficoll 70/400 having comparable collagen type IV signal. The media samples did not indicate the presence of collagen type IV **(Figure 3-3 D)**.

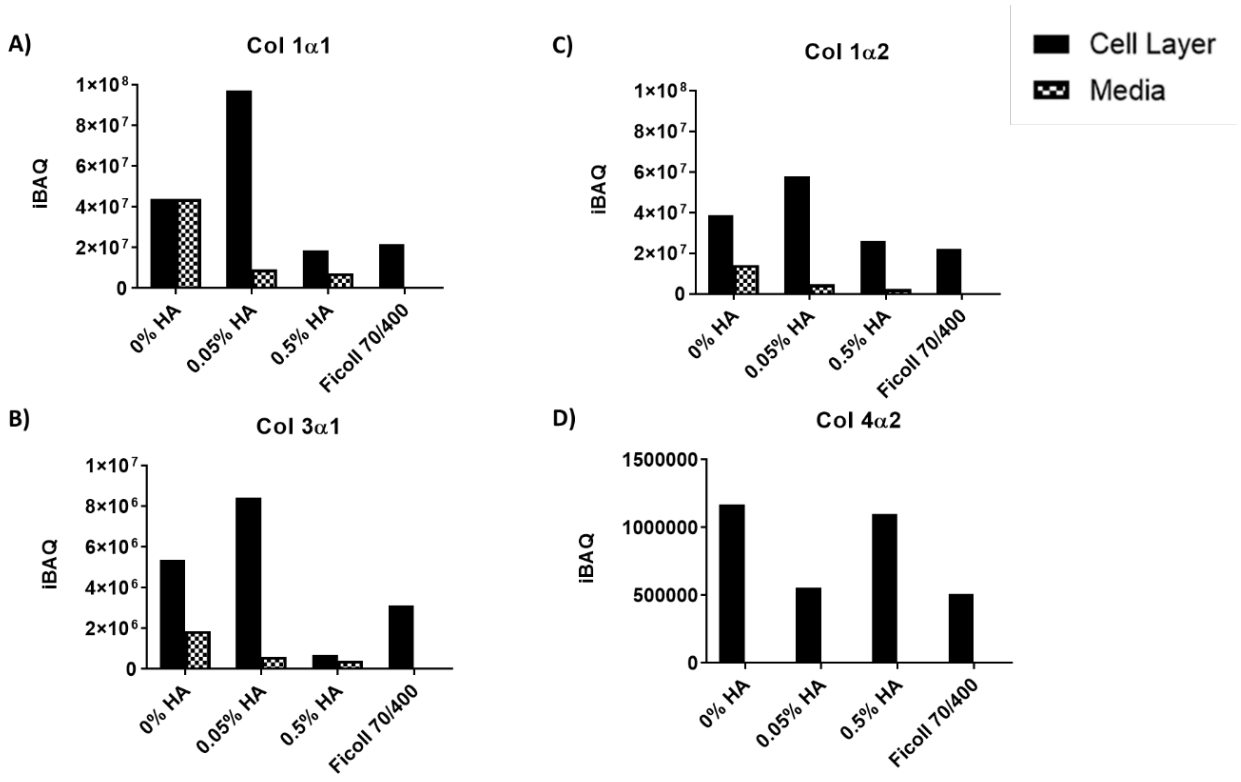

Figure 3-3: Peptide intensity quantified using iBAQ for collagen. **(A, C)** collagen type I, **(B)** collagen type III, and **(D)** collagen type IV present in the cell layer and media samples.

In addition to collagen in the ECM, fibronectin and laminin were also detected in the 14 day CDM samples **(Figure 3-4)**. Fibronectin intensity slightly increased in the presence of Ficoll 70/400, and had similar intensities in the high and low HA conditions **(Figure 3-4 A)**. Laminin indicated an increase intensity in the 0.05%, 0.5% and Ficoll 70/400 conditions compared to the non-treated control **(Figure 3-4 B)**. Laminin has the highest protein signal in the 0.5% HA condition and Ficoll 70/400. Overall, proteomics analysis indicates that HA crowding has an

effect on ECM proteins, such as collagen type I, III, IV, and laminin, compared to the untreated control.

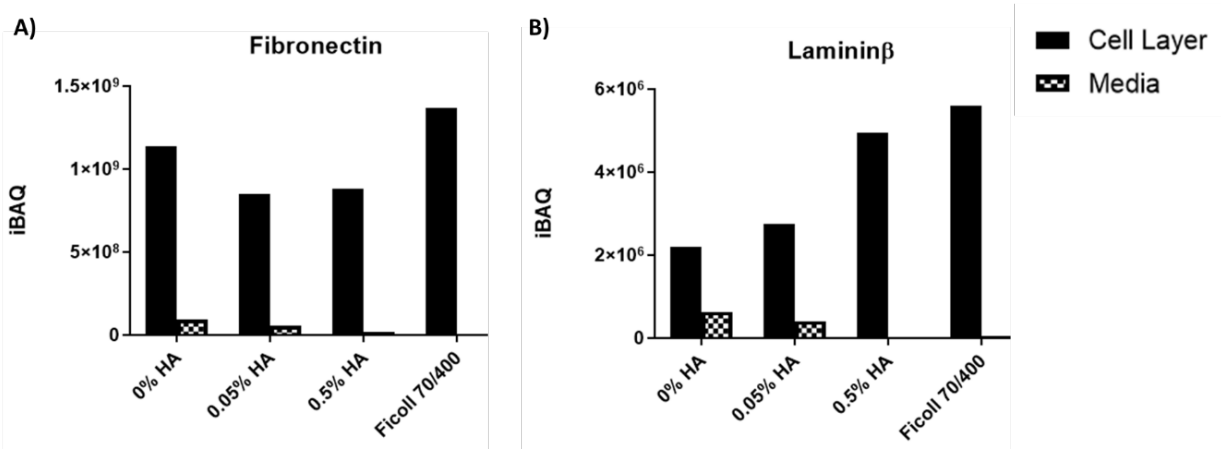

Figure 3-4: Peptide intensity quantified using iBAQ for glycoproteins. **(A)** fibronectin and **(B)** laminin present in the cell layer and media samples.

3.3.3. Quantification of crosslinking enzymes in cell layer and media samples

LC/MS analysis indicated the presence of matrix assembly and crosslinking enzymes **(Figure 3-5)**. PCOLCE-1 was heavily secreted into the media, with crowding conditions decreasing the presence of PCOLCE-1. POLCE was measured at the highest intensity in the 0.05% HA condition. PLOD1, 2, and PLOD3 were also present within the cell layers. PLOD1 and PLOD3 had reduced intensity in the 0.5% and Ficoll 70/400 condition compared to the non-treated control. PLOD2 had increased intensity in both the high and low HA conditions, but no signal was detected in the Ficoll 70/400 condition. LOX had similar expression in all conditions with the exception of the 0.05% HA.

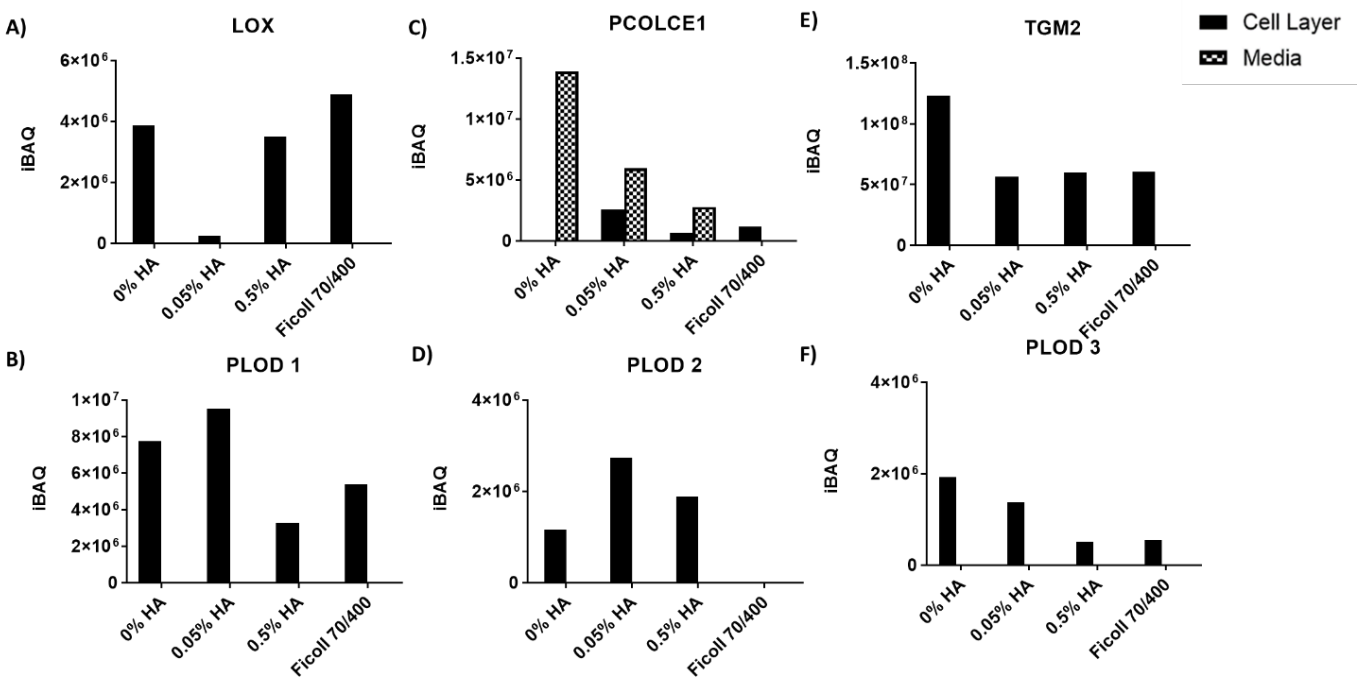

Figure 3-5: Peptide intensity quantified using iBAQ for ECM crosslinking enzymes. **(A)** LOX, **(C)** PCOLCE1, **(E)** TGM2, and **(B,D,F)** PLOD1, PLOD2, and PLOD3 in the cell layer and media samples.

3.3.4. Quantification of proteoglycans in cell layer and media samples

Two proteoglycnas were detected in the proteomics analysis: heparan sulfate and chondroitin sulfate **(Figure 3-6)**. Heparan sulfate had an increase in signal intensity in the 0.5% and Ficoll 70/400 condition. Chondroitin sulfate had the highest intensity at the 0.05% HA condition, and no signal was detected in the 0.5% HA condition. Ficoll 70/400 had comparable intensity to the non-treated control. HA, a non-sulfated glycosaminoglycan was not detected in HA treated or non-treated conditions, which may suggest that exogenous HA was not incorporated into the matrix.

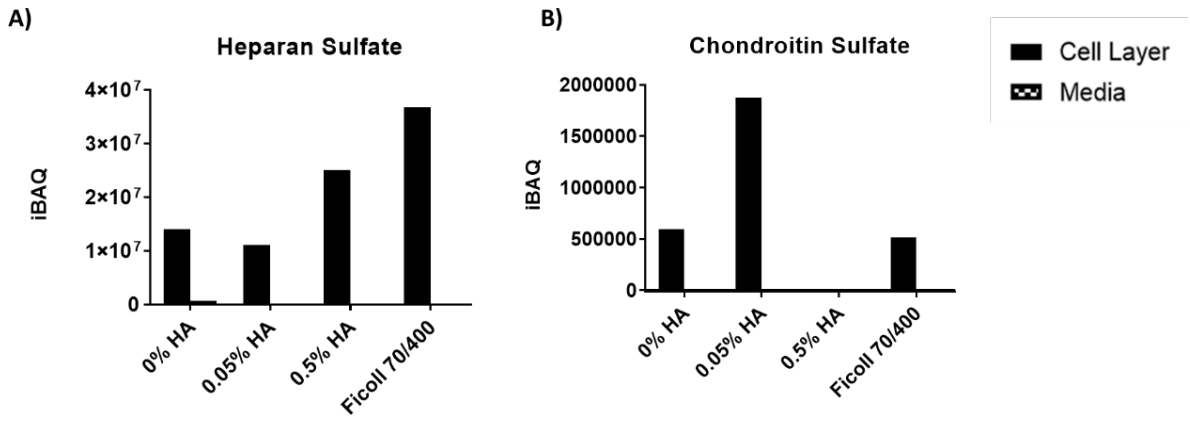

Figure 3-6: Peptide intensity quantified using iBAQ for glycosaminoglycans. **(A)** heparan sulfate and **(B)** chondroitin sulfate present in the cell layer and media samples.

3.3.5. Quantification of MMPs and TIMPs in cell Layer and media samples

MMP1, 2, and 3 as well as TIMP1 were expressed in dermal fibroblasts cultured under MMC conditions **(Figure 3-7)**. MMP1, 2, and 3 greatly increased in the presence of Ficoll 70/400, with the 0.05% and 0.5% HA conditions having minimal MMP expression. This indicates that HA did not induce the expression of MMP. MMP expression was also detected in the media samples with the lowest secretion of MMP present in crowded samples. TIMP1 was expressed in all cell layers, however, a large increase between the crowded conditions and the control were not observed. Crowding also helped sequester TIMP3 at the cell layer, rather than being discarded into the media as waste.

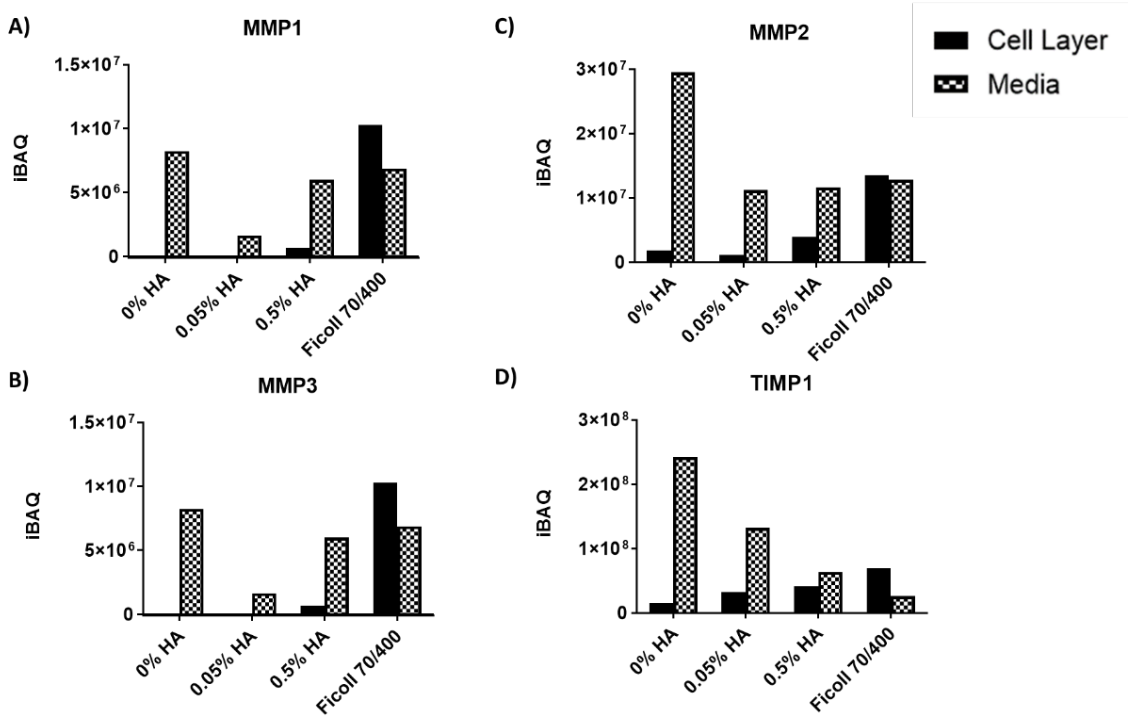

Figure 3-7: Peptide intensity quantified using iBAQ for matrix proteinases. **(A-C)** MMP1, 2, and 3; **(D)** TIMP1 present in the cell layer and media samples.

3.3.6. Presence of pro-angiogenic Molecules

Proteomic analysis indicated the presence of pro- and anti-angiogenic proteins present in the CDM. Twenty proteins, including several ECM-associated proteins were specific to angiogenesis. Three proteins were identified as anti-angiogenic. Several ECM molecules that were previously discussed, such as laminin, collagen, fibrin, and fibronectin, were also present at varying degrees in the sample. Anti-angiogenic factors were also detected and include molecules such as thrombospondin and angiopoietin. A complete list of pro- and anti-angiogenic molecules is included in **Table 3-1**.

3.3.7. Expression of CD44 on Human Dermal Fibroblasts

CD44 is a cell-surface glycoprotein that has been identified as a receptor for hyaluronic acid [20]. HA-CD44 binding is involved in wound repair and extracellular matrix remodeling during embryogenesis [21], and thus it was hypothesized that HA would promote ECM deposition due to its biochemical interaction. Proteomics indicated the presence of CD44 in the cell layer of human dermal fibroblasts (all conditions, **Figure 3-8)**. There are several CD44 isoforms that have been reported in literature [20]. The CD44 isoform detected in these samples was CD44v10. Crowding is not expected to have an effect on receptor expression, however the 0.05% HA condition has the highest iBAQ value compared to the other conditions.

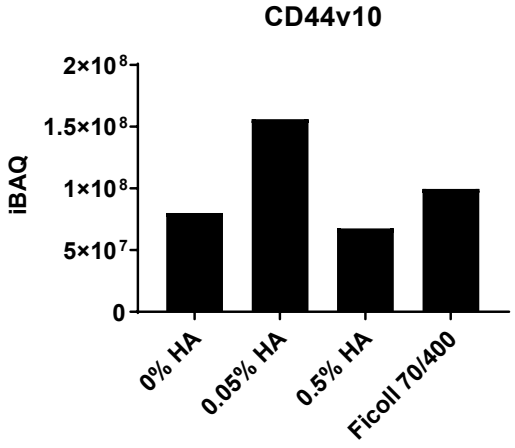

Figure 3-8: Expression of CD44v10 in human dermal fibroblasts.

3.4. Discussion

Proteomics provides a valuable research tool for the global analysis of the ECM protein composition, defined as the "matrisome", as previously coined by Naba *et al* [1, 2, 14]. These techniques, which have been widely used to characterize the ECM of diseased and normal tissue, have been applied to study stromal cell-derived ECM composition [15]. We used this approach for assessing the composition of cell-derived ECM developed under different macromolecular crowding conditions, as well as for diffusion of valuable ECM pre-cursor proteins into the media. This provided us with preliminary results to support the use of HA as a MMC agent for development of CDM biomaterials.

Dermal fibroblasts produced an insoluble ECM after 14 days in culture with ascorbate supplemented HA or Ficoll-based MMC media. Prior to LC/MS analysis, proteins must be solubilized and digested into peptides. However, due to the crosslinked, covalently bonded, and highly glycosylated nature of ECM proteins, traditional solubilizing approaches are not compatible with ECM proteins. There are two approaches recommended for the digestion of ECM proteins. The first is using in solution digestion. In this approach, proteins are solubilized and digested in series of solutions and buffers to allow for digestion and deglycosylation of the protein sample [15]. The second approach used by our contractors, UMass Memorial Medical School, is through in-gel digestion. After separation on a short gel, bands were excised and sent to UMass for in gel digestion, protein reduction, extraction, and LC/MS analysis.

A total of 1,840 proteins were identified at a 90% minimum protein threshold, and 0.1% Prophet false discovery rate. As these samples were collected without decellularization, cellular, nuclear, and cytosolic proteins are also present in the analysis. Albumin was also present in a high ratio due to culturing cells with FBS. However, compared to the other different LC/MS methods, presence of serum is not a significant issue in label free proteomics as its factored into the control sample. Serum may also increase the noise present in the sample, but does not affect the quantification in the label-free method.

Defining the extracellular matrix using proteomics generates a data-rich lists from which proteins of interest were defined using gene ontology categories. However, this was problematic due to several unannotated ECM proteins, and the presence of other categories that incorrectly annotated some ECM proteins [19]. In 2012, the Hynes Lab at MIT defined tissue ECM composition using a bioinformatic approach to predict sets of genes within the matrisome [19]. The matrisome, or the components that comprised the ECM, was categorized into: 1) core

matrisome, and 2) matrisome-associated proteins. Within those categories, proteins were classified as collagens, glycoproteins, proteoglycans, secreted factors, regulators, and ECM-affiliated proteins [19]. Using this approach, core matrisome and matrisome-associated proteins were identified in the CDM developed under MMC. Glycoproteins and ECM-regulators were primarily identified in the core-matrisome and matrisome associated categories, respectively **(Figure 3-2).** Of the 28 collagens identified in mammals, 17 were identified in the CDMs. Collagen types I, III, and IV play the most significant roles in dermal wound repair [22-24], and promotion of angiogenesis [25] were identified at different intensities in each condition tested. Collagen types I and III had the highest expression in the 0.05% HA condition **(Figure 3-3 A-C)**. Both collagen type I alpha-1 and alpha-2 chains were detected, with collagen alpha-1 chains having higher intensity than the alpha-2 in the 0.05% HA condition only. Alternatively, collagen type IV, a basement membrane collagen had the lowest deposition in the 0.05% and Ficoll 70/400 conditions **(Figure 3-3 D)**. In addition to the differential collagen secretion due to presence of crowder type, LC/MS also provided evidence supporting the theory of crowding to limit the diffusion of ECM molecules into the media. The non-crowded condition had the highest intensity of collagen type I and III in the media compared to crowded conditions. While HA-treated samples still indicate the presence of collagen molecules in the media, it was still less than the collagen present in the non-treated control.

Collagen fiber assembly is regulated by different factors, which include post-translational modifications, such as hydroxylation [5, 26, 27] , glycosylation [27], crosslinking [27], and pro-peptide processing [4, 27]; interaction with other matrix components, such as fibronectin; and intracellular modifications [28]. Enzymes, such as lysyl oxidase (LOX), procollagen C-endopeptidase enhancer (PCOLCE1), transglutaminase (TGM2), and procollagen-lysine,2-

oxoglutarate 5-dioxygenase 1 (PLOD) are involved in the post-translational modification of collagen. These enzymes were detected in the CDMs developed under MMC and were differentially expressed depending on the type of crowder used. LOX is an enzyme that mediates formation of collage crosslinks in the extracellular space [29]. Proteomics data indicates that LOX expression was decreased in the 0.05% HA samples compared to the other conditions tested **(Figure 3-5 A)**. However, as we will see in future chapters, the increase in crosslinked collagen present in the 0.05% HA concentration compared to the non-treated and Ficoll 70/400 conditions suggests otherwise, and that follow up studies assessing LOX expression should be completed. PLOD is an intracellular enzyme that catalyzes lysyl hydroxylation prior the formation of the triple helical procollagen molecule [29]. PLOD1, 2, and 3 expression was also dependent on the crowder condition. PLOD 1 and 2 had the highest expression in the 0.05% HA condition, which suggests an increase in crosslinked collagen observed in this condition **(Figure 3-5 B, D, F)**. Alternatively, PLOD3 had a decreased expression pattern under crowding conditions. PCOLCE1, which regulates the enzymatic cleavage of procollagen and increases C-proteinase activity [30], appears to have been secreted into the media in the non-treated control, and sequestered onto the cell layer in the HA and Ficoll 70/400 conditions **(Figure 3-5 C)**. Furthermore, both macromolecules appeared to have reduced the diffusion of the enzyme into the media, thus supporting the use of HA for limiting enzyme diffusion. TGM2 stabilizes collagen assembly through the formation of lysine-based crosslinks, and thus plays a role in collagen crosslinking [31]. TGM expression was highest in the non-treated control, and decreased in the presence of crowder molecules **(Figure 3-5 C)**. The crowder type did not alter TGM expression.

Additional ECM proteins that play a role in the healing cascade, fibronectin and laminin, were also detected. Fibronectin deposition decreased in the HA crowded conditions compared to the non-treated control, and Ficoll 70/400 had higher intensity **(Figure 3-4 A)**. Fibronectin deposition is mediated by the enzyme TGM through TGF-β and interaction with its gelatin-binding domain [32], thus indicating an enzyme-mediated dependence. TGM2 expression supported the high level of fibronectin in the non-treated control, however, fibronectin expression in the crowded conditions was not altered despite the decrease in TGM. Alternatively, laminin deposition increased in the presence of HA and Ficoll 70/400 crowding, with the highest intensity present in the 0.5% HA and Ficoll 70/400 conditions **(Figure 3-4 B)**. Laminin was also detected in the non-treated and 0.05% media conditions.

Glycosaminoglycans (GAGs) are long chains of repeating disaccharide units often found bound to protein cores to form proteoglycans. Chondroitin sulfate (CS) PGs have been shown to assist in collagen polymerization [33], and heparan sulfate (HS) PGs supporting cellular binding to the assembled matrix [34]. Degradation of PG, specifically CS PG [35] and HS PG [36], by proteases secreted in the wound bed has also been shown to modulate proangiogenic responses. HS PGs and CS PGs were present in the CDMs **(Figure 3-6 A-B)**. HS PG increased expression in the presence of 0.5% HA and Ficoll 70/400 compared to the non-treated control and 0.05% HA conditions. CS PG had the highest expression in the 0.05% HA condition. However, it appears that 0.5% HA did not secrete CS PG, possibly suggesting that an elevated viscosity had an adverse effect on CS PG production.

MMP and TIMP expression provide a balance in matrix deposition and assembly *in vivo,* and have been shown to play a role in angiogenesis [37]. MMP1, 2, and 3 expression within the cell layer was increased in the Ficoll 70/400 conditions compared to HA crowding, which did not

increase MMP expression compared to the non-treated control **(Figure 3-7 A-C)**. Alternatively, MMPs were secreted into the media in the non-treated conditions. HA reduced MMP secretion, and did not shown any retention of MMPs at the cell layer, suggesting reduced MMP production. TIMP expression at the cell layer was increased in the presence of crowders compared to the non-treated condition **(Figure 3-7 D)**. Furthermore, TIMP secretion into the media was reduced in the presence of HA and Ficoll 70/400 crowding. In addition to the MMP and TIMP role in matrix deposition, they also play a role in endothelial cell migration and capillary network formation.

Angiogenesis is a highly controlled physiological condition regulated by a balance of angiogenesis stimulating and inhibiting factors. There have been several factors reported in literature that regulate angiogenesis, such as fibroblast growth factors (FGF) [38], transforming growth factor (TGF) [39], hepatocyte growth factor (HGF) [40], tumor necrosis factor (TNFα) [41], and angiopoietins [40], however, these factors are not specific to endothelial cells, and can be secreted by other cells involved in the wound healing process [42]. In addition to those factors, angiogenesis is strongly regulated by the presence of VEGF. As HA plays a role in VEGF production, it was initially hypothesized that HA treatment may induce VEGF secretion via its binding to CD44 , thus stimulating endothelial cell proliferation and sprouting [43]. While dermal fibroblasts expressed an isoform of CD44 **(Figure 3-8)**, proteomics analysis did not indicate the presence of VEGF in the human CDM developed under MMC. ECM components that play a role in angiogenesis, such as collagen, laminin, and fibronectin, were identified in the matrix to different levels of expression. Other research groups have also reported factors as angiogenesis stimulating [25, 44] and inhibiting [44], of which several of those factors were identified in the CDM developed under crowding conditions **(Table 3-1)**. Microvascular

regression is also tightly regulated as angiogenesis inhibitor molecules can cause cells to apoptose [45, 46], alter the composition of the ECM within the microenvironment [47], and reduce EC migration [48].

In summary, a label-free method was used to preliminarily quantify the ECM composition of CDMs developed under MMC conditions, as well as ECM pre-cursor proteins that may have been secreted into the media, thus reducing the overall ECM content that would have been collected at the cell layer. This method defined the ECM composition, however, statistical analysis was not completed, due to the sample size (N=1). Due to the cost-prohibitive nature of these experiments, additional replicates were not performed at this time. Furthermore, alternative LC/MS characterization techniques, such as SILAC labeling would provide a more definitive and quantitative and comparative method of analyzing the ECM composition. Thus, this should be considered next steps in holistic analysis of the ECM. Regardless of limitations, label-free proteomics still provided valuable information regarding the use of HA as a crowder agent compared to a well-characterized crowder, Ficoll,for matrix deposition.

The next chapter further explores the effects of HA on matrix deposition, structure, and organization in human fibroblast cultures.

	Angiogenic Inducing Proteins					
		Molecular Weight	Cell Layer Conditions (Total Unique Peptides)			
			0%	0.05% HA	0.5% HA	Ficoll 70/400
Newman et al 2017 (from conditioned media)	Col 1A1	140	15	29	8	11
	Col 1A2	130	9	20	11	8
	Procollagen C-endopeptidase enhancer 1 precursor	48	0	2	1	1
	Sulfhydryl oxidase precurs	-	-	-	-	-
	Transforming growth fator-B induced high protein ig-h3 precursor	75	20	20	23	22
	Insulin -like growth factor binding protein 7-precursor	29	1	0	1	1
	Laminin subunit gamma (LAMC1)	178	7	12	16	25
	Annexin A2	39	25	28	23	26
	Secreted Protein Acidic and rich in cysteine	35	6	4	6	9
Neve et al, 2014	Col3A1	140	5	13	3	5
	Col4A1	168	4	2	4	2
	Col15	-	-	-	-	-
	Col18	154	2	6	4	6
	Fibrillin	312	41	33	34	46
	Fibulin	77	20	21	19	24
	Fibrin	-	-	-	-	-
	Fibronectin	263	75	77	74	85
	Glypican -1	-	-	-	-	-
	Laminin-1	-	-	-	-	-
	Laminin 8	-	-	-	-	-
	Perlecan	-	-	-	-	-
	Tenascin C	241	66	60	66	76
	Tenascin X	458	1	1	1	10
	Vitronectin	-	-	-	-	-
	Decorin	40	9	10	9	7
	Laminin B1	198	8	6	13	12
	Laminin B2	196	0	3	7	22
	Anti-angiogenic Inducing Proteins					
		Molecular Weight (kDa)	**Cell Layer Conditions (Total Unique Peptides)**			
			0%	**0.05% HA**	**0.5% HA**	**Ficoll 70/400**
Neve et al, 2014	thrombospondin-1	129	37	29	25	27
	thrombospondin-2	130	5	5	3	6
	Angiopoitin relaated protein -2	57	0	0	0	5
	Probability	> 95%	20-49%	0-19%		

Table 3-1: Stimulatory and inhibitory angiogenic molecules reported in literature, and their presence in CDMs developed under MMC.

3.5. References

[1] A. Naba, O.M. Pearce, A. Del Rosario, D. Ma, H. Ding, V. Rajeeve, P.R. Cutillas, F.R. Balkwill, R.O. Hynes, Characterization of the extracellular matrix of normal and diseased tissues using proteomics, Journal of proteome research 16(8) (2017) 3083-3091.
[2] A. Naba, K.R. Clauser, H. Ding, C.A. Whittaker, S.A. Carr, R.O.J.M.B. Hynes, The extracellular matrix: Tools and insights for the "omics" era, 49 (2016) 10-24.
[3] M. Kuo, H. Chen, L. Hahn, C. Hsieh, C. Chiang, Collagen biosynthesis in human oral submucous fibrosis fibroblast cultures, Journal of dental research 74(11) (1995) 1783-1788.
[4] J.F. Bateman, J.J. Pillow, T. Mascara, S. Medvedec, J.A. Ramshaw, W. Cole, Cell-layer-associated proteolytic cleavage of the telopeptides of type I collagen in fibroblast culture, Biochemical Journal 245(3) (1987) 677-682.
[5] S. Murad, D. Grove, K. Lindberg, G. Reynolds, A. Sivarajah, S. Pinnell, Regulation of collagen synthesis by ascorbic acid, Proceedings of the National Academy of Sciences 78(5) (1981) 2879-2882.
[6] D. Hulmes, Collagen diversity, synthesis and assembly, Collagen, Springer2008, pp. 15-47.
[7] C. Frantz, K.M. Stewart, V.M.J.J.C.S. Weaver, The extracellular matrix at a glance, 123(24) (2010) 4195-4200.
[8] D. Greiling, R. Clark, Fibronectin provides a conduit for fibroblast transmigration from collagenous stroma into fibrin clot provisional matrix, Journal of cell science 110(7) (1997) 861-870.
[9] L. Sabatier, D. Chen, C. Fagotto-Kaufmann, D. Hubmacher, M.D. McKee, D.S. Annis, D.F. Mosher, D.P.J.M.b.o.t.c. Reinhardt, Fibrillin assembly requires fibronectin, 20(3) (2009) 846-858.
[10] M.M. Martino, F. Tortelli, M. Mochizuki, S. Traub, D. Ben-David, G.A. Kuhn, R. Müller, E. Livne, S.A. Eming, J.A. Hubbell, Engineering the growth factor microenvironment with fibronectin domains to promote wound and bone tissue healing, Science translational medicine 3(100) (2011) 100ra89-100ra89.
[11] H.A. Ebhardt, A. Root, Y. Liu, N.P. Gauthier, C. Sander, R.J.N.s.b. Aebersold, applications, Systems pharmacology using mass spectrometry identifies critical response nodes in prostate cancer, 4(1) (2018) 26.
[12] D. Gülay Büyükköroğlu, Demir Dora, Filiz Özdemir, Candan Hızel, Techniques for Protein Analysis, in: D.B.a.V. Azevedo (Ed.), Omics Technolgies and Bio-Engineering, Elsevier2017, pp. 591-625.
[13] A. Byron, J.D. Humphries, M.J. Humphries, Defining the extracellular matrix using proteomics, International journal of experimental pathology 94(2) (2013) 75-92.
[14] A. Naba, K.R. Clauser, R.O. Hynes, Enrichment of extracellular matrix proteins from tissues and digestion into peptides for mass spectrometry analysis, JoVE (Journal of Visualized Experiments) (101) (2015) e53057.
[15] H. Ragelle, A. Naba, B.L. Larson, F. Zhou, M. Prijić, C.A. Whittaker, A. Del Rosario, R. Langer, R.O. Hynes, D.G. Anderson, Comprehensive proteomic characterization of stem cell-derived extracellular matrices, Biomaterials 128 (2017) 147-159.
[16] A. Keller, A.I. Nesvizhskii, E. Kolker, R. Aebersold, Empirical statistical model to estimate the accuracy of peptide identifications made by MS/MS and database search, Analytical chemistry 74(20) (2002) 5383-5392.
[17] A.I. Nesvizhskii, A. Keller, E. Kolker, R. Aebersold, A statistical model for identifying proteins by tandem mass spectrometry, Analytical chemistry 75(17) (2003) 4646-4658.
[18] B. Fabre, T. Lambour, D. Bouyssié, T. Menneteau, B. Monsarrat, O. Burlet-Schiltz, M.-P. Bousquet-Dubouch, Comparison of label-free quantification methods for the determination of protein complexes subunits stoichiometry, EuPA Open Proteomics 4 (2014) 82-86.
[19] A. Naba, K.R. Clauser, S. Hoersch, H. Liu, S.A. Carr, R.O. Hynes, The matrisome: in silico definition and in vivo characterization by proteomics of normal and tumor extracellular matrices, Molecular & Cellular Proteomics 11(4) (2012) M111. 014647.
[20] L.T. Senbanjo, M.A. Chellaiah, CD44: a multifunctional cell surface adhesion receptor is a regulator of progression and metastasis of cancer cells, Frontiers in cell and developmental biology 5 (2017) 18.

[21] S. Misra, V.C. Hascall, R.R. Markwald, S. Ghatak, Interactions between hyaluronan and its receptors (CD44, RHAMM) regulate the activities of inflammation and cancer, Frontiers in immunology 6 (2015) 201.
[22] C. Fathke, L. Wilson, J. Hutter, V. Kapoor, A. Smith, A. Hocking, F. Isik, Contribution of bone marrow–derived cells to skin: collagen deposition and wound repair, Stem cells 22(5) (2004) 812-822.
[23] P. Olczyk, Ł. Mencner, K. Komosinska-Vassev, The role of the extracellular matrix components in cutaneous wound healing, BioMed research international 2014 (2014).
[24] G.S. Schultz, G. Ladwig, A. Wysocki, Extracellular matrix: review of its roles in acute and chronic wounds, World wide wounds 2005 (2005) 1-18.
[25] A.C. Newman, M.N. Nakatsu, W. Chou, P.D. Gershon, C.C. Hughes, The requirement for fibroblasts in angiogenesis: fibroblast-derived matrix proteins are essential for endothelial cell lumen formation, Molecular biology of the cell 22(20) (2011) 3791-3800.
[26] M. Yamauchi, M. Sricholpech, Lysine post-translational modifications of collagen, Essays in biochemistry 52 (2012) 113-133.
[27] J. Myllyharju, K.I. Kivirikko, Collagens, modifying enzymes and their mutations in humans, flies and worms, TRENDS in Genetics 20(1) (2004) 33-43.
[28] J. Myllyharju, Intracellular post-translational modifications of collagens, Collagen, Springer2005, pp. 115-147.
[29] Y. Chen, M. Terajima, Y. Yang, L. Sun, Y.-H. Ahn, D. Pankova, D.S. Puperi, T. Watanabe, M.P. Kim, S.H. Blackmon, Lysyl hydroxylase 2 induces a collagen cross-link switch in tumor stroma, The Journal of clinical investigation 125(3) (2015) 1147-1162.
[30] K. Takahara, E. Kessler, L. Biniaminov, M. Brusel, R.L. Eddy, S. Jani-Sait, T.B. Shows, D.S. Greenspan, Type I procollagen COOH-terminal proteinase enhancer protein: identification, primary structure, and chromosomal localization of the cognate human gene (PCOLCE), Journal of Biological Chemistry 269(42) (1994) 26280-26285.
[31] D. Fortunati, D.Y. San Chau, Z. Wang, R.J. Collighan, M. Griffin, Cross-linking of collagen I by tissue transglutaminase provides a promising biomaterial for promoting bone healing, Amino acids 46(7) (2014) 1751-1761.
[32] S.S. Akimov, A.M. Belkin, Cell-surface transglutaminase promotes fibronectin assembly via interaction with the gelatin-binding domain of fibronectin: a role in TGFβ-dependent matrix deposition, Journal of cell science 114(16) (2001) 2989-3000.
[33] T.N. Wight, D.K. Heinegård, V.C. Hascall, Proteoglycans, Cell biology of extracellular matrix, Springer1991, pp. 45-78.
[34] D.S. Grant, C.P. Leblond, H.K. Kleinman, S. Inoue, J.R. Hassell, The incubation of laminin, collagen IV, and heparan sulfate proteoglycan at 35 degrees C yields basement membrane-like structures, The Journal of cell biology 108(4) (1989) 1567-1574.
[35] P. Chan, J. Caron, G. Rosa, M. Orth, Glucosamine and chondroitin sulfate regulate gene expression and synthesis of nitric oxide and prostaglandin E2 in articular cartilage explants, Osteoarthritis and cartilage 13(5) (2005) 387-394.
[36] S. Stringer, The role of heparan sulphate proteoglycans in angiogenesis, Portland Press Limited, 2006.
[37] S.L. Raza, L.A. Cornelius, Matrix metalloproteinases: pro-and anti-angiogenic activities, Journal of Investigative Dermatology Symposium Proceedings, Elsevier, 2000, pp. 47-54.
[38] G. Seghezzi, S. Patel, C.J. Ren, A. Gualandris, G. Pintucci, E.S. Robbins, R.L. Shapiro, A.C. Galloway, D.B. Rifkin, P. Mignatti, Fibroblast growth factor-2 (FGF-2) induces vascular endothelial growth factor (VEGF) expression in the endothelial cells of forming capillaries: an autocrine mechanism contributing to angiogenesis, The Journal of cell biology 141(7) (1998) 1659-1673.
[39] G. Ferrari, B.D. Cook, V. Terushkin, G. Pintucci, P. Mignatti, Transforming growth factor-beta 1 (TGF-β1) induces angiogenesis through vascular endothelial growth factor (VEGF)-mediated apoptosis, Journal of cellular physiology 219(2) (2009) 449-458.

[40] A. Bitto, L. Minutoli, M.R. Galeano, D. Altavilla, F. Polito, T. Fiumara, M. Calò, P.L. Cascio, L. Zentilin, M. Giacca, Angiopoietin-1 gene transfer improves impaired wound healing in genetically diabetic mice without increasing VEGF expression, Clinical Science 114(12) (2008) 707-718.
[41] G. Montrucchio, E. Lupia, E. Battaglia, G. Passerini, F. Bussolino, G. Emanuelli, G. Camussi, Tumor necrosis factor alpha-induced angiogenesis depends on in situ platelet-activating factor biosynthesis, Journal of Experimental Medicine 180(1) (1994) 377-382.
[42] A. Karamysheva, Mechanisms of angiogenesis, Biochemistry (Moscow) 73(7) (2008) 751.
[43] J.F. Murphy, F. Lennon, C. Steele, D. Kelleher, D. Fitzgerald, A.C. Long, Engagement of CD44 modulates cyclooxygenase induction, VEGF generation, and proliferation in human vascular endothelial cells, The FASEB journal 19(3) (2005) 446-448.
[44] A. Neve, F.P. Cantatore, N. Maruotti, A. Corrado, D. Ribatti, Extracellular matrix modulates angiogenesis in physiological and pathological conditions, BioMed research international 2014 (2014).
[45] P.C. Brooks, A.M. Montgomery, M. Rosenfeld, R.A. Reisfeld, T. Hu, G. Klier, D.A. Cheresh, Integrin αvβ3 antagonists promote tumor regression by inducing apoptosis of angiogenic blood vessels, Cell 79(7) (1994) 1157-1164.
[46] F. Re, A. Zanetti, M. Sironi, N. Polentarutti, L. Lanfrancone, E. Dejana, F. Colotta, Inhibition of anchorage-dependent cell spreading triggers apoptosis in cultured human endothelial cells, The Journal of cell biology 127(2) (1994) 537-546.
[47] A.E. Canfield, A.M. Schor, S.L. Schor, M.E. Grant, The biosynthesis of extracellular-matrix components by bovine retinal endothelial cells displaying distinctive morphological phenotypes, Biochemical Journal 235(2) (1986) 375-383.
[48] K. Palanisamy, R.N. Nareshkumar, S. Sivagurunathan, R. Raman, K.N. Sulochana, S. Chidambaram, Anti-angiogenic effect of adiponectin in human primary microvascular and macrovascular endothelial cells, Microvascular research 122 (2019) 136-145.

Chapter 4 : Hyaluronic acid mediated matrix deposition for production of cell-derived matrices

4.1. Introduction

Cell-derived matrices (CDMs) recapitulate natural extracellular matrix (ECM) structures, and their composition can be tailored by altering the cell source [1-3], culture media [2, 4, 5], and growth conditions [1, 6]. Characterization of CDMs has shown that cells can produce a rich ECM composition [4] that retains growth factors and provides signaling cues to support cellular function [7-11] or maintain stem cells in an undifferentiated state [12]. Thus, CDMs may provide advantages compared to uni-molecular ECM protein coatings and scaffolds, such as collagen or fibronectin [13]. Successful development of human CDM biomaterials that support *in vitro* cell culture and serve as scaffolds for cell delivery and tissue regeneration may provide an alternative to current ECM biomaterials, such as Matrigel, without the xenogeneic and immunological limitations.

Despite the many advantages of CDMs, the culture time needed for their production is a limiting factor in their clinical and commercial translation. For example, construction of cultured human cell sheets can take up to 6-28 weeks [14] depending on the cell types used and the required scaffold thickness [15]. The lengthy production time is in part a result of the fact that the enzymatic conversion of procollagen to collagen does not readily occur under standard *in vitro* culture conditions. While some insoluble collagen is assembled at the cell layer, procollagen molecules secreted in the media may be lost when culture medium is exchanged. As a result, development of strong vascular grafts from cell sheets typically takes at least several weeks [16]. Early pioneering work in the study of *in vitro* ECM assembly has shown that, through variations in culture conditions such as low oxygen levels [17], addition of chemically

defined media [4], or addition of macromolecules [18], the reaction kinetics for assembly of mature collagen matrix can be altered. One approach, known as macromolecular crowding (MMC), has been successfully shown to increase ECM deposition and assembly in cultured cells *in vitro* [1, 3, 19, 20]. Briefly, MMC entails the addition of polymeric materials to the cell culture media to create an excluded volume effect and physically limit diffusion of cellular proteins from the cell layer. Addition of neutral polymers to a human skin fibroblast culture was initially studied by Bateman *et al.* in 1987 [18]. The addition of these polymers caused accumulation of collagen at the cell layer due to proteolytic cleavage of collagen N- and C-terminal peptides [18]. While this approach was not referred to as crowding at the time, nor was it utilized as a method in tissue engineering applications for development of cell-assembled sheets, it highlighted the importance of altering the reaction kinetics of precursor ECM proteins at the cell layer to increase CDM deposition.

The approach of using MMC in cell culture for development of CDM biomaterials was not fully appreciated until 20 years later after pioneering work published by Raghunath and Zeugolis [21]. Macromolecular crowding is a biophysical phenomenon that better represents the crowded cell environment *in vivo* than standard cell culture conditions. Macromolecule addition to the culture medium alters the reaction kinetics for conversion of procollagen to mature collagen, as well as its molecular assembly at the cellular layer *in vitro* and the diffusion of other ECM protein precursors [18, 21]. The addition of macromolecules to the media creates an excluded volume effect. The excluded volume effect, or the volume occupied by different macromolecules in the media, is represented by: 1) the space occupied by the added macromolecules themselves (shown schematically in **Figure 2-1)**, and 2) the space created due to steric and electrostatic repulsions between the macromolecules **(Figure 2-1, insert)**.

Depending on the properties of the crowder macromolecule, the volume available for diffusion can be modulated to enhance biological processes *in vitro.*

In general, an ideal crowding agent is soluble in media, has a globular molecular shape, an overall negative charge, is biochemically inert, and acts by steric repulsion. Several synthetic, inert polymers with different molecular weights, charges, and radii have been used as macromolecular crowders, including Ficoll [2, 19, 20, 22, 23], carrageenan [1], dextran sulfate (DxS) [3, 21], and polyvinylpyrrolidone (PVP) [24]. In addition, macromolecular crowding has been used with many different cell types, such as fibroblasts [3, 21, 23], embryonic stem cells (ESC) [12], and mesenchymal stem cells (MSCs) [1]. Hyaluronic acid (HA) has been investigated in the study of collagen fibrillogenesis and matrix organization due to its overall net negative charge in a crowded-like acellular system [25]. HA shares many properties with crowders typically reported in the literature. It is water soluble and forms a self-avoiding random coil-like structure in solution [26, 27], has an overall net negative charge [28], and interacts with the system via steric as well as electrostatic repulsion. In addition to those properties, HA is a macromolecule that is highly expressed during fetal development and abundantly found in the ECM microenvironment of skin fibroblasts [29-31]. It has been shown to play a role in ECM production, organization, and assembly [28, 32, 33]. However, it has not been reported as a crowder in cell-based systems for driving ECM deposition and assembly, or for the development of CDM scaffolds. Thus, the focus of this study was to evaluate the effect of HA as a macromolecule for driving the *in vitro* deposition of ECM proteins important for tissue regeneration.

Proteomics characterization of dermal fibroblast derived fibroblasts suggested that crowding has an effect on matrix deposition and sequestration of precursor proteins to the cell

layer. Furthermore, differences in matrix composition and enzyme profile was dependent on the crowder macromolecule used. This approach provided valuable data supporting the use of HA as a crowder molecule to promote matrix deposition and develop CDM materials. The focus of this study was to evaluate the effect of HA as a macromolecule for driving the *in vitro* deposition of ECM proteins important for tissue regeneration and angiogenesis.

4.2. Materials and Methods

4.2.1. Rheology

Rheological assessment of HA and Ficoll solution fluid viscosity was performed using a MCR 302 WESP (Anton Paar) with a smooth parallel plate configuration. HA solutions at different concentrations were prepared in 1X PBS and sterile filtered. Five hundred microliter volume was loaded onto the stage. A shear rate of 1-1000 s^{-1} was applied to each solution sample to obtain flow curves and viscosity measurements. A sample size of N = 2 was assessed for each condition. Statistical analysis was not completed on these experiments.

4.2.2. Cell culture

Human neonatal fibroblasts (p2-p8, ATCC, CRL 2097) were plated at a density of 25,000 cells/cm^2 and cultured in DMEM (Corning, 15-017 CV) supplemented with 10% v/v fetal bovine serum (Gibco, 16000-044), 1% v/v penicillin/streptomycin (Corning, 30-002-Cl), 1% v/v non-essential amino acids (Corning, 25-025Cl), 1% v/v L-glutamine (Corning, 25- 005Cl) and 1% v/v sodium pyruvate (Corning, 25-001-Cl). Human dermal fibroblasts used stained positive for CD44 **(Supplementary Figure 4-1).**

After 24 hours cells were treated with crowding media. HA media was supplemented with 0.05% w/v or 0.5% w/v high molecular weight hyaluronic acid (HA15M-5, 1.5MDa, LifeCore Biomedical). Ficoll media was prepared by mixing 37.5 mg/mL Ficoll 70 (Sigma, F2878) and 25 mg/mL Ficoll 400 (Sigma, F4375). Untreated cell cultures (without HA or Ficoll) served as the negative control, non-crowded condition. All cultures were supplemented with 100 µM ascorbic acid (Wako, 013-19641). Cells were cultured at standard culture conditions (37°C, 5% CO_2), and media was replaced every 2-3 days. Samples prepared for AFM and characterization of matrix retention were prepared on polydopamine coated surfaces.

4.2.3 SDS-PAGE and silver staining

Cell layers were pepsin/acid digested using 0.1 mg/mL pepsin (Sigma, P6887) reconstituted in 0.05 M cold acetic acid with a pH of 2.2. Samples were centrifuged to collect soluble fractions, and an aliquot was collected and frozen at -80 ºC for Bradford protein analysis. The remaining aliquot of pepsin-digested samples was neutralized with 6 M NaOH and phenol red solution. Protein concentration was normalized to allow for equal loading of protein samples. A collagen standard (Advanced Biomatrix, 5005) prepared in 0.05 M acetic acid for a final concentration of 1mg/mL was used a protein reference. Samples were prepared with 20% Laemmli buffer. Proteins were denatured at 95 ºC for 5 minutes. A 6% Tris-glycine SDS-PAGE gel was used for gel electrophoresis. Gels were stained using SilverQuest staining kit (Invitrogen, LC6070) as specified in the manufacturer's protocol. Gels were fixed for 4 hours in a methanol and acetic acid fixative prior to staining. After appearance of bands, the reaction was stopped and gels were imaged on a ChemiDoc XRS (Bio-Rad).

4.2.4. Sircol soluble collagen assay

Pepsin/acetic acid-digested samples were collected as previously specified. Supernatant was collected and a 100 µl sample was transferred to a 1.7 mL Eppendorf tube. Sircol soluble collagen reagent was prepared using 0.1% direct red 80 and 0.1% Fast green FCF in picric acid solution. Nine hundred microliter reagent volume was added per 100 µl sample and incubated at RT under agitation for 30 minutes to allow for formation of a dye-collagen complex. Samples were centrifuged at 10,000g for 10 minutes to collect pellet. The supernatant was discarded, and the pellet was quenched with 500 µl of 0.5 M NaOH to release collagen. Collagen standards were prepared using bovine type I collagen, and serially diluted using 0.05 M acetic acid. Absorbance measurements were read using Viktor 3 Plate reader (Perkin Elmer) at an absorbance of 550 nm. Soluble collagen concentration was calculated using a standard curve.

4.2.5. Hydroxyproline assay

Cell layers were collected in MilliQ water supplemented with protease and phosphatase inhibitor tablets, and collected using a cell scraper. Samples were collected in a borosilicate glass vial, diluted 1:1 with 12 M HCl, and incubated for 16 hours at 110°C. A citrate buffer (0.03M citric acid, 0.42M sodium acetate, 0.12M tri-sodium citrate dehydrate) was reconstituted in isopropanol and water solution (1:2). The final pH of the citrate buffer was between 6.5 -7. Chloramine T reagent was reconstituted in citrate buffer for a final concentration of 0.04 M. Ehlrich's reagent was prepared by reconstituting p-dimethylaminobenzaldehyde (p-DMAB) in a isopropanol/water solution for a final concentration of 0.68 M. Both chloramine T and Ehlrich's reagents were prepared fresh immediately before use. Collagen standards were prepared using bovine type 1 collagen diluted 1:1 in 12 M HCl, and incubated for 16 hours at 110°C.

Experimental and standard samples were allowed to cool to room temperature prior to handling. Hydrolyzed protein samples were transferred to an Eppendorf tube and centrifuged for 10 minutes at 10,000 g to collect the soluble fraction. One hundred microliters of the supernatant was neutralized with 6 M NaOH for a final pH of 7. Chloramine T reagent was added to all experimental and standard samples for a final concentration of 0.025M. Samples were vortexed and allowed to oxidize in chloramine T for 25 minutes at room temperature. Following the incubation period, Ehlrich's reagent was added for a final concentration of 0.5M, vortexed, and incubated at 70°C for 15 minutes. Absorbance was measured at 550nm in a 100 µl volume. The concentrations of unknown samples was calculated from collagen standard curve.

4.2.6. Immunocytochemistry of ECM proteins and quantification

Fibroblasts cultured for 3 days, 7 days, or 14 days were fixed using 4% paraformaldehyde/PBS (Alfa Aesar, J61899) for 10 minutes at room temperature. After fixation, cells were incubated in 2% w/v bovine serum albumin (HyClone, 25-529F) reconstituted in 1X DPBS for two hours at room temperature to minimize non-specific binding. The following primary antibody solutions were prepared in 2% BSA and incubated with cells overnight at 4 °C: collagen type I (Abcam, ab34710, 1:500), collagen type III (Abcam, ab7778,1:250), collagen type IV (Abcam, ab6486, 1:250), laminin (Sigma-Aldrich, L9933, 1:50), and fibronectin (Santa Cruz Biotechnology, sc-59826,1:200). After primary antibody incubation, cell layers were rinsed in 1X DPBS and incubated in secondary antibody solution consisting of goat anti-mouse 568 (Life Technologies, A11004) and goat anti-rabbit 488 (Life Technologies, A11005) or goat anti-rabbit 594 (Life Technologies, A11012) at 1:400 dilution in 1X DPBS depending on primary

antibody species. Cells were counterstained with DAPI and imaged using a Zeiss Axiovert microscope.

ICC images were quantified as specified in **Figure 4-1**. Each condition was imaged in five different regions of interest (ROI) per sample. Mean gray values (MGV) of each detected fluorescent sample for the areas measured were obtained using an iterative threshold algorithm on ImageJ (National Institute of Health). DAPI counts were determined using Image J algorithms. MGVs were normalized to the number of cells present in the frame analyzed, as determined by DAPI counts. Pixel distribution as represented by MGV, and MGV normalized relative to the DAPI counts per ROI were quantified and graphed. MGVs were normalized to the 3-day non-treated control samples.

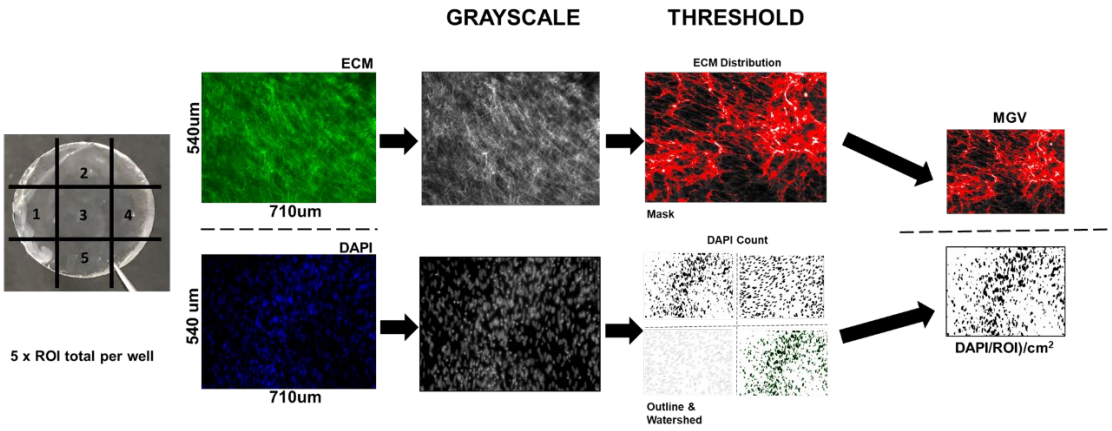

Figure 4-1: Schematic illustrating the quantification method used to measure ECM distribution as a function of mean gray value (MGV), and DAPI cell count. Image J algorithms were used to measure MGV and obtain DAPI counts from ICC images.

4.2.7. DNA quantification assays

Quantification of cellular density under crowding conditions was assessed using PicoGreen dsDNA assay (Invitrogen, P7589). Briefly, human fibroblasts were cultured as

specified above. After 3, 7, and 14 days, media was removed, cell layer rinsed with 1X DPBS, and cells were trypsinized using 0.25% Trypsin/0.05M EDTA for 10 minutes at 37 °C, 20% O_2 and 5% CO_2. Cells were neutralized using complete DMEM, collected with a cell scraper, and then centrifuged to collect the cell pellet. Pellet was resuspended in 1X Tris-EDTA buffer, and lysate was used to analyze total dsDNA content. Cell number was assessed by total dsDNA content calculated from the standard dsDNA curve.

Quantification of dsDNA for calculation of collagen per DNA (µg/ µg) was assessed using PicoGreen dsDNA assay, however, sample was obtained from the cell layer collected as specified in *Section 4.2.4.* A small aliquot was collected and diluted 10-fold prior to measuring dsDNA as specified in the previous paragraph.

4.2.8. Raman microspectroscopy

For Raman spectroscopic imaging, fibroblasts were cultured for 3 days, 7 days or 14 days in glass bottom µ-dishes (ibidi GmbH, Martinsried, Germany) at different crowding conditions and fixed using 4% paraformaldehyde/PBS (Alfa Aesar) for 10 minutes at room temperature. The samples were rinsed and covered with PBS before the measurements. Images of an area of 200x200 µm were acquired with a customized Raman microspectroscope system (WiTec alpha300R, WiTec GmbH, Ulm, Germany), equipped with a green laser (532 nm), a CCD camera (grating of 600 g/mm) and a 63x water dipping objective (Carl Zeiss GmbH, Jena, Germany) as previously described in detail [34]. Acquisition settings were a laser power of 40 mW, an integration time of 0.5 s and a pixel resolution of 2 x 2 µm. Raman imaging enabled generation of a map of the sample that provided a specific spectrum in every pixel. For analysis and separation of spectral differences, True Component Analysis (TCA) was performed as

described before [34]. Briefly, Raman spectra of pixels that contained similar spectral information were identified as one component and presented as an intensity heat map. TCA enabled the marker-independent localization and identification of certain molecular structures.

4.2.9. Dimethyl methylene blue assay

Pepsin/acetic acid-digested samples were collected as previously specified. Samples were centrifuged to collect insoluble fractions. Pellet was frozen at -80°C until ready for use. Pellets were digested in 1mg/mL papain (Sigma, P3375) digestion buffer prepared in 0.1M sodium phosphate solution (pH 6.5) supplemented with 5mM cysteine hydrochloride (Sigma, 30120). Solutions was prepared fresh before use and sterile filtered prior to adding 200 µl digestion solution to pellet. Samples were digested overnight in a 65°C water bath. Dimethyl methylene blue (DMMB) reagent was prepared using DMMB (Sigma, 341088), sodium chloride (Sigma S7653), and glycine (Sigma, 50046) distilled in water. The solution pH was adjusted to 3.0 using 0.1 M glacial acetic acid. Chondroitin-6-sulfate (CS-6, Sigma, 6737) was used as a standard, and dilutions were prepared in 0.1 M sodium phosphate buffer. A 50 µl sample volume was incubated with 200 µl DMMB solution, and absorbance values were measured using SpectraMx 250 reader at an absorbance of 525nm (Molecular Devices).Standard curve was generated by fitting the CS-6 concentrations to respective absorbance values using a 4-PL regression. The concentrations of the experimental samples was calculated using the 4PL regression equation generated from mycurvefit.com.

4.2.10. Quantitative reverse transcriptase polymerase chain reaction (qRT-PCR)

Expression of ECM genes and ECM-associated genes was investigated by a quantitative reverse transcriptase-polymerase chain reaction (qRT-PCR). After 3, 7 or 14 days in culture fibroblasts and their developed CDMs were trypsinized and collected in an Eppendorf tube for RNA isolation. Cell pellet from four wells were collected and pooled at the time points specified above under crowded culture conditions. Total RNA extraction was completed using the E.Z.N.A total RNA kit (OMEGA Biotek, R6834) as specified in the manufacturer's protocol. Briefly, cells were lysed in TRK lysis buffer supplemented with β-mercaptoethanol and mechanically disrupted using a 21-gauge needle. RNA was purified on a HiBind RNA mini column. The purity and concentration of the total RNA was evaluated using a Nanodrop (ThermoFisher). Samples with A260/280 ratio greater than 1.7 were used in the experiments. An RT-RT first strand DNA kit (Qiagen, 95048) was used to prepare cDNA samples from the total RNA. The prepared cDNA was monitored using SYBR Green master mix (ThermoFisher, A25741) using an Applied Biosystems thermal cycler (AB7500). Results were quantified using the ΔΔCt method [35], and fold changes were assessed through normalizing to the endogenous reference gene *GAPDH* and normalized relative to the non-crowded media condition. The selected primer pairs for each gene are specified in **Supplementary Table 4-1.** All experiments were performed with a minimum of three biological replicates, unless otherwise specified, and the differences were calculated relative to the non-crowded control.

4.2.11. Confocal laser scanning microscopy

Cell-derived matrices were prepared as previously specified using ibidi Plates. CDMs were fixed at 3, 7, and 14 days using 4% paraformaldehyde, and stained simultaneously using

collagen type I antibody (Abcam, Ab 6308) at a dilution of 1:500, and a goat- anti-rabbit 488 secondary antibody at 1:400. Z-stack and tile scan images were obtained using a confocal laser scanning microscope (LSM 710, Zeiss, Oberkochen, Germany). An argon 488 nm laser and diode 405 nm laser were used to acquire images for thickness measurements. Images were stitched and a 3-D render was generated using ZEN black software. CD44 staining (1:500 dilution) was also imaging using LSM confocal.

4.2.12. Preparation of polydopamine coated surfaces

Polydopamine (Sigma, H8502) was reconstituted in 100 mM bicine (Sigma, B3876) solution prepared at pH 8.5. Coverslips placed in 24-well plates were incubated with polydopamine solution overnight at room temperature under rotation. After 24 hours, polydopamine solution was removed, and multi-well plates rinsed for 5 minutes under distilled water. Multi-well plates were sterilized under ultraviolet light for 30 minutes prior to use.

4.2.13. Decellularization of CDMs

CDMs cultured for 14 days on polydopamine-coated surfaces were decellularized as previously described [36], under sterile conditions . Briefly, media was aspirated and cell layers rinsed in distilled water for 5 minutes. Distilled water was aspirated, and cell layer was incubated in 0.6 M KCl solution for 1 hour at RT. The KCl solution was aspirated, and cell layer was incubated in 1M KI solution for 1 hour. Cell layers were rinsed in distilled water before repeating the KCl and KI solution incubation. A 50 U/mL DNase I (Worthington Biochemical, LS002004) was prepared in a 1X solution diluted from a 10X stock (10X stock: 20mM $MgCl_2$, 200mM Tri-HCl, pH 8.3). DNase solution was incubated for 1 hour at 37°C before rinsing.

4.2.14. Assessment of decellularized CDMs and matrix retention

Decellularized CDMs and their corresponding non-decellularized controls were fixed and stained for retained ECM proteins as specified in *Section 4.2.5.* In addition, decellularized CDMs were assessed for total DNA content compared to a non-decellularized control using a PicoGreen dsDNA assay as specified in *Section 4.2.6.*

4.2.15. Atomic force microscopy

Matrix viscoelasticity measurements were performed using an Asylum MFP-3D-BIO atomic force microscope [37]. A conical tip DNP cantilever (Bruker) with nominal spring constant 0.06N/m was calibrated for spring constant and inverse optical lever sensitivity (invOLS) before each measurement to ensure accuracy of measurements. The cantilever was programmed to indent at 2μm/s until a trigger force of 10 nN was achieved. Measurements were gathered in 8 x 8, 20 x 20μm force maps for the decellularized conditions, with three force maps gathered per matrix. Samples were blinded to negate location selection biases. Stiffness values $\boldsymbol{E}$ were determined by fitting the data over a 500nm indentation range after initial contact using the conical geometry Hertzian fit model [38].

$$E = \frac{kd\pi(1-\nu^2)}{2\Delta^2 \tan\phi}$$

where $\boldsymbol{k}$ is the spring constant of the cantilever, $\boldsymbol{d}$ is the deflection of the cantilever, $\boldsymbol{\nu}$ is the Poisson's ratio (Here, 0.5 for an assumed uncompressible material), $\boldsymbol{\Delta}$ is the sample indentation depth, and $\boldsymbol{\Phi}$ is the half angle of the conical tip (17.5°). An automated MATLAB code was utilized to determine the initial contact position and fit the Hertz model over the 500nm indentation range [39].

4.2.16. Statistical analysis

All experiments were completed in triplicate unless otherwise stated. Statistical analysis was performed to determine significance amongst the experimental conditions using GraphPad Prism 7 software. Data is reported as the mean ± standard error of the mean (SEM). One-way ANOVA followed by Tukey's post-hoc multiple comparisons within conditions was completed. If normality assumptions were violated, Kruskal–Wallis test followed by Dunn's post-hoc analysis was completed. A two-way ANOVA followed by Tukey's or Sidak's multiple comparison tests were completed if two factors were analyzed. Statistical significance is reported at $p < 0.05$.

4.3. Results

4.3.1. Characterization of viscosity

The viscosities of the 0.05% HA, 0.5% HA, and Ficoll 70/400 solutions at a shear rate of 100 s^{-1} were 2.36 mPa-s, 139.1 mPa-s, and 1.17 mPa-s, respectively **(Figure 4-2)**. The viscosities for the 0.05% HA and Ficoll 70/400 were comparable to each other, and are representative of physiological solution viscosity (blood viscosity: 3.36 mPa-s 100 s^{-1}) [40]. The similarities in viscosity between the 0.05% HA and Ficoll 70/400 solution allow comparison of the effects of charge and type of crowder molecule independent of differences in viscosity. The 0.5% HA solution allowed

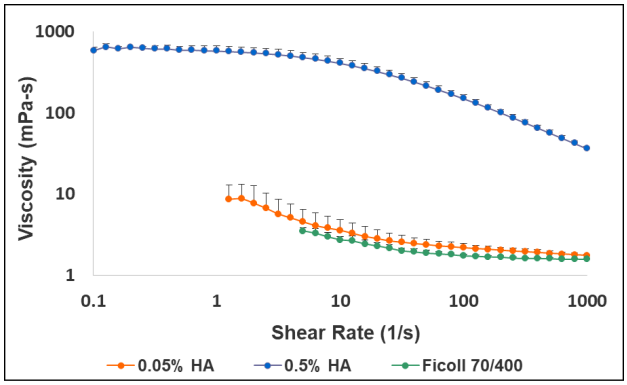

	Viscosity @ Shear Rate 100 s^{-1} (mPa-s)		
Condition	0.05% HA	0.50% HA	Ficoll 70/400
Viscosity	2.36	139.1	1.17

Figure 4-2: Rheological analysis of HA media prepared at different concentrations, and compared to the Ficoll 70/400 media. All values represent mean and standard deviation from two experimental replicates.

assessment of the effects of viscosity as a crowding factor for matrix deposition compared to the less viscous 0.05% HA solution.

4.3.2. Effects of MMC on cell morphology

Dermal fibroblasts cultured under macromolecular crowding conditions were imaged. Fibroblasts are physically crowded in culture to induce a secretory rather than proliferative state. Fibroblast appear to maintain their long, spindle like morphology at days 7 and 14 **(Figure 4-3).** While it is very difficult to observe cellular details due to physical crowding, HA crowded cells appear to have a flattened, wider cell body.

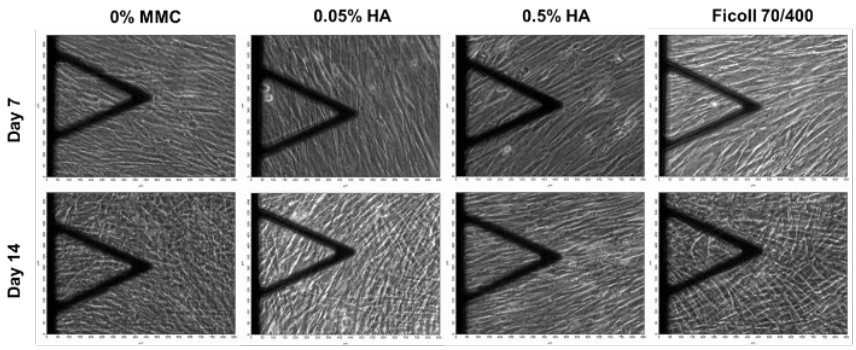

Figure 4-3: Phase contrast images of non-decellularized 7 and 14- day cell derived matrices imaged using atomic force microscopy (AFM).

4.3.3. Quantitative assessment of soluble and total collagen fractions

Human fibroblasts cultured under untreated, 0.05%, or 0.5% HA, or Ficoll 70/400, for 3 and 14 days under macromolecular-crowded cultures, were pepsin/acid treated and evaluated for collagen deposition using SDS-PAGE and silver staining, which allows for qualitative assessment of the alpha, beta, and gamma regions present in the sample **(Figure 4-4 A)**. The collagen footprint seen in the 3-day cell layer samples indicates darker intensity bands within the lower molecular weight alpha region and the higher molecular weight crosslinked beta region in the HA crowded conditions compared to the non-treated control. Darker intensity bands are seen at the 14-day cell layers due to the increased culture time. Qualitative assessment of the crowded

samples indicate that the 0.05% w/v HA treatment increased alpha-1 collagen chains (alpha region), and showed darker intensity bands in the beta and gamma regions compared to the other three conditions [20, 41]. Covalent crosslinking within the beta and gamma regions suggest presence of mature collagen molecules, and formation of a stable collagen matrix. Pepsin-treated samples were then analyzed quantitatively for soluble collagen using the Sircol soluble collagen assay **(Figure 4-4 B)**. Soluble collagen levels were comparable in all conditions at the 3-day cell layers with no statistically significant differences between treatment groups. Differences in soluble collagen concentrations were observed in the 14-day cell layer samples, with the 0.05% HA condition having a statistically significant effect on soluble collagen concentration compared to the other conditions.

Total collagen, including soluble and insoluble fractions, was measured using a hydroxyproline assay **(Figure 4-4 C)**. Hydroxyproline assay results indicated no change in collagen concentration at the 3 day time point. An increase in hydroxyproline was observed in all conditions at 14 days, with the 0.05% HA conditions having the highest collagen concentration, which was significantly higher than the 0.5% HA and Ficoll 70/400 treated samples. Ficoll 70/400 significantly decreased collagen content compared to the untreated control. This trend was similar to the soluble collagen concentration measurements obtained using the Sircol Assay.

Evaluation of collagen deposition per microgram of DNA indicates that 0.5% HA increased collagen production compared to non-treated control and other crowded conditions within 3 days of culture **(Supplementary Figure 4-2)**. Both concentrations of HA did not alter collagen production on a per cell level at day 14. However, Ficoll 70/400 significantly decreased collagen content compared the non-treated and HA treated conditions. This trend was similar to the soluble collagen concentration observed using the Sircol Assay.

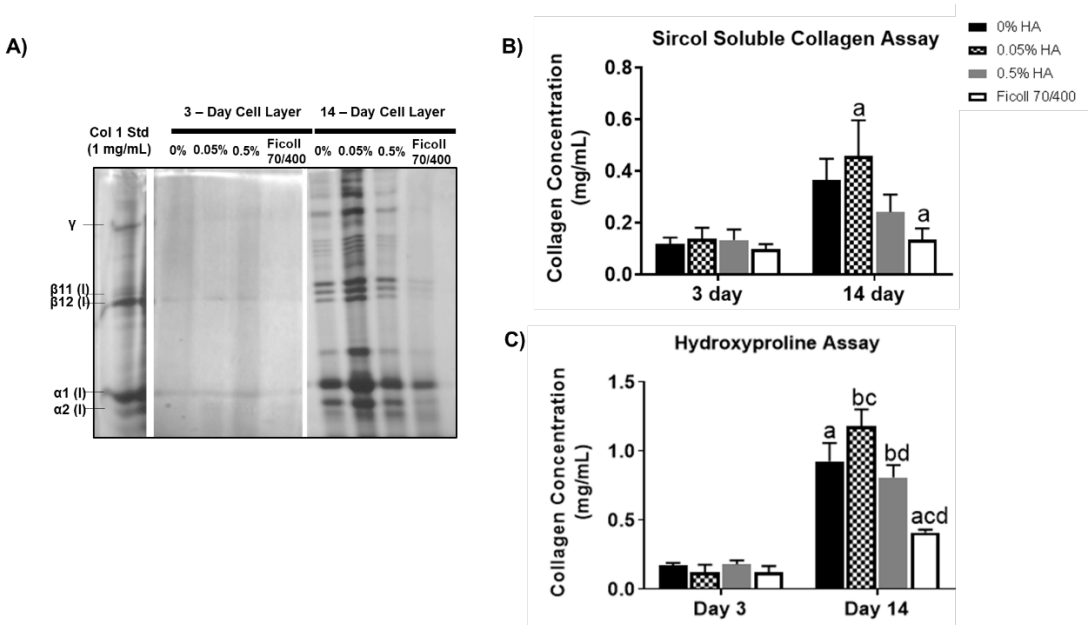

Figure 4-4: Assessment of collagen deposition in 3 and 14 day cell-derived matrices prepared under HA and Ficoll 70/400 crowding conditions. **(A)** SDS-PAGE and silver stained gel of pepsin-acetic acid digested cell layer samples. Bovine collagen type I standard (1mg/mL) was used as a positive control. Image represents data collected from four experimental replicates. **(B)** Complementary quantitative Sircol soluble collagen assay of pepsin-acetic acid digested cell layer samples at 3 and 14 days. All values represent mean and standard error of the mean (SEM) from four experimental replicates. Statistically significant differences between conditions at 14 days is indicated by $^{a}p < 0.05$. **(C)** Total collagen quantification using hydroxyproline assay of MMC cultures CDMs at 3 and 14 days. All values represent mean and SEM from four experimental replicates. Statistically significant differences between conditions at 14 days is indicated by: $^{c}p < 0.0001$, $^{a}p < 0.001$, $^{d}p < 0.01$ $^{b}p < 0.05$.

4.3.4. ECM deposition

In order to assess the effects of HA on ECM composition and deposition, CDMs were qualitatively assessed using immunocytochemistry (ICC) for different ECM proteins after 3, 7 and 14 days in culture. The following ECM proteins were studied: collagen types I and III, and basement membrane collagen type IV, as well as laminin and cellular fibronectin. Based on previous literature, we expected to observe a significant increase in ECM deposition in the Ficoll 70/400 conditions, and hypothesized that HA treatment would also increase ECM deposition. After treatment of dermal fibroblasts with HA or Ficoll 70/400 mix media supplemented with 100 µM ascorbate, no significant changes in ECM deposition due to crowding were observed in collagen types I, III, and IV (**Figure 3 A-C**). A trend of increased collagen type III and IV deposition was

observed in HA and Ficoll 70/400 treated conditions, but the differences were not statistically significant.

The 0.05% HA condition increased laminin deposition after 3 days in culture compared to the negative control and Ficoll 70/400-treated samples, however a significant difference was not observed **(Figure 4-5 A-C)**. Cellular fibronectin deposition was significantly increased on a per cell basis after 3 days, with the 0.5% HA having the highest effect at all time points studied **(Figure 4-6 B, D, F)**. Quantification of mean gray values (MGV) for immunofluorescent images indicated that Ficoll 70/400 and HA crowding increased collagen types III, IV, fibronectin and laminin compared to the non-treated controls **(Figure 4-5 A-F, Figure 4-6 A-D)**.

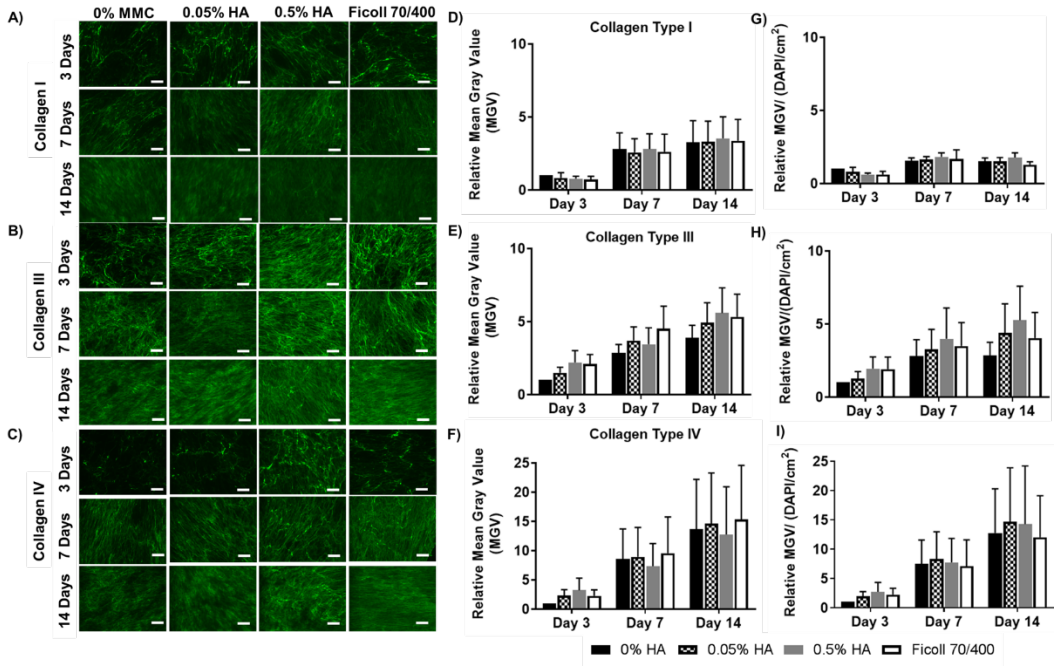

Figure 4-5: Collagen deposition in 3, 7, and 14 day cell-derived matrices prepared under HA and Ficoll 70/400 crowding conditions. **(A-C)** Representative immunocytochemistry images of collagen distribution in cell-derived matrices at 3, 7, and 14-day time points. Scale Bar: 100µm. **(D-F)** Quantification of pixel distribution using iterative thresholding to represent mean collagen deposition. **(G-I)** Mean gray values normalized to the number of cells per ROI within each image. All values represent mean and standard error of the mean from four experimental replicates.

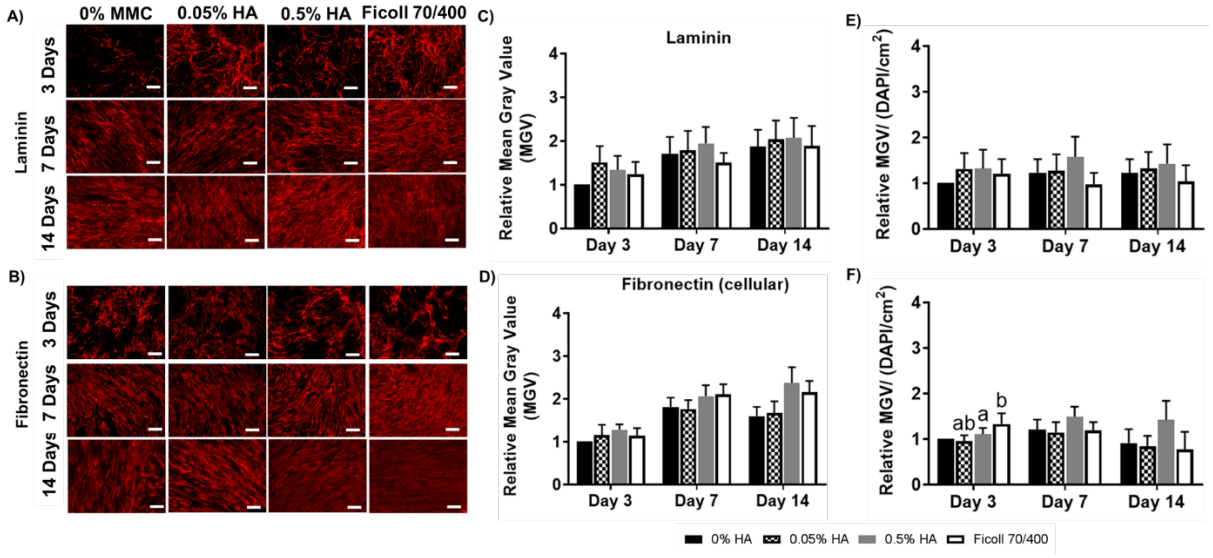

Figure 4-6: Fibronectin and laminin deposition in in 3, 7, and 14 day cell-derived matrices prepared under HA and Ficoll 70/400 crowding conditions. Representative immunocytochemistry images of **(A)** laminin and **(B)** fibronectin distribution in cell-derived matrices at 3, 7, and 14-day time points. Scale Bar: 100µm. **(C-D)** Quantification of pixel distribution using iterative thresholding to represent overall fibronectin and laminin deposition. **(E-F)** Mean gray values normalized to number of cells per ROI within each image. All values represent mean and standard error of the mean from four experimental replicates. Statistically significant differences between conditions at day 3 is indicated by $^{a}p < 0.01$, $^{b}p < 0.05$.

4.3.5. DNA quantification

Corresponding DAPI-positive cell counts from ICC experiments were also obtained from each image. Quantification of cell count indicated that there was an increase in cell number in the Ficoll 70/400-treated conditions **(Figure 4-7 A)**. The increase in cell number in the Ficoll 70/400-treated samples compared to

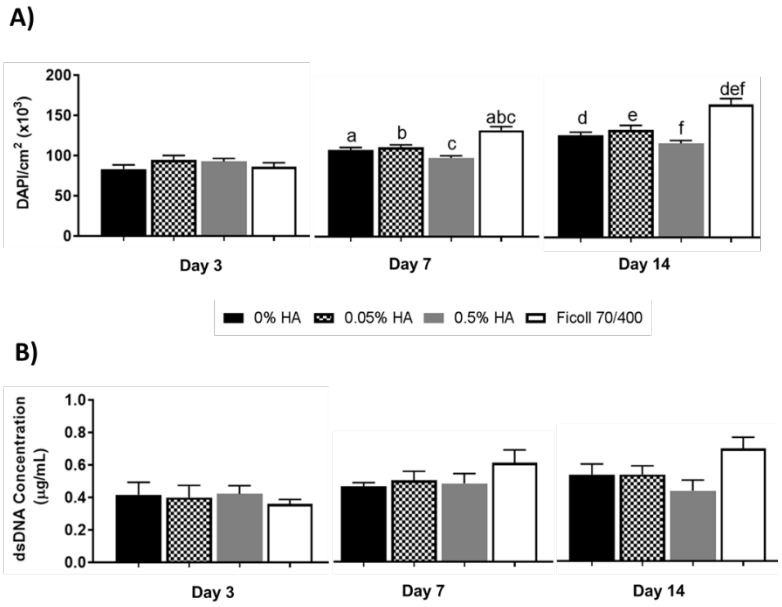

Figure 4-7: Assessment of cell quantity 3, 7, and 14 day cell-derived matrices prepared under HA and Ficoll 70/400 crowding conditions. **(A)** Quantification of DAPI-stained cells per region of interest (ROI) using Image J. All values represent mean and standard error of the mean from twenty experimental replicates. Statistically significant differences between means of non-crowded condition to crowded conditions at days 7 and 14 is indicated by $^{c,f}p < 0.0001$, $^{a}p < 0.001$, $^{b,d}p < 0.01$, $^{e}p < 0.05$. **(B)** Measurement of dsDNA concentration using PicoGreen assay.

the HA-treated samples suggests that cells are in a more proliferative rather than secretory state, and thus are not producing as much matrix. Normalizing the mean gray values (MGV) from immunofluorescent images to the cell number within each region of interest (ROI) indicated an increasing trend collagen type III, IV, laminin, and fibronectin deposition on a per cell basis **(Figure 4-5 H-I and Figure 4-6 E-F)**. There were no observed differences in collagen type I secretion on a per cell basis among all conditions **(Figure 4-5 G)**.

To follow up on the observed increase in DAPI-stained nuclei in Ficoll 70/400-treated cultures, we measured dsDNA concentration. The dsDNA concentration, which correlates to the number of cells in the sample, indicated that HA did not increase the dsDNA concentration compared to the non-crowded control at each time point **(Figure 4-7 B).** However, the dsDNA concentration in Ficoll 70/400 condition increased at the 14-day time point.

4.3.6. Raman microspectroscopy

Raman imaging allowed for spectral mapping of the selected sample area within cell layers cultured for 3, 7, or 14 days. True component analysis (TCA) identified three major spectral components in the images: nuclei (blue), glycosaminoglycans/proteoglycans (green), and collagen (magenta) **(Figure 4-8 A)**. One component was assigned to the cell nuclei, identified by characteristic peaks at 786, 1253 or 1332 cm^{-1} due to vibrations in the phosphate backbone and the bases of DNA [42, 43]. The other two components showed peaks related to ECM proteins. One component contained peaks at 667, 817, 950 and 1250 cm^{-1} assigned mainly to collagen. The second ECM component revealed peaks such as 425, 803, 882 and 1065 cm^{-1} related to glycosaminoglycans and proteoglycans [44]. Mapping of these structures revealed different matrix compositions depending on culture time and crowding conditions **(Figure 4-8**

B). In comparison to non-crowded samples, deposition of collagen and proteoglycans appeared to be greater after 3 days of culture in crowded samples, and continued over the 14-day period. In addition to an overall increase in ECM production, an altered matrix composition was observed with HA crowding. Within 3 days of culture, an increased deposition of the collagen component was detected in samples treated with HA. Over time, collagen appeared to be elevated in HA crowding in comparison to non-crowded and Ficoll 70/400 samples. The second ECM component, mainly containing spectral information on proteoglycans, showed similar amounts for all samples after 14 days.

4.3.7. Quantitative assessment of sulfated glycosaminoglycans

The sulfated GAG concentration for the CDMs prepared under untreated, HA, and Ficoll crowding at day 3 were: 0.55 μg/mL, 0.53 μg/mL, 0.79 μg/mL, and 072 μg/mL **(Supplementary Figure 4-3)**. Sulfated GAG concentration was not significant between all crowder conditions at day 3 and day 7, however, the 0.5% HA and Ficoll 70/400 crowded samples have higher sGAG content. The sGAG concentration increased at 14 days with the 0% and 0.05%, having approximately 1.50 μg/mL. The 0.5% and Ficoll 70/400 conditions had higher concentrations within the matrix, 1.87 μg/mL and 2.02 μg/mL, respectively. This increase was not significant compared to the control, however, indicates an MMC or viscosity mediated effect on sGAG content in CDMs.

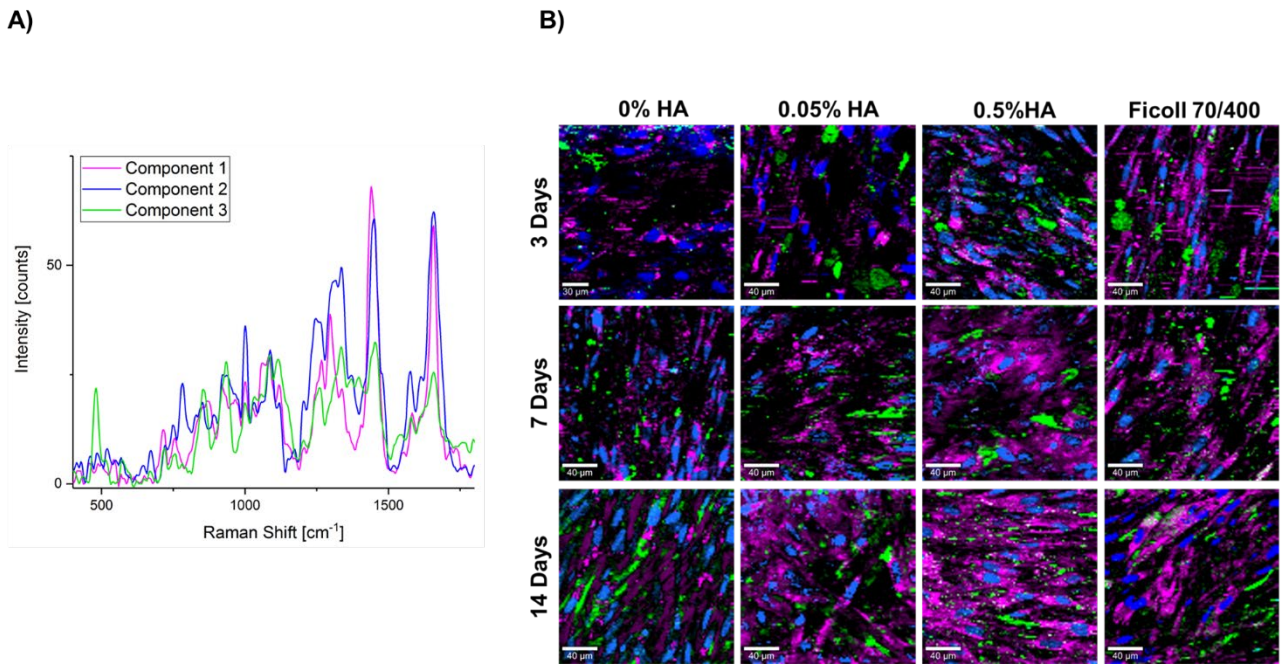

Figure 4-8: Raman microspectroscopy images of 3, 7 and 14-day cultures prepared under HA and Ficoll 70/400 crowding conditions. **(A)** True component analysis (TCA) identified three major spectral components that were assigned to nuclei (blue), collagens (magenta) and glycosaminoglycans/proteoglycans (green). **(B)** Representative images of identified components from TCA analysis. Scale bar: 40µm. Images represent data collected from one experiment.

4.3.8. ECM molecules gene expression

Evaluation of expression of collagen genes demonstrated that cells cultured in the presence of Ficoll 70/400 and the 0.5% HA condition have a modest, ~2-fold increase in *COL1A1, COL3A1,* and *COL4A1* expression within 3 days in culture **(Figure 4-9 A-C)**. The 0.05% HA condition increased at day 7 compared to the other conditions, but this change was not apparent at the later time points. At all time points studied, Ficoll 70/400 decreased *LOX* expression compared to HA and negative control conditions with a significant decrease at day 7 **(Figure 4-9 F)**. The crowding conditions also did not have a significant effect on fibronectin and laminin gene expression **(Figure 4-9 D-E)**. MMC mediated effects were observed in *LOX* gene expression. At all time

points studied, Ficoll 70/400 decreased *LOX* expression compared to HA and negative control conditions with a significant decrease observed at day 7 **(Figure 4-9 F)**.

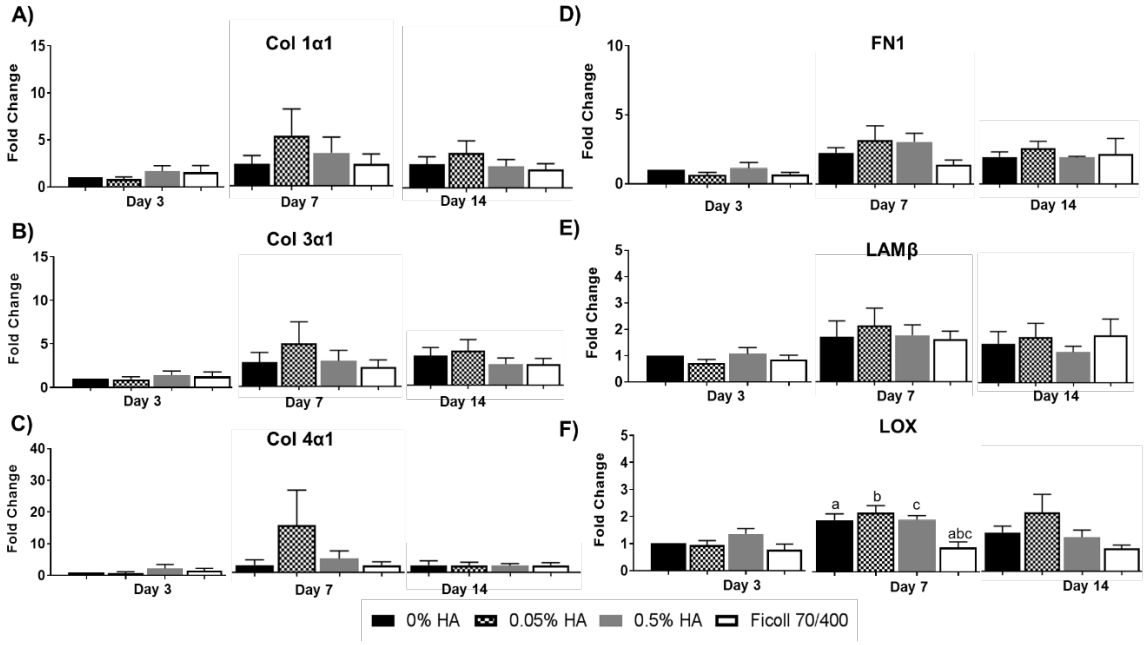

Figure 4-9: Quantitative RT-PCR analysis of (A-C) collagen, (D) glycoproteins (fibronectin), (E) laminin, and (F) lysyl oxidase. All values represent mean and standard error of the mean from at least three experimental replicates. Statistically significant differences between means of non-crowded condition to crowded conditions at day 7 for LOX is indicated by $^{a,b,c}p < 0.05$.

4.3.9. ECM-associated gene expression

Ficoll 70/400 significantly increased *MMP1* and *MMP2* gene expression compared to HA and non-crowder treated cultures **(Figure 4-10 A-B)**. Furthermore, HA did not increase *MMP1* and *MMP2* gene expression compared to non-treated cultures. Ficoll 70/400 increased *MMP8* expression compared to the non-treated control similar to other MMPs studied **(Supplementary Figure 4-4 A)**. *MMP9* expression was increased in the 0.5% HA conditions, and Ficoll 70/400 did not compared to the non-treated **(Supplementary Figure 4-4 B)**. HA did not significantly increase *TIMP1* gene expression compared to untreated cultures **(Figure 4-10 C)**. Furthermore,

Ficoll 70/400 significantly decreased *TIMP3* expression compared to non-treated and HA-treated cultures at day 3 **(Figure 4-10 D)**. This decrease in *TIMP3* expression was also apparent at day 7 compared to HA-treated cultures. There were no changes in *TIMP3* expression at day 14 among all conditions.

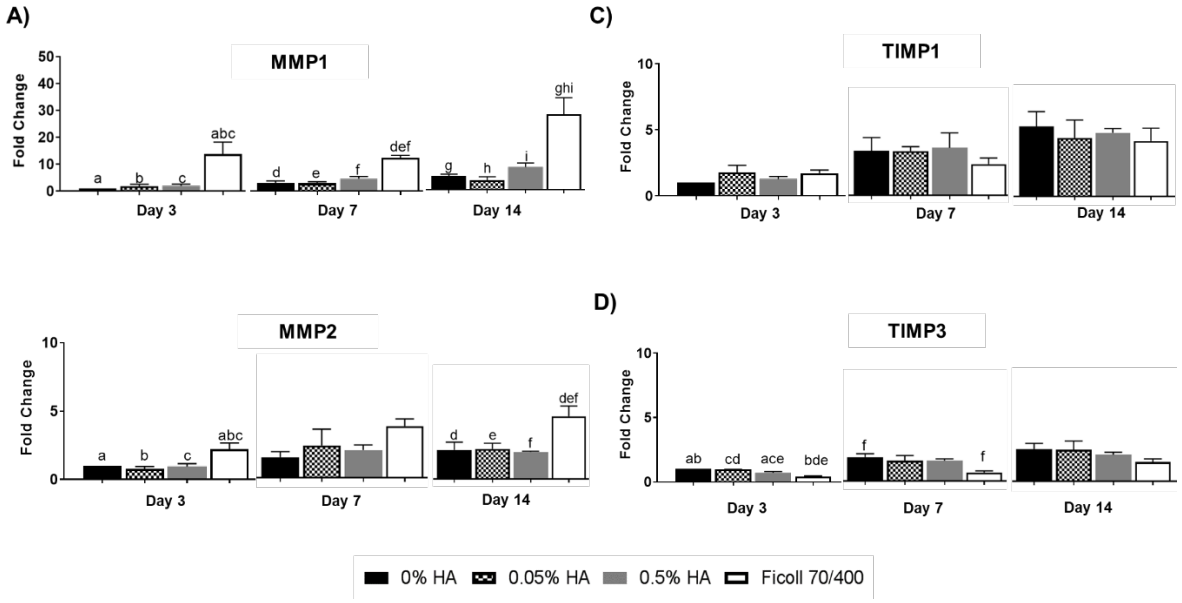

Figure 4-10: Quantitative RT-PCR analysis of **(A-B)** matrix metalloproteinases and **(C-D)** tissue inhibitors of metalloproteinases. All values represent mean and standard error of the mean from at least three experimental replicates. Statistically significant differences between means of non-crowded condition to crowded conditions for *MMP1* is indicated by $^{d,e,f}p < 0.0001$, $^{h}p < 0.001$, $^{a,g,i}p < 0.01$, $^{b,\ c}p < 0.05$, for *MMP2*: $^{a\text{-}f}p < 0.05$; and for *TIMP3* at day 3: $^{b,d}p < 0.001$ and $^{a,c,e,f}p < 0.05$.

4.3.10. Incorporation of hyaluronic acid in CDM and effects on HAS gene expression

HABP staining indicated presence of hyaluronic acid in all conditions **(Supplementary Figure 4-5 A)**, indicating that the exogenous HA was not incorporated into the CDMs. HA crowding does not appear to increase expression of genes involved with HA production. HA crowding does not significantly increase *HAS2* expression compared to the non-crowded condition **(Supplementary Figure 4-5 B).** *HAS3* expression increases over time and increased when cultured under the 0.05% HA condition **(Supplementary Figure 4-5 C)**.

4.3.11. Polydopamine coating and decellularization of CDMs developed under crowding

Polydopamine coating was used to promote adherence of CDMs to tissue culture polystyrene surface to enable decellularization and functional characterization (**Supplementary Figure 4-6)**. CDMs prepared on polydopamine surfaces were decellularized using hyperosmotic solutions followed by DNase treatment. PicoGreen dsDNA assay indicated >95% cell removal **(Figure 4-11 A)** and imaging indicated lack of DAPI-positive signal from the matrices, respectively **(Figure 4-11 B-F)** using this technique. ICC characterization of the decellularized 14-day CDMs indicated that collagen types I, III, IV as well as laminin and fibronectin were retained at the surface.

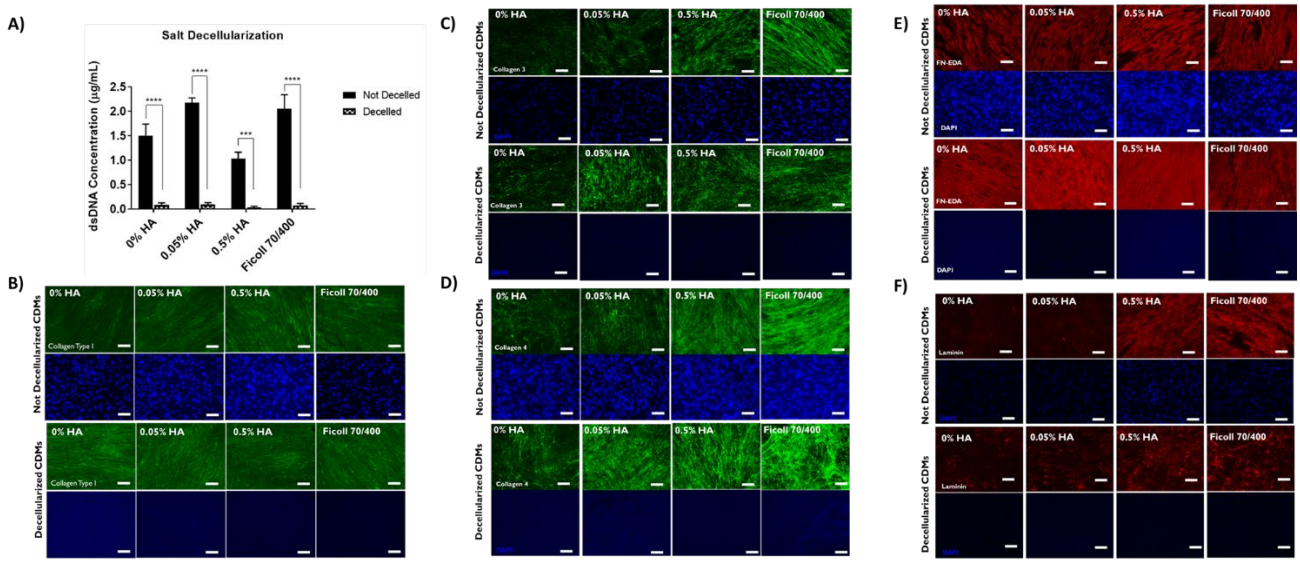

Figure 4-11: Samples decellularized using osmotic diffusion techniques. (**A)** PicoGreen assay was used to quantify dsDNA content of decellularized versus non-decellularized conditions. All values represent mean and standard error of the mean from three experimental replicates. Statistically significant differences between means of decellularized versus non-decellularized conditions is indicated by $^{****}p < 0.0001$ and $^{***}p < 0.001$. DAPI staining and ECM matrix retention for **(B)** collagen type I, **(C)** collagen type III, **(D)** collagen type IV **(E)** fibronectin, and **(F)** laminin. Images represent data from two experimental replicates.

4.3.12. Characterization of CDMs using AFM

To assess the effects of HA treatment on CDM mechanics, CDMs prepared by cells cultured for 14 days on polydopamine-coated surfaces were used to measure matrix stiffness using atomic force microscopy (AFM) nanoindentation. There is a minimum specimen thickness required for nanoindentation to prevent inaccurate stiffness measurements due to contacting the surface of the tissue culture dish. CDM sample thickness was obtained using collagen Z-stack and tile scan images of collagen type I stained samples using a confocal laser scanning microscope **(Figure 4-12)**. The CDM thickness increased over time for all conditions, but increase was not dependent on the crowding conditions. The mean thicknesses of the CDMs obtained at 7 days and 14 days was 18µm and 30µm, respectively **(Figure 4-12)**. The 14-day time point was selected for nanoindentation tests since sufficient matrix layer was retained post decellularization **(Figure 4-13).**

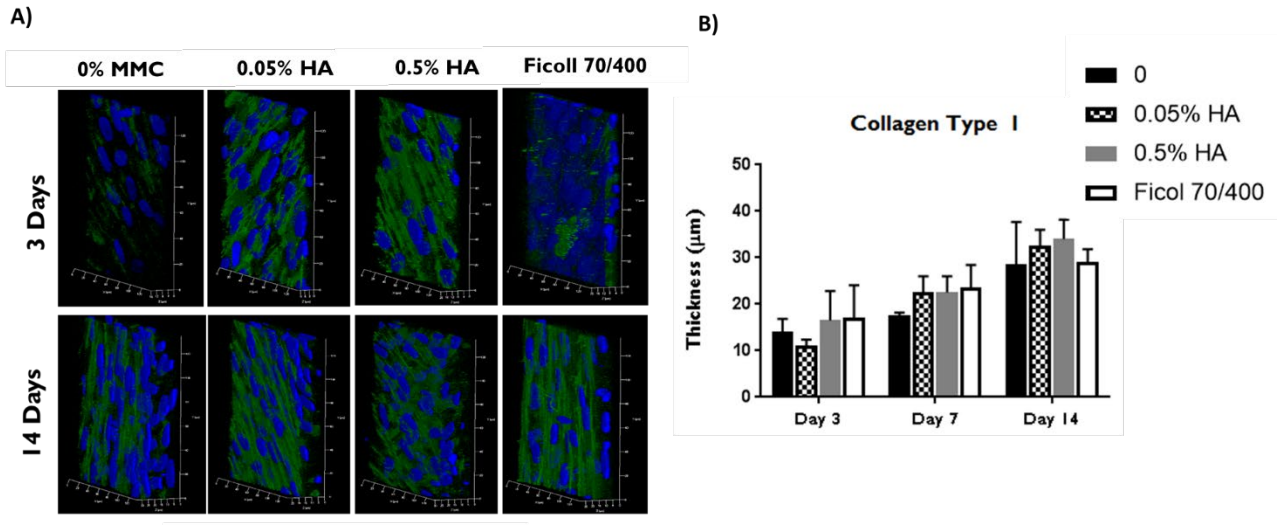

Figure 4-12: (A) Confocal laser scanning microscopy z-stack and tile scan image of collagen type I immunostaining. **(B)** Quantified CDM thickness at 3, 7, and 14 days. All values represent mean and standard error of the mean from two experimental replicates.

The stiffness values for the dermal fibroblast CDMs cultured with 0%, 0.05% HA, 0.5% HA, and Ficoll 70/400 were 15.8 kPa, 16.2 kPa, 11.85 kPa, and 4.5 kPa, respectively **(Figure 4-13)**. The differences in the stiffness of the CDM developed under 0, 0.05 or 0.05% HA crowding were not statistically significant from each other, however, indicate increased matrix density compared to the Ficoll 70/400 condition. The measured stiffness for the Ficoll 70/400-treated CDM was significantly different from the non-treated control and the 0.05% HA condition.

Stiffness measurements of CDMs were also collected without decellularization of the substrate to study ECM structure. At day 7, both HA treated matrices were comparable to the non-treated control, and measured about 7.5kPa **(Supplementary Figure 4-7)**. Ficoll 70/400 treated CDMs measured about 3.9kPa, however this was not significantly lower than the other conditions. Significant differences in stiffness measurements were apparent at day 14 **(Supplementary Figure 4-7)**. At day 14, the stiffness measurements for the non-treated, 0.05% HA, 0.5% HA, and Ficoll 70/400 treated cultures were 7.8 kPa, 5.3 kPa, 3.7 kPa, and 3.4 kPa, respectively. The non-treated control and the 0.05% HA were not statistically different from each other, however, the 0.5% HA and the Ficoll 70/00 were statistically significant compared to the non-treated control.

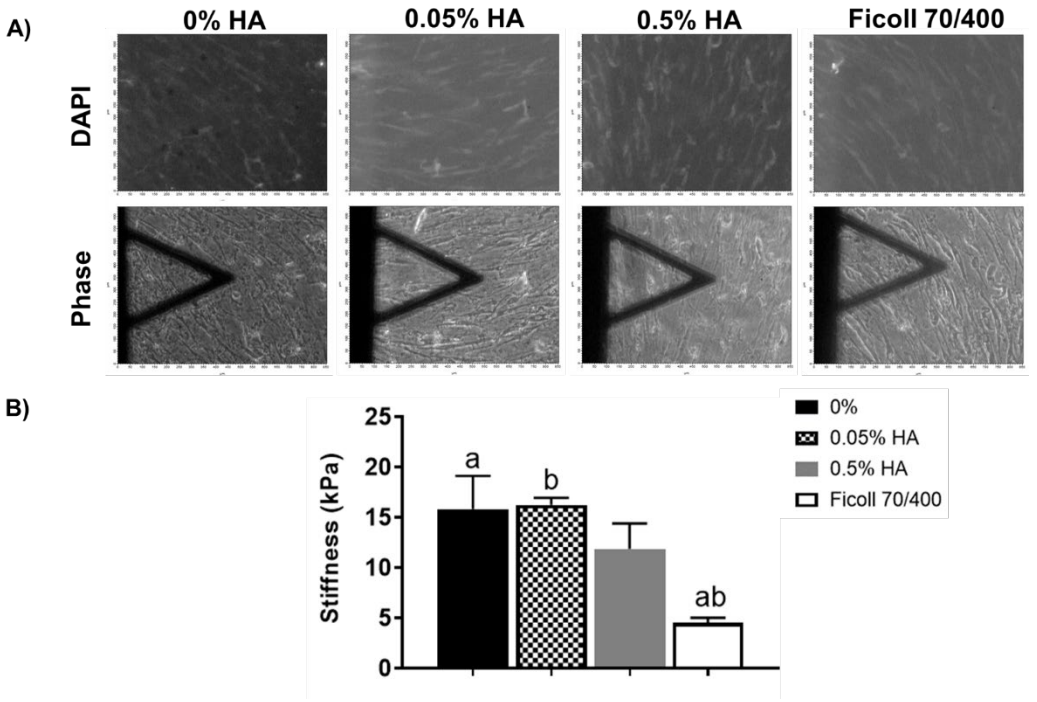

Figure 4-13: (A) Atomic force microscopy phase contrast and DAPI images of decellularized cell layers. **(B)** Stiffness values of decellularized 14-day cell-derived matrices prepared on polydopamine-coated surfaces. All values represent mean and standard error of the mean from four experimental replicates. Statistically significant differences between means of non-crowded condition to crowded conditions is indicated by $^{a, b}p < 0.05$.

4.4 Discussion

The goal of this aim was to assess the effects of MMC, specifically HA, on ECM deposition and composition, as well as explore possible effects contributing to the changes between conditions. Macromolecular crowding is governed by the excluded volume effect as well as viscosity, and we explored the effects of different macromolecules sizes and solution viscosities on ECM production in dermal fibroblasts.

While the excluded volume effect is a major contributing factor to cellular responses to crowding, there are other factors such as viscosity [45, 46], diffusion [47], and direct physical interactions between crowders and secreted proteins that may also be involved in matrix deposition [48]. It has been previously reported that changes in viscosity due to crowding alter

diffusion rates for enzyme and factors involved in different cellular processes [49-51]. Small proteins, such as enzymes, are more sensitive to differences in viscosity than larger proteins, and thus have a reduced diffusion coefficient in the system [47, 50].

HMW HA was used, which has an increased viscosity at higher concentrations [52]. Ficoll, a sucrose-based macromolecule that has been well-characterized as a macromolecular crowder for collagen deposition, was used as a positive control [19, 23]. Different molecular weight Ficoll molecules (Ficoll 70 Da and Ficoll 400 Da) were used to prepare a crowded solution representative of physiological crowding and viscosity, as previously reported [24, 40]. The viscosities of the 0.05% HA and Ficoll 70/400 solutions at a shear rate of 100 s^{-1} were 2.36 mPa-s, and 1.17 mPa-s, respectively **(Figure 4-2)**, and are representative of viscosities of physiological solutions (e.g., blood viscosity: 3.36 mPa-s 100 s^{-1}) [40]. Although the solution viscosity of 0.5% HA was ~60-fold higher than the 0.05% HA solution, the 0.5% HA concentration used was not high enough to be considered a hydrogel, and thus the solution can be considered a crowded rather than confined environment [53, 54].

The effects of crowder molecule type and solution viscosity on ECM deposition were assessed using various techniques. Pepsin/acid treated soluble fraction of human dermal fibroblasts cultured under MMC indicated differences in the collagen footprint, which was also supported by the complementary assessment of soluble collagen using the Sircol assay **(Figure 4-4)**. The bands present in the beta and gamma regions suggest the presence of alpha-1 collagen chains that were covalently crosslinked to an alpha-2 chain and adjacent alpha-1 chains prior to digestion, respectively [20, 41]. MMC did not significantly change soluble collagen presence after 3 days in culture, however, differences between MMC treated samples were apparent at 14 days. The 0.05% HA condition had the highest SDS-PAGE band intensities in all three collagen

regions compared to the negative control, which was also supported by the highest measured soluble collagen concentration in the Sircol assay. Ficoll 70/400 decreased soluble collagen deposition compared to the negative control, whereas, the 0.05% HA condition increased soluble collagen deposition. It is possible that the high viscosity in the 0.5% w/v HA culture induced adverse effects on protein stability, thus reducing the collagen deposited compared to the 0.05% HA condition [24]. However, despite the increase in viscosity, the 0.5% HA condition still had higher intensity collagen bands in the different regions compared to the less viscous Ficoll 70/400-treated cultures.

Dermal fibroblasts natively secrete collagen in their ECM and exhibit low matrix turnover [55-58]. However, the addition of 0.05% HA to the culture media increased the amount of collagen compared to the non-treated control, despite elevated proteolytic activity in the presence of bovine serum [23]. This is compared to the Ficoll 70/400 condition, which significantly decreased the amount of collagen present in the CDM. The decrease in collagen in CDM of Ficoll 70/400-treated cultures may have contributed to the observed statistically significant decrease in the stiffness values measured in Ficoll 70/400-treated CDM **(Figure 4-13)** compared to untreated and 0.05% HA-treated CDM samples.

Despite concerns that viscosity has an adverse effect on protein deposition, relative MGV quantification of ECM distribution at day 3 indicates that effects on collagens type III and IV, as well as laminin, were also comparable to the Ficoll 70/400-treated conditions **(Figure 4-5 - 4-6)**. Overall deposition of cellular fibronectin was not affected by the presence of crowder agents, however, a significant increase was observed on a per cell basis within 3 days of culture. Raman microspectroscopy was also used as an additional, marker-independent method to characterize ECM composition in fibroblast cultures **(Figure 4-8)**. Raman spectral mapping showed MMC-

mediated changes in collagen and proteoglycan deposition within 3 days of culture, with HA increasing matrix deposition compared to Ficoll 70/400-treated and untreated control. As Raman microspectroscopy is a label-free method, it eliminates any variation that may result from differences in antibody epitope specificity, staining protocols, and imaging techniques. Raman imaging results showed the potential of this technique for an unbiased, marker-independent approach for characterization of ECM composition in cell-derived matrices that also provides a holistic approach for ECM molecule detection.

A possible explanation for the differences in matrix deposition observed in Raman imaging may be due to MMC-mediated changes in cell density, which would address the question if more matrix is being made because more cells are present. Quantification of cell count and dsDNA concentration indicated that there was an increase in cell number in the Ficoll 70/400-treated conditions **(Figure 4-7)**. The increase in cell number in the Ficoll 70/400-treated samples compared to the HA-treated samples suggests that cells are in a more proliferative rather than secretory state, and thus are not producing as much matrix.

An alternative explanation for the varying effects of crowding on ECM deposition can be due to a direct effect on ECM gene expression. Previous literature has shown that Ficoll does not have a significant effect on ECM-associated gene expression in human corneal fibroblasts [23]. Furthermore, a study conducted by Monterio *et al*, evaluating the effects of HMWHA and PEG-based products used for cutaneous fillings on human dermal fibroblast viability only showed a 2-fold increase on *COL1A1* gene expression compared to the non-treated control [5]. These results were comparable to what we observed on HMWHA effects on *COL1A1*, *COL3A1*, and *COL4A1* gene expression **(Figure 4-9)**. Thus, we hypothesized that crowding would not have a significant effect on ECM gene expression. Significant differences were not observed in collagen,

fibronectin, or laminin gene expression, however, MMC mediated effects were apparent in *LOX*. The significant decrease in *LOX* expression due to Ficoll 70/400 treatment may contribute to in the collagen footprint in the SDS-PAGE While significant changes were not observed in ECM-associated genes, MMP expression was significantly affected by the type of macromolecule.

Commercially available biomaterials require devitalization via dehydration or decellularization in order to prevent any immunogenic interaction with the host. Thus, CDMs were decellularized in order to characterize their structural and functional properties. A common problem when working with *in vitro* CDMs synthesized by high cell density cultures on plastic surfaces is detachment of the cells and matrix. As decellularization protocols typically entail stringent membrane disrupting components and extensive washing, CDMs were cultured on a polydopamine-coated surface for studies requiring decellularized CDMs. Polydopamine provides a functional backbone to allow for adherence of amine and thiol groups in ECM proteins, and thus prevents the disruption of the CDM from the culture surface [59, 60]. A hyperosmotic decellularization approach was used for removal of cellular content as it minimized loss of CDM composition, and preserved matrix composition, structure, and organization [36]. PicoGreen assay and DAPI imaging indicated removal of cellular content from CDMs without removal of key ECM proteins important for tissue regeneration and angiogenesis. Decellularized CDMs were used to characterize MMC-mediated effects on CDM stiffness.

Matrix stiffness is regulated by several factors, such as increased collagen deposition [20] and GAG deposition [61, 62], crosslinking [63], and matrix metalloproteinase activity [64]. In our studies, the decrease in matrix stiffness in the presence of Ficoll 70/400 and 0.5% HA crowding suggests that there may be a macromolecule type and viscosity-mediated effect on CDM organization and assembly. Previous work using non-FBS containing media reported an

increase in stiffness of MSC cytoskeleton in response to Ficoll 70/400 crowding [20], and thus the associated ECM [65, 66]. However, in our studies, Ficoll 70/400 significantly decreased CDM stiffness compared to the non-treated and 0.05% HA conditions. While we reported upregulation in *MMP1/2* gene expression only, Ficoll-treated cultures are known to exhibit high MMP activity [67], which could have resulted in a high matrix turnover contributing to the reduced stiffness observed. In addition to the effect of crowder on MMP expression, previous literature has also shown a HMWHA dependent up-regulation in *LOX* expression in MSCs[68]. While HMWHA did not increase *LOX* expression in dermal fibroblasts, Ficoll 70/400 media induced a significant decrease in *LOX* expression at day 7 compared to the untreated and HA-crowded conditions. The decrease in *LOX* gene expression, and corresponding effects on matrix crosslinking may also explain observed differences in stiffness. The differences in the 0.05% HA and 0.5% HA CDM stiffness may be attributed to differences in matrix deposition profiles due to media viscosity. These differences indicate that crowding can be used to develop substrates with tunable mechanical properties, which have applications in studying stromal cell differentiation. For example, MSCs have been shown to differentiate into different phenotypes depending on the rigidity of the substrate used [69]. Various culture substrates, such as uni-molecular ECM components [65, 69, 70] and polyacrylamide [71], have been used with varying degrees of stiffness to study cell-substrate interactions. However, these substrates are not representative of the native microenvironment composition. Decellularized cell-derived substrates can be tailored using different crowder molecules to develop heterogeneous ECM substrates of various stiffness to support future applications of CDMs.

Previous literature studying the effects of negatively charged crowders on other cell types such as, embryonic lung fibroblasts and mesenchymal stromal/stem cells (MSCs), showed

significant effects on collagen and fibronectin deposition at the cell layer compared to the non-treated control [1, 20, 21]. Other studies have shown that the effects of MMC can further be amplified through the use of non-bovine derived sera [23]. The differences in study findings suggest that the effects of MMC are dependent on the baseline collagen synthesis and degradation rates of each cell type. Dermal fibroblasts are characterized by lower collagen synthesis per day (~4%) compared to lung fibroblasts (10%) [58]. However, lung fibroblasts have higher matrix turnover rates than dermal fibroblasts, thus resulting in less collagen content overall in lung fibroblasts [55-58]. Similar to embryonic lung fibroblasts, MSCs have high MMP to TIMP ratio, suggesting a high matrix turnover rate in these cell lines [72]. As a result of the higher matrix turnover rates, lung fibroblasts and MSCs are more sensitive to changes in external stimuli that increase their matrix deposition. In comparison, dermal fibroblasts are less sensitive to crowder-induced changes in matrix production as they already exhibit, high matrix density due to lower turnover. It has also been shown that increased fetal serum supplementation may increase proteolytic enzyme activity compared to alternative serum sources [3]. In the current study, dermal fibroblasts cultured under HA crowding and FBS still supported increased, but non-significant, matrix deposition. These studies suggest that the effects of crowding is cell-type dependent, and that it is crucial to study macromolecule effects on specific cell types in order to maximize ECM production for a particular application.

In this study, we showed that application of HMW HA as a macromolecular crowder in human dermal fibroblast cultures did not significantly increase ECM gene expression or deposition (measured by immunocytochemistry) compared to untreated controls. However, treatment with 0.05% HA increased soluble collagen and insoluble collagen crosslinks, as indicated by SDS-PAGE and quantitative collagen assays (Sircol and hydroxyproline).

The 0.05% HA concentration and Ficoll 70/400 solutions had similar viscosities, 0.05% HA cell layers had significantly higher soluble collagen, collagen crosslinks, and *LOX* transcript levels, as well as matrix stiffness, whereas Ficoll 70/400 had significantly higher MMP gene expression. The effects of macromolecule type on cell proliferation may also contribute to differences observed in matrix deposition. An increase in dsDNA and DAPI counts indicate that Ficoll 70/400 promotes a more proliferative state in dermal fibroblastsThis may also indicate that different crowding molecules modulate matrix stiffness, likely due to effects on protease and crosslinking genes.

Previous studies using different cell lines have indicated differences in collagen composition and crosslinking, as well as matrix mechanical properties, thus, highlighting differences in crowder-cell interaction, and importance of developing media formulations dependent on the cellular system used for CDM production. These studies were completed on dermal fibroblasts which may not be as sensitive to significant increases in matrix deposition compared to other cell types. Future studies may include alternative cell types, modification of cell culture media formulations, and/or changing the culture environment. In the context of other literature published in the field, this study provides insight into the different effects that macromolecules in culture media can have on different cell types, suggesting that extensive characterization of cell types, media, and crowders are needed to successfully apply macromolecular crowding for development of biomanufactured CDMs.

Alterations in media viscosity using HA crowding will be studied in the next chapter to further understand the effects of viscosity on crowding.

4.5 Acknowledgements

We would like to thank the Katja Schenke-Layland and her lab, especially Julia Marzi, at the University of Tubingen for their support in Raman microspctroscopy image acquisition and data analysis. We would also like to thank Tanja Dominko and David Dolivo for providing scientific and technical feedback on the project, assistance with primer design, and training on qRT-PCR experiments. We would like to thank Silke Keller at the Fraunhofer Institute for her training on the confocal laser scanning microscope. Finally, we would like to thank Daniel Lawler for his help on ImageJ macros script writing for bulk analysis of all ICC images.

4.6 References

[1] D. Cigognini, D. Gaspar, P. Kumar, A. Satyam, S. Alagesan, C. Sanz-Nogués, M. Griffin, T. O'Brien, A. Pandit, D.I. Zeugolis, Macromolecular crowding meets oxygen tension in human mesenchymal stem cell culture-A step closer to physiologically relevant in vitro organogenesis, Scientific Reports 6 (2016) 30746.
[2] M. Patrikoski, M.H.C. Lee, L. Mäkinen, X.M. Ang, B. Mannerström, M. Raghunath, S. Miettinen, Effects of Macromolecular Crowding on Human Adipose Stem Cell Culture in Fetal Bovine Serum, Human Serum, and Defined Xeno-Free/Serum-Free Conditions, Stem cells international 2017 (2017) 6909163.
[3] A. Satyam, P. Kumar, X. Fan, A. Gorelov, Y. Rochev, L. Joshi, H. Peinado, D. Lyden, B. Thomas, B. Rodriguez, M. Raghunath, A. Pandit, D. Zeugolis, Macromolecular crowding meets tissue engineering by self-assembly: A paradigm shift in regenerative medicine, Advanced Materials 26(19) (2014) 3024-3034.
[4] J.-E.W. Ahlfors, K.L. Billiar, Biomechanical and biochemical characteristics of a human fibroblast-produced and remodeled matrix, Biomaterials 28(13) (2007) 2183-2191.
[5] M.R. Monteiro, I.L. dos Santos Tersario, S.V. Lucena, Culture of human dermal fibroblast in the presence of hyaluronic acid and polyethylene glycol: effects on cell proliferation, collagen production, and related enzymes linked to the remodeling of the extracellular matrix, Surg Cosmet Dermatol 5(3) (2013) 222-5.
[6] P. Kumar, A. Satyam, D. Cigognini, A. Pandit, D.I. Zeugolis, Low oxygen tension and macromolecular crowding accelerate extracellular matrix deposition in human corneal fibroblast culture, Journal of tissue engineering and regenerative medicine 12(1) (2018) 6-18.
[7] M.L. Decaris, B.Y. Binder, M.A. Soicher, A. Bhat, J.K. Leach, Cell-derived matrix coatings for polymeric scaffolds, Tissue engineering Part A 18(19-20) (2012) 2148-2157.
[8] H. Ragelle, A. Naba, B.L. Larson, F. Zhou, M. Prijić, C.A. Whittaker, A. Del Rosario, R. Langer, R.O. Hynes, D.G. Anderson, Comprehensive proteomic characterization of stem cell-derived extracellular matrices, Biomaterials 128 (2017) 147-159.
[9] S. Sart, T. Ma, Y. Li, Extracellular matrices decellularized from embryonic stem cells maintained their structure and signaling specificity, Tissue Engineering Part A 20(1-2) (2013) 54-66.
[10] G. Tour, M. Wendel, I. Tcacencu, Cell-derived matrix enhances osteogenic properties of hydroxyapatite, Tissue Engineering Part A 17(1-2) (2010) 127-137.
[11] Y. Mao, T. Block, A. Singh-Varma, A. Sheldrake, R. Leeth, S. Griffey, J. Kohn, Extracellular matrix derived from chondrocytes promotes rapid expansion of human primary chondrocytes in vitro with reduced dedifferentiation, Acta biomaterialia 85 (2019) 75-83.
[12] Y. Peng, M.T. Bocker, J. Holm, W.S. Toh, C.S. Hughes, F. Kidwai, G.A. Lajoie, T. Cao, F. Lyko, M. Raghunath, Human fibroblast matrices bio-assembled under macromolecular crowding support stable propagation of human embryonic stem cells, Journal of tissue engineering and regenerative medicine 6(10) (2012) e74-e86.
[13] J.M. Aamodt, D.W. Grainger, Extracellular matrix-based biomaterial scaffolds and the host response, Biomaterials 86 (2016) 68-82.
[14] J.-M. Bourget, R. Gauvin, D. Larouche, A. Lavoie, R. Labbé, F.A. Auger, L. Germain, Human fibroblast-derived ECM as a scaffold for vascular tissue engineering, Biomaterials 33(36) (2012) 9205-9213.
[15] M.Y. Tondreau, V. Laterreur, R. Gauvin, K. Vallières, J.-M. Bourget, D. Lacroix, C. Tremblay, L. Germain, J. Ruel, F.A. Auger, Mechanical properties of endothelialized fibroblast-derived vascular scaffolds stimulated in a bioreactor, Acta Biomaterialia 18 (2015) 176-185.
[16] M. Peck, D. Gebhart, N. Dusserre, T.N. McAllister, N. L'Heureux, The evolution of vascular tissue engineering and current state of the art, Cells Tissues Organs 195(1-2) (2012) 144-158.
[17] V. Falanga, V. Su Wen Qian, D. Danielpour, M.H. Katz, A.B. Roberts, M.B. Sporn, Hypoxia upregulates the synthesis of TGF-β1 by human dermal fibroblasts, Journal of Investigative Dermatology 97(4) (1991) 634-637.

[18] J.F. Bateman, J.J. Pillow, T. Mascara, S. Medvedec, J.A. Ramshaw, W. Cole, Cell-layer-associated proteolytic cleavage of the telopeptides of type I collagen in fibroblast culture, Biochemical Journal 245(3) (1987) 677-682.
[19] M.C. Prewitz, A. Stißel, J. Friedrichs, N. Träber, S. Vogler, M. Bornhäuser, C. Werner, Extracellular matrix deposition of bone marrow stroma enhanced by macromolecular crowding, Biomaterials 73 (2015) 60-69.
[20] A.S. Zeiger, F.C. Loe, R. Li, M. Raghunath, K.J. Van Vliet, Macromolecular crowding directs extracellular matrix organization and mesenchymal stem cell behavior, PloS one 7(5) (2012) e37904.
[21] R.R. Lareu, K.H. Subramhanya, Y. Peng, P. Benny, C. Chen, Z. Wang, R. Rajagopalan, M. Raghunath, Collagen matrix deposition is dramatically enhanced in vitro when crowded with charged macromolecules: the biological relevance of the excluded volume effect, FEBS letters 581(14) (2007) 2709-2714.
[22] P. Benny, C. Badowski, E.B. Lane, M. Raghunath, Making more matrix: enhancing the deposition of dermal–epidermal junction components in vitro and accelerating organotypic skin culture development, using macromolecular crowding, Tissue Engineering Part A 21(1-2) (2014) 183-192.
[23] P. Kumar, A. Satyam, X. Fan, E. Collin, Y. Rochev, B.J. Rodriguez, A. Gorelov, S. Dillon, L. Joshi, M. Raghunath, Macromolecularly crowded in vitro microenvironments accelerate the production of extracellular matrix-rich supramolecular assemblies, Scientific reports 5 (2015) 8729.
[24] R. Rashid, N.S.J. Lim, S.M.L. Chee, S.N. Png, T. Wohland, M. Raghunath, Novel use for polyvinylpyrrolidone as a macromolecular crowder for enhanced extracellular matrix deposition and cell proliferation, Tissue Engineering Part C: Methods 20(12) (2014) 994-1002.
[25] N. Saeidi, K.P. Karmelek, J.A. Paten, R. Zareian, E. DiMasi, J.W. Ruberti, Molecular crowding of collagen: a pathway to produce highly-organized collagenous structures, Biomaterials 33(30) (2012) 7366-7374.
[26] J.P. Berezney, O.A. Saleh, Electrostatic effects on the conformation and elasticity of hyaluronic acid, a moderately flexible polyelectrolyte, Macromolecules 50(3) (2017) 1085-1089.
[27] A. La Gatta, M. De Rosa, I. Marzaioli, T. Busico, C. Schiraldi, A complete hyaluronan hydrodynamic characterization using a size exclusion chromatography–triple detector array system during in vitro enzymatic degradation, Analytical biochemistry 404(1) (2010) 21-29.
[28] C.B. Knudson, W. Knudson, Hyaluronan-binding proteins in development, tissue homeostasis, and disease, The FASEB Journal 7(13) (1993) 1233-1241.
[29] B.J. Larson, M.T. Longaker, H.P. Lorenz, Scarless fetal wound healing: a basic science review, Plastic and reconstructive surgery 126(4) (2010) 1172.
[30] M.T. Longaker, E.S. Chiu, M.R. Harrison, T.M. Crombleholme, J.C. Langer, B.W. Duncan, N.S. Adzick, E.D. Verrier, R. Stern, Studies in fetal wound healing. IV. Hyaluronic acid-stimulating activity distinguishes fetal wound fluid from adult wound fluid, Annals of surgery 210(5) (1989) 667.
[31] B.A. Mast, R.F. Diegelmann, T.M. Krummel, I.K. Cohen, Hyaluronic acid modulates proliferation, collagen and protein synthesis of cultured fetal fibroblasts, Matrix 13(6) (1993) 441-446.
[32] C. Fieber, P. Baumann, R. Vallon, C. Termeer, J.C. Simon, M. Hofmann, P. Angel, P. Herrlich, J.P. Sleeman, Hyaluronan-oligosaccharide-induced transcription of metalloproteases, Journal of cell science 117(2) (2004) 359-367.
[33] C.B. Knudson, Hyaluronan and CD44: strategic players for cell–matrix interactions during chondrogenesis and matrix assembly, Birth Defects Research Part C: Embryo Today: Reviews 69(2) (2003) 174-196.
[34] J. Marzi, E.M. Brauchle, K. Schenke-Layland, M.W. Rolle, Non-invasive functional molecular phenotyping of human smooth muscle cells utilized in cardiovascular tissue engineering, Acta biomaterialia 89 (2019) 193-205.
[35] K.J. Livak, T.D. Schmittgen, Analysis of relative gene expression data using real-time quantitative PCR and the 2− ΔΔCT method, methods 25(4) (2001) 402-408.
[36] A.R. Gillies, L.R. Smith, R.L. Lieber, S. Varghese, Method for decellularizing skeletal muscle without detergents or proteolytic enzymes, Tissue engineering part C: Methods 17(4) (2010) 383-389.

[37] W. Linthicum, M.-T. Thanh, M. Vitolo, Q. Wen, Effects of PTEN Loss and Activated KRAS Overexpression on Mechanical Properties of Breast Epithelial Cells, International journal of molecular sciences 19(6) (2018) 1613.
[38] H. Hertz, Uber die beruhrung faster elastischer Korper, Journal für die reine und angewandte. Mathematik 92 (1881) 156-171.
[39] G. Thomas, N.A. Burnham, T.A. Camesano, Q. Wen, Measuring the mechanical properties of living cells using atomic force microscopy, Journal of visualized experiments: JoVE (76) (2013).
[40] R.S. Rosenson, A. Mccormick, E.F. Uretz, Distribution of blood viscosity values and biochemical correlates in healthy adults, Clinical Chemistry 42(8) (1996) 1189-1195.
[41] Analysis of Type I Collagen Products, in: A. BioMatrix (Ed.) Carlsbad, CA.
[42] N. Stone, C. Kendall, J. Smith, P. Crow, H. Barr, Raman spectroscopy for identification of epithelial cancers, Faraday discussions 126 (2004) 141-157.
[43] A.J. Ruiz-Chica, M.A. Medina, F. Sánchez-Jiménez, F.J. Ramírez, Characterization by Raman spectroscopy of conformational changes on guanine–cytosine and adenine–thymine oligonucleotides induced by aminooxy analogues of spermidine, Journal of Raman Spectroscopy 35(2) (2004) 93-100.
[44] R. Ellis, E. Green, C.P. Winlove, Structural analysis of glycosaminoglycans and proteoglycans by means of Raman microspectrometry, Connective tissue research 50(1) (2009) 29-36.
[45] T. Laurent, A. Ogston, The interaction between polysaccharides and other macromolecules. 4. The osmotic pressure of mixtures of serum albumin and hyaluronic acid, Biochemical Journal 89(2) (1963) 249.
[46] T.C. Laurent, An early look at macromolecular crowding, Biophysical chemistry 57(1) (1995) 7-14.
[47] M.M. Hansen, L.H. Meijer, E. Spruijt, R.J. Maas, M.V. Rosquelles, J. Groen, H.A. Heus, W.T. Huck, Macromolecular crowding creates heterogeneous environments of gene expression in picolitre droplets, Nature nanotechnology 11(2) (2016) 191.
[48] I. Kuznetsova, B. Zaslavsky, L. Breydo, K. Turoverov, V. Uversky, Beyond the excluded volume effects: mechanistic complexity of the crowded milieu, Molecules 20(1) (2015) 1377-1409.
[49] M. Golkaram, S. Hellander, B. Drawert, L.R. Petzold, Macromolecular crowding regulates the gene expression profile by limiting diffusion, PLoS computational biology 12(11) (2016) e1005122.
[50] M. Tabaka, T. Kalwarczyk, J. Szymanski, S. Hou, R. Holyst, The effect of macromolecular crowding on mobility of biomolecules, association kinetics, and gene expression in living cells, Frontiers in Physics 2 (2014) 54.
[51] M.J. Morelli, R.J. Allen, P.R. Ten Wolde, Effects of macromolecular crowding on genetic networks, Biophysical journal 101(12) (2011) 2882-2891.
[52] M.K. Cowman, T.A. Schmidt, P. Raghavan, A. Stecco, Viscoelastic properties of hyaluronan in physiological conditions, F1000Research 4 (2015) 622.
[53] A.P. Minton, The influence of macromolecular crowding and macromolecular confinement on biochemical reactions in physiological media, Journal of biological chemistry 276(14) (2001) 10577-10580.
[54] H.-X. Zhou, G. Rivas, A.P. Minton, Macromolecular crowding and confinement: biochemical, biophysical, and potential physiological consequences, Annu. Rev. Biophys. 37 (2008) 375-397.
[55] J. Davidson, Biochemistry and turnover of lung interstitium, European Respiratory Journal 3(9) (1990) 1048-1063.
[56] O. Eickelberg, E. Köhler, F. Reichenberger, S. Bertschin, T. Woodtli, P. Erne, A.P. Perruchoud, M. Roth, Extracellular matrix deposition by primary human lung fibroblasts in response to TGF-β1 and TGF-β3, American Journal of Physiology-Lung Cellular and Molecular Physiology 276(5) (1999) L814-L824.
[57] G. Laurent, Dynamic state of collagen: pathways of collagen degradation in vivo and their possible role in regulation of collagen mass, American Journal of Physiology-Cell Physiology 252(1) (1987) C1-C9.
[58] G.J. Laurent, Rates of collagen synthesis in lung, skin and muscle obtained in vivo by a simplified method using [3H] proline, Biochemical Journal 206(3) (1982) 535-544.

[59] H. Lee, S.M. Dellatore, W.M. Miller, P.B. Messersmith, Mussel-inspired surface chemistry for multifunctional coatings, science 318(5849) (2007) 426-430.
[60] H. Lee, J. Rho, P.B. Messersmith, Facile conjugation of biomolecules onto surfaces via mussel adhesive protein inspired coatings, Advanced Materials 21(4) (2009) 431-434.
[61] A. Takahashi, A. Majumdar, H. Parameswaran, E. Bartolák-Suki, B. Suki, Proteoglycans maintain lung stability in an elastase-treated mouse model of emphysema, American journal of respiratory cell and molecular biology 51(1) (2014) 26-33.
[62] E. Brauchle, J. Kasper, R. Daum, N. Schierbaum, C. Falch, A. Kirschniak, T.E. Schäffer, K. Schenke-Layland, Biomechanical and biomolecular characterization of extracellular matrix structures in human colon carcinomas, Matrix Biology 68 (2018) 180-193.
[63] K.R. Levental, H. Yu, L. Kass, J.N. Lakins, M. Egeblad, J.T. Erler, S.F. Fong, K. Csiszar, A. Giaccia, W. Weninger, Matrix crosslinking forces tumor progression by enhancing integrin signaling, Cell 139(5) (2009) 891-906.
[64] A. Haage, I.C. Schneider, Cellular contractility and extracellular matrix stiffness regulate matrix metalloproteinase activity in pancreatic cancer cells, The FASEB Journal 28(8) (2014) 3589-3599.
[65] J. Solon, I. Levental, K. Sengupta, P.C. Georges, P.A. Janmey, Fibroblast adaptation and stiffness matching to soft elastic substrates, Biophysical journal 93(12) (2007) 4453-4461.
[66] K. Kurpinski, J. Chu, C. Hashi, S. Li, Anisotropic mechanosensing by mesenchymal stem cells, Proceedings of the National Academy of Sciences 103(44) (2006) 16095-16100.
[67] X.M. Ang, M.H. Lee, A. Blocki, C. Chen, L.S. Ong, H.H. Asada, A. Sheppard, M. Raghunath, Macromolecular crowding amplifies adipogenesis of human bone marrow-derived mesenchymal stem cells by enhancing the pro-adipogenic microenvironment, Tissue Engineering Part A 20(5-6) (2013) 966-981.
[68] C.P. El-Haibi, G.W. Bell, J. Zhang, A.Y. Collmann, D. Wood, C.M. Scherber, E. Csizmadia, O. Mariani, C. Zhu, A. Campagne, Critical role for lysyl oxidase in mesenchymal stem cell-driven breast cancer malignancy, Proceedings of the National Academy of Sciences 109(43) (2012) 17460-17465.
[69] A.J. Engler, S. Sen, H.L. Sweeney, D. Discher, Matrix elasticity directs stem cell lineage specification, Cell 126(4) (2006) 677-689.
[70] J. He, J. Guo, B. Jiang, R. Yao, Y. Wu, F. Wu, Directing the osteoblastic and chondrocytic differentiations of mesenchymal stem cells: matrix vs. induction media, Regenerative biomaterials 4(5) (2017) 269-279.
[71] R.J. Pelham, Y.-l. Wang, Cell locomotion and focal adhesions are regulated by substrate flexibility, J Proceedings of the National Academy of Sciences 94(25) (1997) 13661-13665.
[72] T.P. Lozito, W.M. Jackson, L.J. Nesti, R.S. Tuan, Human mesenchymal stem cells generate a distinct pericellular zone of MMP activities via binding of MMPs and secretion of high levels of TIMPs, Matrix Biology 34 (2014) 132-143.

Chapter 5 : High Molecular Weight HA Dose Response on Dermal Fibroblasts

5.1. Introduction

The goal of this project was to develop a CDM with pro-angiogenic properties that would also support the exogenous delivery of antimicrobial peptides through the increased presence of crosslinked collagen. Production of CDMs is often limited by the prolonged culture time due to the diffusion of extracellular matrix pre-cursor proteins into the media, which are ultimately discarded as waste during media changes. Macromolecular crowding is used as an approach to limit the diffusion of extracellular matrix pre-cursor proteins, thus altering the reaction kinetics for conversion of pro-collagen to mature collagen [1, 2]. The addition of macromolecules to the media creates an excluded volume effect. The excluded volume effect, or the volume occupied by different macromolecules in the media, is represented by: 1) the space occupied by the added macromolecules themselves (shown schematically in **(Chapter 2, Figure 2-1)**, and 2) the space created due to steric and electrostatic repulsions between the macromolecules **(Chapter 2, Figure 2-1, insert)**. Depending on the properties as well as concentration of the crowder macromolecule, the volume available for diffusion can be modulated to enhance biological processes *in vitro.* In addition to the excluded volume effect, macromolecular crowding can also be explained through the effects of changes in viscosity. The increase in viscosity due to addition of macromolecules can also alter the diffusion profile of small enzymes and proteins, thus affecting matrix deposition. Small enzymes and proteins are the most sensitive to changes in viscosity, and thus has a direct effect on matrix deposition.

High molecular weight (HMW) HA has been previously studied for ECM deposition [3, 4]. However, lower concentrations of HMW HA were used, and thus did not significantly alter

the viscosity of the media. Furthermore, these studies were not completed in the context of a macromolecular crowder, but rather studied how HA-containing products affect fibroblast viability. We have shown that HMWHA at 0.05% (low viscosity) and 0.5% (high viscosity) have an effect on matrix properties through changes in soluble collagen concentration (Sircol assay), increase in total collagen concentration (hydroxyproline assay), and changes in matrix stiffness properties. While increased viscosity can help promote matrix deposition at the cell layer and reduce diffusion of ECM precursor molecules into the media, increasing the viscosity of the media may also result in adverse effects on protein folding and stability [5]. Furthermore, for bioreactor manufacturing applications, higher solution viscosities may cause challenges in scale-up reactor based cultures due to high shear rates required. The higher concentration of HMWHA in scaled up cultures may also present a significant cost burden during production as HMWHA itself is expensive, and use at higher concentrations with frequent media changes can substantially increase the cost of production.

As a result, it is important to determine the ideal concentration of HA as a crowder molecule. The objective of this project was to identify the concentrations of HA that increase collagen production compared to the negative control, non-treated cultures without causing any adverse effects on matrix production. Ficoll 70/400 was used a positive control for viscosity measurements only as this condition has been previously assessed in our work characterizing HA as a crowder molecule. Identifying an ideal concentration of HA provides information into the production of CDMs using HA crowding.

5.2. Materials and Methods

5.2.1. Rheology

Rheological assessment of HA and Ficoll solution fluid viscosity was completed using a MCR 302 WESP (Anton Paar) with a smooth parallel 25mm plate configuration. HA solutions at different concentrations were prepared in 1X PBS and sterile filtered. Five hundred microliter volume was loaded onto the stage. A shear rate of 1-1000 s^{-1} was applied to each solution sample to obtain flow curves and viscosity measurements. A sample size of N = 2 was assessed for each condition. Statistical analysis was not completed on these experiments.

5.2.2. Cell Culture

Human neonatal fibroblasts (p2-p8, ATCC, CRL 2097) were plated at a density of 25,000 cells/cm^2 and cultured in DMEM (Corning, 15-017 CV) supplemented with 10% v/v fetal bovine serum (Gibco, 16000-044) , 1% v/v penicillin/streptomycin (Corning, 30-002-Cl), 1% v/v non-essential amino acids (Corning, 25-025Cl), 1% v/v L-glutamine (Corning, 25- 005Cl) and 1% v/v sodium pyruvate (Corning, 25-001-Cl) for 24 hours prior to culture with crowding media. HA media was supplemented with 0.05% w/v, 0.1% w/v, 0.25% w/v, or 0.5% w/v high molecular weight hyaluronic acid (HA15M-5, 1.5MDa, LifeCore Biomedical, USA). Untreated cell cultures served as the negative control, non-crowded condition. All cultures were supplemented with 100μM ascorbic acid (Wako, 013-19641). Cells were cultured at standard culture conditions (37°C, 5% CO_2), and media was replaced every 2-3 days.

5.2.3. Immunocytochemistry

Fibroblasts cultured for 3 days, 7 days, or 14 days were fixed using 4% paraformaldehyde/PBS (Alfa Aesar, J61899) for 10 minutes at room temperature. After fixation, cells were incubated in 2% w/v bovine serum albumin (HyClone, 25-529F) reconstituted in 1X DPBS for two hours at room temperature to minimize non-specific binding. The following primary antibody solutions were prepared in 2% BSA and incubated with cells overnight at 4C: collagen type III (Abcam, ab7778,1:250), collagen type IV (Abcam, ab6486, 1:250), and fibronectin (Santa Cruz Biotechnology, sc-59826,1:200). After primary antibody incubation, cell layers were rinsed in 1X DPBS and incubated in secondary antibody solution consisting of goat anti-mouse 568 (Life Technologies, A11004) and goat anti-rabbit 488 (Life Technologies, A11005) or goat anti-rabbit 594 (Life Technologies, A11012) at 1:400 dilution in 1X DPBS depending on primary antibody species. Cells were counterstained with DAPI and imaged using a Zeiss Axiovert microscope.

Each condition was imaged in five different regions of interest (ROI) per sample. Mean gray values (MGV) of each detected fluorescent sample for the areas measured were obtained using an iterative threshold algorithm on ImageJ (National Institute of Health). DAPI counts were determined using Image J algorithms. MGVs were normalized to the number of cells present in the frame analyzed, as determined by DAPI counts. Pixel distribution as represented by MGV, and MGV normalized relative to the DAPI counts per ROI were quantified and graphed. MGVs were normalized to the 3-day non-treated control samples.

5.2.4. SDS-PAGE and Silver Staining

Cell layers were pepsin-digested using 0.1 mg/mL pepsin (Sigma, P6887) reconstituted in 0.05M cold acetic acid with a pH of 2.2. An aliquot was collected for Sircol soluble collagen assay and total protein measurement using Bradford. Aliquots were frozen at -80ºC until use. The remaining aliquot of pepsin-digested samples was neutralized with 6M NaOH and phenol red solution. Protein concentration was normalized to allow for equal loading of protein samples. A collagen standard (Advanced Biomatrix, 5005) prepared in 0.05M acetic acid for a final concentration of 1mg/mL was used a protein reference. Samples were prepared with 20% Laemmli buffer. Proteins were denatured at 95ºC for 5 minutes. A 6% Tris-glycine SDS-PAGE gel was used for gel electrophoresis. Gels were stained using SilverQuest staining kit (Invitrogen, LC6070) as specified in the manufacturer's protocol. Gels were fixed for 4 hours in a methanol and acetic acid fixative prior to staining. After appearance of bands, the reaction was stopped and gels were imaged on a ChemiDoc XRS (Bio-Rad).

5.2.5. Sircol Soluble Collagen Assay

Pepsin-acetic acid-digested samples were collected as previously specified. Sircol soluble collagen reagent was prepared using 0.1% direct red 80 and 0.1% Fast green FCF in picric acid solution. 900 µl reagent volume was added per 100 µl sample and incubated at RT under agitation for 30 minutes to allow for formation of a dye-collagen complex. Samples were centrifuged at 10,000g for 10 minutes to collect pellet. The supernatant was discarded, and the pellet was quenched with 500 µl of 0.5M NaOH to release collagen. Collagen standards were prepared using bovine type I collagen, and serially diluted using 0.05M acetic acid. Absorbance

measurements were read using Viktor 3 Plate reader (Perkin Elmer) at an absorbance of 550nm. Soluble collagen concentration was calculated using a standard curve.

5.2.6. Statistical Analysis

All experiments were completed in triplicate unless otherwise stated. Statistical analysis was performed to determine significance amongst the experimental conditions using GraphPad Prism 7 software. Data is reported as the mean ± standard error of the mean (SEM). One-way ANOVA followed by Tukey's post-hoc multiple comparisons within conditions was completed. If normality assumptions were violated, Kruskal–Wallis test followed by Dunn's post-hoc analysis was completed. A two-way ANOVA followed by Tukey's multiple comparison tests were completed if two factors were analyzed. Statistical significance is reported at $p < 0.05$.

5.3. Results

5.3.1. Characterizing solution viscosity

The viscosities of the 0.01% HA, 0.05% HA, 0.1% HA, 0.25% HA, and 0.5% HA at a shear rate of 100 s^{-1} were 1.34 mPa-s, 2.36 mPa-s, 5.26 mPa-s, 31.23 mPa-s, and 139.1 mPa-s, respectively **(Figure 5-1)**. The viscosities of the different HA concentrations were compared to Ficoll 70/400, which at a shear rate of 100 s^{-1} was 1.17 mPa-s. The viscosities for the 0.05% HA and 0.01% HA were comparable to Ficoll 70/400, and are most representative of

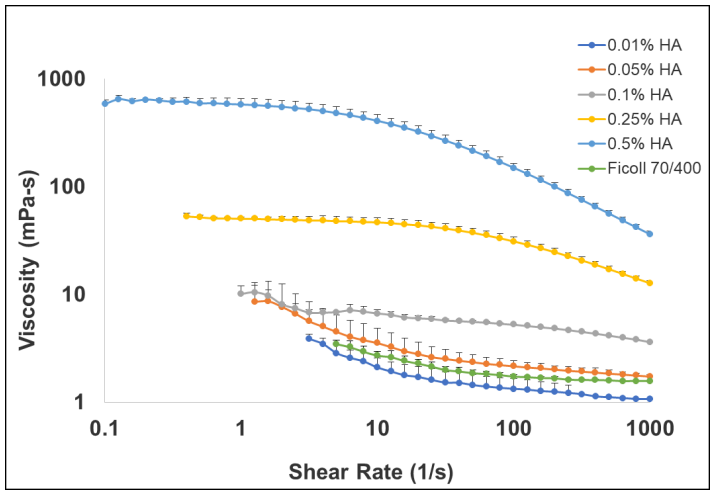

Figure 5-1: Viscosity measurements for different concentrations of HMWHA solutions compared to Ficoll 70/400.

physiological solution viscosity (blood viscosity: 3.36 mPa-s 100 s^{-1}) [6]. Viscosity values represent measurements obtained from two independently prepared solutions with standard deviation reported on the graph.

5.3.2. Assessment of soluble collagen

Human fibroblasts cultured under untreated, 0.05%, 0.1% HA, 0.25% HA, or 0.5% HA for 14 days under macromolecular-crowded cultures, were pepsin/acid treated and evaluated for collagen deposition using SDS-PAGE and silver staining. This technique allows for qualitative assessment of the alpha, beta, and gamma regions present in the sample **(Figure 5-2 A)**. The collagen footprint seen in the 0.05% HA cell layer samples indicates darker intensity bands within the lower molecular weight alpha region and the higher molecular weight crosslinked beta region compared to the non-treated control. Qualitative assessment of the crowded samples indicate that the 0.05% w/v HA treatment increased alpha-1 collagen chains (alpha region), and showed darker intensity bands in the beta region compared to the other conditions. The 0.1% w/v HA

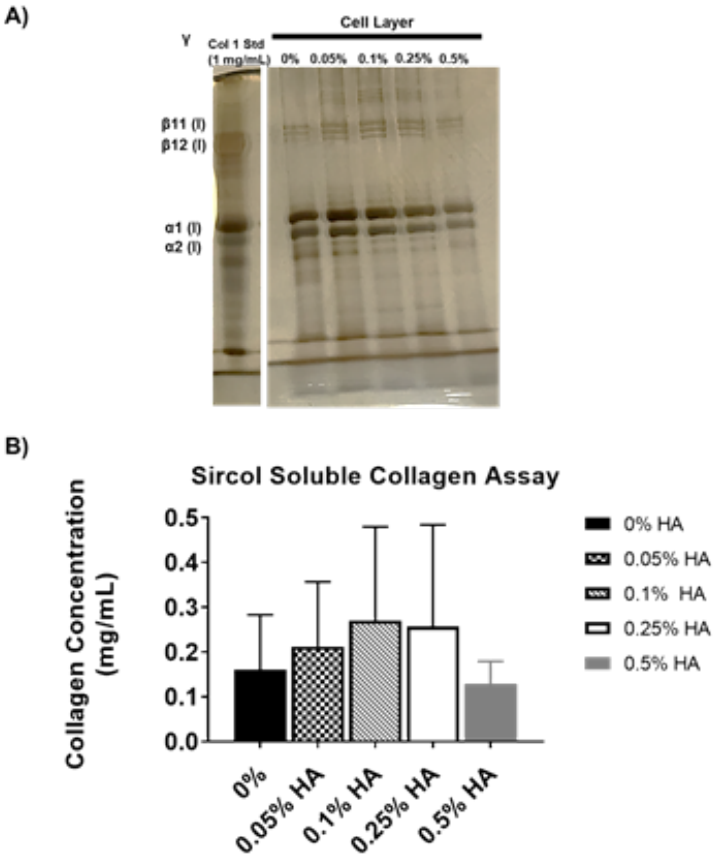

Figure 5-2: Assessment of collagen deposition in 14-day cell-derived matrices prepared under different HA crowding conditions. **(A)** SDS-PAGE and silver stained gel of pepsin/acetic acid digested cell layers. Bovine type I collagen was used as a positive control. **(B)** Complimentary quantitative Sircol soluble collagen assay of pepsin/acetic acid digested cell layers. All values represent mean and standard error of the mean from three independent experimental replicates. Statistical significance between conditions was not present.

condition has alpha and beta region bands that are slightly darker compared to the 0.05% HA condition. The intensity of the bands in the 0.25% HA condition is lower compared to the less viscous solutions. The 0.5% HA condition has the lowest band intensity compared to untreated as well as all other HA conditions. Image represents data collected from three independent experiments**.**

A complimentary Sircol collagen assay was completed using the pepsin/acid collected samples from the SDS-PAGE/Silver staining experiment. There were differences in soluble collagen concentrations observed at the 14-day cell layer samples. Soluble collagen concentrations for the 0.1% and 0.25% HA treated conditions were 0.27 mg/mL and 0.25 mg/mL, respectively, compared to the 0.05% HA condition which was 0.21 mg/mL **(Figure 5-2 B)**. While significant differences were not observed, these conditions were higher than the 0.5% HA condition.

5.3.3. ECM Deposition

In order to assess the effects of HA on ECM composition and deposition, CDMs were qualitatively assessed using immunocytochemistry (ICC) for different ECM proteins after 3, 7 and 14 days in culture. The following ECM proteins were studied: collagen types III and type IV, as well as cellular fibronectin **(Figures 5.3-5.5)**.

After treatment of dermal fibroblasts with the different HA media supplemented with 100 μM ascorbate, qualitative assessment indicates increase in collagen type III and type IV in all crowder conditions compared to the non-treated control within 3 days of culture. Quantitative assessment of collagen III and collagen IV did not indicate any statistically significant increases in HA treated compared to untreated condition, however, and increasing trend was observed. The

0.25% HA condition had increased fibronectin deposition compared to the non-treated control within 3 days. Furthermore, the 0.25% HA and 0.5% HA conditions increased the cellular fibronectin deposited on a per cell basis compared to the other HA conditions as well as the non-treated control. However, these results were not significant.

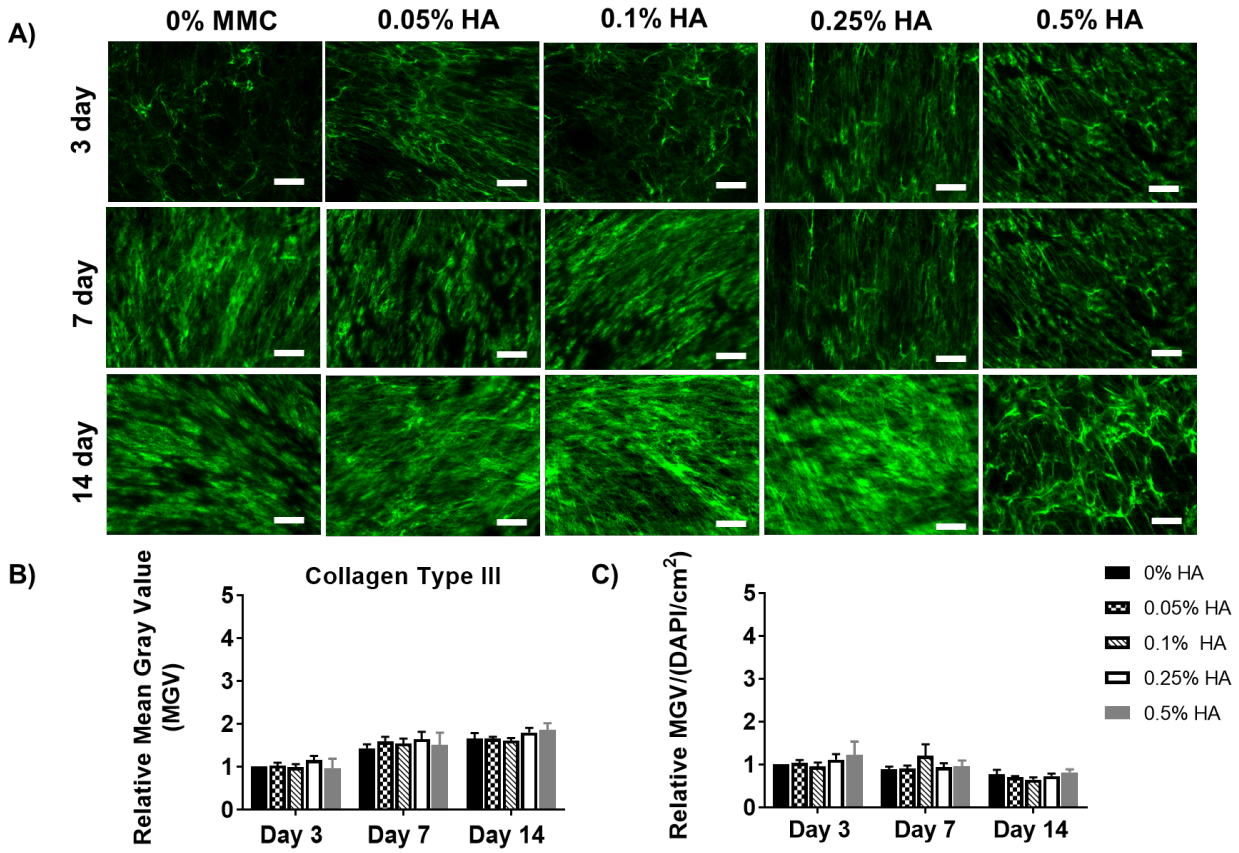

Figure 5-3: Collagen type III deposition in 3, 7, and 14 day samples under HA crowding **(A)** Representative ICC images of collagen type III distribution in CDMs at 3, 7, and 14 day time points. Scale bar: 100 µm. **(B)** Quantification of pixel distribution using iterative thresholding to represent mean collagen deposition. **(C)** Mean gray values normalized to number of cells per ROI within each image. Values represent averages and SEM from four independent experimental replicates.

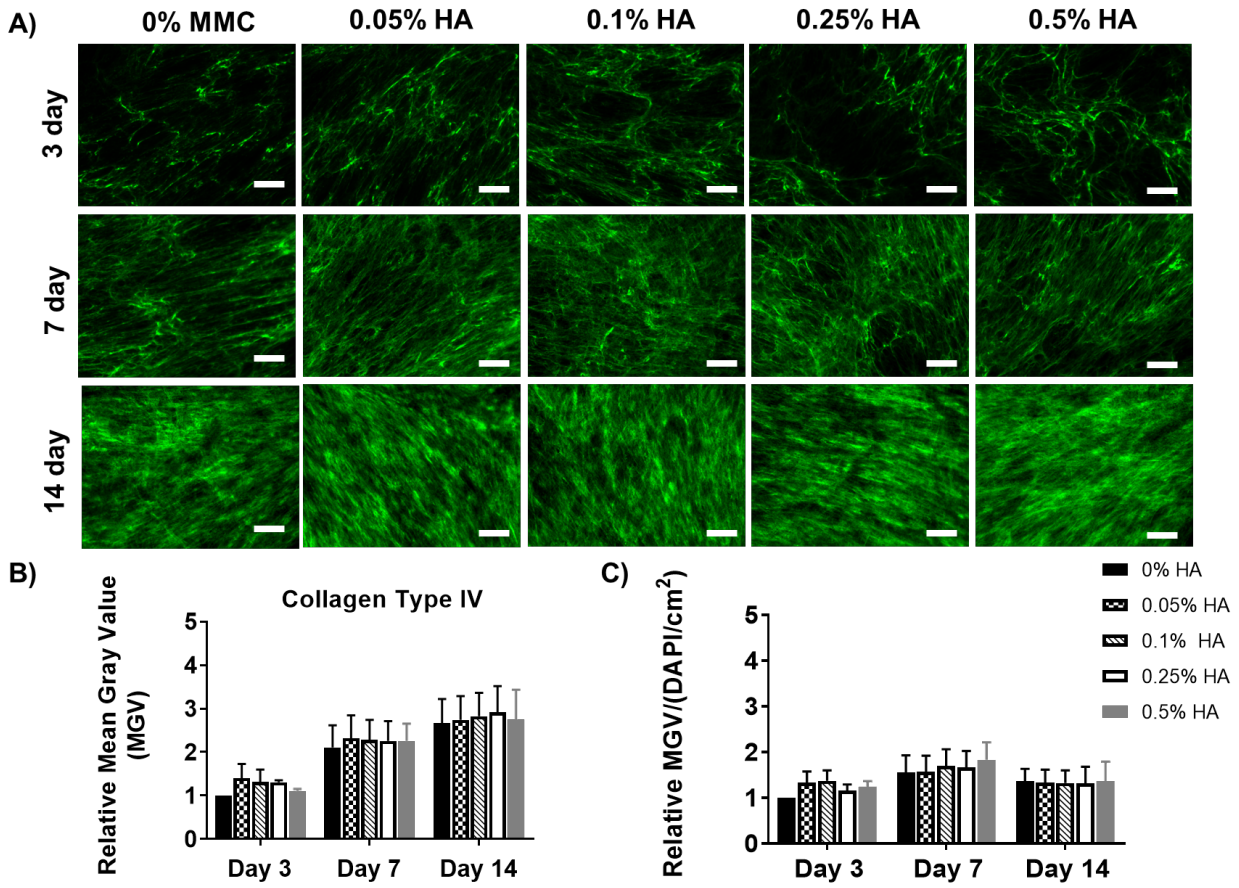

Figure 5-4: Collagen type IV deposition in 3, 7, and 14 day samples under HA crowding **(A)** Representative ICC images of collagen type IV distribution in CDMs at 3, 7, and 14 day time points. Scale bar: 100 µm. **(B)** Quantification of pixel distribution using iterative thresholding to represent mean collagen deposition. **(C)** Mean gray values normalized to number of cells per ROI within each image. Values represent averages and SEM from four independent experimental replicates.

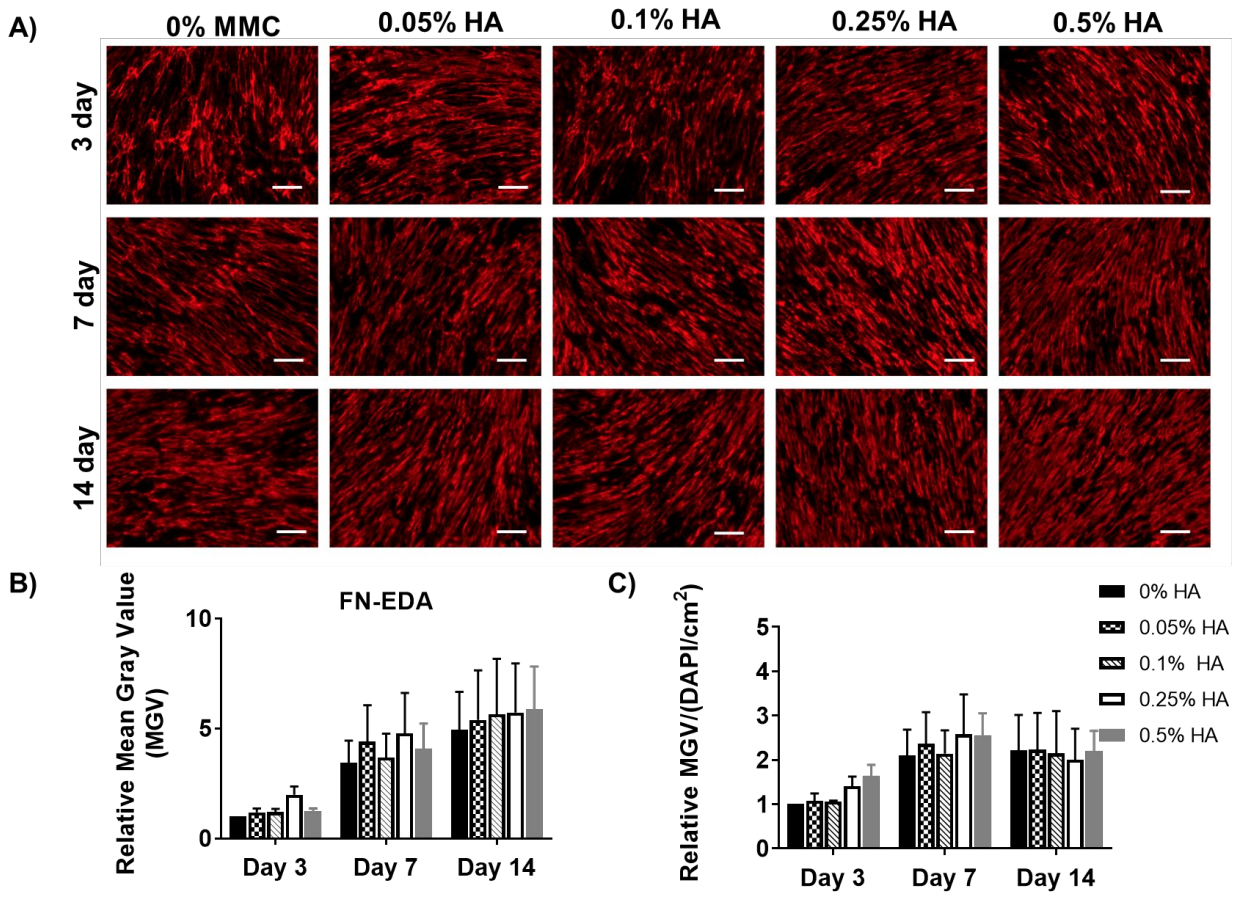

Figure 5-5: Fibronectin deposition in 3, 7, and 14 day samples under HA crowding **(A)** Representative ICC images of collagen type IV distribution in CDMs at 3, 7, and 14 day time points. Scale bar: 100 µm. **(B)** Quantification of pixel distribution using iterative thresholding to represent mean collagen deposition. **(C)** Mean gray values normalized to number of cells per ROI within each image. Values represent averages and SEM from three independent experimental replicates.

5.4. Discussion

The objective of this study was to optimize the HA macromolecule concentration in media to promote increased ECM deposition. Macromolecular crowding has been shown to promote ECM deposition *in vitro* through the excluded volume effect and changes in viscosity. The excluded volume effect is dependent on polydispersity index and macromolecule size; and the effects of viscosity is dependent on concentration and solubility in solution.

As a natural macromolecule present *in vivo*, HA has been shown to play a role in ECM deposition, organization, and assembly [7]. Previous work has also explored the effects of HMWHA on dermal fibroblast proliferation and collagen deposition [3, 4]. However, the concentrations and cell densities used in the culture were not representative of a crowded environment; and thus the effects of HA as a crowder in cellular systems had not been explored until now.

In this study, we used different concentrations of HA (0.05%, 0.1%, 0.25%, and 0.5% HA) to study the effects of HA concentration and solution viscosity on ECM deposition **(Figure 5.1)**. The viscosity of the 0.1% HA and 0.25% HA concentrations exceeded that of physiological conditions, however, it was closer in viscosity to the 0.05% HA condition, and it was hypothesized that those concentrations would have similar matrix deposition profiles. ICC characterization and quantification of ECM deposition on a per cell basis, do not indicate significant changes in collagen type III deposition and fibronectin within 3 days of culture in the 0.25% and 0.5% HA conditions compared to the non-treated control **(Figure 5.3, 5.5),** however there is an increasing trend. A significant increase was not observed for collagen type IV, but an increase was observed in the 0.05% and 0.1% compared to the non-treated control **(Figure 5.4)**. Furthermore, silver staining and complimentary Sircol assay showed increases in collagen deposition up until 0.1% compared to the non-treated control **(Figure 5.2)**. The concentration of collagen decreased in 0.25% and 0.5% treated cultures indicating that the increased viscosity had an effect on protein deposition. It is apparent from these experiments, that conditions with similar viscosities have comparable effects on matrix deposition. As a macromolecule for promoting matrix deposition, the 0.05% and 0.1% HA would be the most effective in CDM deposition, and supports the use of the 0.05% HA condition for further characterization of

CDMs. In the next chapter, we investigate the applications of CDMs for antimicrobial peptide adsorption to support the overall goal of developing a pro-regenerative scaffold to treat and prevent infection.

5.5. Acknowledgements

We would like to thank Amanda J. Rickards for working on this project during her REU project, and would like to acknowledge REU Grant for funding support (NSF EEC 1559819).

5.6. References

[1] R.R. Lareu, K.H. Subramhanya, Y. Peng, P. Benny, C. Chen, Z. Wang, R. Rajagopalan, M. Raghunath, Collagen matrix deposition is dramatically enhanced in vitro when crowded with charged macromolecules: the biological relevance of the excluded volume effect, FEBS letters 581(14) (2007) 2709-2714.
[2] J.F. Bateman, J.J. Pillow, T. Mascara, S. Medvedec, J.A. Ramshaw, W. Cole, Cell-layer-associated proteolytic cleavage of the telopeptides of type I collagen in fibroblast culture, Biochemical Journal 245(3) (1987) 677-682.
[3] B.A. Mast, R.F. Diegelmann, T.M. Krummel, I.K. Cohen, Hyaluronic acid modulates proliferation, collagen and protein synthesis of cultured fetal fibroblasts, Matrix 13(6) (1993) 441-446.
[4] M.R. Monteiro, I.L. dos Santos Tersario, S.V. Lucena, Culture of human dermal fibroblast in the presence of hyaluronic acid and polyethylene glycol: effects on cell proliferation, collagen production, and related enzymes linked to the remodeling of the extracellular matrix, Surg Cosmet Dermatol 5(3) (2013) 222-5.
[5] L. Breydo, K.D. Reddy, A. Piai, I.C. Felli, R. Pierattelli, V.N. Uversky, The crowd you're in with: effects of different types of crowding agents on protein aggregation, Biochimica et Biophysica Acta (BBA)-Proteins and Proteomics 1844(2) (2014) 346-357.
[6] R.S. Rosenson, A. Mccormick, E.F. Uretz, Distribution of blood viscosity values and biochemical correlates in healthy adults, Clinical Chemistry 42(8) (1996) 1189-1195.
[7] C.B. Knudson, Hyaluronan and CD44: strategic players for cell–matrix interactions during chondrogenesis and matrix assembly, Birth Defects Research Part C: Embryo Today: Reviews 69(2) (2003) 174-196.

Chapter 6 : Cell-derived materials for antimicrobial peptide delivery

6.1. Introduction

Chronic wounds are characterized by prolonged inflammatory stage and impaired blood flow to the wound bed, and thus delay the wound healing response. As a result of the delayed closure, there is higher potential for a wound bed to become infected. An infected wound poses several challenges to a patient's overall health, and is an expensive yet preventable economic burden. In the United States alone, there are 6.5 million patients [1] that have some type of chronic wound, and of those wounds there is a 50% chance of a wound bed becoming infected, making treatment more challenging and expensive [2, 3].

A wound bed is considered infected if bacterial concentration exceeds 10^5 or 10^6 bacteria colony forming-units [4]. The most commonly identified pathogen present in chronic wounds is *Staphylococcus aureus,* with methicillin resistant *Staphylococcus aureus* (MRSA) accounting for 20-50% of chronic wound cases [5]. Standard of care for infected wounds includes surgical debridement followed by administration of antibiotics. While systemic antibiotics do not effectively reduce the bacterial colony count, topical antibiotics have been shown to be effective [6]. Despite the effectiveness of antibiotics, medical care is being challenged by the rising threat of antibiotic resistance [7]. Furthermore, prolonged use of an antibiotic course has been shown in inhibit wound healing.

In addition to the use of antibiotics, silver and chemical -based dressings have been widely used to treat infection. Silver based dressings are more commonly used in the clinic, with multiple reports claiming improved rates of healing [8]. However, these findings are also conflicting, as silver has been shown to be cytotoxic to cells at the wound bed, and thus inhibit wound closure [8-10]. Thus, there is a clinical need for the development of biomaterials with

antimicrobial properties. An alternative approach is through the use of naturally occurring antimicrobial peptides that play a role in the wound healing process.

Antimicrobial peptides (AMPs) are short, naturally occurring peptides present within the innate immune system of living organisms. Due to the large variety of AMP structures and sequences, their mechanism of action is currently under investigation. However, the general mechanism of action is through membrane disruption of different microbial organisms [11]. For peptides with an overall cationic charge, it is accepted that the mechanism of action is initially mediated by electrostatic interaction with negatively charged microbial membranes followed by bivalent cation exchange, leading to membrane permeabilization [12, 13]. AMPs have been explored as alternatives to conventional antimicrobial agents, such as metallic compounds and quaternary ammoniums due to their broad-spectrum activity and lower cytotoxicity [13, 14]. Their several alternative mechanisms of action positions AMPs as potential therapeutic technology to address the rising challenge of antibiotic resistance [15].

While AMPs have several advantages, challenges associated with their cytotoxicity at higher doses, poor *in vivo* stability, and high costs of production have hindered their commercial application in wound healing [16]. These challenges are being addressed through different approaches to binding peptides to surfaces to facilitate peptide delivery and reduce toxicity. While AMPs have been shown to bind to different substrates, such as metals [17] and synthetic polymers [18], their binding to biomaterials for regenerative applications have only recently been explored [19].

AMPs can bind to surfaces through physical methods, such as adsorption [20], electrostatic attraction, or layer-by-layer assembly within polyelectrolyte multilayer films [21]. The layer-by-layer assembly technique is based on alternating cationic and anionic layers on a

substrate with AMPs sandwiched between the layers [21]. This method provides controlled release, however, peptides are restricted to the innermost layers and are not in contact with surrounding environment, which is important for microbial activity [13]. Chemical methods, such as polyethylene glycol (PEG)-mediated covalent binding [13, 22] have also been reported for immobilizing AMPs to surfaces. Tethering or covalent binding to surfaces through PEG spacers can reduce the required therapeutic concentration [23], improve peptide stability [23], and also provide a method for controlled release [24]. However, stable polymers must be used to prevent PEG chain cleavage due to polymer degradation [25]. Furthermore, covalent immobilization methods have also been shown to have cytotoxic effects [26].

Collagen binding domains (CBDs) have also been explored as a method to bind bioactive molecules, such as growth factors [27] and small proteins [28, 29], to different surfaces. The binding of CBDs is due to site specific affinity binding to collagen molecules [30, 31], with the strength of binding described by dissociation constants [19, 32]. There are several types of CBDs reported with various amino acid compositions, charges, and dissociation constants [19]. CBDs have also been shown to improve binding of growth factors to the ECM of retinal tissue surfaces [29, 33]. However, binding or release of peptides from biopolymeric materials that can be used for tissue engineering applications has not been explored until recently [19, 26, 28]. Integrin- and fibronectin-binding sequences derived from mammalian collagen molecules have been shown to improve the stability of collagen-like proteins through non-covalent binding to a mechanically stable silk biomaterial [28]. Collagenase- and fibronectin-derived CBDs have also been shown to improve the stability of AMPs when bound to bovine collagen type 1 wound dressings [19].

One particular class of AMPs, cathelicidins, are mammalian-derived peptides that are characterized by a conserved cathelin-like domain on their N-terminus and a variable, active

domain on the C-terminus. The only human cathlicdiin, hCAP-18, contains a 37 amino acid sequence known as LL37. The LL37 peptide is cleaved from the hCAP-18 pre-cursor via via serine proteases [34, 35]. In addition to its antimicrobial properties, LL37 has been shown to have anti-inflammatory [35], pro-regenerative, and pro-angiogenic properties [34]. The binding of LL37 via collagenase- (cCBD) and fibronectin- (fCBD) derived CBDs to commercially available engineered, bovine collagen type I scaffolds compared to an unmodified LL37 controls showed improved retention of the CBD-LL37s to the scaffold, and that the peptide retained its antimicrobial activity against Gram-positive and Gram-negative bacteria [19]

Collagen is a major ECM component that plays a role in the wound healing response, and binding AMPs to collagen via CBDs can potentially improve AMP stability and reduce cytotoxicity *in vivo.* While tissue-derived collagen biopolymers are successful commercially [36], limitations such as xenogeneic source, tissue availability, post-processing procedures, have lead researchers to seek alternative sources of ECM as potential delivery vehicles [37]. Cell-derived matrices provide an alternative ECM source as they are rich in collagen, and thus can also be used to bind CBD modified peptides for biomaterial development. They have several advantages in that they are human cell-derived, heterogeneous extracellular matrix materials that recapitulate the native microenvironment. ECM-based dressings have been shown to play a major role in reepithelialization, as individual ECM components play an active role in cell recruitment and growth factor secretion [38]. CDMs also have a rich collagen composition that can support adsorption of AMP binding via CBDs. While there are several advantages and applications for CDMs, their commercial translation has been hindered due to the required culture time needed for sufficient accumulation of ECM materials.

Previous work assessing CBD-LL37 binding and activity utilized homogenous, engineered bovine collagen type I scaffolds [19]. The objective of this aim was to study the use of a heterogeneous, human cell-derived materials for binding of CBD-LL37, as well as its antimicrobial activity. We only utilized the collagenase derived CBD (cCBD-LL37), as a preliminary approach for adsorption to CDMs. The first part of this aim focuses on the use of CDMs developed under MMC conditions for cCBD-LL37 binding and microbial activity against a model microorganism, *E. coli*, and will be referred to as MMC CDMs. Due to the differences in collagen composition and structure within the MMC CDMs, we hypothesized that samples with higher collagen amounts would have the highest log-reduction values due to increased binding of cCBD-LL37. However, it is important to emphasize that these CDMs were developed as 2-D *in vitro* cultures, and for clinical translation, a biomanufacturing process must be adopted. The second part of the aim focuses on using a biomanufactured CDM, which was developed by our collaborators, Histogen, Inc. These 3-D scaffolds will be referred to as *hECM* to differentiate from the MMC developed 2-D materials.

Histogen is a startup company based in San Diego, CA that has developed an approach for scaled production of CDMs. They have developed a method that uses neonatal fibroblasts cultured on dextran microcarrier beads suspended in bioreactors under hypoxic conditions and chemically defined medium for up to 8 weeks [39]. Their approach highlights the efficacy of combining multiple methods to increase CDM production. The ECM slurry that is secreted by human cells can be collected to develop CDM biomaterials for applications in wound healing. The ECM slurry is versatile in that the final material can be formulated into different types of biomaterials. For example, the slurry can be digested to develop a hydrogel or lyophilized to

develop a sponge-like scaffold. The material developed from the ECM slurry will be referred to in this chapter as human ECM (hECM) to differentiate between CDMs developed under MMC.

Using the hECM materials developed by Histogen, our goal was to assess the adsorption and activity of cCBD-LL37 to develop a pro-regenerative, antimicrobial hECM biomaterial for treatment of chronic wounds. To support product development, we used Histogen's hECM in lyophilized and hydrogel formats and assessed cCBD-LL37 adsorption. The antimicrobial activity was assessed against *E. coli*.

Ultimately, scaled production of CDMs would support development of a stable, AMP-loaded ECM-biomaterial, which can be used to promote wound healing and reduce infection. Furthermore, MMC may potentially be combined in a bioreactor culture to promote ECM deposition during production.

6.2. Materials and Methods

6.2.1. Preparation of polydopamine coating

Polydopamine (Sigma, H8502) was reconstituted in 100 mM bicine (Sigma, B3876) solution prepared at pH 8.5. Coverslips placed in 24-well plates were incubated with polydopamine solution overnight at room temperature under rotation. After 24 hours, polydopamine solution was removed, and multi-well plates rinsed for 5 minutes under distilled water. Multi-well plates were sterilized under ultraviolet light for 30 minutes prior to use for cell culture.

6.2.2. Cell Culture

Human dermal fibroblasts (CRL 2097) were cultured as previously described in complete DMEM (Corning, 15-017 CV) supplemented with 10% v/v fetal bovine serum (Gibco, 16000-044) , 1% v/v penicillin/streptomycin (Corning, 30-002-Cl), 1% v/v non-essential amino acids (Corning, 25-025Cl), L-glutamine (Corning, 25- 005Cl) and 1% v/v sodium pyruvate (Corning, 25-001-Cl). Cells were trypsinized and centrifuged at 1100 rpm. Supernatant was removed, and pellet was resuspended in complete DMEM, and maintained in T75 flasks.

6.2.3. Culture of Cell-Derived Matrices (In vitro) under MMC

HDFs (p3-p8) were plated at a density of 25,000 cells/cm^2 and cultured in complete DMEM for 24 hours prior to culture with crowding media. Crowding media was supplemented with 0.05% w/v or 0.5% w/v high molecular weight hyaluronic acid (HA15M-5, 1.5MDa, LifeCore Biomedical, USA). Ficoll media was prepared by mixing 37.5 mg/mL Ficoll 70 (Sigma, F2878) and 40 mg/mL Ficoll 400 (Sigma, F4375) in standard DMEM. Crowded conditions were compared to a non-crowded treated negative control condition. All conditions were supplemented with 100µM ascorbic acid (Wako, 013-19641). Cells were cultured at standard culture conditions (37°C, 5% CO_2), and media was replaced every 2-3 days. CDMs were cultured for 14 days prior to decellularization.

6.2.4. Decellularization of CDMs developed under MMC

CDMs cultured for 14 days on polydopamine-coated surfaces were decellularized as previously described [40] . Briefly, media was aspirated and cell layers rinsed in distilled water for 5 minutes. Distilled water was aspirated, and cell layer was incubated in 0.6 M KCl solution

for 1 hour at RT. The KCl solution was aspirated, and cell layer was incubated in 1M KI solution for 1 hour. Cell layers were rinsed in distilled water before repeating the KCl and KI solution incubation. Cell layers were rinsed in distilled water and incubated with 50 U/mL DNase I (Worthington Biochemical, LS002004) in a solution prepared from a 10X stock (20mM $MgCl_2$, 200mM Tri-HCl, pH 8.3). DNase solution was aspirated, and cell layers rinsed prior to storage in 1X PBS (culture grade) supplemented with 1% Pen/Strep at 4 °C for up to 1 month. All decellularization steps were completed under sterile conditions.

6.2.5. Lyophilized Histogen (hECM) Scaffolds + Peptide Loading

Biomanufactured cell-derived ECM biomaterial was provided to us by Histogen, Inc. Briefly, neonatal fibroblasts were cultured on dextran microcarrier beads in 1L bioreactors under hypoxic conditions for up to 8 weeks [39]. Culture was collected debeaded and decellularized, and provided as an ECM slurry **(Figure 6-1 A)**. ECM slurry was rinsed seven times in sterile MilliQ water, until the sample doubled in volume. Non-peptide and AMP-loaded hECM scaffolds were prepared. Briefly, a volume of 224 µL of stock cCBD –LL37 peptide (1340 µM) was added per 1mL ECM slurry. Serial dilutions with non-peptide loaded hECM was used to prepare CDM slurry solutions at difference concentrations. ECM slurry was pipetted into a 12-well plate, and lyophilized at a freezing rate of 0.25°C/ min and freezing temperature of 55°C to produce a porous, hECM scaffold **(Figure 6-1, B, top panel)**.

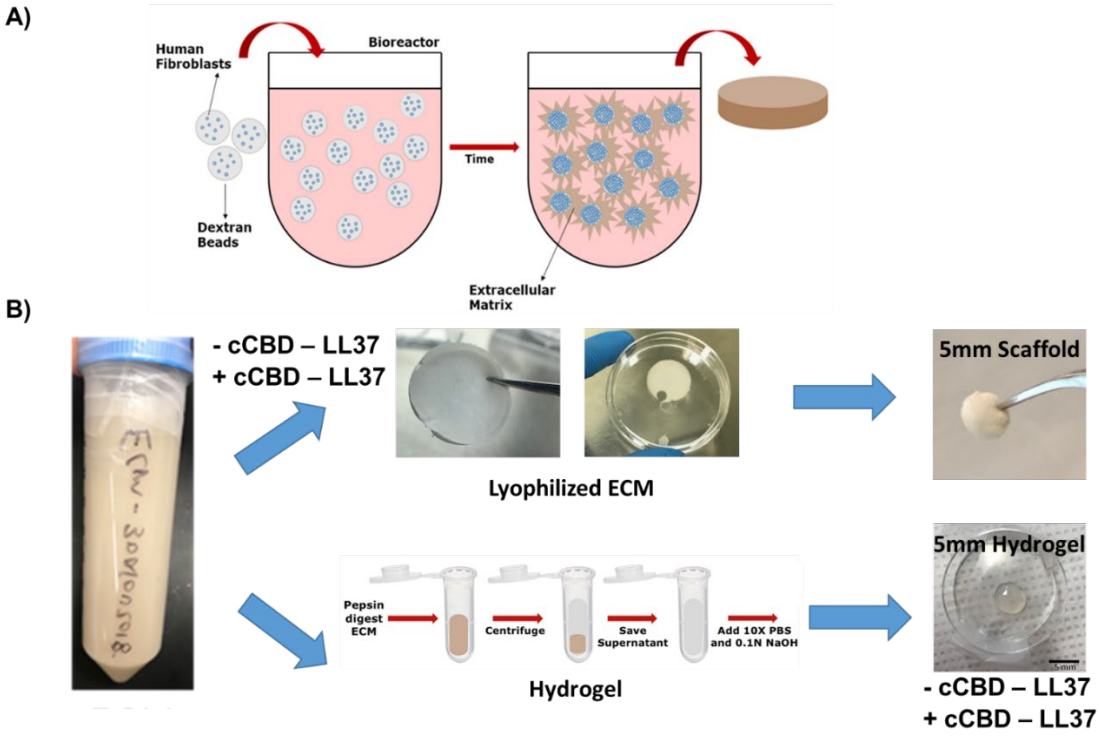

Figure 6-1: (A) Schematic illustrating the biomanufacturing process of Histogen's cell-derived ECM slurry (hECM). (**B)** ECM slurry formulated with or without cCBD –LL37 can be processed as lyophilized ECM sheets or ECM hydrogels. Peptide is incorporated into ECM slurry prior to lyophilization for formation of dry scaffolds. Lyophilized scaffolds developed from Histogen, Inc. are referred to as hECM. Alternatively, peptides can be added to hydrogel solution prior to crosslinking.

6.2.6. Bacterial strains and culture

Escherichia coli (ATCC HB101) was purchased from ATCC. Bacteria was cultured in Mueller Hinton Broth (MHB, Sigma, 70192) prepared at 9.8g/L. Fresh cultures were prepared from colonies freshly plated on Mueller Hinton Agar (MHA, Sigma, 70191) stock plate, and cultured for 12 hours at 37°C. A 0.5 McFarland standard dilution was prepared to make a $1x10^8$ colony forming units (CFU/mL), and then diluted 100-fold for a final concentration of $1x10^6$ prior to culture.

6.2.7. Turbidity Assay

All CDM samples (MMC CDMs (2-D) and hECMs (3-D)) were handled under sterile conditions for each part of this protocol. Decellularized CDM scaffolds prepared under MMC conditions were rinsed 3x in 1X DPBS prior to peptide loading to remove residual antibiotics used in the storage solution. CDMs from each condition were hydrated with peptides or sterile phosphate buffered saline as a negative control in a humidified, hydrophobic paraffin surface (Parafilm) at 37°C for 2 hours. The CDMs were loaded with peptide by adsorbing 20 µL *c*CBD–LL37 solution prepared at a final concentration of 300 µM. After CDMs were incubated with peptide (or control solution), CDMs were transferred to a multi-well plate, and rinsed 3x in MHB. CDMs were inoculated with bacteria at a final concentration of $2x10^5$ CFU/mL (**Figure 6-2, top panel, MMC CDMs)**. CDMs were incubated with bacteria for 1 hour at 37°C to allow for adherence at the CDM layer. After incubation, bacteria was aspirated, and CDMs were rinsed 3x in MHB. Five hundred microliters of fresh MHB was added to each well, and CDMs were incubated for 16 hours at 37°C.

The lyophilized hECM scaffolds provided by Histogen were assessed using a modified turbidity assay. Briefly, 50 µL of fresh MHB was added to each well. CDMs were inoculated with 50 µl bacteria for a final concentration of $5x10^5$ CFU/mL. CDMs were incubated for 16 hours at 37°C. Growth and sterility controls were also prepared. A schematic illustrating the methodology used for this experiment is seen in **Figure 6-2 (bottom panel, hECM)**. After incubation, scaffolds were transferred to cassette for tissue processing **(**Section 6.2.10: *Immunofluorescence and Histology***)**, and OD 600 was measured using a Victor 3 Plate reader (Perkin Elmer). Growth and sterility controls were also prepared. A schematic illustrating the

methodology used for this experiment is seen in **Figure 6-3.** A 100 µL aliquot was transferred to a 96 well plate, and OD 600 was measured using a Victor 3 Plate reader (Perkin Elmer).

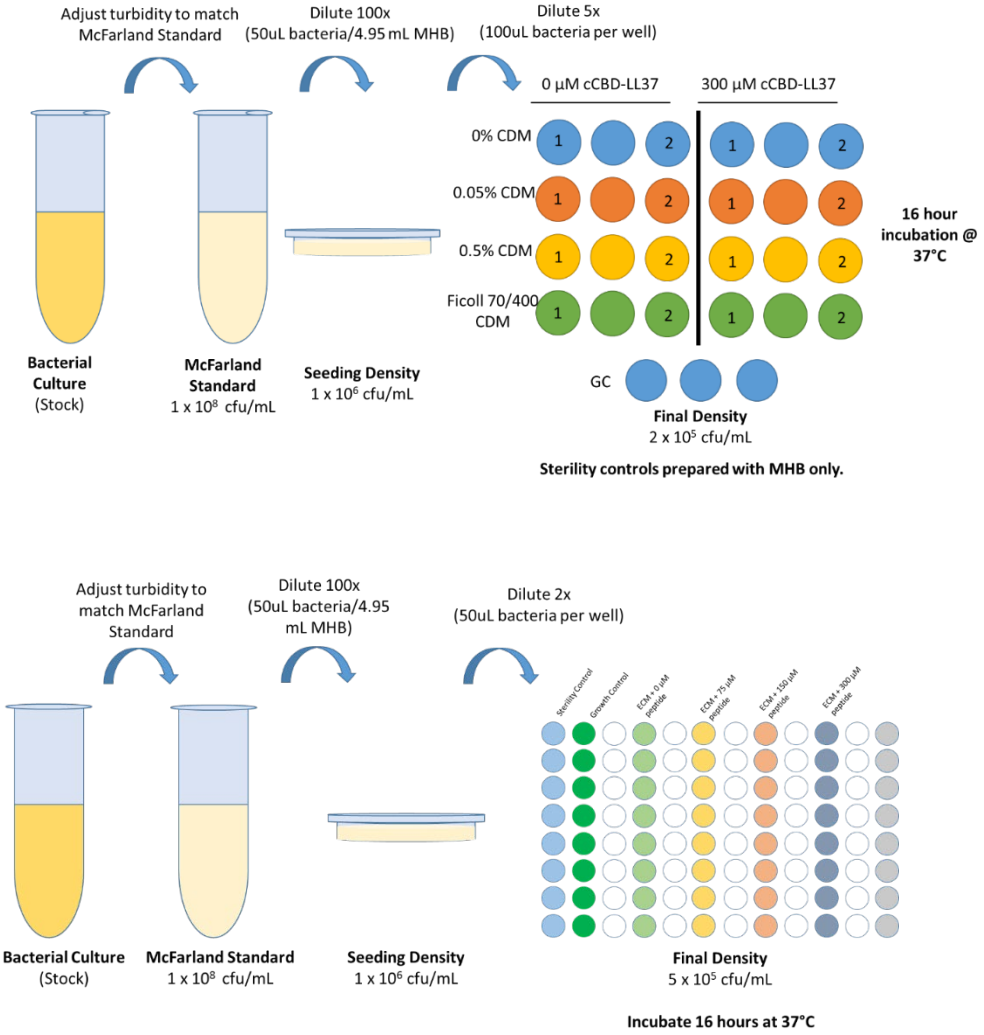

Figure 6-2: Schematic illustrating the microbial inoculation of decellularized CDMs prepared under MMC conditions (top panel). Schematic illustrating the microbial inoculation of decellularized CDMs prepared under MMC conditions (bottom panel)

6.2.8. Colony Count Assays

A bacterial dilution was prepared at 1:1x10^6 CFU/mL from the bacterial suspensions cultured as specified in **(*Section 6.2.7:***

Turbidity Assay), and plated on agar plates for assessment of microbial growth. Agar plates were incubated at 37 °C, imaged on the Bio-Rad GelDoc imaging system, and colonies were counted using Image J cell counter plug in. A schematic illustrating the methodology used for preparing the microbial agar plating is seen in **Figure 6-3.**

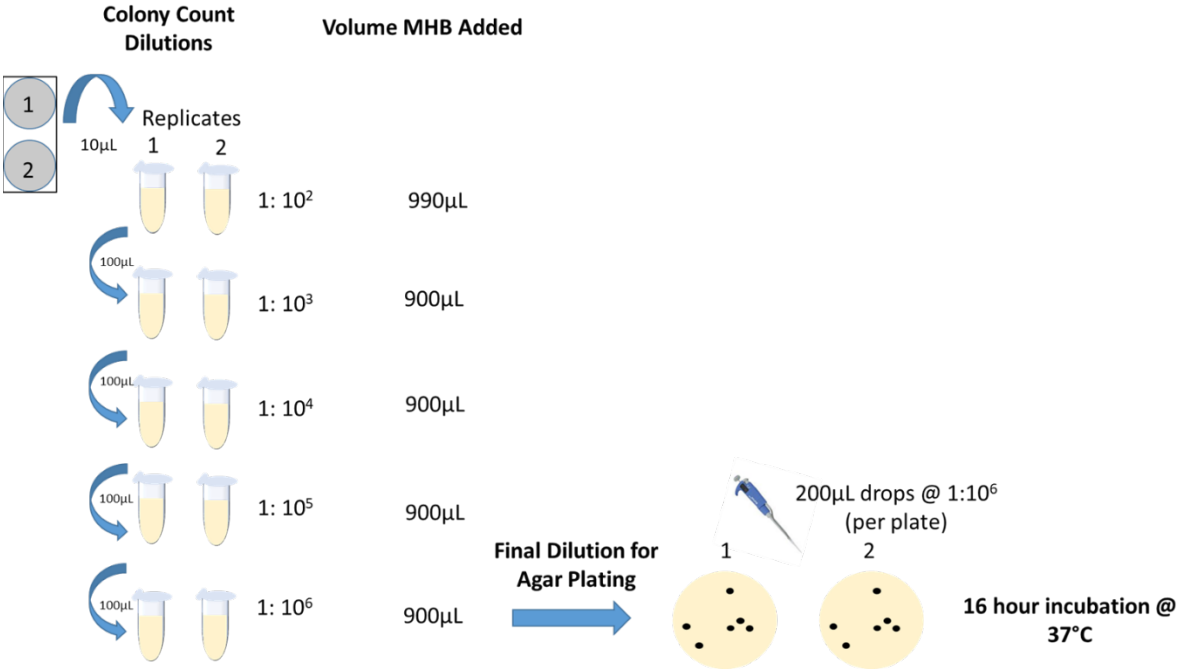

Figure 6-3: Schematic illustrating microbial agar plate cultures for colony count assays.

6.2.9. Calculation of log and percent reduction

Colony counts were obtained after 1:10^6 dilution of the bacterial cultures incubated on the CDMs for 16 hours were plated on agar plates. The colony counts for the non-peptide and peptide loaded controls were calculated using **Equation 1** [41] and **Equation 2** [41]:

$$\textbf{log growth reduction}(\textbf{16 h}) = \textbf{log CFU}(\textbf{negative control})(\textbf{16 h}) - \textbf{log CFU}(\textbf{sample})(\textbf{16 h})$$

Equation 1: Equation for calculating log growth reduction due to presence of peptide.

$$\textbf{Percent Reduction (16h)} = 100 * \frac{(\#\ \textbf{viable organisms before treatment} - \#\ \textbf{of viable organisms after treatment})}{\#\ \textbf{viable organisms before treatment}}$$

Equation 2: Equation for calculating percent reduction due to presence of peptide.

6.2.10. Immunofluorescence and Histology

MMC CDMs prepared on coverslips were fixed in 4% paraformaldehyde for 10 minutes. Histogen ECM scaffolds were stored in tissue processing cassettes, and fixed in 10% neutral buffered formalin for 1 hour followed by 70% ethanol incubation. After processing, paraffin embedding, and sectioning, slides were deparaffinized and antigen retrieval was completed in citrate buffer using a pressure cooker. Samples were blocked in 5% normal goat serum solution for 2 hours at RT prior to incubation with primary antibody. Sections were incubated in anti-LL37 at 1:500 in 3% NGS solution (Anaspec, 55927) overnight at 4°C. After primary antibody incubation, sections layers were rinsed in 1X DPBS and incubated in goat anti-rabbit 488 secondary solution (Life Technologies, A11005) at 1:400 dilution in 1X DPBS. Sections were counterstained with DAPI and imaged using a Zeiss Axiovert microscope.

6.2.11. Scanning Electron Microscopy

Scanning electron microscopy (SEM) images of lyophilized CDMs loaded with different concentrations of peptide (0 μM, 0.15 μM, 0.625 μM, 2.5 μM, 10 μM, 75 μM, 150 μM, and 300 μM) to visualize surface topography. Scaffolds with concentration range 0.15 μM - 10 μM were prepared at Histogen, LLC. All other scaffolds were prepared at WPI. Dry scaffolds were sputtered with an 8 nm coating of Pt/Pd (Cressington Scientific Instruments). SEM images were acquired at University of Massachusetts Medical School Electron Microscopy Core (Worcester,

MA) with an FEI Quanta 200 FEG MKII SEM (FEI). Images were acquired at 100x magnification, 9mm working distance, and 15kV high vacuum conditions.

6.2.12. Statistical Analysis

All experiments were completed in triplicates unless otherwise stated with equivalent sample sizes within each independent experiments. Statistical analysis was performed to determine significance amongst the experimental conditions using GraphPad Prism 7 software. Data is reported as the mean ± standard error of the mean (SEM). Two -way ANOVA followed by Sidak's multiple comparisons between peptide and non-peptide loaded conditions was completed.

6.3. Results

6.3.1. Effect of Peptide Loaded MMC CDMs on E. coli

CDM MMCs loaded with 300 μM cCBD- LL37 resulted in decreased the OD590 readings compared to the non-peptide loaded controls **(Figure 6-4 A)**, which suggests that the peptide maintained its activity when bound to the CDM. It appears that the Ficoll 70/400 CDM loaded with peptide had the highest absorbance value compared to the other conditions, which indicates that the samples had higher turbidity, and thus higher *E. coli burden.* The non-peptide loaded CDMs had comparable turbidity to the growth control, which indicates that the CDM did not have intrinsic antimicrobial effects on *E. coli*.

A follow-up colony count assay also indicated that the Ficoll 70/400 peptide loaded CDMs had the highest colony counts on the agar plates compared to the other conditions **(Figure 6-4 B)**. There were no significant differences in turbidity between the conditions, but modest

differences were observed in the colony counts on the CDMs prepared using different crowder molecules. While turbidity measurements did not indicate that the CDM had an antimicrobial effect on *E. coli*, a reduction in the colony counts was observed between the GC and control CDMs. However, it is possible that polydopamine coating may have contributed to this decrease [42]. Despite this decrease, there was not any significance between the GC and any of the non-peptide loaded CDMs.

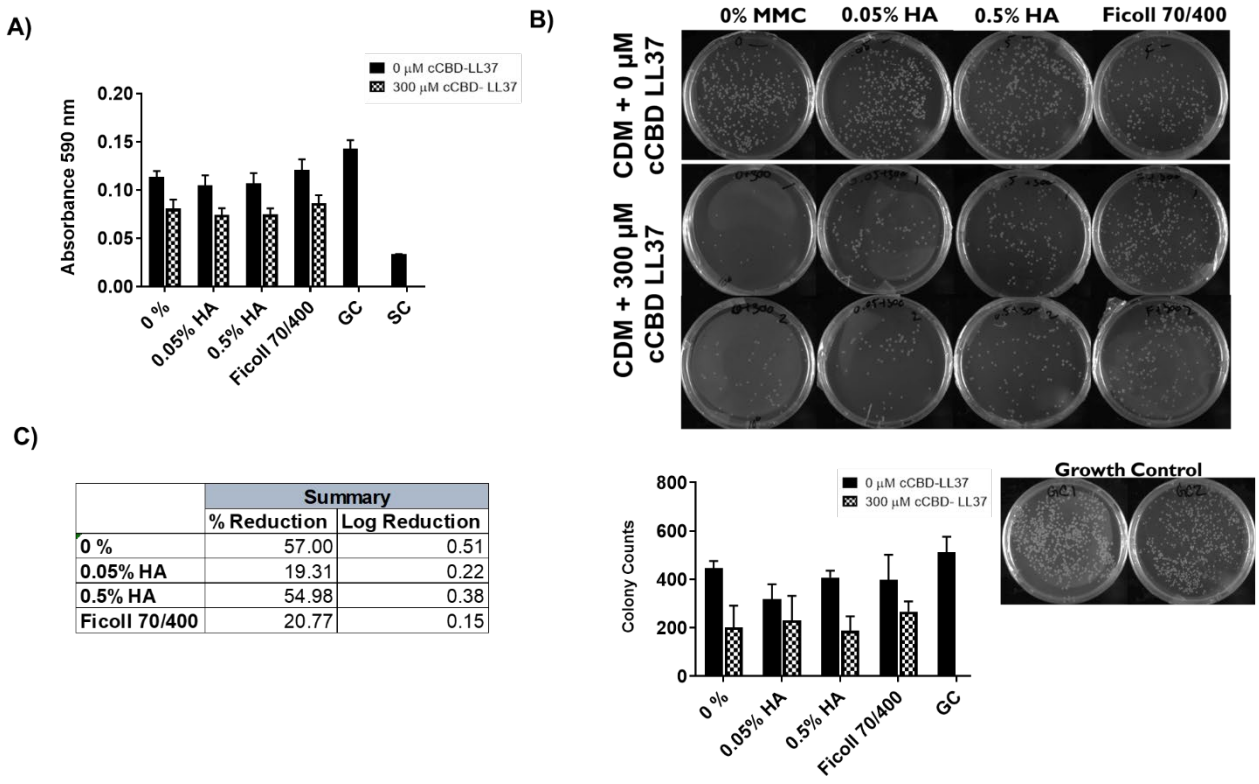

Figure 6-4: (A) Turbidity measurements after CDMs were exposed to Gram negative E. *coli* for 16 hours. **(B)** Colonies formed on agar plates after culture with non-peptide (first row) loaded and peptide loaded (second and third rows) CDMs for 16 hours, and quantification of the number of colonies formed. **(C)** Calculated percent and log reduction in peptide loaded CDMs. Values represent means and the standard error of the mean from three experimental replicates.

6.3.2. Peptide Adsorption on MMC CDMs

CDMs with and without peptides used for the microbial turbidity assays were fixed, and stained for LL37 to indicate the presence of cCBD-LL37. ICC indicates lack of LL37 present on the non-loaded peptide CDMs **(Figure 6-5)**. LL37 was detected in samples in which cCBD-LL37 was adsorbed onto the collagen in the CDM samples. Ficoll 70/400 peptide loaded CDMs appeared to have the least peptide binding present.

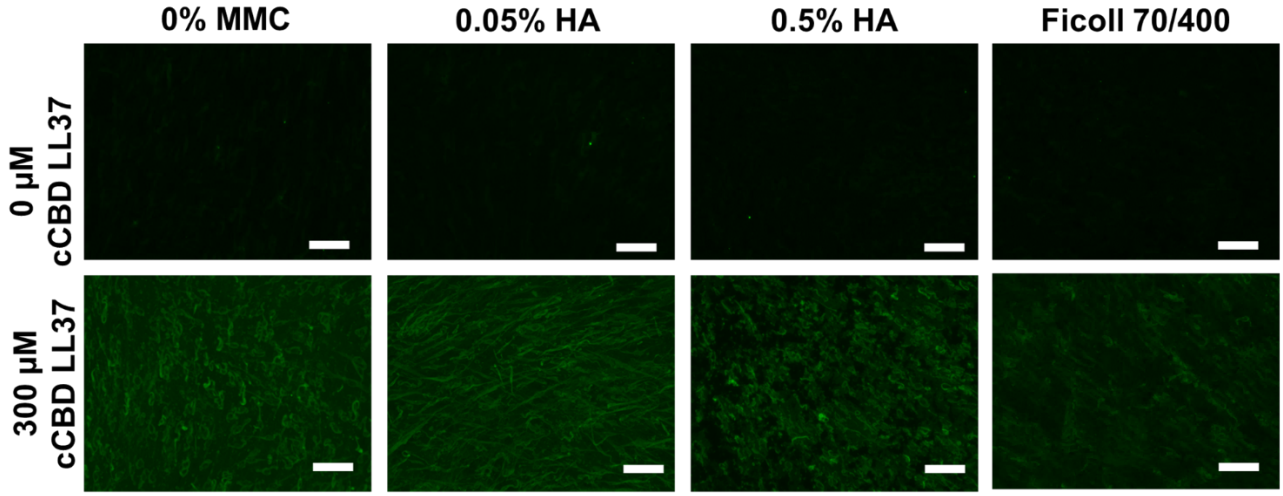

Figure 6-5: Representative immunocytochemistry images of CDMs stained with anti-LL37 and visualized with AlexaFluor_488-conjugated secondary antibody after exposure to E. coli for 16 h. Scale bar: 100 µm. Representative images from three experimental replicates.

6.3.3 Effect of Peptide Loaded Lyophilized CDMs on E. coli

Lyophilized CDMs with and without peptide were inoculated with *E. coli.* Colony count assay indicates complete microbial eradication at cCBD-LL37 concentrations of 75 µM or higher **(Figure 6-6)**. This is indicated by the zero colony growth present on agar plates with *E.coli* incubated with CDM scaffolds loaded with peptide concentrations of 75 µM or higher. CDMs with and without peptides used for the microbial turbidity assays were fixed, and stained for assessment of collagen distribution and cCBD-LL37 binding. ICC indicates presence of cCBD-LL37 in peptide loaded CDM compared to the negative control **(Figure 6-7)**.

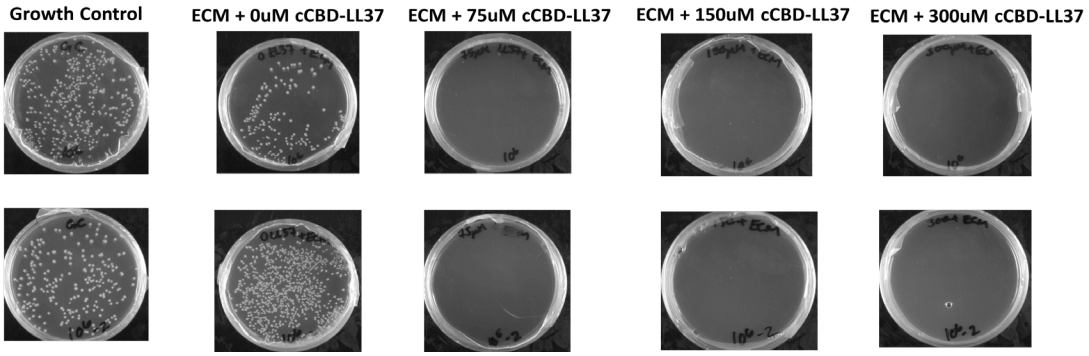

Sample Name	Number of Colonies Counted
ECM + 0 µM cCBD-LL37	496. 5 ± 456
ECM + 75 µM cCBD-LL37	0 ± 0
ECM + 150 µM cCBD-LL37	0 ± 0
ECM + 300 µM cCBD-LL37	0 ± 0
Growth Control	332 ± 130

Figure 6-6: *A*gar plates smeared with *E. coli* suspension cultured with CDMs loaded with different concentrations of cCBD-LL37 (top panel). Quantitative representation of the number of colonies formed (bottom panel). Images and counts represent samples from two independent replicates.

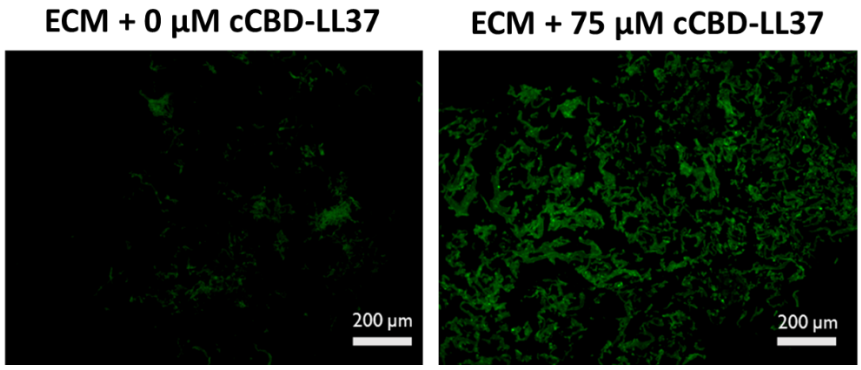

Figure 6-7: Representative immunocytochemistry images of hECM CDMs stained with anti-LL37 and visualized with AlexaFluor_488-conjugated secondary antibody after exposure to E. coli for 16 h. Scale bar: 200 µm.

6.3.4 Surface Topography of Lyophilized hECM

SEM images indicate differences in porosity due to presence of cCBD-LL37 peptide **(Figure 6-9)**. The pore size appeared to decrease in the CDM scaffolds with increasing concentration of cCBD-LL37 peptide. Scaffolds loaded with peptide appeared to have a denser structure compared to the non-peptide loaded control.

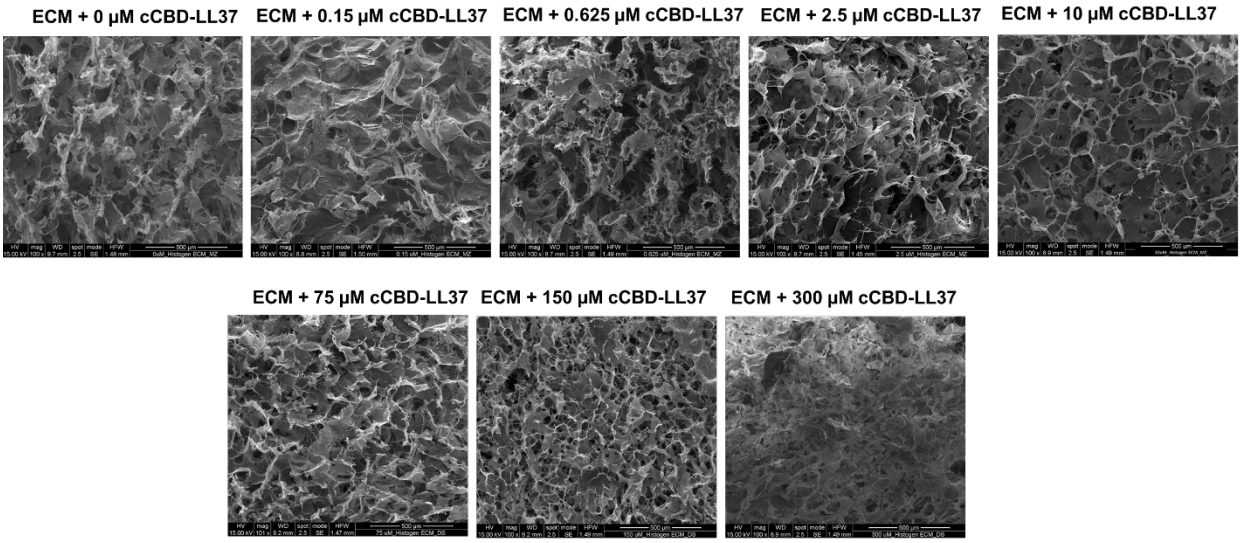

Figure 6-8: SEM images of cCBD-LL37 loaded lyophilized scaffolds (hECM). The following concentrations are listed in the specified order: 0 µM, 0.15 µM , 0.625 µM, 2.5 µM, 10 µM, 75 µM, 150 µM, and 300 µM. Scale bar: 500 µm.

6.4. Discussion

The cCBD-LL37 peptide has been previously shown to bind to bovine type I collagen in commercially available wound dressings, and retain its activity [19]. CDMs are also composed of collagens that can support peptide binding through collagen binding domains (CBD). The objective of this experiment was to determine if CDMs prepared under *in vitro* MMC conditions can functionally support cCBD-LL37 binding to the collagen molecule present in the samples.

The characterization of CDMs prepared under MMC pre-decellularization **(Figures 4-5, 4-6)** and post-decellularization **(Figure 4-11)** indicate the presence of collagen within the ECM structure, which suggests that cell-derived materials can also be used for antimicrobial peptide adsorption. Decellularized CDMs prepared under MMC were used to test whether cCBD-LL37 adsorbs to the collagen present. Industry standards define a log reduction of less than 0.5 as an indication of no antimicrobial activity [41, 43]. The log reductions for all of the CDMs cultured

under MMC conditions were calculated to be 0.5 and less, thus indicating minimal antimicrobial activity. The CDM developed under non-crowder conditions had the highest log reduction compared to the MMC treated CDMs. We hypothesized that the 0.05% HA CDM would have a higher, if not comparable, log reduction to that of the 0% CDM due to the higher amount of collagen present in the sample as indicated by Sircol **(Chapter 4, Figure 4-4 B)** and hydroxyproline assays **(Chapter 4, Figure 4-4 C)**. Furthermore, while there was not decrease in turbidity values between the GC and non-peptide loaded CDMs, agar plating indicated a decrease in colony counts. It has been previously reported that polydopamine coatings have a strong antibacterial effect against *E. coli* [42]. It is common that polydopamine needs to be modified with other agents, to impart its antibacterial effect [44], however, Su *et al.* reported increased antibacterial activity by incorporating shaking mechanism to create roughened polydopamine layers [42].

The peptide maintains antimicrobial activity as indicated by the decreased absorbance and colony counts observed between the non-peptide loaded control and the 300 µM cCBD-LL37 peptide loaded CDMs. Immunocytochemistry staining of the CDMs cultured with *E. coli* were fixed, stained with anti-human LL37 to assess binding and distribution of the peptide on the material. Immunofluorescence indicates the presence of cCDB-LL37 on CDMs, with a decrease in peptide intensity in the Ficoll 70/400 condition. The decrease in cCBD-LL37 binding in the Ficoll 70/400 CDM, and the associated increase in colony count suggests that less peptide may be bound to the CDM due to the decreased collagen amount observed in previous experiments. As ICC is a qualitative method to assess presence of peptide on CDMs, a quantitative approach, such as ELISA, can be used to compare the amount of peptide bound to each CDM.

The insignificant reduction in microbial growth reported for the MMC CDMs does not suggest that the peptide was not active, but rather that there were less collagen binding sites for the peptide to bind to compared to a fairly homogeneous collagen scaffolds, such as Puracol. The concentration of 300 uM selected for assessment of antimicrobial activity on CDMs was preliminarily based on previous experiments completed using cCBD-LL37 on Primatrix collagen scaffolds (data not shown). However, the concentration of cCBD-LL37 used is dependent on the number of collagen binding sites present in the substrate, and should be calculated accordingly. Theoretical calculations using the collagen concentration of digested samples may provide an estimate to the available binding sites present. However, as CDMs are heterogeneous materials, we would need to also determine the ratio of collagen type I present compared to the other ECM proteins. It is also important to note that the MMC CDMs used for cCBD-LL37 binding were also decellularized, and thus the quantified collagen amount may not necessarily be the same as in CDMs pre-decellularization. While immunofluorescence staining indicated that collagen was retained at the surface, a quantitative technique, such as hydroxyproline assay, would need to be used in order to assess collagen content post-decellularization. This would provide a more representative description of the amount of collagen present in each MMC developed CDM to support peptide binding.

We hypothesized that the peptide adsorbs to the collagen due to affinity interaction of the cCBD to collagen in the CDMs. In order to support our hypothesis, additional controls are needed for future studies. One control would be to bind cCBD-LL37 to a glass substrate alone, as the peptide has been shown to adsorb glass surfaces [45]. Another control would be using unmodified LL37. Unmodified LL37 has also been shown to adsorb to collagen scaffolds [19]. However, this binding mechanism is possibly due to electrostatic-based adsorption between the

peptide and the substrate [20, 46]. Thus, loading CDMs with unmodified LL37 would allow us to control for binding mechanism of the peptide, and to assess its retention on the surface. Time-course studies can be completed to further assess the adsorption and activity of the cCBD -LL37 peptide with the CDMs. Finally, due to the heterogeneous nature of CDMs, it is expected that there would be less collagen binding sites compared to a homogenous collagen scaffold. An alternative CDM control, such as a heterogeneous protein film (i.e. Matrigel), would control for the composition of the CDM, and its ability to adsorb to cCBD-LL37.

While the CDMs supported peptide binding, significant log reduction in microbial growth was not observed. This may be due to an insufficient collagen density and scaffold thickness to support peptide binding via its CBD. The CDMs tested were developed *in vitro* under 2-dimensional culture conditions in order to assess the effects of crowding on ECM deposition. However, to translate a CDM into a biomaterial to support clinical application, a scaled up manufacturing process must be utilized to support a significantly higher collagen production.

Histogen, LLC developed a manufacturing approach primarily for collected fibroblast conditioned media, which ultimately led to production of an ECM slurry composed of ECM proteins, growth factors, and cytokines that can ultimately support regenerative applications [39]. As seen in **Figure 6-1,** the ECM produced is a very viscous, slurry like material that depending on its processing method can be used to develop CDM sponges/scaffolds or hydrogels. Utilizing the collagen present in the CDM, we mixed the slurry with cCBD-LL37 prior to lyophilization to support development of an antimicrobial scaffold.

Lyophilized CDMs were prepared at the following concentrations: 0 μM, 75 μM, 150 μM, and 300 μM and inoculated with a model microorganism, *E. coli*, to assess peptide activity. After inoculation, colony count assays were completed on agar plates. This approach was similar

to “time kill” assay AATCC 100-2004 test method: Assessment of antibacterial finishes on textile materials [41, 43]. The acceptance criteria for antimicrobial products according to industry standards is a minimum of 3-log-reduction, which indicates strong antimicrobial activity [41]. According to the colony count assays, complete eradication of microbial colonies occurred at a minimum concentration of 75 μM, as indicated by lack of colony growth on the agar plates **(Figure 6-7).** Complete eradication indicates that >3-log reduction was achieved. In order to reduce cost of production, we can further narrow down the minimum concentration for microbial killing to be between 0 μM – 75 μM. We collected the scaffolds post-incubation in MHB to assess for presence of peptide. ICC staining indicated that cCBD- LL37 was still bound to the CDM scaffolds **(Figure 6-7)**. SEM imaging of the lyophilized materials in the presence of increasing concentrations of peptide indicated a decreased in pore size **(Figure 6-8)**. Despite the decrease in porosity, the scaffolds still maintained a pore structure that would promote cell adhesion and migration [47].

It is important to note that assessment of microbial activity for a scaffold that is to be used as a dressings in clinical applications must be performed on a completely decellularized and sterilized material. Histology images indicate that the material still contains DNA components, and further decellularization is currently being addressed. Sterilization techniques are also being explored with supporting assessment on peptide activity. Furthermore, Histogen ECM material is versatile, and can also be developed to produce scaffolds in a hydrogel format.

6.5. Acknowledgments

We would like to thank Histogen, LLC, specifically Michael Zimber, PhD, for his support and mentorship throughout the STTR project. A special thank you to Jyotsna Patel and all the undergraduate research assistants that helped with specimen processing, sectioning, staining and imaging. This work has been supported through the National Science Foundation IGERT Grant No. NSF DGE 1144804 and STTR Grant No. NSF IIP 1521294.

6.6. References

[1] C.K. Sen, G.M. Gordillo, S. Roy, R. Kirsner, L. Lambert, T.K. Hunt, F. Gottrup, G.C. Gurtner, M.T. Longaker, Human skin wounds: a major and snowballing threat to public health and the economy, Wound Repair and Regeneration 17(6) (2009) 763-771.
[2] P. Bowler, B. Duerden, D.G. Armstrong, Wound microbiology and associated approaches to wound management, Clinical microbiology reviews 14(2) (2001) 244-269.
[3] P.G. Bowler, B.J. Davies, The microbiology of infected and noninfected leg ulcers, International journal of dermatology 38(8) (1999) 573-578.
[4] M.C. Robson, A. Barbul, Guidelines for the best care of chronic wounds, Wound repair and regeneration 14(6) (2006) 647-648.
[5] F. Werdin, M. Tennenhaus, H.-E. Schaller, H.-O. Rennekampff, Evidence-based management strategies for treatment of chronic wounds, Eplasty 9 (2009).
[6] S. Diehr, A. Hamp, B. Jamieson, Do topical antibiotics improve wound healing?, Clinical Inquiries, 2007 (MU) (2007).
[7] Impacts of antibiotic-resistant bacteria : Thanks to penicillin-- He will come home!, DIANE Publishing.
[8] H. Vermeulen, J.M. van Hattem, M.N. Storm-Versloot, D.T. Ubbink, S.J. Westerbos, Topical silver for treating infected wounds, Cochrane Database of Systematic Reviews (1) (2007).
[9] S. Sheikpranbabu, K. Kalishwaralal, D. Venkataraman, S.H. Eom, J. Park, S. Gurunathan, Silver nanoparticles inhibit VEGF-and IL-1β-induced vascular permeability via Src dependent pathway in porcine retinal endothelial cells, Journal of nanobiotechnology 7(1) (2009) 8.
[10] S.B. Zou, W.Y. Yoon, S.K. Han, S.H. Jeong, Z.J. Cui, W.K. Kim, Cytotoxicity of silver dressings on diabetic fibroblasts, International wound journal 10(3) (2013) 306-312.
[11] R.E. Hancock, H.-G. Sahl, Antimicrobial and host-defense peptides as new anti-infective therapeutic strategies, Nature biotechnology 24(12) (2006) 1551.
[12] L.A. Clifton, M.W. Skoda, A.P. Le Brun, F. Ciesielski, I. Kuzmenko, S.A. Holt, J.H. Lakey, Effect of divalent cation removal on the structure of gram-negative bacterial outer membrane models, Langmuir 31(1) (2014) 404-412.
[13] M. Bagheri, M. Beyermann, M. Dathe, Immobilization reduces the activity of surface-bound cationic antimicrobial peptides with no influence upon the activity spectrum, Antimicrobial agents and chemotherapy 53(3) (2009) 1132-1141.
[14] S.A. Onaizi, S.S. Leong, Tethering antimicrobial peptides: current status and potential challenges, Biotechnology advances 29(1) (2011) 67-74.
[15] F. Guilhelmelli, N. Vilela, P. Albuquerque, L. Derengowski, I. Silva-Pereira, C. Kyaw, Antibiotic development challenges: the various mechanisms of action of antimicrobial peptides and of bacterial resistance, Frontiers in microbiology 4 (2013) 353.
[16] R. Eckert, Road to clinical efficacy: challenges and novel strategies for antimicrobial peptide development, Future microbiology 6(6) (2011) 635-651.
[17] M. Gabriel, K. Nazmi, E.C. Veerman, A.V. Nieuw Amerongen, A. Zentner, Preparation of LL-37-grafted titanium surfaces with bactericidal activity, Bioconjugate chemistry 17(2) (2006) 548-550.
[18] S. Ye, K.T. Nguyen, A.P. Boughton, C.M. Mello, Z. Chen, Orientation difference of chemically immobilized and physically adsorbed biological molecules on polymers detected at the solid/liquid interfaces in situ, Langmuir 26(9) (2009) 6471-6477.
[19] L.D. Lozeau, J. Grosha, D. Kole, F. Prifti, T. Dominko, T.A. Camesano, M.W. Rolle, Collagen tethering of synthetic human antimicrobial peptides cathelicidin LL37 and its effects on antimicrobial activity and cytotoxicity, Acta biomaterialia 52 (2017) 9-20.
[20] K. Kristensen, J.R. Henriksen, T.L. Andresen, Adsorption of cationic peptides to solid surfaces of glass and plastic, PLoS One 10(5) (2015) e0122419.

[21] O. Etienne, C. Picart, C. Taddei, Y. Haikel, J. Dimarcq, P. Schaaf, J. Voegel, J. Ogier, C. Egles, Multilayer polyelectrolyte films functionalized by insertion of defensin: a new approach to protection of implants from bacterial colonization, Antimicrobial agents and chemotherapy 48(10) (2004) 3662-3669.
[22] L.D. Lozeau, T.E. Alexander, T.A. Camesano, Proposed mechanisms of tethered antimicrobial peptide chrysophsin-1 as a function of tether length using QCM-D, The Journal of Physical Chemistry B 119(41) (2015) 13142-13151.
[23] F. Costa, I.F. Carvalho, R.C. Montelaro, P. Gomes, M.C.L. Martins, Covalent immobilization of antimicrobial peptides (AMPs) onto biomaterial surfaces, Acta biomaterialia 7(4) (2011) 1431-1440.
[24] C.S. Kwok, C. Wan, S. Hendricks, J.D. Bryers, T.A. Horbett, B.D. Ratner, Design of infection-resistant antibiotic-releasing polymers: I. Fabrication and formulation, Journal of controlled release 62(3) (1999) 289-299.
[25] J. Ulbricht, R. Jordan, R. Luxenhofer, On the biodegradability of polyethylene glycol, polypeptoids and poly (2-oxazoline) s, Biomaterials 35(17) (2014) 4848-4861.
[26] M.E. Cassin, A.J. Ford, S.M. Orbach, S.E. Saverot, P. Rajagopalan, The design of antimicrobial LL37-modified collagen-hyaluronic acid detachable multilayers, Acta biomaterialia 40 (2016) 119-129.
[27] H. Sekiguchi, K. Uchida, O. Matsushita, G. Inoue, N. Nishi, R. Masuda, N. Hamamoto, T. Koide, S. Shoji, M. Takaso, Basic Fibroblast Growth Factor Fused with Tandem Collagen-Binding Domains from Clostridium histolyticum Collagenase ColG Increases Bone Formation, BioMed research international 2018 (2018).
[28] B. An, T.M. DesRochers, G. Qin, X. Xia, G. Thiagarajan, B. Brodsky, D.L. Kaplan, The influence of specific binding of collagen–silk chimeras to silk biomaterials on hMSC behavior, Biomaterials 34(2) (2013) 402-412.
[29] R. Sistiabudi, A. Ivanisevic, Collagen-binding peptide interaction with retinal tissue surfaces, Langmuir 24(5) (2008) 1591-1594.
[30] R. Bauer, J.J. Wilson, S.T.L. Philominathan, D. Davis, O. Matsushita, J. Sakon, Structural comparison of ColH and ColG collagen-binding domains from Clostridium histolyticum, Journal of bacteriology 195(2) (2013) 318-327.
[31] C.E. Tye, G.K. Hunter, H.A. Goldberg, Identification of the type I collagen-binding domain of bone sialoprotein and characterization of the mechanism of interaction, Journal of Biological Chemistry 280(14) (2005) 13487-13492.
[32] E. Nègre, T. Vogel, A. Levanon, R. Guy, T.J. Walsh, D.D. Roberts, The collagen binding domain of fibronectin contains a high affinity binding site for Candida albicans, Journal of Biological Chemistry 269(35) (1994) 22039-22045.
[33] R. Sistiabudi, J. Paderi, A. Panitch, A. Ivanisevic, Modification of native collagen with cell-adhesive peptide to promote RPE cell attachment on Bruch's membrane, Biotechnology and bioengineering 102(6) (2009) 1723-1729.
[34] R. Ramos, J.P. Silva, A.C. Rodrigues, R. Costa, L. Guardão, F. Schmitt, R. Soares, M. Vilanova, L. Domingues, M. Gama, Wound healing activity of the human antimicrobial peptide LL37, Peptides 32(7) (2011) 1469-1476.
[35] R.R. Ramos, L. Domingues, F. Gama, LL37, a human antimicrobial peptide with immunomodulatory properties, (2011).
[36] N.J. Turner, S.F. Badylak, The use of biologic scaffolds in the treatment of chronic nonhealing wounds, Advances in wound care 4(8) (2015) 490-500.
[37] L.E. Fitzpatrick, T.C. McDevitt, Cell-derived matrices for tissue engineering and regenerative medicine applications, Biomaterials science 3(1) (2015) 12-24.
[38] G.S. Schultz, G. Ladwig, A. Wysocki, Extracellular matrix: review of its roles in acute and chronic wounds, World wide wounds 2005 (2005) 1-18.
[39] R.S. Kellar, M. Hubka, L.A. Rheins, G. Fisher, G.K. Naughton, Hypoxic conditioned culture medium from fibroblasts grown under embryonic-like conditions supports healing following post-laser resurfacing, Journal of cosmetic dermatology 8(3) (2009) 190-196.

[40] A.R. Gillies, L.R. Smith, R.L. Lieber, S. Varghese, Method for decellularizing skeletal muscle without detergents or proteolytic enzymes, Tissue engineering part C: Methods 17(4) (2010) 383-389.
[41] C. Wiegand, M. Abel, P. Ruth, P. Elsner, U.-C. Hipler, In vitro assessment of the antimicrobial activity of wound dressings: influence of the test method selected and impact of the pH, Journal of Materials Science: Materials in Medicine 26(1) (2015) 18.
[42] L. Su, Y. Yu, Y. Zhao, F. Liang, X. Zhang, Strong antibacterial polydopamine coatings prepared by a shaking-assisted method, Scientific reports 6 (2016) 24420.
[43] Standard Guide for Assessment of Antimicrobial Activity Using a Time-Kill Procedure.
[44] J. Jiang, L. Zhu, L. Zhu, H. Zhang, B. Zhu, Y. Xu, Antifouling and antimicrobial polymer membranes based on bioinspired polydopamine and strong hydrogen-bonded poly (N-vinyl pyrrolidone), ACS applied materials & interfaces 5(24) (2013) 12895-12904.
[45] L.D. Lozeau, M.W. Rolle, T.A. Camesano, Mechanistic predictions of the influence of collagen-binding domain sequences on human LL37 interactions with model lipids using quartz crystal microbalance with dissipation, Biointerphases 14(2) (2019) 021006.
[46] T. Osaki, L. Renner, M. Herklotz, C. Werner, Hydrophobic and electrostatic interactions in the adsorption of fibronectin at maleic acid copolymer films, The Journal of Physical Chemistry B 110(24) (2006) 12119-12124.
[47] M.M. Stevens, J.H. George, Exploring and engineering the cell surface interface, Science 310(5751) (2005) 1135-1138.

Chapter 7 : Summary, Future Work, and Future Directions

7.1. Summary

The goal of this work was to develop a human cell-derived, natural, functional, ECM-rich biomaterial that can also be used for the exogenous delivery of antimicrobial peptides. An example of an ECM rich, proangiogenic material that is commercially available for *in vitro* research application only, is Matrigel®. Developing a human cell-derived version of Matrigel® would provide an ECM-based product that can simultaneously be used as an injectable hydrogel for tissue repair and promotion of capillary network formation at the wound bed. Furthermore, a human-derived Matrigel can also provide a delivery vehicle for cells and therapeutic agents, such as antimicrobial peptides.

The approach we utilized for the development of a human cell-derived biomaterial is the use of macromolecule crowding (MMC). Hyaluronic acid (HA) has not been used as a crowder molecule despite its native role as crowding macromolecules *in vivo*. We used Ficoll 70/400 as a positive control as its effect on crowding has been established in literature. In this study, we have shown that high molecular weight (HMW) HA has a crowding effect on ECM deposition in human dermal fibroblasts. Crowding was assessed through the excluded volume effect (the presence of macromolecules in the media) as well as through changes in viscosity (high versus low concentration of HMWHA). ICC did not indicate significant increases in collagen type I collagen type III, collagen type IV, fibronectin, and laminin deposition within 3 days, however, Sircol, hydroxyproline, and SDS-PAGE indicate an increase in the collagen footprint in the 0.05% HA treated condition compared to untreated control. This may support the use of HA as a macromolecular crowder, although the observed increases were not statistically significant. Deposition levels were comparable to that of Ficoll 70/400-treated cultures. Alternatively, it

seemed that the 0.05% HA concentration increased soluble collagen and formation of collagen crosslinks, as indicated by darker bands in the beta and gamma regions. The increased collagen crosslinks may be supported by increase in *LOX* gene expression. The 0.05% HA concentration and Ficoll 70/400 solutions had similar viscosities, which may explain similarities in matrix deposition profiles. The differences seen in soluble collagen concentration, collagen crosslinking, *MMP* and *LOX* transcript levels, between those two conditions suggest macromolecule-mediated effects on dermal fibroblasts. We have shown that HMWHA is as effective as Ficoll for increasing matrix deposition at early time points. This effect may be due to an HA-induced secretory cell profile and lack of changes in MMP gene expression levels compared to the non-treated control.

To assess the functional and mechanical properties of the CDMs developed under crowding conditions, it was crucial to remove cellular content to allow for characterization of CDM functional properties. This would allow us to test the CDM as a scaffold for endothelial sprouting and loading of LL37 via a collagen binding domain, and to measure the stiffness of the CDM material (without cells) using AFM. A hyperosmotic decellularization approach with DNase treatment was utilized in order to remove cellular content without affecting matrix retention. This method removed >95% of DNA content, while retaining important ECM proteins, such as collagen types I, III, and IV, as well as laminin and fibronectin.

The retained matrix post-decellularization was used to assess changes in structural characteristics of the CDM, specifically stiffness. Changes in CDM stiffness were observed in the presence of the 0.5% HA and Ficoll 70/400 treated cultures.A cell migration assay using Cytodex beads was used to assess endothelial cell sprouting after being cultured on different CDM surfaces (**Appendix 2**). Cytodex bead assay appeared to support endothelial cell migration

as indicated by the sprouts formed on the 0.05%, 0.5%, and Ficoll 70/400 within 6 hours of culture, which was comparable to the Matrigel positive control. Quantification was not completed to assess number of sprouts due to small sample size.

Loading of cCBD –LL37 to the CDMs developed under MMC and LL37 staining indicated a reduced binding of the peptide on the Ficoll 70/400 treated CDM. The decreased LL37-positive signal on the Ficoll 70/400 treated CDM as well as the increase in colony counts indicate that less collagen may be available for binding. This further highlights the variation macromolecule induced difference on matrix composition.

Overall, results indicate that HA acts as a crowder molecule and can possibly modulate matrix properties, such as stiffness and crosslinked collagen, due to effects on proteinase and crosslinking genes. This study also introduced a facile method for developing mechanically tunable CDM materials depending on the crowding molecule and concentration, which can ultimately support the use of CDM scaffolds as substrates for the study of stem cell expansion and differentiation [1, 2]. The use of CDMs as a substrate material would be more representative of a native ECM environment due to its heterogeneous composition compared to homogenous ECM protein coatings.

7.2. Future Work

7.2.1. Assess MMP activity

Trancriptomics and qRT-PCR studies indicate that Ficoll 70/400 induces an increase in MMP gene expression compared to HA and non-treated controls. However, changes in gene expression do not necessarily mean translation into a functionally active protein. In order to follow up on MMP activity, zymography experiments need to be completed on lysates collected

from CDMs treated under different MMC conditions. Zymography is an electrophoretic technique utilizing gelatin embedded in polyacrylamide gels to measure MMP2 and MMP9 proteolytic activity [3]. Areas of gelatin degradation indicate proteolytic activity. Alternatively, MMP fluorescence resonance energy transfer (FRET) assay can also be used to assess MMP activity. In its initial state, the FRET peptide is intact and its fluorescence is quenched by the other part. After addition of samples containing MMPs, the FRET peptide is cleaved and the fluorescent activity of the FRET peptide is recovered. Changes in fluorescence compared to the blank is an indication of MMP activity. We also included a recombinant MMP as a positive control for this assay. As the substrate in the assay is a sequence that is recognized by all MMPs, this assay does not differentiate between the different MMPs that are present in the sample. It measures total MMP activity present. We hypothesized that an increase in MMP2 activity will be observed in the Ficoll 70/400 condition compared to the non-treated and HA crowded condition.

7.2.2. Proteomics

Due to the cost-inhibitive nature of proteomics analysis, small sample sizes were used for each experiment. The preliminary proteomics study was completed on non-decellularized samples with a sample size of one. In order to properly characterize the CDM as a substrate or scaffold for regenerative applications, a proteomics analysis post-decellularization is crucial to assess matrix and associated matrix molecule retention.

7.2.3. Transwell Inserts

Limitations within our research platform included the thicknesses of the developed cell-derived substrate. The thickness reported from a 2D *in vitro* culture was from 25-30 μm. The

limitation in scaffold thickness was preliminarily addressed using Transwell inserts (**Appendix 3**) that would support infiltration of gases and nutrients from the bottom of the scaffold through a permeable membrane as well as from the top. Culturing dermal fibroblasts on Transwells supported histological characterization of the collagen structure in each sample, however, further characterization is needed, such as assessment of collagen content, in order to use the thicker scaffolds for other experiments, such as hydrogel development or angiogenesis assays.

7.2.4. Hydrogel formulations

Another limitation was in the development of a hydrogel from MMC-derived CDMs comparable to other hydrogel substrates, such as Matrigel. A minimum collagen concentration of 0.5mg/mL is required for supramolecular collagen assembly to occur [4]. When tested at the minimum concentration, there appeared to formation of collagen hydrogels at the 0.05% HA and Ficoll 70/400 conditions, however, gel assembly was observed after overnight incubation at 37°C, and gelation was only assessed using an invert test. Qualitatively, the hydrogel also appeared to be soft, which is expected as stiffness measurements increase with higher collagen concentrations [4]. Scale up studies to increase the concentration of collagen would be required to properly assess hydrogel formation from CDMs.

7.2.5. Angiogenesis assays

In this thesis, we assessed the functional activity of CDMs developed under MMCs using a modified Cytodex Bead assay **(Appendix 2)**. In this assay, endothelial cells were cultured on the surface of Cytodex beads and then plated on decellularized CDMs. While we did see short, endothelial sprouts from the 0.05% HA, 0.5% HA, and Ficoll 70/400 conditions, not many

sprouts formed as seen in previous publications . [5]. This may be due to several limitations in our approach, specifically working in a 2-D environment versus 3-D. One approach for developing a 3D-scaffold is to use Transwell inserts or CDM hydrogels to develop to support endothelial cell culture. HUVECs can then be cultured on 3-D scaffolds using multiple approaches. The first approach utilizes creation of endothelial cell 'spheroids' that can be cultured on the surface of the CDM, and sprouting can be assesses from the cell mass [6]. Alternatively, agarose wells can be created on the surface of the CDMs to allow localized culturing of a concentrated bolus of HUVECs, and assessing migration from those specific areas [7]. Previous literature has also shown that incorporating fibroblasts in the culture, can promote secretion of several molecules that are important to angiogenesis [8]. Nakatsu *et al.* recommended addition of fibroblasts to the top of the 3-D substrate to allow for growth factor secretion that would promote angiogenesis [5]. An *ex vivo* approach that may also be utilized to assess angiogenesis of CDMs is the use of rat mesentery. The rat mesentery provides a translucent window to allow assessment of treatment, lacks physiological angiogenesis, and has very sparse microvessel network similar to adult tissue [9]. Furthermore, it replicates a clinical assay as the responses observed reflect the metabolic, cellular, and molecular alternations that would be induced by the treatment [9]. This assessment provides information regarding microvascular extension, density, and sprouting without relying on endothelial cells of micro- or macrovascular origin, which have been shown to have different phenotypes and responses to treatments [10, 11]. A hydrogel developed from CDMs under MMC may also support the use of this assay to assess sprouting. In order to form a hydrogel, a minimum collagen concentration of 0.5 mg/mL is required for supramolecular collagen assembly to occur [4].

7.2.6. Biochemical effects of HA

HA is a natural bioactive molecule that is known to interact with cell surface receptors, CD44 and RHAMM. In order to characterize HA as an external stimuli for crowding experiments, it is important to determine if HA is also contributing a direct biochemical effect by binding to cell surface receptors, in addition to its biophysical effect. This can be determined using binding/blocking assays to CD44 or RHAMM, and determining if exogenous addition of HA to the cell culture would still have the same effect on matrix deposition as previously observed. However, receptor blocking/binding assays are challenging due to the presence of several CD44/RHAMM isoforms.

7.3. Alternative strategies and future directions

There are several different approaches that when combined with MMC may ultimately promote ECM deposition, and support CDM production. The first approach is to select an appropriate cell source/type as different stimuli will induce different responses for each cell. Furthermore, genetic modification of a cell source may also be an option for matrix production. After selection of cell source, approaches such as low oxygen cultures and bioreactor cultures may be applied with MMC techniques to tailor the compositions and properties of the CDMs.

7.3.1 Hypoxic Culture Conditions

During embryonic and fetal wound healing, the developed ECM is characterized by increased levels of glycosaminoglycans, such as hyaluronic acid and chondroitin sulfate [12], which plays a role in the scar-free wound healing response. Embryonic microenvironments are characterized by low oxygen (2%-5%) levels, which is required for the regulation of embryonic

and progenitor cells in an undifferentiated state [13]. Fetal ECM developed under hypoxic conditions increases collagen type IIII expression, and supports the deposition of fine reticular fibers that is similar to uninjured skin [14]. Thus, ECM developed under hypoxic conditions may provide valuable insight in the development of scaffolds for scar-free wound healing responses. Bioreactor cultures have also been combined with hypoxic culture techniques for regulation of matrix production in an embryonic like microenvironment [15]

Furthermore, hypoxic cultures may also support a pro-angiogenic microenvironment. Hypoxia is a potent stimulator for the production of several pro-and anti-angiogenic factors [16, 17]. Pro-angiogenic factors that are stimulated under hypoxic culture conditions include VEGF, angiopoietin- 1/- 2 FGF, PDGF, and PAI-1 [16]. Anti-angiogenic factors induced under hypoxic culture conditions include thrombospondin-1, angiostatin, and endostatin [16]. In response to hypoxia, hypoxia-inducible factor 1α (HIF-1α) synthesis increases VEGF levels, thus regulating the secretion of proangiogenic factors [16, 18, 19]. Hypoxic conditions have also been applied to macromolecular crowding based cultures. Cigognini *et al.* showed a small increase in MSC collagen type I and III deposition in the presence of carrageenan crowding at low oxygen conditions [20]. The use of hypoxic culture is dependent on cell type, however, as decreases in collagen have also been observed [21]. In human dermal fetal fibroblasts, specifically, hypoxia induced accumulation of HIF-1, which promoted increased ECM deposition through changes in crosslinking genes [22].

The combination of hypoxic culture conditions and macromolecular crowding can promote increased matrix production and deposition, respectively, depending on the cell type selected for production of CDMs. Therefore, the combination of these techniques can potentially produce a CDM with pro-regenerative and pro-angiogenic properties.

7.3.2 Chemically Defined and Serum Free Media

Chemically defined media containing different supplements and growth factors has been shown to increase matrix production in human dermal fibroblasts [23]. It is defined as a media with known concentrations of all of its components, and is entirely free of animal derived components, such as fetal bovine serum, bovine serum albumin, and human serum [24]. In chemically defined media, recombinant human albumin or a synthetic chemical, such as polyvinyl alcohol is used instead of serum. Chemically defined media is the purest and most consistent cell culture environment, and has several advantages in that there is minimal batch to batch variability due to lack of serum presence, eliminates the risks of contaminants, and has low protein content [25]. Ahlfors *et al.* showed significant increases in collagen and protein content in dermal fibroblasts cultured under chemically defined media conditions [23]. The media contained several different growth factors, such as epidermal growth factor, fibroblast growth factors, as well as several other additives, such as insulin, ethanolamine, dexamethasone, and 500μM ascorbate. However, it was not specified if recombinant human albumin was used. Frequent media changes may have led to the discard of ECM pre-cursor proteins that may have potentially led to increased matrix deposition at the cell layer. Thus, the addition of crowders can further promote matrix deposition by sequestering the pre-cursor proteins that would be secreted into the media. Furthermore, the addition of crowders would not alter the definition of a chemically defined media, as the crowders are not animal derived and would be added at known concentrations.

Serum-free media is an alternative type of defined media that, unlike chemically defined media, contains human or bovine serum albumin. These media formulations are erroneously described as chemically defined media [26]. Studies have shown the use of human serum and

human serum albumin in crowder based media, and noted an increase in collagen deposition, especially under lower serume concentrations [27, 28]. These studies were compared to fetal bovine serum supplemented media, which showed that high serum concentrations increased proteinase activity, and thus reduced overall collagen deposition. Substitution of human serum or human serum albumin at lower concentrations with crowder molecules was the optimal media formulation for collagen deposition, and supports the addition of crowders to serum free media as a potential alternative.

7.3.3 Cell Source

In developing cell-derived matrices for applications in dermal repair, cell sources can be derived from local, systemic, and progenitor cell populations [17]. Cell sources include fibroblasts [29], keratinocytes [29], and adipocytes [2]. Systemic and progenitors cells can reside in the bone marrow system [20, 30-32]. Progenitor cells may also arise from local stem cell niches or embryonic stem cells cultured *in vitro* [1]. Embryonic stem cells provide a very attractive production source for development of CDMs due to their totipotency and indefinite differentiation potential. The cell source is dependent on the end-application for the CDM, as different cells will produce matrices with different compositions. For applications in dermal repair as well as developing substrates to study stem cell differentiation, various cell types such as dermal [29], lung [28, 33], and corneal [27] fibroblasts, bone marrow-derived MSCs [20, 30-32], embryonic stem cells [1], and adipose stem cells [2] have been studied under macromolecular crowding. Different cell sources may have different sensitivities to crowder induced matrix deposition, such as Ficoll 70/400 induced elevation in MMP activity in dermal fibroblast cultures compared to other studies reported in literature.

An additional approach to developing an angiogenic scaffold is the use of cancer cells for development of the CDM. Cancer cells are characterized by an ECM-rich, and well vascularized environment, and may potentially be used after decellularization of the tumor. Culturing under hypoxic and crowding conditions can drive the development an ECM rich, angiogenesis promoting scaffold. This is a similar approach to the highly pro-angiogenic, mouse tumor derived commercial ECM, Matrigel® [34]. While Matrigel® lacks any clinical application, the concept of using an ECM-rich pro-angiogenic tumor may provide an alternative source of cells for matrix production. However, as the cells are tumor derived, extensive decellularization and matrix characterization is necessary. Overall, proper selection of cell source can be utilized with different culture techniques such as bioreactor based cultures, low oxygen conditions, as well as macromolecular crowding development of CDMs.

7.3.4 Genetically Modified Cells for Production of CDMs

Cell-derived ECM scaffolds can also be produced using cells that are genetically modified to increase production of ECM-proteins and growth factors to promote healing and angiogenesis. Previous work has demonstrated the use of biomimetic peptide based matrices for localized targeting of a genes. Trentin *et al.* presented localized targeting of HIF-1α lacking the oxygen sensitive degradation domain via fibrin based matrices leading to upregulation of VEGF when implanted in a full thickness dermal model [19]. Similar approaches have also been utilized for increased FGF production [35]. This approach utilized an ECM based delivery vehicle as a biomaterial for *in vivo* studies, and modification of cells at the site of transplantation. A similar approach for localized gene delivery would be culturing an immortalized cell lines within the biomimetic material to allow for modification, digesting the matrix material, and

utilizing the genetically modified cells for production of CDMs. Other approaches for gene therapy such as the use of mammalian derived viral vectors or non-viral vectors [36] can also be used to modify specific cell lines for development of ECM based CDM. Modification of cell lines for up-regulation of ECM and ECM-crosslinking genes, such as collagen and lysyl oxidase, would allow development of a matrix producing cell factory. The same approach can also be used for pro-angiogenesis growth factor associate genes, such as VEGF, PDGF, or FGF, to allow increased production of angiogenesis promoting factors. Gene modification has also been presented as a novel approach to allow decellularization of a CDM through apoptotic cell death mechanisms thus preventing any modification or disruption in the synthesized matrix [37, 38]. This would be an interesting decellularization approach to study as it would minimize on sample preparation time, and reduce any matrix proteins lost in the decellularization process.

7.3.5 Microcarrier-bioreactor cultures

The use of MMC in culture may provide a method to supplement the development of CDMs using bioreactor microcarrier cultures [15, 39]. Microcarrier cultures provide scaled manufacturing of CDMs, however, the culture period is still on the order of months. The combination of MMC culture techniques in bioreactor cultures can help accumulate ECM pre-cursor proteins to the surface of microcarriers rather than being discarded as waste. The scale-up procedure combined with techniques to reduce waste of discarded ECM proteins may potentially provide a method to reduce the culture time of CDMs, and reduce manufacturing costs. While this approach is not the focus of this thesis project, it provides a method to consider for future applications of CDM production.

7.4. Conclusion

Cell-derived matrices have several advantages that would support their use for dermal repair in clinical applications, as well as a culture substrate for *in vitro* research platforms. They can be tailored depending on the desired specification through selection of cell source; and composition can be varied depending on the culture conditions utilized. While their commercialization is hindered due to prolonged culture periods, there are several methods and techniques that can be utilized to aid in the biomanufacturing process. Macromolecular crowding in combination with other scale up techniques may address some of the limitations associated with CDMs. The presence of crowders may help sequester the ECM pre-cursor proteins at the surface, rather than being discarded as waste during media changes.

7.5. References

[1] R. Nair, S. Shukla, T.C. McDevitt, Acellular matrices derived from differentiating embryonic stem cells, Journal of Biomedical Materials Research Part A: An Official Journal of The Society for Biomaterials, The Japanese Society for Biomaterials, and The Australian Society for Biomaterials and the Korean Society for Biomaterials 87(4) (2008) 1075-1085.
[2] M. Patrikoski, M.H.C. Lee, L. Mäkinen, X.M. Ang, B. Mannerström, M. Raghunath, S. Miettinen, Effects of Macromolecular Crowding on Human Adipose Stem Cell Culture in Fetal Bovine Serum, Human Serum, and Defined Xeno-Free/Serum-Free Conditions, Stem cells international 2017 (2017) 6909163.
[3] T.M. Leber, F.R. Balkwill, Zymography: a single-step staining method for quantitation of proteolytic activity on substrate gels, Analytical biochemistry 249(1) (1997) 24-28.
[4] Y.-l. Yang, L.M. Leone, L.J. Kaufman, Elastic moduli of collagen gels can be predicted from two-dimensional confocal microscopy, Biophysical journal 97(7) (2009) 2051-2060.
[5] M.N. Nakatsu, C.C. Hughes, An optimized three-dimensional in vitro model for the analysis of angiogenesis, Methods in enzymology 443 (2008) 65-82.
[6] Z. Dong, B.D. Zeitlin, W. Song, Q. Sun, E. Karl, D.M. Spencer, H.V. Jain, T. Jackson, G. Núñez, J.E. Nör, Level of endothelial cell apoptosis required for a significant decrease in microvessel density, Experimental cell research 313(16) (2007) 3645-3657.
[7] G. Alessandri, K. Raju, P.M. Gullino, Mobilization of capillary endothelium in vitro induced by effectors of angiogenesis in vivo, Cancer research 43(4) (1983) 1790-1797.
[8] A.C. Newman, M.N. Nakatsu, W. Chou, P.D. Gershon, C.C. Hughes, The requirement for fibroblasts in angiogenesis: fibroblast-derived matrix proteins are essential for endothelial cell lumen formation, Molecular biology of the cell 22(20) (2011) 3791-3800.
[9] K.C. Norrby, Rat mesentery angiogenesis assay, JoVE (Journal of Visualized Experiments) (52) (2011) e3078.
[10] I. Lang, M.A. Pabst, U. Hiden, A. Blaschitz, G. Dohr, T. Hahn, G. Desoye, Heterogeneity of microvascular endothelial cells isolated from human term placenta and macrovascular umbilical vein endothelial cells, European journal of cell biology 82(4) (2003) 163-173.
[11] I. Solomon, M. O'Reilly, L. Ionescu, R.S. Alphonse, S. Rajabali, S. Zhong, A. Vadivel, W.C. Shelley, M.C. Yoder, B. Thébaud, Functional Differences Between Placental Micro-and Macrovascular Endothelial Colony-Forming Cells, Stem cells translational medicine 5(3) (2016) 291-300.
[12] K. Rolfe, A. Grobbelaar, A review of fetal scarless healing, ISRN dermatology 2012 (2012).
[13] M.C. Simon, B. Keith, The role of oxygen availability in embryonic development and stem cell function, Nature reviews Molecular cell biology 9(4) (2008) 285.
[14] R. Carter, K. Jain, V. Sykes, D. Lanning, Differential expression of procollagen genes between mid- and late-gestational fetal fibroblasts, Journal of Surgical Research 156(1) (2009) 90-94.
[15] R.S. Kellar, M. Hubka, L.A. Rheins, G. Fisher, G.K. Naughton, Hypoxic conditioned culture medium from fibroblasts grown under embryonic-like conditions supports healing following post-laser resurfacing, Journal of cosmetic dermatology 8(3) (2009) 190-196.
[16] B.L. Krock, N. Skuli, M.C. Simon, Hypoxia-induced angiogenesis: good and evil, Genes & cancer 2(12) (2011) 1117-1133.
[17] A.D. Metcalfe, M.W. Ferguson, Tissue engineering of replacement skin: the crossroads of biomaterials, wound healing, embryonic development, stem cells and regeneration, Journal of the Royal Society Interface 4(14) (2006) 413-437.
[18] V. Falanga, V. Su Wen Qian, D. Danielpour, M.H. Katz, A.B. Roberts, M.B. Sporn, Hypoxia upregulates the synthesis of TGF-β1 by human dermal fibroblasts, Journal of Investigative Dermatology 97(4) (1991) 634-637.

[19] D. Trentin, H. Hall, S. Wechsler, J.A. Hubbell, Peptide-matrix-mediated gene transfer of an oxygen-insensitive hypoxia-inducible factor-1α variant for local induction of angiogenesis, Proceedings of the National Academy of Sciences 103(8) (2006) 2506-2511.
[20] D. Cigognini, D. Gaspar, P. Kumar, A. Satyam, S. Alagesan, C. Sanz-Nogués, M. Griffin, T. O'Brien, A. Pandit, D.I. Zeugolis, Macromolecular crowding meets oxygen tension in human mesenchymal stem cell culture-A step closer to physiologically relevant in vitro organogenesis, Scientific Reports 6 (2016) 30746.
[21] T.B. McKay, J. Hjortdal, S. Priyadarsini, D. Karamichos, Acute hypoxia influences collagen and matrix metalloproteinase expression by human keratoconus cells in vitro, PloS one 12(4) (2017) e0176017.
[22] D.M. Gilkes, S. Bajpai, P. Chaturvedi, D. Wirtz, G.L. Semenza, Hypoxia-inducible factor 1 (HIF-1) promotes extracellular matrix remodeling under hypoxic conditions by inducing P4HA1, P4HA2, and PLOD2 expression in fibroblasts, Journal of Biological Chemistry 288(15) (2013) 10819-10829.
[23] J.-E.W. Ahlfors, K.L. Billiar, Biomechanical and biochemical characteristics of a human fibroblast-produced and remodeled matrix, Biomaterials 28(13) (2007) 2183-2191.
[24] D.W. Jayme, S.R. Smith, Media formulation options and manufacturing process controls to safeguard against introduction of animal origin contaminants in animal cell culture, Cytotechnology 33(1-3) (2000) 27-36.
[25] S. Yao, S. Chen, J. Clark, E. Hao, G.M. Beattie, A. Hayek, S. Ding, Long-term self-renewal and directed differentiation of human embryonic stem cells in chemically defined conditions, Proceedings of the National Academy of Sciences 103(18) (2006) 6907-6912.
[26] S.N. Usta, C.D. Scharer, J. Xu, T.K. Frey, R.J. Nash, Chemically defined serum-free and xeno-free media for multiple cell lineages, Annals of translational medicine 2(10) (2014).
[27] P. Kumar, A. Satyam, X. Fan, E. Collin, Y. Rochev, B.J. Rodriguez, A. Gorelov, S. Dillon, L. Joshi, M. Raghunath, Macromolecularly crowded in vitro microenvironments accelerate the production of extracellular matrix-rich supramolecular assemblies, Scientific reports 5 (2015) 8729.
[28] A. Satyam, P. Kumar, X. Fan, A. Gorelov, Y. Rochev, L. Joshi, H. Peinado, D. Lyden, B. Thomas, B. Rodriguez, M. Raghunath, A. Pandit, D. Zeugolis, Macromolecular crowding meets tissue engineering by self-assembly: A paradigm shift in regenerative medicine, Advanced Materials 26(19) (2014) 3024-3034.
[29] P. Benny, C. Badowski, E.B. Lane, M. Raghunath, Making more matrix: enhancing the deposition of dermal–epidermal junction components in vitro and accelerating organotypic skin culture development, using macromolecular crowding, Tissue Engineering Part A 21(1-2) (2014) 183-192.
[30] M.C. Prewitz, A. Stißel, J. Friedrichs, N. Träber, S. Vogler, M. Bornhäuser, C. Werner, Extracellular matrix deposition of bone marrow stroma enhanced by macromolecular crowding, Biomaterials 73 (2015) 60-69.
[31] R. Rashid, N.S.J. Lim, S.M.L. Chee, S.N. Png, T. Wohland, M. Raghunath, Novel use for polyvinylpyrrolidone as a macromolecular crowder for enhanced extracellular matrix deposition and cell proliferation, Tissue Engineering Part C: Methods 20(12) (2014) 994-1002.
[32] A.S. Zeiger, F.C. Loe, R. Li, M. Raghunath, K.J. Van Vliet, Macromolecular crowding directs extracellular matrix organization and mesenchymal stem cell behavior, PloS one 7(5) (2012) e37904.
[33] R.R. Lareu, D.I. Zeugolis, M. Abu-Rub, A. Pandit, M. Raghunath, Essential modification of the Sircol Collagen Assay for the accurate quantification of collagen content in complex protein solutions, Acta biomaterialia 6(8) (2010) 3146-3151.
[34] H.K. Kleinman, G.R. Martin, Matrigel: basement membrane matrix with biological activity, Seminars in cancer biology, Elsevier, 2005, pp. 378-386.
[35] D. Larocca, M. Brug, K. Jensen-Pergakes, E. Ravey, A. Gonzalez, A. Baird, Evolving phage vectors for cell targeted gene delivery, Current pharmaceutical biotechnology 3(1) (2002) 45-57.
[36] C. Hardee, L. Arévalo-Soliz, B. Hornstein, L. Zechiedrich, Advances in non-viral DNA vectors for gene therapy, Genes 8(2) (2017) 65.

[37] P. Bourgine, C. Le Magnen, S. Pigeot, J. Geurts, A. Scherberich, I. Martin, Combination of immortalization and inducible death strategies to generate a human mesenchymal stromal cell line with controlled survival, Stem cell research 12(2) (2014) 584-598.
[38] P.E. Bourgine, B.E. Pippenger, A. Todorov Jr, L. Tchang, I. Martin, Tissue decellularization by activation of programmed cell death, Biomaterials 34(26) (2013) 6099-6108.
[39] Y. Zhou, M. Zimber, H. Yuan, G.K. Naughton, R. Fernan, W.-J. Li, Effects of human fibroblast-derived extracellular matrix on mesenchymal stem cells, Stem Cell Reviews and Reports 12(5) (2016) 560-572.

Appendix 1: Chapter 4 Supplementary Figures

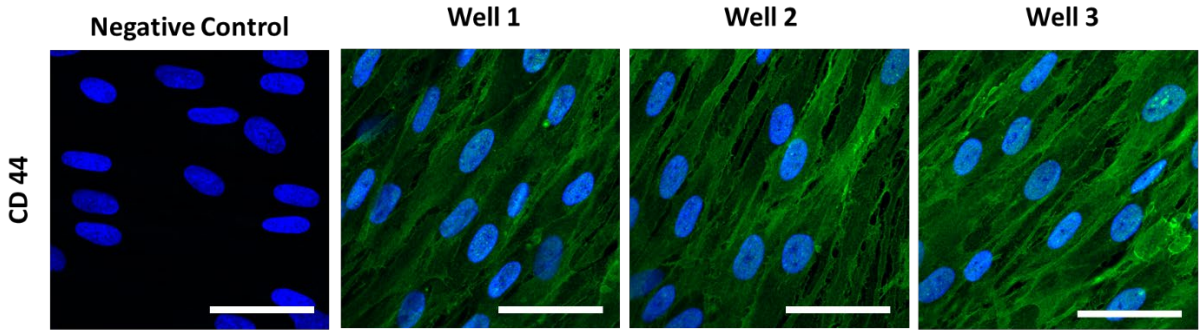

Supplementary Figure 4-1: Laser scanning microscopy of CD44 positive primary human neonatal foreskin fibroblasts. Sample size: N = 1 (biological), n = 3 (technical). Scale bar: 50 µm.

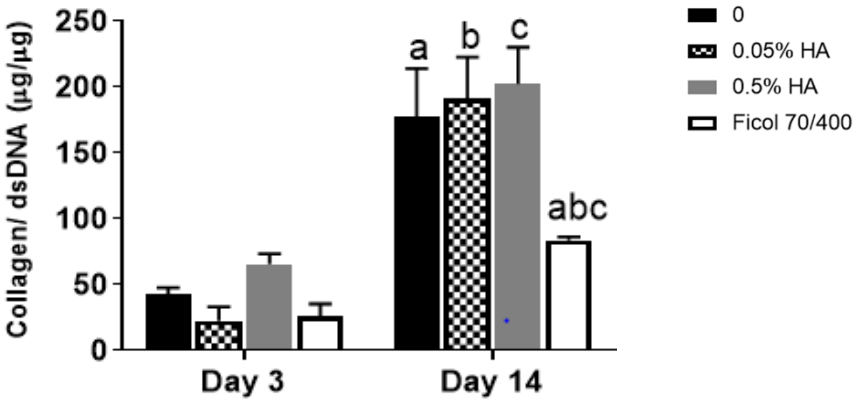

Supplementary Figure 4-2: Assessment of collagen deposition in 3 and 14 day cell-derived matrices prepared under HA and Ficoll 70/400 crowding conditions. Total collagen quantification using hydroxyproline assay of MMC cultures CDMs at 3 and 14 days. Data presented as collagen amount (µg) per dsDNA amount (µg). All values represent mean and SEM from four experimental replicates. Statistically significant differences between conditions at 14 days is indicated by: $^{bc}p < 0.01$, $^{a}p < 0.05$.

.

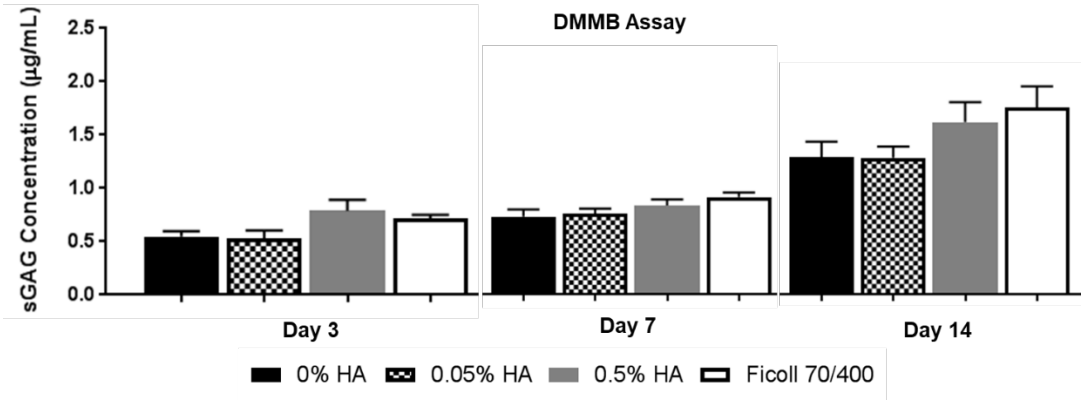

Supplementary Figure 4-3: Assessment of GAG deposition in 3, 7, and 14 day cell-derived matrices prepared under HA and Ficoll 70/400 crowding conditions. Sulfated GAG concentrations measured using DMMB assay.

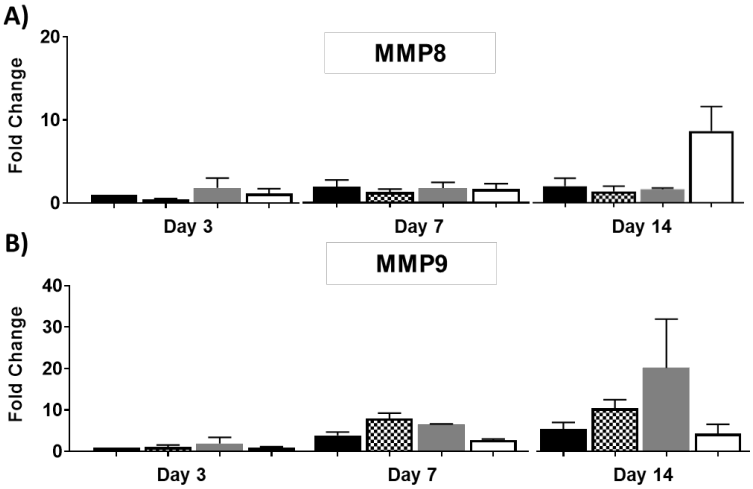

Supplementary Figure 4-4: Quantitative RT-PCR analysis of **(A)** MMP 8 and **(B)** MMP9. All values represent mean and standard error of the mean from at least three experimental replicates.

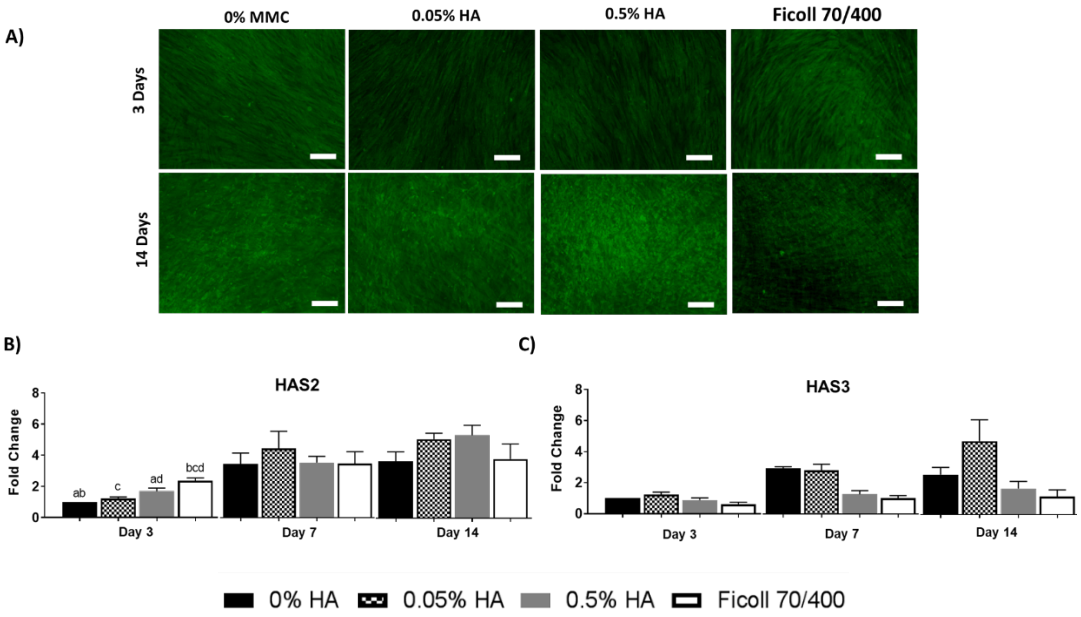

Supplementary Figure 4-5: **(A)** Hyaluronic acid binding protein (HABP) staining of 3 and 14 day fibroblasts cultured under HA and Ficoll 70/400 crowding. **(B)** Quantitative RT-PCR analysis of hyaluronic acid producing genes HAS2 and **(C)** HAS3. Scale bar: 100 µm.

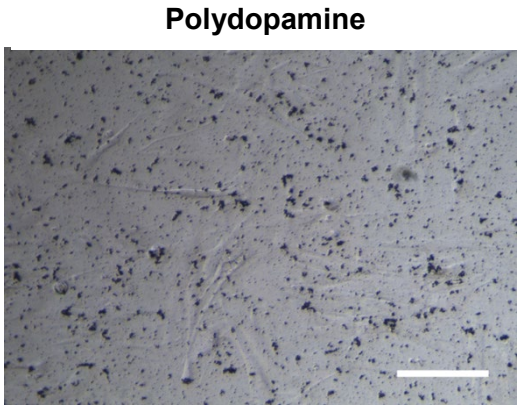

Supplementary Figure 4-6: Image of polydopamine coated coverslip with fibroblasts cultured for 24 hours. Scale bar :100 µm.

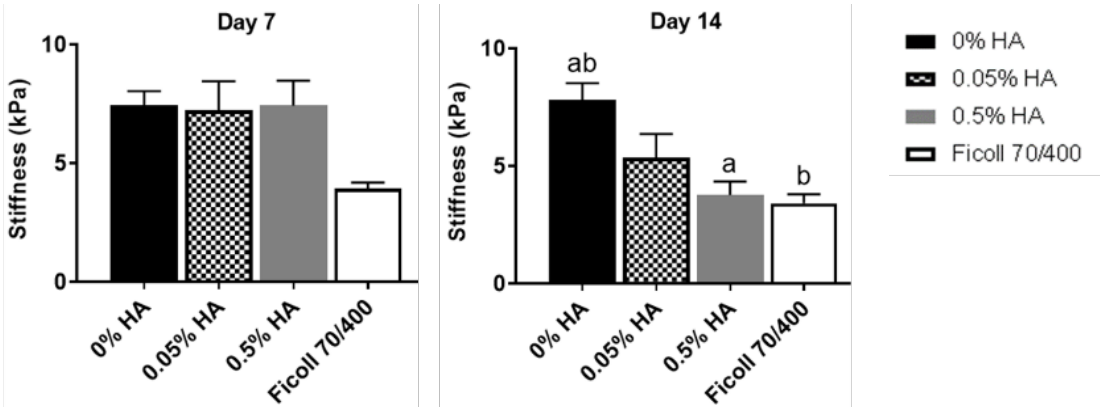

Supplementary Figure 4-7 Atomic force microscopy (AFM) nanoindentation of non-decellularized 7 and 14-day cell-derived matrices. Stiffness measurements of non-decellularized 7 and 14-day CDMs. Sample size: N = 3. Statistically significant difference between means of non-crowded control (0% HA) versus 0.05% HA and Ficoll 70/400 is indicated by: $^{b,}p < 0.01$, $^{a,}p < 0.05$.

Extracellular Matrix Genes		
	Primer Sequence	
Gene	Forward	Reverse
Col1A1	GTC AGG CTG GTG TGA TGG G	GCC TTG TTC ACC TCT CTC GC
Col13A1	GGA CAC AGA GGC TTC GAT GG	CTC GAG CAC CGT CAT TAC CC
Col4A1	TGG TGA CAA AGG ACA AGC AG	GGT TCA CCC TTT GGA CCT G
FN1	CCA CAG TCG GGT CAG GAG	CTG GCC GAA AAT ACA TTG TAA A
LAMB	GAC AGT GGA CGC CAG TTT G	GCA CAG TCG TCA CAT CTG GA
ELN	GGA TTC CAG TTG TCC CAG GT	CTG CTT CTG GTG ACA CAA CC
Matrix Crosslinking Genes		
LOX	CTC TTG CTG TCC TCC GCT C	ATC TTG GTC GGC TGG GTA AG
Matrix Metalloproteases Genes		
	Primer Sequence	
Gene	Forward	Reverse
MMP1	GAT AAC CTG GAT CCA TAG ATC GTT	GCA TAT CGA TGC TGC TCT TTC
MMP2	GGT CTT GGG AGT GCT CCA G	CGA TGA TGA CCG CAA GTG
MMP8	AAG ATC ATG TTC TCC CTG AAG AC	TAC TGG TTG CTT GGT AAT TGG T
MMP9	CGC CTC TGG AGG TTC GAC	AAG CGG TCC TGG CAG AAA TAG
Inhibitors of MMPs Genes		
	Primer Sequence	
Gene	Forward	Reverse
TIMP1	TGG AAG CCC TTT TCA GAG	GGC TGT GAG GAA TGC ACA
TIMP3	GTG CAA CTT CGT GGA GAG GT	AGC AGG ACT TGA TCT TGC AGT
HA Synthesis Genes		
	Primer Sequence	
Gene	Forward	Reverse
HAS2	CAG ACA GGC TGA GGA CGA CT	AGA CTC CAA AGA GTG TGG TTC C
HAS3	TGC GAC TCT GAC ACT GTG C	TCC ATG AGT CGT ACT TGT TGA GG
Housekeeping Gene		
	Primer Sequence	
Gene	Forward	Reverse
GAPDH	TTC ACA CCC ATG ACG AAC AT	GAG TCC ATC GGC GTC TTC AC

Supplementary Table 4-1: Quantitative RT-PCR primer sequences.

Appendix 2: Functional Properties of Cell-derived Matrices Prepared under Macromolecular Crowding- Pilot Study to Assess Angiogenesis

A2.1. Introduction

Chronic wounds have a delayed healing response due to the impaired blood flow present at the wound bed, thus developing pro-angiogenic scaffolds is crucial to promoting a pro-healing environment. There are several commercially available products on the market that have been clinically shown to promote wound closure and formation of granulation tissue; however few have evaluated capillary formation/improvement of blood flow to the wound bed as a clinical endpoint. Several synthetic polymers such as, poly-methacrylates [1], poly- L-lactic-glycolic acid [2], polycaprolactone [2], and self-assembling synthetic peptides [3], have been shown to provide varying degrees of pro-angiogenic stimulus. Due to concern that synthetic polymers can elicit non-physiological cellular responses and induce effects created by the scaffold degradation [2, 4], there has been a research shift towards chemically-derivatized or underivatized components of the extracellular matrix (ECM) [5]. These materials are often homogenous sources of ECM components, such as collagen [6], fibrin [7], hyaluronic acid (HA) [6, 8], or laminin [9], as these proteins have been shown to play a crucial role in the wound healing process, especially for angiogenesis.

ECM-based biomaterials used for wound repair are often xenogeneic-derived, decellularized or devitalized products. Tissue-derived ECM has several advantages, but they are limited in application due to availability of tissue source, large variability between different sources, and likely immunogenic response to xenogeneic derived materials [10]. Matrigel® is an example of a decellularized, xenogeneic tissue-derived ECM protein material that has been characterized for the support of capillary network formation [11]. Matrigel® is rich in basement

membrane proteins and pro-angiogenic growth factors, such as laminin, collagen type IV, fibronectin, and VEGF, however it has limited clinical utility due to its xenogeneic origin and immunological consequences, and is not specific to endothelial cell sprouting [11]. The development of a human cell-derived material with a similar ECM composition and properties to that of Matrigel®, may have potential clinical applications, and provide a human *in vitro* platform for studying cell propagation or stromal cell differentiation.

CDMs are a heterogeneous source of ECM proteins that can be tailored to clinical applications depending on the cell source and/or culture conditions. Due to the rich ECM protein composition, CDMs can potentially be used to develop a human cell-derived "Matrigel-like" material. Similar to other ECM scaffolds, CDMs have been shown to contain various ECM proteins to support cellular growth [12], bind growth factors [13], and provide signaling cues for cellular function [14]. For example, enzymatic degradation of collagen induces vascular permeability, and the accumulation of collagen fragments provides a chemotactic response for endothelial cell migration [14]. Fibronectin is another ECM molecule that is crucial to healing, as it provides collagen and heparin sulfate proteoglycan binding sites, and thus acts as a substrate for promoting cell adhesion and migration [13]. Laminin also provides functional binding sites for collagen and proteoglycans, and play a crucial role in epithelialization and angiogenesis [9].

Angiogenesis is defined as the growth of blood vessels from an existing vascular structure [15, 16], and is vital to the development of new tissues during embryogenesis as well as during tissue remodeling and repair throughout a lifespan. It is a highly controlled physiological process regulated by a balance of angiogenesis stimulating and inhibiting factors [17]. Over the past 40 years, research has focused on developing clinical therapies aimed at restoring the balance between angiogenesis promoting and inhibiting factors[18]. It has been

shown that the stimulation of angiogenesis can have therapeutic benefit to treat diseases, such as ischemic heart disease, and wound healing.

Hyaluronic acid has therapeutic potential as a pro-angiogenic stimulus that can support the development of vascularized and vascular-inducing functional materials for clinical applications [8]. Fibroblast-like cells exogenously treated with HA exhibited increased expression of TGF-β [8, 19], VEGF [19], and IL-8 [8] as well as ECM proteins [8] that are important to the angiogenesis process. The study of microvascular network formation using the co-culture of endothelial cells and fibroblasts highlight the important role each cell type plays [20, 21]. While HA provides stimuli for endothelial cell proliferation, fibroblasts further enhance the formation of capillary structures through production of extracellular matrix molecules [22] and proangiogenic factors [23]. The production and retention of proangiogenic growth factors and ECM molecules within cell-derived matrices developed under HA stimulus, as well as changes in its biomechanical properties, may be a strategy to modulate the response of incorporated endothelial cells. Furthermore, the ECM molecules produced under the HA stimulus may provide directional guidance for endothelial cell outgrowth [6]. We hypothesized that developing CDMs under HA-based crowding conditions will produce a pro-angiogenic matrix that can support endothelial cell migration, and thus capillary sprouting. Our goal is to develop a substrate that would promote formation of capillary sprouts from existing vessels in the vicinity of the wound, thus providing support of tissue remodeling and repair during the wound healing process.

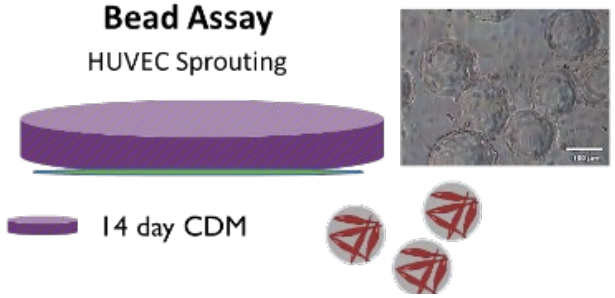

Supplementary Figure A2-1: Schematic illustrating the method for 14-day cell-derived matrices for assessment of endothelial cell sprouting.

In this chapter, we preliminarily characterize the functional properties, specifically endothelial cell sprouting, of decellularized CDMs using a Cytodex Bead assay. An overview of the experimental approach shown in **Supplementary Figure A2-1.**

A2.2. Materials and Methods

A2.2.1 Preparation of polydopamine coating

Dopamine hydrochloride (Sigma, H8502) was reconstituted in 100mM bicine (Sigma, B3876) solution prepared at pH 8.5 [24, 25]. Coverslips placed in 24-well plates were incubated with polydopamine solution overnight at room temperature under rotation. After 24 hours, polydopamine solution was removed, and multiwall places rinsed for 5 minutes under distilled water. Multi-well plates were sterilized under ultraviolet light for 30 minutes prior to use for cell culture.

A2.2.2 Cell Culture- Human Dermal Fibroblasts and Human Umbilical Vein Endothelial Cells

Human dermal fibroblasts (CRL 2097) were cultured as previously described and used to prepare CDMs. CDMs were cultured under crowding conditions and decellularized as previously described in **Chapter 4.**

Human umbilical vein endothelial cells (HUVECs) (ATCC, PCS-100-010) were cultured in VasculLife Endothelial basal media supplemented with LifeFactor VEGF kit (LifeLine, LL-0003). Complete media was prepared as specified in the manufacturer protocol. Briefly, basal media was supplemented with the following at the specified final concentration: recombinant human (rh) FGF (5ng/mL), ascorbic acid (50µg/mL), hydrocortisone (1µg/mL), FBS (2% v/v), L-glutamine (10mM), rhIGF-1 (15ng/mL), rhEGF (5ng/mL), rhVEGF (5ng/mL), heparin sulfate

(0.75U/mL), gentamicin (30mg/mL), and amphotericin B (15µg/mL). Cells were trypsinized with 0.05% Trypin/EDTA, neutralized with complete media, and centrifuged at 1100 rpm. Supernatant was removed, and pellet was resuspended in complete LifeLine-VEGF media, and maintained in 145cm^2 petri dishes. Media was removed, and supplemented with fresh complete media every 48 hours. Cells were cultured at standard culture conditions (37°C, 5% CO_2).

A2.2.3 HUVEC Sprouting Assays

Cytodex-3 (Sigma, C3275) beads (0.1g) were measured and hydrated in sterile 1X PBS -/- (Caisson, PBL06) followed by overnight sterilization in 70% ethanol solution under rotation. After 24 hours, beads were allowed to settle, ethanol was removed, and beads rinsed 3x with sterile 1X PBS. Beads were resuspended for a final concentration of 2.5mg/mL, which is equivalent to 7500 beads/mL (1 g = 3x10^6 beads). HUVECs were loaded with cell tracker red CMPTX dye (Invitrogen, C34552) reconstituted in serum-free LifeLine basal media at a final concentration of 1µM and incubated for 30 minutes under standard culture conditions. After incubation, cell layer was rinsed twice with sterile 1xPBS, and cultured as specified above. Cytodex-3 beads can be loaded with 400 cells/bead as specified in manufacturer protocol. A cell density of 3 x 10^6 cells/mL was mixed with 1mL bead suspension (7500 beads/mL) in 1mL complete media in a 1.7ml Eppendorf tube. Cell number can be scaled according to experimental set up. Bead/cell suspension was mixed under rotation for 4 hours at 37°C. Beads coated with cells were transferred to a 65cm^2 tissue culture dish, and cultured overnight in complete media to remove unbound cells. Coated beads were collected, and allowed to settle prior to resuspending in 1mL complete media, and plating onto decellularized CDMs at a density of ~50,000 cells per CDM, which is approximately 125 beads per sample. CDMs were cultured for up to 48 hours, and imaged at 6, 18, and 48 hour

time points using a Leica DMIL microscope. A schematic illustrating the process for bead coating is seen in **Figure A-2**.

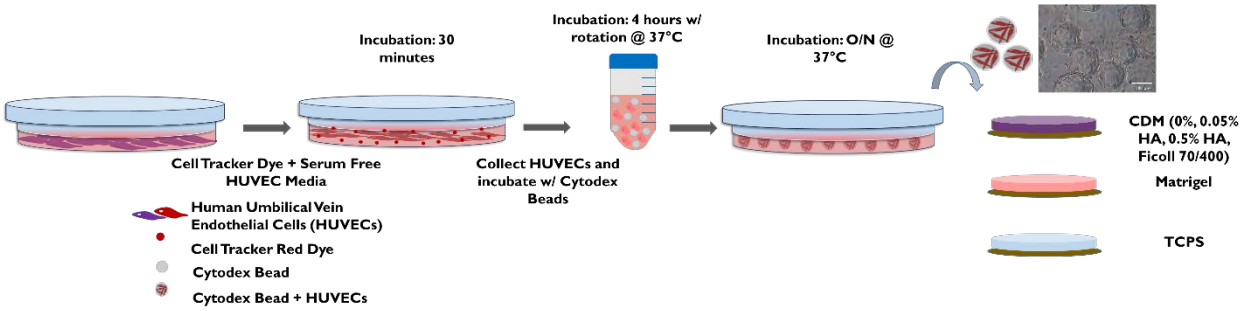

Supplementary Figure A2-2: Schematic illustrating the cytodex bead assay used to assess endothelial cell sprouting on the surface of decellularized CDMs

A2.2.3 Statistical Analysis

Statistical analysis for quantification of number and length of endothelial sprouts was not completed as the experiment represents a small sample size.

A2.3. Results

A2.3.1 Cytodex Bead Assay for HUVEC Sprouting

Capillary sprouting was assessed using a Cytodex bead assay [7] with human umbilical vein endothelial cells cultured on the CDMs **(Supplementary Figure A2-3).** Matrigel™, which is commonly used in angiogenesis assays, was used as a positive control ECM substrate to assess sprouting. Tissue culture polystyrene (TCPS) was used as a negative, non-matrix, control to assess the effects of the media alone on endothelial cell sprouting. A capillary sprout is defined as a cellular extension or endothelial cell migration, from the edge of the Cytodex bead. Short, single, capillary sprouts was observed in the 0.05% and 0.5% HA conditions as well as Ficoll 70/400. Sprouting on the Matrigel condition was comparable to the observations made on the CDMs.

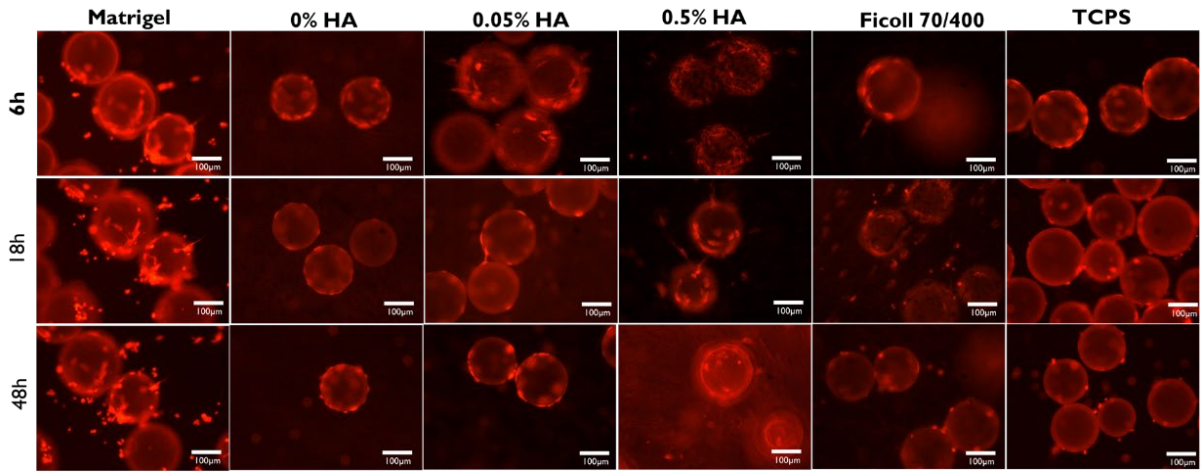

Figure A2-3: Cytodex bead assay to assess HUVEC migration on CDMs developed under MMC. Scale bar: 100 µm.

A2.4. Discussion

Angiogenesis can occur *in vivo* through four different mechanisms: sprouting, intussusceptions, elongation, and the incorporation of endothelial precursor cells into vessel walls [26]. Physiological angiogenesis occurs as a sequence of different events which includes vascular initiation, formation, maturation, remodeling, and regression [26]. There are several *ex vivo* and *in vitro* assays that are typically used to assess angiogenesis. *Ex vivo* assays, such as chick chorioallantoic membrane (CAM), rat aortic ring and rabbit corneal assays have been used to assess stimulators and inhibitors of angiogenesis [27], and are often recommended over *in vitro* assays for assessing the functional response of a biomaterial as they assess angiogenesis as a whole process rather than just one component of it. Due to their cost-inhibitory nature and requirement on animals for material harvest, alternative techniques have been utilized. For example, endothelial cell migration assays, such as Boyden or bead assays, are most frequently used for measuring angiogenesis. Alternative techniques rely on cell proliferation or differentiation into tubule structures as a measure of angiogenesis [27]. While these approaches

only assess isolated processes of angiogenesis, such as proliferation, differentiation, or migration, they provide easily quantified measures directly from endothelial cells, and thus provide an initial screen of the CDM prior to *ex vivo* or *in vivo* assessment. However, it is important to keep in mind that *in vitro* assays are limited by the heterogeneity of endothelial cell populations [27].

Our initial experiments were designed to assess endothelial cell migration and network of cell sprouts. From these experiments, it was observed that HUVECs cultured on CDMs anchored to the edge of the well and formed a network of cell sprouts (data not shown), which is not representative of the material as a whole. This indicates that endothelial cells require solid, support structure to anchor to and sprout from, which has also been reported in literature [12]. The type of matrix used for an *in vitro* angiogenesis assay has a strong effect on endothelial cell differentiation. For example, coating endothelial cells on collagen types 1 and III result in a proliferative state, however culturing on collagen types IV or laminin leads to extensive tube formation with little proliferation [27]. The heterogeneous ECM nature of Matrigel makes it a powerful *in vitro* ECM-based model for assessing angiogenic potential, and thus we used Matrigel as a control in our experiments. CDMs are also characterized by a heterogeneous ECM nature, and we hypothesized that HMWHA, compared to an inert macromolecule (Ficoll), crowding would support the development of CDMs with properties that support endothelial cell sprouting.

We qualitatively assessed angiogenesis using a cell migration assay via a bead assay. The Cytodex bead assay utilizes a 3-dimensional (3-D) structure, such as a fibrin based hydrogel or Matrigel, to assess capillary sprouting as well as lumen formation of endothelial cells coated to a dextran bead, and embedded within a hydrogel [20]. This approach is advantages over other *in*

vitro approaches as it allows quantitative measurement of cell migration and lumen formation simultaneously. For our assay, we modified a technique reported in Newmann *et al* [20]. Instead of utilizing a hydrogel/ 3-D structures, we assessed sprouting on a CDM substrate layer (i.e. coating) that only provided 2-dimensional (2-D) contact to the endothelial cells. CDMs supported short, thin HUVEC sprouts in the 0.05% HA, 0.5% HA, and Ficoll 70/400 conditions. The time points selected represent the initiation of sprouting/migration (4-6 hours) [28] and initiation of regression (after 30 hours) [29]. The sprouts were only observed at the 6 hour time point. No sprouts were observed at 18 and 48 hours. Capillary network formation is a transient response, and endothelial cells may have regressed over time [29, 30]. Endothelial cell regression within *in vitro* assays have been related to endothelial cell mediated activation of MMPs [29, 30] or apoptosis.

The sprouting observed in this assay was not comparable to sprouting reported for ECM based-hydrogels that are typically used for assessing angiogenesis, suggesting that it may not be the best method to assess sprouting on a 2-D surface due to small contact area between the bead and the matrix [7, 20]. A hydrogel developed from CDMs under MMC may better support the use of this assay to assess sprouting. In order to form a hydrogel, a minimum collagen concentration of 0.5 mg/mL is required for supramolecular collagen assembly to occur [31]. To address the limitation of the *in vitro,* we attempted to develop a MMC developed CDM hydrogel to support 3-D encapsulation of endothelial cells for assessment sprouting. When tested at the minimum concentration, there appeared to formation of collagen hydrogels at the 0.05% HA and Ficoll 70/400 conditions, however, gel assembly was observed after overnight incubation at 37°C, and gelation was only assessed using an invert test. Due to the prolonged time required for gelation, the hydrogels were not used to assess sprouting.

The bead assay completed above using the CDM substrates on the polydopamine coating representative of one experiment, thus statistical analysis was not performed and conclusions regarding the effects of CDMs on endothelial cell sprouting cannot be made. Additional information provided by AFM and proteomics studies may provide insight into creating a favorable angiogenic environment. Previous literature has reported that stiffness also has an effect on endothelial cell sprouting [32-35]. Matrix stiffness can be regulated by several factors, such as increased collagen deposition [36, 37] and GAG deposition [38, 39], crosslinking [40], and matrix metalloproteinase activity [41]. Increased matrix concentration within collagen and fibrin matrices, has been shown to have a negative effect on angiogenesis, as the increased density acts as a physical barrier preventing endothelial cell migration [37, 42]. Previous literature has shown that CDMs developed under Ficoll 70/400 crowding do not support capillary network formation [12]. Alternatively to matrix density, matrix stiffness can also increase due to an elevation in matrix crosslinking enzymes [43]. Endothelial cells have been shown to be mechanosensitive to matrix stiffness [44, 45], indicating the effect of CDM mechanical properties on supporting sprouting. Collagen gels with increased collagen crosslinks have been shown to increase the number extensions from embedded multicellular spheroids [33]. In this study, the increased crosslinks in the collagen gel changed the stiffness from 3kPa to 5kPa [33], which is still softer than the stiffness reported for the 0% and 0.05% HA CDMs, which were ~15kPa. The relationship between increased crosslinking and sprouting would support the observed sprouting from the 0.05% HA CDM, as the 0.05% HA condition has higher crosslinked collagen as observed in silver staining characterization of the CDMs (**Chapter 4, Figure 4-4).**

Two-dimensional substrates have also been used to assess endothelial sprouting. In 2-D surfaces, capillary networks more readily form on substrates with stiffness values of 1kPa

compared to 10kPa [35]. This suggests that the 0.5% or Ficoll 70/400 CDMs 2-D substrates would be able to support endothelial cell sprouting, as their measured stiffness is ~11 kPa and ~ 5kPa, respectively. However, the relationship between stiffness and sprouting is also dependent on other factors, such as scaffold thickness [32, 34] and how the endothelial cells are cultured on the substrate (i.e. in suspension versus encapsulated) [32].

A proteomic analysis was also completed on CDMs prepared at 14 days can provide information regarding the composition of CDMs favorable to angiogenesis. The data obtained from this experiment indicated the expression of pro- and anti-angiogenic factors that are expressed in each CDM **(Chapter 3, Table 3-1).** Several important pro-angiogenic factors have been reported to play an important role in promoting capillary sprouting [14], and were identified in the proteomics analysis completed. ECM components that play a role in angiogenesis, such as collagen, laminin, and fibronectin, were identified in the matrix to different levels of expression. Other research groups have also reported factors as angiogenesis stimulating [14, 20] and inhibiting [14], of which several of those factors were identified in the CDM developed under crowding conditions. For example, angiogenesis stimulating factors that were present in the CDM include fibrin, decorin, and fibulin. Anti-angiogenic factors that were reported include thrombospondin 1 /2 and angiopoitin-2.

A2.5. Acknowledgements

We would like to acknowledge our undergraduate research assistant Paige Waligora for her help in developing the *in vitro* angiogenesis assays.

A2.6. References

[1] A. Bakshi, O. Fisher, T. Dagci, B.T. Himes, I. Fischer, A. Lowman, Mechanically engineered hydrogel scaffolds for axonal growth and angiogenesis after transplantation in spinal cord injury, Journal of Neurosurgery: Spine 1(3) (2004) 322-329.
[2] H.-J. Sung, C. Meredith, C. Johnson, Z.S. Galis, The effect of scaffold degradation rate on three-dimensional cell growth and angiogenesis, Biomaterials 25(26) (2004) 5735-5742.
[3] D.A. Narmoneva, O. Oni, A.L. Sieminski, S. Zhang, J.P. Gertler, R.D. Kamm, R.T. Lee, Self-assembling short oligopeptides and the promotion of angiogenesis, Biomaterials 26(23) (2005) 4837-4846.
[4] C. Laurencin, H. Pierre-Jacques, R. Langer, Toxicology and biocompatibility considerations in the evaluation of polymeric materials for biomedical applications, Clinics in laboratory medicine 10(3) (1990) 549-570.
[5] E.L. Pardue, S. Ibrahim, A. Ramamurthi, Role of hyaluronan in angiogenesis and its utility to angiogenic tissue engineering, Organogenesis 4(4) (2008) 203-214.
[6] C. Borselli, O. Oliviero, S. Battista, L. Ambrosio, P.A. Netti, Induction of directional sprouting angiogenesis by matrix gradients, Journal of Biomedical Materials Research Part A 80(2) (2007) 297-305.
[7] M.N. Nakatsu, C.C. Hughes, An optimized three-dimensional in vitro model for the analysis of angiogenesis, Methods in enzymology 443 (2008) 65-82.
[8] M.A. Mariggiò, A. Cassano, A. Vinella, A. Vincenti, R. Fumarulo, L.L. Muzio, E. Maiorano, D. Ribatti, G. Favia, Enhancement of fibroblast proliferation, collagen biosynthesis and production of growth factors as a result of combining sodium hyaluronate and aminoacids, International Journal of immunopathology and Pharmacology 22(2) (2009) 485-492.
[9] J. Dixelius, L. Jakobsson, E. Genersch, S. Bohman, P. Ekblom, L. Claesson-Welsh, Laminin-1 promotes angiogenesis in synergy with fibroblast growth factor by distinct regulation of the gene and protein expression profile in endothelial cells, Journal of Biological Chemistry 279(22) (2004) 23766-23772.
[10] L.E. Fitzpatrick, T.C. McDevitt, Cell-derived matrices for tissue engineering and regenerative medicine applications, Biomaterials science 3(1) (2015) 12-24.
[11] H.K. Kleinman, G.R. Martin, Matrigel: basement membrane matrix with biological activity, Seminars in cancer biology, Elsevier, 2005, pp. 378-386.
[12] V. Magno, J. Friedrichs, H.M. Weber, M.C. Prewitz, M.V. Tsurkan, C. Werner, Macromolecular crowding for tailoring tissue-derived fibrillated matrices, Acta biomaterialia 55 (2017) 109-119.
[13] X. Zhou, R.G. Rowe, N. Hiraoka, J.P. George, D. Wirtz, D.F. Mosher, I. Virtanen, M.A. Chernousov, S.J. Weiss, Fibronectin fibrillogenesis regulates three-dimensional neovessel formation, Genes & development 22(9) (2008) 1231-1243.
[14] A. Neve, F.P. Cantatore, N. Maruotti, A. Corrado, D. Ribatti, Extracellular matrix modulates angiogenesis in physiological and pathological conditions, BioMed research international 2014 (2014).
[15] T.H. Adair, J.-P. Montani, Overview of angiogenesis, Angiogenesis (2010) 1-8.
[16] T.H. Adair, J.-P. Montani, Angiogenesis, Colloquium Series on Integrated Systems Physiology: From Molecule to Function, Morgan & Claypool Life Sciences, 2010, pp. 1-84.
[17] A. Karamysheva, Mechanisms of angiogenesis, Biochemistry (Moscow) 73(7) (2008) 751.
[18] M.G. Tonnesen, X. Feng, R.A. Clark, Angiogenesis in wound healing, Journal of Investigative Dermatology Symposium Proceedings, Elsevier, 2000, pp. 40-46.
[19] Y.T. Lee, H.J. Shao, J.H. Wang, H.C. Liu, S.M. Hou, T.H. Young, Hyaluronic acid modulates gene expression of connective tissue growth factor (CTGF), transforming growth factor-β1 (TGF-β1), and vascular endothelial growth factor (VEGF) in human fibroblast-like synovial cells from advanced-stage osteoarthritis in vitro, Journal of Orthopaedic Research 28(4) (2010) 492-496.
[20] A.C. Newman, M.N. Nakatsu, W. Chou, P.D. Gershon, C.C. Hughes, The requirement for fibroblasts in angiogenesis: fibroblast-derived matrix proteins are essential for endothelial cell lumen formation, Molecular biology of the cell 22(20) (2011) 3791-3800.

[21] R. Costa-Almeida, M. Gomez-Lazaro, C. Ramalho, P.L. Granja, R. Soares, S.G. Guerreiro, Fibroblast-endothelial partners for vascularization strategies in tissue engineering, Tissue Engineering Part A 21(5-6) (2014) 1055-1065.
[22] C. Tonello, B. Zavan, R. Cortivo, P. Brun, S. Panfilo, G. Abatangelo, In vitro reconstruction of human dermal equivalent enriched with endothelial cells, Biomaterials 24(7) (2003) 1205-1211.
[23] I. Hartlapp, R. ABE, R.W. SAEED, T. PENG, W. VOELTER, R. BUCALA, C.N. METZ, Fibrocytes induce an angiogenic phenotype in cultured endothelial cells and promote angiogenesis in vivo, The FASEB Journal 15(12) (2001) 2215-2224.
[24] H. Lee, S.M. Dellatore, W.M. Miller, P.B. Messersmith, Mussel-inspired surface chemistry for multifunctional coatings, science 318(5849) (2007) 426-430.
[25] H. Lee, J. Rho, P.B. Messersmith, Facile conjugation of biomolecules onto surfaces via mussel adhesive protein inspired coatings, Advanced Materials 21(4) (2009) 431-434.
[26] F.M. Spinelli, D.L. Vitale, G. Demarchi, C. Cristina, L. Alaniz, The immunological effect of hyaluronan in tumor angiogenesis, Clinical & translational immunology 4(12) (2015) e52.
[27] Z. Tahergorabi, M. Khazaei, A review on angiogenesis and its assays, Iranian journal of basic medical sciences 15(6) (2012) 1110.
[28] C.A. Staton, S.M. Stribbling, S. Tazzyman, R. Hughes, N.J. Brown, C.E. Lewis, Current methods for assaying angiogenesis in vitro and in vivo, International journal of experimental pathology 85(5) (2004) 233-248.
[29] G.E. Davis, K. Pintar, R.S. Allen, S.A. Maxwell, Matrix metalloproteinase-1 and-9 activation by plasmin regulates a novel endothelial cell-mediated mechanism of collagen gel contraction and capillary tube regression in three-dimensional collagen matrices, Journal of cell science 114(5) (2001) 917-930.
[30] W.B. Saunders, K.J. Bayless, G.E. Davis, MMP-1 activation by serine proteases and MMP-10 induces human capillary tubular network collapse and regression in 3D collagen matrices, Journal of cell science 118(10) (2005) 2325-2340.
[31] Y.-l. Yang, L.M. Leone, L.J. Kaufman, Elastic moduli of collagen gels can be predicted from two-dimensional confocal microscopy, Biophysical journal 97(7) (2009) 2051-2060.
[32] A. Sieminski, R.P. Hebbel, K. Gooch, The relative magnitudes of endothelial force generation and matrix stiffness modulate capillary morphogenesis in vitro, Experimental cell research 297(2) (2004) 574-584.
[33] F. Bordeleau, B.N. Mason, E.M. Lollis, M. Mazzola, M.R. Zanotelli, S. Somasegar, J.P. Califano, C. Montague, D.J. LaValley, J. Huynh, Matrix stiffening promotes a tumor vasculature phenotype, Proceedings of the National Academy of Sciences 114(3) (2017) 492-497.
[34] D.J. LaValley, C.A. Reinhart-King, Matrix stiffening in the formation of blood vessels, Advances in Regenerative Biology 1(1) (2014) 25247.
[35] B.N. Mason, A. Starchenko, R.M. Williams, L.J. Bonassar, C.A. Reinhart-King, Tuning three-dimensional collagen matrix stiffness independently of collagen concentration modulates endothelial cell behavior, Acta biomaterialia 9(1) (2013) 4635-4644.
[36] A.S. Zeiger, F.C. Loe, R. Li, M. Raghunath, K.J. Van Vliet, Macromolecular crowding directs extracellular matrix organization and mesenchymal stem cell behavior, PloS one 7(5) (2012) e37904.
[37] L.T. Edgar, C.J. Underwood, J.E. Guilkey, J.B. Hoying, J.A. Weiss, Extracellular matrix density regulates the rate of neovessel growth and branching in sprouting angiogenesis, PloS one 9(1) (2014) e85178.
[38] A. Takahashi, A. Majumdar, H. Parameswaran, E. Bartolák-Suki, B. Suki, Proteoglycans maintain lung stability in an elastase-treated mouse model of emphysema, American journal of respiratory cell and molecular biology 51(1) (2014) 26-33.
[39] E. Brauchle, J. Kasper, R. Daum, N. Schierbaum, C. Falch, A. Kirschniak, T.E. Schäffer, K. Schenke-Layland, Biomechanical and biomolecular characterization of extracellular matrix structures in human colon carcinomas, Matrix Biology 68 (2018) 180-193.

[40] K.R. Levental, H. Yu, L. Kass, J.N. Lakins, M. Egeblad, J.T. Erler, S.F. Fong, K. Csiszar, A. Giaccia, W. Weninger, Matrix crosslinking forces tumor progression by enhancing integrin signaling, Cell 139(5) (2009) 891-906.
[41] A. Haage, I.C. Schneider, Cellular contractility and extracellular matrix stiffness regulate matrix metalloproteinase activity in pancreatic cancer cells, The FASEB Journal 28(8) (2014) 3589-3599.
[42] V.L. Cross, Y. Zheng, N.W. Choi, S.S. Verbridge, B.A. Sutermaster, L.J. Bonassar, C. Fischbach, A.D. Stroock, Dense type I collagen matrices that support cellular remodeling and microfabrication for studies of tumor angiogenesis and vasculogenesis in vitro, Biomaterials 31(33) (2010) 8596-8607.
[43] P. Lu, V.M. Weaver, Z. Werb, The extracellular matrix: a dynamic niche in cancer progression, J Cell Biol 196(4) (2012) 395-406.
[44] C.A. Reinhart-King, M. Dembo, D.A. Hammer, Cell-cell mechanical communication through compliant substrates, Biophysical journal 95(12) (2008) 6044-6051.
[45] J. Huynh, N. Nishimura, K. Rana, J.M. Peloquin, J.P. Califano, C.R. Montague, M.R. King, C.B. Schaffer, C.A. Reinhart-King, Age-related intimal stiffening enhances endothelial permeability and leukocyte transmigration, Science translational medicine 3(112) (2011) 112ra122-112ra122.

Appendix 3: Developing Cell-Derived Matrices with Macromolecular Crowding using Transwell Inserts

A3.1. Introduction

Research completed on cell-derived matrices (CDMs) within this dissertation project have focused on using two-dimensional (2D) cultures. After culture for 14 days under crowder conditions, the thickness of CDMs ranged from 25-30 μm. This system was ideal for assessing the effects of crowding on collagen deposition using techniques such as, immunocytochemistry, SDS-PAGE, and silver staining. Histological staining, however, was very challenging due to strong differential binding of anionic dyes to 2D- surfaces. As a result of the strong dye affinity as well as the large size of the dye molecules, staining 2-D surface with traditional histology stain diminish fine structural details within the sample [1]. Furthermore, there was a limitation in the thickness of sample that would be collected due to the unidirectional nutrient and gas exchange. Alternatively, permeable supports enable cellular nutrient and gas exchange to occur bidirectionally, thus increasing the matrix deposited, and providing a thicker sample for sectioning. CDMs have been successfully cultured on permeable meshes, and supported processing for histological staining in Ahlfors *et al* [2].

Paraffin processing of CDM sections grown on permeable scaffolds provides a thick specimen that can be embedded and provided several sections for histological analysis using Hematoxylin and Eosin (H&E) and Picrosirius red (PSR)/Fast green (FG). H&E combines the use of two dyes to assess for nuclear and collagen content. Hematoxylin is a cationic, deep blue purple stain that specifically binds to negative charged nucleic acids present in the sample [3], and provides nuclear detail and definition. Eosin is a light to deep pink stain that binds to positively proteins in the cell cytoplasm and extracellular matrix to varying degrees [3]. The

stain provides a technique to assess collagen density, distribution, and scaffold thickness. PSFG is an additional technique that combines two dyes for assessing collagen density and distribution. Fast green binds to non-collagenous proteins, with picrosirius binding to collagen in the ECM.

Both staining techniques provide qualitative assessment of collagen distribution in the matrix, however, there is poor specificity towards thin collagen fibers [1]. However, this limitation could be addressed by utilizing collagen inherent birefringent properties. To address the challenge of specificity and provide relevant information regarding collagen organization within a sample, it was discovered that Sirius red dissolved in picric acid solution consistently stained thin collagen fibers, without fading, and can greatly increase the birefringence properties of collagen, as picrosirius red is a birefringent molecule itself [4-6]. Sulfonic acid groups present in the Sirius red stain bind to the basic groups along the length of the collagen fibers, or parallel to it, thus greatly enhancing the birefringent properties of collagen [6, 7]. This method eventually became the standard for the analysis of collagen due to the birefringent properties provided by collagen's molecular structure [7-10]. This method is typically utilized when only linear polarized light is used, as collagen fibers that are aligned parallel to the transmission axis of the polarized filter appear dark and does not provide a hue [10]. Picrosirius red in combination with circular polarized light provides a method to identify all collagen fibers, while also assessing fiber hue and spatial distribution of the different colors [1]. Using picrosirius red/fast green staining with polarized imaging, we can assess collagen fiber network formation and distribution.

A3.2. Materials and Methods

A3.2.1 Cell culture

Human neonatal fibroblasts (p2-p8, ATCC, CRL 2097) were cultured as previously described and plated at a density of 428,000 cells/cm^2 in transwell inserts (Corning, 3450) for a total seeding density of 2 x 10^6 cells per insert as specified in previous protocols [2].

A3.2.2 Tissue Processing and Histology

Cell-derived matrices cultured on transwell inserts for 14 days were removed from the mesh, placed in a tissue cassette, fixed in 10% neutral buffered formalin for 1 hour, and stored in 70% ethanol solution until processing. CDMs were processed, paraffin embedded, and 5 μm sections were transferred onto charged slides. Tissue sections were then deparaffinzed, prior to staining. Hematoxylin & eosin (H&E) staining was used to examining collagen density, distribution, and matrix thickness. Picrosirius red/fast green staining was used for collagen density and collagen fibril distribution. Bright field imaging was used for H&E using a Leica DMI microscope. Bright field and polarized light filter was used to image PSFG samples using a Nikon Eclipse microscope and P-T diascopic polarizing filter (Microvideo Systems, MDN11920). Human skin or umbilical cord tissue was used as a positive control to assess staining technique. A sample size of N =1 scaffold with three sections per scaffold were stained and imaged.

A3.3. Results

A3.3.1 Hematoxylin and Eosin Staining

CDMs prepared under all MMC conditions shows several layers of cells and their associate extracellular space distributed throughout the section **(Supplementary Figure A3-1)**. The 0% and 0.05% HA scaffolds have a lightly packed collagen density, and appear to be approximately 100 µm in thickness. The 0.5% HA CDM appears to have a denser, tightly packed cellular layers and appears to be approximately 50 µm in thickness. The Ficoll 70/400 CDM collagen distribution appeared to be diffuse, and as not tightly packed compared to the other samples. Despite the lower qualitative collagen density staining pattern, the thickness for this sample is approximately 100 µm. Previous data for CDMs developed under 2D cultures indicated that the thickness ranged from 20-30 µm (Chapter 4, Figure 4-12). The differences in sample thickness support the use of transwell inserts for development of 3D CDM scaffolds. A sample size of one was used for this experiment, and thus thickness measurements were not quantified.

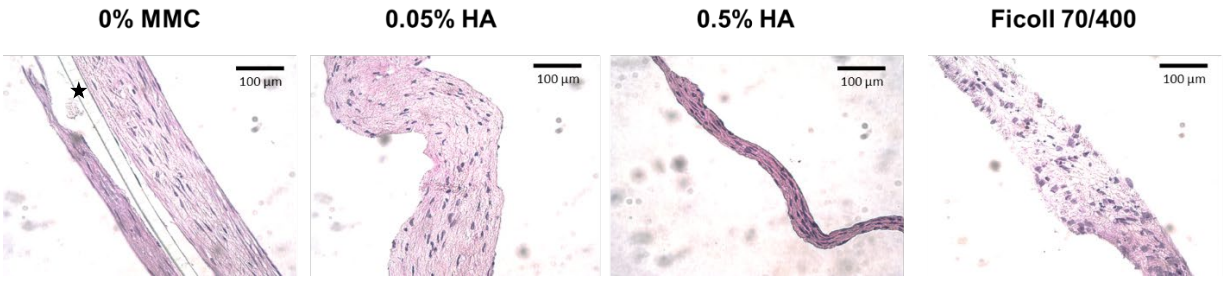

Supplementary Figure A3-1: Brightfield imaging of H&E stain of CDMs developed under MMC. Scale bar: 100 µm. Asterisk indicates presence of transwell inserts in tissue sections. Sample size: N =1.

A3.3.2 Picrosirius Red/Fast Green Staining and Polarized Light Microscopy

CDMs prepared under all MMC conditions stained with H&E indicate the presence of collagen. The PSFG staining shows that the 0%, 0.05% HA, and 0.5% HA condition had tightly

packed collagen density, with the 0.5% HA having the densest structure. CDM prepared under Ficoll 70/400 had a diffuse, thin collagen staining pattern. Polarized light imaging also shows the distribution of collagen fibers **(Supplementary Figure A3-2, Bottom Panel)**. The non-treated control CDM was characterized by a yellowish hue (birefringence coloration). CDMs prepared under both concentrations of HA had a yellow/orange hue, with the 0.5% HA condition exhibiting stronger birefringent fibers. The Ficoll 70/400 CDM had a greenish hue, with weakly birefringent scattered collagen fibers.

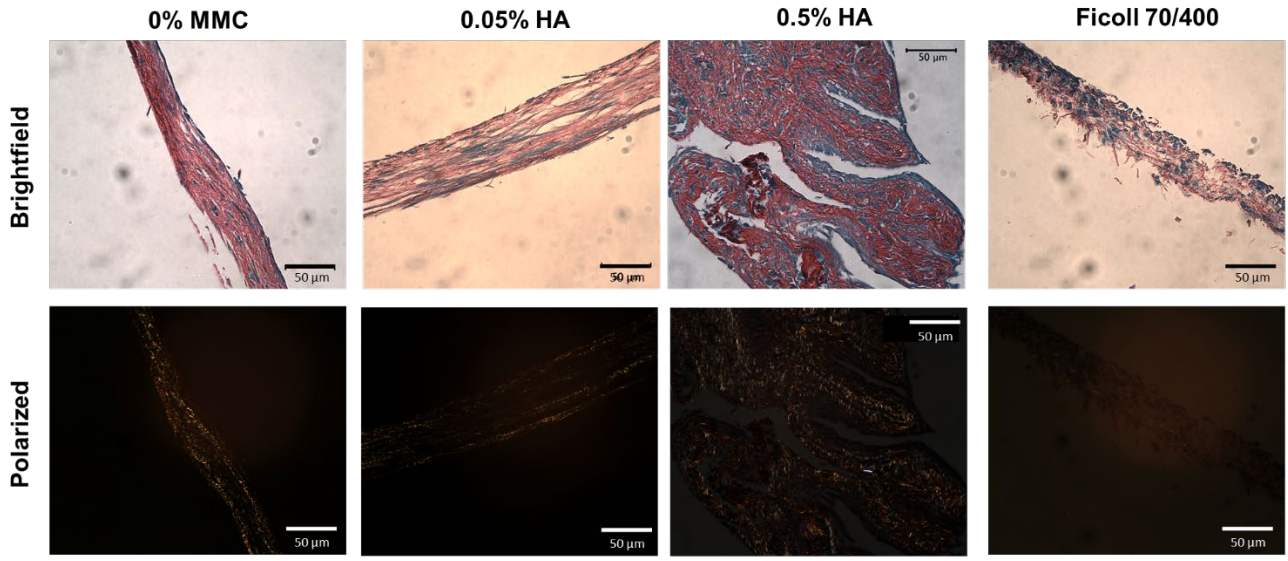

Supplementary Figure A3-2: Brightfield and polarized imaging of CDMs prepared under MMC crowding. Scale bar: 50 µm. Sample size: N =1.

A3.4. Discussion

CDMs cultured on transwell inserts were initially stained with H&E to assess for cell distribution and specimen thickness. The CDMs prepared on transwell inserts were not decellularized sections, and show the presence of nuclear content in the sections **(Supplementary Figure A3-1)**. For use as a 3D-biomaterial, decellularization process previously discussed in **Chapters 4** can be applied, and evaluating the efficacy of the procedure with thicker specimen in terms of matrix retention would need to be completed.

CDMs prepared under all MMC conditions show collagen distribution and density in the samples, and may provide information regarding sample thickness **(Supplementary Figure A3-1)**. The 0% and 0.05% HA scaffolds have a packed collagen density, and appear to be approximately 100 µm in thickness. The 0.5% HA CDM appears to have a denser, tightly packed collagen presence compared the non-treated control and the 0.05% HA sample. The 0.5% HA conditions appears to be approximately 50 µm in thickness. The Ficoll 70/400 CDM collagen distribution appeared to be diffuse, and as not tightly packed compared to the other samples, and appears to be approximately 100 µm despite the lower qualitative collagen density staining pattern. Thickness was not quantified throughout the entire sample block in this experiment as an N = 1 was prepared. Furthermore, due to concerns regarding ECM folding during sample folding during transfer to tissue cassettes and paraffin embedding, this method does not give an accurate description of thickness, as previous method used to assess CDM thickness did not indicate an MMC dependent effect on thickness **(Chapter 4, Figure 4-12)**. However, collagen type I immunostaining imaged as a Z-stack using a confocal laser scanning microscope did indicate MMC dependent differences in collagen density between the HA and Ficoll 70/400 treated CDMs.

PSFG is a collagen staining technique that provides information regarding collagen density, presence of non-collagenous proteins, and through the use of polarized light microscopy can also provide information regarding collagen fiber size and distribution. Collagen is an anisotropic material that interacts with light depending on the orientation of the molecule relative to the incident of light. When polarized light hits a collagen molecule, light is refracted into rays traveling at different speeds and vibrations directed at 90° to one another [6]. When collagen molecules are stained with PSFG, their birefringent properties are enhanced due as picrosirius

red is a birefringent molecule itself [4-6]. It has been reported that collagen types I, II, and III bind an average of 126 molecules of Sirius dye per collagen molecule present [11].

Brightfield imaging of PSFG indicated that the 0%, 0.05% HA, and 0.5% HA condition had tightly packed collagen density, with the 0.5% HA having the most dense structure. CDM prepared under Ficoll 70/400 had a diffuse, thin collagen staining pattern. Polarized light imaging indicate changes in the collagen fiber distribution in each CDM. The change in color of the of the PSR-stained collagen fibers due to polarized light imaging provides information regarding collagen fiber thickness. Thick collagen fibers have a red/orange hue and thinner collagen fibers having a yellow/green hue. The non-treated control CDM as well as both HA treated CDMs are characterized by a hue indicative of thicker collagen fibers exhibiting stronger birefringent properties compared to the Ficoll 70/400 treated condition. The Ficoll 70/400 CDM had a greenish hue, with weakly birefringent scattered collagen fibers that may correspond to molecular disorganization or collagen degradation.

Some groups have suggested that hue color provides information regarding collagen fiber type; for instance, collage type III, characterized by a green hue, while thicker collagen type I fibers have a reddish/orange/yellow hue [8]. It is still possible that the thinner, green fibers may be thinner, immature collagen type I fibers [1] or indicate the presence of collagen fiber degradation [12, 13]. Collagen degradation is dependent on the activity of MMPs, which help maintain the balance between collagen degradation and production for maintenance of tissue mechanical properties. MMP1 is specifically a collagenase molecule that degrades collagen type I. Ficoll 70/400 treated samples significantly increased MMP1 gene and protein expression as indicated by qRTPCR, transcriptomic, as well as proteomic experiments thus supporting the increased green collagen hue present. Alternatively, the green hue present in this sample may

indicate higher collagen type III distribution compared to collagen type I. While fixation time and method was kept consistent for all samples, the green hue may be due to a prolonged fixation time, as a loner fix time has also been attributed to a decrease the in staining intensity, especially for thinner collagen fibers [14]. However, the green hue is more likely due to reasons discussed earlier since the other conditions as well as the tissue control slide had different hues indicating even staining, and that fixation technique was not an issue.

The use of transwell inserts to make CDM scaffolds provided additional characterization techniques to assess collagen density and distribution. Transwell inserts provide bidirectional nutrient and gas exchange thus resulting in a thicker scaffold that can be used to assess functional properties of CDMs developed under MMC conditions. Ahlfors *et al* also used transwell inserts to develop CDMs under chemically defined media conditions [2]. Histological staining indicated thicker CDM samples, however, this experiment also utilized an ascorbate concentration that was 5x higher than what was reported in this dissertation project. Furthermore, MMC was used as a technique to promote sequestration of ECM precursor proteins at the cell layer (Chapter 3, Proteomics). Thus, this method can be used with alternative techniques that focus on driving matrix production alone.

A3.5. Acknowledgements

We would like to thank Jyotsna Patel for her help and support in tissue processing and staining.

A3.6. References

[1] L. Rich, P. Whittaker, Collagen and picrosirius red staining: a polarized light assessment of fibrillar hue and spatial distribution, Braz J Morphol Sci 22(2) (2005) 97-104.
[2] J.-E.W. Ahlfors, K.L. Billiar, Biomechanical and biochemical characteristics of a human fibroblast-produced and remodeled matrix, Biomaterials 28(13) (2007) 2183-2191.
[3] A.H. Fischer, K.A. Jacobson, J. Rose, R. Zeller, Hematoxylin and eosin staining of tissue and cell sections, Cold Spring Harbor Protocols 2008(5) (2008) pdb. prot4986.
[4] F. Sweat, H. Puchtler, S.I. Rosenthal, Sirius red F3BA as a stain for connective tissue, Archives of pathology 78 (1964) 69-72.
[5] H. Puchtler, F.S. Waldrop, L.S. Valentine, Polarization microscopic studies of connective tissue stained with picro-sirius red FBA, Beiträge zur Pathologie 150(2) (1973) 174-187.
[6] L. Rittié, Method for picrosirius red-polarization detection of collagen fibers in tissue sections, Fibrosis, Springer2017, pp. 395-407.
[7] L.C.U. Junqueira, G. Bignolas, R. Brentani, Picrosirius staining plus polarization microscopy, a specific method for collagen detection in tissue sections, The Histochemical journal 11(4) (1979) 447-455.
[8] L. Junqueira, W.a. Cossermelli, R. Brentani, Differential staining of collagens type I, II and III by Sirius Red and polarization microscopy, Archivum histologicum japonicum 41(3) (1978) 267-274.
[9] P. Whittaker, D.R. Boughner, R. Kloner, Analysis of healing after myocardial infarction using polarized light microscopy, The American journal of pathology 134(4) (1989) 879.
[10] P. Whittaker, P.B. Canham, Demonstration of quantitative fabric analysis of tendon collagen using two-dimensional polarized light microscopy, Matrix 11(1) (1991) 56-62.
[11] L. Junqueira, G. Bignolas, R. Brentani, A simple and sensitive method for the quantitative estimation of collagen, Analytical biochemistry 94(1) (1979) 96-99.
[12] L.F. Borges, P.S. Gutierrez, H.R.C. Marana, S.R. Taboga, Picrosirius-polarization staining method as an efficient histopathological tool for collagenolysis detection in vesical prolapse lesions, Micron 38(6) (2007) 580-583.
[13] L. Junqueira, M. Zugaib, G. Montes, O. Toledo, R. Krisztan, K. Shigihara, Morphologic and histochemical evidence for the occurrence of collagenolysis and for the role of neutrophilic polymorphonuclear leukocytes during cervical dilation, American Journal of Obstetrics and Gynecology 138(3) (1980) 273-281.
[14] V. Constantine, R. Mowry, Selective staining of human dermal collagen: I. An analysis of standard methods, Journal of Investigative Dermatology 50(5) (1968) 414-418.